The regulation of subfornical organ neurons

by

Colleen S. Peterson

A thesis submitted to the Faculty of Graduate Studies of

The University of Manitoba

in partial fulfilment of the requirements of the degree of

Master of Science

Department of Biological Sciences

University of Manitoba

Winnipeg

Abstract

While the central nervous system (CNS) plays a critical role in the regulation of homeostasis, most of the CNS is isolated from constituents of the periphery by a blood-brain-barrier (BBB). The subfornical organ (SFO) is a specialised structure known as a sensory circumventricular organ (sensory CVO) which lacks a BBB, expresses a wide variety and density of membrane receptors, and sends projections to numerous nuclei critical in regulation of homeostasis. Thus the SFO is situated to sense and integrate information about the physiological state of the body and transduce this information to homeostatic control centres in the CNS.

The manuscripts comprising this thesis are focused on investigation of the regulation of the rat SFO to maintain homeostasis. In the first manuscript, we investigated the effect of overnutrition in the postnatal pre-weaning stage on gene expression in the SFO by RNAseq, and observed significantly altered expression of 12 transcripts. In the second manuscript, we combined the transcriptomics data from the first chapter with expression data from a previously published microarray study to produce a list of ion channels and G-protein-coupled receptors expressed within the SFO. We also investigated voltage-gated K^+, Na^+, and Ca^{2+} currents in SFO neurons, and validated the presence of receptors for the peptide hormones substance P, endothelin, and neurotensin via electrophysiology, in an effort to correlate gene expression data with physiology. Due to the markedly high expression of receptors for neurotensin revealed by the transcriptomics data, in the third manuscript we investigated the electrical effects of neurotensin on SFO neurons. Patch clamp electrophysiology experiments revealed that neurotensin increases the electrical excitability of SFO neurons via an increase in nonselective cation conductance and attenuation of delayed-rectifier voltage-gated K^+ currents.

Together, these manuscripts represent a significant contribution to our knowledge of the regulation of SFO neurons, thereby improving our understanding of the CNS regulation of homeostasis. We expect these data to be of particular interest to researchers focused on the physiology of homeostasis and the treatment of obesity, hypertension, and metabolic syndrome.

Contributions of authors

Chapter 2 is co-authored between Colleen S. Peterson, Shuo Huang, Samantha A. Lee, Dr. Alastair V. Ferguson, and Dr. W. Mark Fry. Colleen S. Peterson carried analyses and co-wrote the first draft of the manuscript with Dr. W. Mark Fry. Dr. W. Mark Fry and Dr. Alastair V. Ferguson designed the study. Shuo Huang dissected out the brain tissue for RNAseq, Samantha A. Lee weighed rats and recorded their weights. All authors contributed to manuscript edits.

The remaining chapters are authored by Colleen S. Peterson under the supervision of Dr. W Mark Fry.

Acknowledgements

I would like to thank my advisor Dr. Mark Fry for all the support, encouragement, and all the reading and editing. You believed in and encouraged me when I didn't believe in myself, and I'm a better scientist because of it.

Thank you to my committee members Dr. Jay Treberg and Dr. Mike Jackson for all their comments and suggestions: my thesis is better for it.

Thank you also to my lab mates Todd Curtaz, Rayna Hamilton, Anjelica Bodnaryk, Megan Belyea, and Jodi Ruckhall. You were all a pleasure to work with and I will miss your suggestions and banter. I believe in all of you and wish you the best in your future careers.

I would also like to acknowledge staff at the Animal Holding Facility for taking care of our animals, and The University of Manitoba Faculty of Graduate Studies and NSERC for funding.

Finally, to my husband Joel, thank you for your endless support these past seven years, and for the upcoming years too. Two degrees down and I couldn't have done either without you.

Table of contents

List of tables

List of figures

Appendix

List of abbreviations

AgRP – agouti-related peptidev

Ahsa2 – AHA1, activator of heat shock protein ATPase 2

ARC – arcuate nucleus of the hypothalamus

AP – area postrema

BBB – blood-brain barrier

BNST – bed nucleus of the stria terminalis

cAMP – cyclic adenosine monophosphate

CART – cocaine/amphetamine regulated transcript

cGMP – cyclic guanosine monophosphate

CHO – Chinese hamster ovary cells

Chordc1 – cysteine and histidine-rich domain-containing protein 1

CNS – central nervous system

Cracr2b – EF-hand calcium-binding domain-containing protein 4A

Creld2 – cysteine-rich with EGF-like domain protein 2

CVO – circumventricular organ

DREADD – designer receptors exclusively activated by designer drugs

Elovl1 – elongation of very long chain fatty acids protein 1

EPSP – excitatory post-synaptic potential

ET – endothelin β

ETRA – endothelin receptor A

ETRB – endothelin receptor B

GPCR – G-protein-coupled receptor

HEK293 – human embryonic kidney cells

Hspb1 – heat shock 27 kDa protein 1

Hsph1 – heat shock protein 105 kDa

I_A – transient K^+ current

Il-1β – interleukin 1-beta

I_K – delayed-rectifier K^+ current (non-inactivating)

I_{NSC} – nonselective cation current

IP_3 – inositol triphosphate

IPSP – inhibitory post-synaptic potential

LH – lateral hypothalamus

LOC100910245 – tibose-phosphate pyrophosphokinase 2-like

αMSH – alpha melanocyte stimulating hormone

Manf – mesencephalic astrocyte-derived neurotrophic factor

MAPK – mitogen-activated protein kinase

MC4R – melanocortin receptor 4

MPN – medium preoptic nucleus

NPY – neuropeptide Y

Nts – neurotensin

NTS – nucleus tractus solaris

NTSR – neurotensin receptor

OVLT – organum vasculosum of the lamina terminalis

PKC – protein kinase C

PNS – peripheral nervous systems

POMC – proopiomelanocortin

PVN – paraventricular nucleus of the hypothalamus

RNAseq – RNA sequencing

Slc24a4 – solute carrier family 24 member 4

SFO – subfornical organ

SON – supraoptic nucleus

SORT1 – sortilin receptor 1

SorLa/LR11 - sorting protein-related receptor

SP – substance P

TACR1 – tachykinin receptor 1

VMN – ventromedial nucleus of the hypothalamus

VTA – ventral tegmental area

1. Introduction

This thesis is comprised of three manuscripts investigating the role of the subfornical organ (SFO) in central regulation of homeostasis (Chapters 2-4). In chapter 2, we examined the effects of early postnatal overnutrition using a small litter model (from birth to weaning) on gene expression in the SFO using RNAseq. In chapter 3, we mined transcriptomic data from the control group in the second chapter and from the control data of a previously published SFO microarray transcriptome (Hindmarch et al., 2008) to develop a validated list of ion channel and G-protein-coupled receptor (GPCR) transcripts expressed in the SFO. The ion channels and GPCRs expressed within the SFO can give us insight in to the intrinsic electrical properties of SFO neurons and the mechanisms behind them, as well as the sensing ability of the SFO. Furthermore, the validated transcriptome data provided us with a list of GPCRs and ligand-gated ion channels known to be expressed, but whose activity at the SFO is unexplored. From this list we noted a particular high level of expression of two receptors for neurotensin: NTSR2 and NTSR3. Therefore, in the fourth chapter we studied the electrical effects of neurotensin on dissociated SFO neurons using whole cell patch clamp electrophysiology. This research will be of particular interest to those investigators focused on the central regulation of homeostasis and the perturbations of these systems in human health issues including obesity, hypertension, and metabolic syndrome.

1.1. Obesity

Self-reported adult obesity rates in Canada have increased from 17.9% in 2009 to 27.8% in 2017 (Statistics Canada, 2015, 2019) and are predicted to increase worldwide in coming years (Twells et al., 2014). The increasing availability of palatable high-fat, high-sugar foods, larger portion sizes (Nielsen and Popkin, 2019), and technological advances which have lead to a

decreased need for physical activity (Epstein et al., 2000) are most often cited as the major causes of the obesity epidemic. The increase in obesity is of particular concern as excess body fat is associated with increased risk for type II diabetes (Ohlson et al., 1985; Lundgren et al., 1989), hypertension (Berchtold et al., 1977), heart disease (Berchtold et al., 1977), and some cancers (Calle et al., 2003). In addition to personal health and quality of life concerns, obesity places a burden on healthcare systems. In Canada, obesity-related healthcare spending is estimated between 4.6 to 7.1 billion dollars annually (~4% of the health care budget (Public Health Agency of Canada and Canadian Institute for Health, 2011)). Considering these factors, there is an urgent need for the development of improved prevention strategies and treatments for obesity, and the first steps include gaining a better understanding of the central nervous systems (CNS) that regulate homeostasis.

1.1.2. Predisposing factors

Obesity is caused by an imbalance of energy intake versus expenditure leading to positive energy balance, typically by overeating and under exercising. While the apparent solution is to correct this imbalance via decreasing food intake and increasing exercise, this solution fails for many due to a combination of physiological and psychological factors (Herriot et al., 2008). There are many factors which complicate the effective treatment of obesity, including genetic, environmental, and physiological components. In a small number of cases, a single loss-of-function mutation in an important energy balance gene can cause severe obesity. For example, loss-of-function of the satiety hormone leptin or its receptor results in persistent hunger and as a consequence unsuppressed feeding in humans (Froguel et al., 1998) and rodent models (Pelleymounter et al., 1995). Similar effects are seen in loss-of-function mutations in other genes such as the melanocortin receptor 4 (MC4R) (Kobayashi et al., 2002) and proopiomelanocortin

(POMC) (Yaswen et al., 1999), a precursor to the satiety signal α-melanocyte stimulating hormone (αMSH) (Biebermann et al., 1998). Even the presence of one functional copy of these genes may not fully rescue the phenotype, producing individuals with variable severity of obesity for some genes (Valette et al., 2014). More commonly, predisposition toward obesity is inherited in functional variants of energy balance genes. Genome-wide association studies have identified single nucleotide polymorphisms in as many as 870 genes associated with obesity, including those with verified roles in regulation of energy balance (Locke et al., 2015; Akiyama et al., 2017; Yengo et al., 2018). However, genetic variability in these genes explains only 5% of BMI variance (Yengo et al., 2018), suggesting that other factors play a larger role in the current obesity epidemic.

Once an individual becomes obese, physiological changes make weight loss more difficult (McNay et al., 2012). While many obese people show increased serum levels of the satiety hormone leptin (Considine et al., 1996), this is proposed to occur in parallel to central leptin resistance (Frederich et al., 1995), preventing feelings of fullness and ultimately acting to promote continued overfeeding. Similarly, some obese individuals show varying levels of resistance to insulin (Yamashita et al., 1996), which also acts as a satiety signal at the CNS (Brief and Davis, 1984).

In addition to genetic predisposition and adult physiological changes, overnutrition at both prenatal and early postnatal stages are associated with the development of obesity (Shankar et al., 2008; Habbout et al., 2012) and related conditions such as hypertension (Campbell et al., 1996; Yim et al., 2013) and perturbations of glucose homeostasis (Siemelink et al., 2002) in adulthood, though this thesis will focus only on the effects of early postnatal overnutrition. The propensity toward obesity due to early overnutrition is in part due to alterations of energy

balance circuits. Rodent studies show that early postnatal high fat diets results in fewer anorexigenic and orexigenic projections from the arcuate nucleus of the hypothalamus (ARC) to the paraventricular nucleus of the hypothalamus (PVN) (Schipper et al., 2013). However, within the ARC and the PVN, orexigenic galanin neuron densities are increased (Plagemann et al., 1999a, 1999b). The response of neurons to energy balance signalling molecules are also altered in some cases: early postnatal overnutrition results in weaker responses to leptin and insulin (Davidowa and Plagemann, 2007; Glavas et al., 2010), and inverse effects of the anorexigenic signals cocaine-amphetamine regulated transcript (CART), NPY, and corticotropin releasing hormone in hypothalamic neurons (Davidowa et al., 2003, 2004; Davidowa and Plagemann, 2004). Notably, much of the research on the effects of early postnatal overnutrition on central regulation of energy balance has focused on hypothalamic centres (see section 1.2), however several nuclei outside the hypothalamus such as the ventral tegmental area (VTA) and sensory circumventricular organs (sensory CVOs) also contribute to energy balance (Contreras et al., 1982; Cador et al., 1986; Smith et al., 2008). This will be further explored with a focus on gene expression (Chapter 2).

The genetic, environmental, and physiological influences make the treatment of obesity surprisingly complex. Unravelling the ways in which energy balance homeostasis is altered in obese individuals can aid in the prevention and treatment of obesity. However, to decipher the ways in which the CNS regulation of energy balance is altered to promote obesity, we first need to understand how these systems work in a healthy individual.

1.2. CNS hypothalamic regulation of energy balance

Multiple hypothalamic nuclei contribute to the regulation of energy balance. Early lesion studies identified the lateral hypothalamus (LH), ventromedial nucleus (VMN), and later the

PVN as key nuclei coordinating energy balance: lesions of the LH reduce feeding and body weight (Boyle and Keesey, 1975; Grossman et al., 1978), whereas the VMN lesions have the reverse effect (Anand and Brobeck, 1951). At that time the LH and VMN were thought to be the major sites for regulation of energy balance. However, other nuclei were also shown to play important roles: lesions of the PVN also cause hyperphagia and increased body weight (Sims and Lorden, 1986). Furthermore, the PVN sends efferent projections to the medulla which modulate gastric motility (Saper et al., 1976; Rogers and Hermann, 1987).

Since the 1980s, the ARC has been recognised as a major regulator and possibly the main coordination centre of energy balance. The ARC contains 2 main populations of neurons involved in regulation of energy balance, both of which send axonal projections to the LH, VMN, and the PVN (Broberger et al., 1998; Wang et al., 2015): anorexigenic POMC/CART neurons, and orexigenic NPY/agouti-related peptide (NPY/AgRP) neurons. POMC/CART and NPY/AgRP neurons are thought to act antagonistically to suppress and promote feeding, respectively (Yaswen et al., 1999; Aponte et al., 2011). NPY/AgRP neurons also send inhibitory synaptic connections to POMC/CART neurons which allow inhibition of anorexigenic signals when orexigenic signals are detected (Roseberry et al., 2004; Atasoy et al., 2012). Critical energy balance signals also act in opposing ways on these neurons to promote a unified message. The satiety signal leptin depolarises POMC/CART neurons and promotes expression of its anorexigenic signals (Qiu et al., 2010), while hyperpolarising NPY/AgRP neurons to decrease inhibitory input to POMC/CART neurons (Baver et al., 2014). Conversely, the hunger hormone ghrelin activates NPY/AgRP neurons while also acting on POMC/CART neurons to inhibit firing (Cowley et al., 2003). However, leptin and ghrelin are produced outside the CNS (Zhang et al., 1994; Kojima et al., 1999) and as large peptide hormones are not capable of passively

crossing the blood-brain barrier (BBB), as are numerous other homeostatic signalling molecules. How then do these nuclei monitor energy balance?

1.3. The blood-brain-barrier protects and isolates the CNS

Most areas of the CNS, including the hypothalamus is protected via a BBB composed of tight junctions between endothelial cells and astrocyte end-feet (Figure 1.1A and B) (Reese and Karnovsky, 1966). The BBB prevents polar molecules and macromolecules from freely passing in to the interstitial fluid between neurons, allowing for tighter regulation of the internal environment of the brain (Figure 1.1B). Herein lies a paradox in that the CNS is also critical in the maintenance of homeostasis, which requires monitoring of signals in the circulation from other systems, including signalling molecules such as peptides and large hormones which cannot normally cross the BBB.

Some molecules may pass the BBB via passive diffusion (Fischer et al., 1998), though this is not possible for some larger hydrophilic signals. A limited number of signalling molecules are specifically moved across the BBB via a saturable transporter, for example leptin (Koistinen et al., 1998) and insulin (Duffy and Pardridge, 1987). There are also some situations where the BBB can become “leaky”, such as during inflammation (Reijerkerk et al., 2013), some pathological states such as Alzheimer’s (Sun-young et al., 2013) and lupus (Alexander et al., 2011), as well as in periventricular areas in mice which show a leaky choroid plexus (Ueno et al., 2000). However, in these scenarios the BBB is not consistently and non-specifically open, posing a problem for the prompt detection of signals of the physiological state of the periphery.

1.4. Sensory circumventricular organs lack a blood-brain-barrier

Sensory CVOs are unique structures in that they lack a BBB. Sensory CVOs are located adjacent to ventricles, and contain extensive vasculature and fenestrated capillaries to facilitate movement of blood and cerebrospinal fluid across sensory CVO cell bodies (Gross, 1992). Sensory CVO vasculature slows perfusion of blood across the CVOs, thereby allowing blood and important signals contained therein to come in contact with the CVO cell bodies for longer (Gross, 1991). Furthermore, sensory CVOs express a large variety of peptide and hormone receptors (Hindmarch et al., 2008; Szathmari et al., 2013), and send many projections to important homeostatic control centres (Phillips and Camacho, 1981; Lind et al., 1982; Shapiro and Miselis, 1985), positioning them as detectors and transducers of the body's physiological state. Three sensory CVOs exist in the mammalian brain: the organum vasculosum of the lamina terminalis (OVLT) in the anterior wall of the 3rd ventricle, the area postrema (AP) in the brainstem, and the SFO in the anteroventral 3rd ventricle (Figure 1.2). The present studies will focus on the SFO and its roles in homeostasis.

1.5. The subfornical organ

1.5.1. Anatomy of the subfornical organ

The SFO is a sensory circumventricular organ with well-established roles in regulation of cardiovascular output (Mangiapane and Simpson, 1983; Dai et al., 2013; Black et al., 2018), hydromineral balance (Felix, 1976; Mangiapane and Simpson, 1980; Oka et al., 2015), energy balance (Smith et al., 2008, 2010), and lesser roles in immune function (Roth et al., 2002; Cerqueira et al., 2016) and reproduction (Limonta et al., 1981; Donevan et al., 1989). In line with these roles, the SFO sends axonal projections to homeostatic centres including the median preoptic nucleus (MPN) (Lind et al., 1982, 1984), the PVN (Miselis, 1982), the supraoptic

nucleus (SON) (Lind et al., 1982; Sawchenko and Swanson, 1983), the ARC, (Gruber et al., 1987; Whyment et al., 2004), the LH (Burton et al., 1976; Miselis, 1982), the bed nucleus of the stria terminalis (BNST) (Swanson and Lind, 1986; McKinley et al., 2003; Hollis et al., 2008) and the OVLT (Lind et al., 1982). The SFO also receives synaptic input from many of these areas including the LH, the ARC (Rosas-Arellano et al., 1996), the MPN (Gruber et al., 1987), the nucleus of the solitary tract (NTS) (Miselis, 1982), the PVN, and the SON (Gruber et al., 1987).

The SFO can be separated into two regions with differences in anatomy, protein expression, and subtle differences in electrical behaviour: the rostrodorsal outer shell or peripheral SFO (hereafter referred to as shell SFO), and the ventromedial core (hereafter referred to as core SFO) (Figure 1.3). Anatomically, the shell and core SFO regions differ in both capillary structure and projections. The core SFO contains a dense network of long capillaries with considerable surface area; in contrast, the shell SFO has narrower capillaries (Gross, 1991). Whereas the shell SFO sends axonal projections to hypothalamic centres such as the magnocellular cells of the PVN (Kawano and Masuko, 2010), the LH, and the SON, the core SFO region primarily projects to the limbic BNST (Swanson and Lind, 1986; McKinley et al., 2003; Hollis et al., 2008) in addition to hypothalamic nuclei including the parvocellular cells of the PVN (Kawano and Masuko, 2010). The different projections from neurons in these zones suggest there are distinct physiological roles for the core and shell SFO. Notably, the magnocellular cells of the PVN secrete the neurohormones oxytocin and vasopressin via the posterior pituitary (Lobo Antunes and Zimmerman, 1978), whereas the parvocellular cells of the PVN secrete corticotropin releasing hormone (Paull and Gibbs, 1983; Piekut and Joseph, 1986), vasopressin (Piekut and Joseph, 1986), and thyrotropin-releasing hormone (Liposits et al., 1987) on to the anterior pituitary.

The differences between the core and shell regions are also reflected in the expression of various proteins. Although the physiological significance is not yet clear, the expression profile of calcium binding proteins calbindin and calretinin is distinct between shell and core SFO neurons, such that shell SFO neurons express calretinin and core SFO neurons express calbindin. This allows shell and core SFO neurons to be readily distinguished by their expression of calretinin and calbindin (McKinley et al., 2003; Huang et al., 2019), respectively. Differences also exist in the expression of angiotensin II (Lind et al., 1984), and its receptor (Lenkei et al., 1995; Giles et al., 1999), the former which shows increased expression in the shell SFO, and the latter which is more densely expressed in the core SFO. Furthermore, expression differences between shell and core SFO cells are not limited to neurons, as differential expression is also evident in glial cells and SFO vascular elements (Pócsai and Kálmán, 2015). The distribution of proteins in the shell and core SFO continues to be investigated, as these differences likely underlie the differences in electrical behaviour and physiological roles between shell and core SFO neurons (Lind et al., 1984; Pócsai and Kálmán, 2015; Huang et al., 2019)

Using an RNA gold nanoparticle molecular beacon probe to label calbindin in live neurons, Huang et al. examined the differences in electrical properties of calbindin-positive versus calbindin-negative neurons via patch clamp electrophysiology (Huang et al., 2019). In general, a greater proportion of calbindin-positive neurons were spontaneously active than calbindin-negative neurons, though they on average fired less. The firing pattern between spontaneous calbindin and non-calbindin neurons also differed, as calbindin neurons showed a propensity to burst firing as opposed to tonic firing. The increased spontaneous activity may be related to the mean more depolarised resting membrane potential in core neurons and their increased transient Na^+ current density. These properties represent average differences between

the core and shell populations, and cannot necessarily be used to identify individual neurons, as these two populations overlap in these properties. Similarly, Anderson et al. (Anderson et al., 2001) examined the electrophysiological properties of SFO neurons projecting to the PVN and observed increased transient K^+ currents, but noted that this property, while ubiquitous in those neurons, was not unique enough to distinguish them by K^+ current alone (Anderson et al., 2001). For this reason, divergent protein expression remains a more effective tool for separating SFO neuron subtypes.

1.5.2. Differential receptor expression in the subfornical organ

In line with its role as a sensor of physiological state, the SFO expresses an abundance of receptors for signalling molecules. A microarray study which examined the effects of fasting and water restriction on gene expression in the SFO revealed the expression of numerous receptors, including multiple receptors known to be involved in energy balance and blood pressure regulation (Hindmarch et al., 2008). Receptor expression will be further discussed in chapter 3.

The SFO contains several subpopulation of cells, in which individual neurons may express only a subset of the transcripts discovered via microarray (Hindmarch et al., 2008) and RNAseq (Chapters 2 and 3). Multiple studies show only a proportion of SFO neurons respond to any particular signalling molecule (Ono et al., 2008; Dai et al., 2013; Lakhi et al., 2013; Black et al., 2018; also explored in chapter 4), and that subsets of SFO neurons may have opposing responses to the same signal (Dai et al., 2013; Lakhi et al., 2013; Black et al., 2018), due to the complement of ion channels expressed within them. For example, insulin (Lakhi et al., 2013), brain-derived neurotrophic factor (Black et al., 2018), and apelin (Dai et al., 2013) elicit either a depolarising, hyperpolarising, or no response in dissociated SFO neurons. In some cases, the ability to respond to a specific signal is reflected along the anatomic lines: leptin receptors are

preferentially expressed in the core SFO (Smith et al., 2008) whereas vasopressin receptors are preferentially expressed in the shell SFO (McKinley et al., 2003). The differing behaviours of SFO neurons to signals may also be connected to differing physiological responses: photoactivation of SFO neurons shows some SFO neurons acts to drive thirst whereas others supress it (Oka et al., 2015).

1.5.3. The subfornical organ contributes to osmoregulation and regulation of cardiovascular output

One of the first established roles for the SFO to detect circulating angiotensin to modulate blood pressure and thirst (Mangiapane and Simpson, 1980). Direct microinjection of angiotensin II to the SFO was shown to increase blood pressure and water drinking (Mangiapane and Simpson, 1979, 1980), which was reduced by SFO lesion (Massi et al., 1986; Mumford et al., 1989). Stimulation of the SFO results in greater vasopressin release (Ferguson and Kasting, 1986), via projections to SON (Wilkin et al., 1989) and excitatory projections to PVN vasopressin neurons (Tanaka et al., 1987; Ferguson, 1988). The magnocellular neurons of the PVN and SON release vasopressin and oxytocin as neurotransmitters on to the posterior pituitary (Brimble et al., 1978), whereas the PVN parvocellular neurons which release vasopressin as a neurotransmitter on the anterior pituitary (Brimble et al., 1978), and send axonal projections to the median eminence (Ferguson et al., 1984a), medulla (Ferguson et al., 1984b), the spinal cord (Bains and Ferguson, 1995) including preganglionic cells of the autonomic nervous system (Swanson and Kuypers, 1980). The end result of angiotensin-biding at the SFO is release of vasopressin in to the circulation to increase blood pressure via vasoconstriction (Friedman and Pauls, 1952) and to regulate water homeostasis via the renal system (Ganote et al., 1968), and potentially activation of the sympathetic nervous system and modulation of the baroreceptor

reflex (Townend et al., 1995; Potts et al., 1999; Sayk et al., 2015). Furthermore, circulating vasopressin acts on the SFO to decrease blood pressure (Smith and Ferguson, 1997) in a negative feedback loop of the renin-angiotensin system. Since these seminal experiments, research has shown the SFO to affect cardiovascular output and hydromineral balance in response to a variety signalling molecules (Simpson and Routtenberg, 1972; Wall et al., 1992; Smith et al., 2007; Smith and Ferguson, 2012; Dai et al., 2013; Kuksis et al., 2014; Cerqueira et al., 2016; Black et al., 2018), allowing the SFO to detect numerous signals from multiple peripheral and central sites, and integrate these signals to produce the appropriate output to homeostatic control centres.

Many of the signals which modulate the electrical activity of SFO neurons also have demonstrated roles in other aspects of homeostasis: leptin (Smith et al., 2008; Smith and Ferguson, 2012), ghrelin (Mimee et al., 2013), and adiponectin (Alim et al., 2010) alter the electrical excitability of SFO neurons and modulate cardiovascular output at the SFO, but also have roles in energy balance (Rentsch et al., 1995; Nakazato et al., 2001; Polson and Thompson, 2003).

1.5.4. The subfornical organ contributes to regulation of energy balance

Early research hinted at a role for the SFO in regulation of energy balance. The SFO sends and receives projections to and from numerous homeostatic nuclei implicated in energy balance, including the LH (Burton et al., 1976; Miselis, 1982; Gruber et al., 1987), PVN (Miselis, 1982; Larsen et al., 1991; Cottrell and Ferguson, 2004), and ARC (Gruber et al., 1987; Rosas-Arellano et al., 1996; Whyment et al., 2004). Furthermore, an early SFO lesion study which was primarily focused on fever also noted changes in feeding and body fat (Takahashi et al., 1997). More recently, numerous studies have confirmed that SFO is involved in energy balance and begun to investigate the mechanisms by which the SFO contributes to energy

homeostasis. A transcriptome of the SFO by microarray uncovered the expression of receptors for key signalling molecules with known roles in regulation of energy balance, including leptin, amylin, and insulin (Hindmarch et al., 2008). Electrophysiology studies have since confirmed that leptin (Smith et al., 2008), ghrelin (Pulman et al., 2006), and insulin (Lakhi et al., 2013), among other feeding signals (Pulman et al., 2006; Ono et al., 2008; Alim et al., 2010) can alter the electrical excitability of SFO neurons. Importantly, electrical stimulation of the SFO induces feeding in satiated rats (Smith et al., 2010). Thus, in recent years it has become clear that in addition to its roles in the osmoregulation and cardiovascular output, the SFO can sense circulating satiety and transduce this information to other nuclei to affect behaviour. However, many receptors revealed by microarray (Hindmarch et al., 2008) and RNAseq (chapters 2 and 3) as expressed in the SFO have not yet been investigated, including those whose ligands have roles in regulation of energy balance.

1.6. The neuromedin family of signalling peptides

In the second and third chapter of this thesis, we performed RNAseq on the rat SFO and developed a list of ion channels and GPCRs with validated expression in the SFO. One family of receptors we observed to be strongly expressed in the SFO, which were not previously studied at the SFO, were the neuromedin family of receptors. The first neuromedin was extracted from porcine spinal cord and dubbed neuromedin U for its ability to stimulate contractile effects when injected in to a rodent uterus (Minamino et al., 1985). Numerous neuromedins were subsequently discovered (Leeman, 1973; Kangawa et al., 1983; Minamino et al., 1983) and can now be divided in to 4 subgroups: 1. the bombesin-like neuropeptides neuromedin B and C, 2. the tachykinin-like neuropeptides neuromedin K and L, 3. the neurotensin-like neuropeptides neurotensin and neuromedin N, and 4. neuromedin U-like neuropeptides neuromedin U and S.

Among these, the highest level of expression observed in the SFO was for neurotensin receptors. Therefore, to investigate the role of neurotensin receptors at the SFO, in the fourth chapter we examined the electrical effects of neurotensin application to dissociated SFO neurons.

1.6.1. Neurotensin

The neurotensin peptide was first extracted from bovine hypothalamus in 1973, in a study where the authors describe neurotensin to have a powerful hypotensive action in rodents (Carraway and Leeman, 1973). However, further research revealed that the effect of neurotensin on blood pressure can be variable depending on species: in rodents and dogs, both coronary and intracerebroventricular injections of neurotensin decreases blood pressure (Carraway and Leeman, 1973; Ertl et al., 1993), whereas the opposite is seen resulting from intravenous or intracerebroventricular injections guinea pigs (Kérouac et al., 1981). In humans, intravenous injection of neurotensin does not appear to effect blood pressure, though the doses used were lower than all but the lowest dose used in coronary injections in dogs (0.004-0.03 µg/kg/min in humans vs 0.03-3 µg/kg/min) (Blackburn et al., 1980b; Rosell et al., 1980), which may explain the absence of a response to intravenous injection of neurotensin in humans. As intracerebroventricular injections are an invasive technique, it is not typically used for basic research in humans, and is typically reserved for research in to treatment of neurodegenerative disorders (Miller et al., 2012) or gliomas (Merchant et al., 1992). Thus it is not clear how neurotensin in the brain effects blood pressure in humans. However, intravenous injection of neurotensin in humans causes vasoconstriction specifically within adipose tissue (Rosell et al., 1980), an effect also seen in dogs (Rosell et al., 1978), indicating some concordance between humans and animal models. Furthermore, neurotensin's effects on blood pressure are complicated: some studies show bi- and triphasic effects on blood pressure in rats (Oishi et al.,

1981; Rioux et al., 1982). While intracerebroventricular injection of neurotensin (Rioux et al., 1981) and direct injection of neurotensin to the NTS (Kubo and Kihara, 1990; Ciriello and Zhang, 1997) both decrease blood pressure in rats, direct injection of neurotensin to the VTA potentiates the hypertensive effects of vasopressin (Van Den Buuse and Catanzariti, 2000). The varying effects of neurotensin on blood pressure may then be modulated by a combination of central action at multiple nuclei and peripheral action.

Since these early studies, the pathways by which neurotensin modulates blood pressure remain under investigation. Multiple pathways are likely involved: neurotensin inhibits noradrenaline release from perivascular fibres (Tsuda and Masuyama, 1993), and acts on the renin-angiotensin system (Rioux et al., 1982). Notably, neurotensin does not appear to affect isolated rabbit pulmonary arteries or rat aortal rings at doses which decrease blood pressure (Obara et al., 1989; Di Paola and Richelson, 1990), though a more potent neurotensin analogue caused vasodilation of aortal rings (Di Paola and Richelson, 1990), and coronary injections of neurotensin appear to cause vasoconstriction of the coronary artery in guinea pigs (Ertl et al., 1993). Given the expression of neurotensin receptors at the SFO and the established role of the SFO in regulation of cardiovascular output, the SFO may be one site of central neurotensin action to modulate blood pressure. Moreover, neurotensinogenic projections from the ARC to the SFO are thought to be responsible for the cardiovascular and fluid homeostatic effects of ARC stimulation, potentially via local vasodilation of vessels within the SFO (Rosas-Arellano et al., 1996).

In addition to regulation of blood pressure, neurotensin is implicated in numerous homeostatic processes including feeding (Levine et al., 1983; Ratner et al., 2016), digestion (Andersson et al., 1976a, 1977; Blackburn et al., 1980a), thirst (Stanley et al., 1983; Hawkins et

al., 1989), thermoregulation (Nemeroff et al., 1977), in addition to non-homeostatic roles in psychiatric disorders including schizophrenia (O'Connor, 2001; For review see Cáceda et al., 2006). Because the SFO is primarily involved in homeostatic regulation, this thesis will focus on neurotensin's homeostatic roles. While neurotensin production occurs both peripherally (Sundler et al., 1977; Goedert et al., 1984) and centrally (Carraway and Leeman, 1973; Goedert et al., 1984), these populations appear to regulate different systems. In some cases, peripheral injections show no effect when central injections do: intracisternal injection of neurotensin in mice shows an antinociceptive effect not seen from intravenous neurotensin (Clineschmidt and McGuffin, 1977). In other cases, neurotensin may show opposing effects from central and peripheral administration: whereas intracisternal neurotensin injection causes hypothermia (Nemeroff et al., 1977), one research group has reported hyperthermia resulting from peripheral injection (Clineschmidt et al., 1979).

However, central and peripheral actions of neurotensin are not universally separable. Feeding and drinking behaviours appear to be simultaneously regulated by neurotensin at both central and peripheral levels: intravenous injection of neurotensin shows dipsogenic effects (Stanley et al., 1983) and studies show injection of neurotensin in to the cerebral ventricle (Hawkins et al., 1989) or activation of neurotensinogenic neurons promotes drinking (Brown et al., 2019; Kurt et al., 2019), in particular in the LH. Intracerebroventricular (Levine et al., 1983), hypothalamic, (Stanley et al., 1983) and systemic (Ratner et al., 2016) injections of neurotensin generate an anorectic effect. In addition to effects on appetite, neurotensin inhibits both gastric motor function (Andersson et al., 1977; Blackburn et al., 1980a) and release of gastric acid and pepsin (Andersson et al., 1976b), and is critical for fat uptake (Kim et al., 2016). The effects on

gastric function appear to be due to local neurotensin released from the ilium, though central autonomic regulation cannot be ruled out.

Given the distinct and sometimes contradictory roles of peripheral and central neurotensin, the peptide was long-assumed to not penetrate the blood-brain-barrier (Nemeroff et al., 1977). However, a recent study showed that peripheral injection of neurotensin activates nuclei implicated in regulation of energy balance including the AP, NTS, and PVN (Ratner et al., 2016). While a transport kinetics study published in the same year showed that neurotensin is capable of crossing the BBB (Gevaert et al., 2016) at rates similar to those reported for leptin (Banks et al., 1996, 1999) (0.75 μl/g-min vs 0.587-0.894 μl/g-min), blocking BBB transport via pegylation of neurotensin does not remove its anorexic effects. Moreover, peripherally injected pegylated neurotensin still activates secondary messenger pathways in the CNS and was further found to increase POMC expression in the ARC to decrease feeding (Ratner et al., 2016). This study suggests that neurotensin acts at a structure which lies outside the BBB to influence central regulation of energy balance. While the investigators did see activation of another sensory CVO, the AP, the activity of the SFO was not reported.

1.6.2. Neurotensin receptors

To date 4 neurotensin receptors (NTSR) have been proposed: two GPCRs NTSR1 and 2, and two single transmembrane domain receptors NTSR3, also known as sortilin 1 (SORT1), and SorLa/LR11. NTSR1 and NTSR2 are the most similar of the neurotensin receptors, though they only share 64% amino acid sequence homology (Chalon et al., 1996), which likely accounts for differences in their binding affinities. NTSR1 shows higher affinity for neurotensin than NTSR2 (Tanaka et al., 1990; Chalon et al., 1996), but does not bind the neurotensin agonist levocabastine as NTSR2 does (Chalon et al., 1996), allowing for the pharmacological

identification of the neurotensin GPCRs. Though NTSRs are expressed both within (Carraway and Leeman, 1973; Goedert et al., 1984) and outside (Sundler et al., 1977; Goedert et al., 1984) the CNS, NTSRs are most highly expressed in the brain, at a level 6-100x greater than in peripheral tissues as shown by autoradiograph of mRNA expression (Tanaka et al., 1990). Within the CNS, NTSR2 shows a much broader expression profile, such that no area with NTSR1 expression is without NTSR2 expression at some level, though only the substantia nigra and the VTA show strong expression of both receptors (Fassio et al., 2000; Sarret et al., 2003b). Conversely, a number of areas show high levels of NTSR2 expression with no apparent NTSR1 expression, including ependymal cells, the SFO, and the ARC (Walker et al., 1998; Fassio et al., 2000; Sarret et al., 2003b). Furthermore, while both NTSR1 (Elde et al., 1990) and NTSR2 (Sarret et al., 1998; Walker et al., 1998) are expressed in neurons, in rats NTSR2 expression is more pronounced in astrocytes, glia, and ependymal cells (Walker et al., 1998), though in mice NTSR2 expression is primarily found in neurons (Sarret et al., 1998). There are also developmental differences between NTSR1 and NTSR2 expression: NTSR1 is expressed above adult levels at birth (Sato et al., 1992), whereas NTSR2 is not expressed until PD14 and does not reach adult expression levels until PD30 (Sarret et al., 1998); the significance of differences in NTSR1 and NTSR2 expression in development is not clear.

NTSR3, a single-transmembrane domain receptor, shows no significant homology to the GPCRs NTSR1 and 2. *In situ* hybridisation and immunohistochemistry data show NTSR3 expression overlaps with NTSR1 and NTSR2 in the brain, and in some cases is likely co-expressed in the same cells (Sarret et al., 2003a). However, electron microscopy from the same study revealed that NTSR3 has a primarily (though not exclusively) subcellular localisation, and it is possible that NTSR3's ability to bind neurotensin (Mazella et al., 1998) is related to its roles

in ligand sorting and turnover (Petersen et al., 1997) as opposed to detection of extracellular neurotensin. However, NTSR3 may still play a role in signalling: NTSR1 heterodimersation with NTSR3 in the HT29 cell line showed differences in NTSR1 IP_3 and MAPK activity than NTSR1 alone (Martin et al., 2002). Notably, this has not been observed in neurons, nor in association with NTSR2. Furthermore, two studies have observed direct electrical effects of neurotensin on some neurons which was not mediated by NTSR1 or NTSR2 (Bose et al., 2015), though due to a lack of NTSR3-specific agonists or antagonists, the authors could not confirm NTSR3 was responsible as opposed to an unknown neurotensin receptor. A 4^{th} neurotensin receptor most similar to NTSR3 has also been proposed: SorLa/LR11 can bind neurotensin in addition to other ligands including various propeptides and apolipoprotein E (Jacobsen et al., 2001). Similar to NTSR3, SorLa/LR11 shows a primarily subcellular localisation, expressing approximately 10% on the outer membrane, and is proposed to mediate ligand sorting, trafficking, and endocytosis (Jacobsen et al., 2001). Currently, the roles of the NTSR3 and SorLa/LR11 receptors are not well understood, and this thesis will focus primarily on the neurotensin GPCRs.

Neurotensin GPCRs may couple with a multiple intracellular signalling pathways. The most common pathway appears to be the phospholipase C through $G_{\alpha q/11}$ coupling. For example, neurotensin's excitation of periaqueductal grey neurons results in increased intracellular Ca^{2+} and can be blocked via an anti-$G_{q/11}$ antibody or an IP_3 blocker, though not a protein kinase C blocker (Li et al., 2017). However in other neurons, protein kinase C appears to be essential to neurotensin's effects (Thibault et al., 2011). Activation of the phospholipase C pathway by neurotensin receptors has been reported in other CNS cells, including striatal neurons (Weiss et al., 1988), midbrain dopamine neurons (Farkas et al., 2017), and possibly cortex cells (Sato et al., 1991). One group examining rat brain slices found neurotensin increased IP_3 in the

hypothalamus, midbrain, frontal cortex, hippocampus, striatum, pons-medulla, and the cerebellum (Ert et al., 1984). However, in some cases, neurotensin receptors in neurons are coupled to G_{α} or $G_{\alpha i/o}$ subunits and use the cAMP-mediated pathway. Multiple studies have shown that neurotensin's effect in some dopamine neurons involve activation of cAMP and protein kinase A pathways (Malmersjö et al., 2009; Shi and Bunney, 2018). More evidence exists for cAMP/cGMP-dependent pathways activated by neurotensin in cell lines, including immortalised neuroblastoma N1E-115 cells (Amar et al., 1985; Bozou et al., 1989) CHO cells (Yamada et al., 1993), and HEK293 cells (Slusher et al., 1994). Thus is appears the neurotensin receptors couple to different intracellular signalling pathways or may activate different parts of the same pathway depending on the cell subtype, leading to differing responses in different cells.

1.7. Aims of the present thesis

Given the role of the SFO in osmoregulation, cardiovascular output, and energy balance, it is a site of particular interest to the study of perturbations of these processes, including obesity and hypertension. In the three papers contained in this thesis, we performed experiments to address the mechanisms by which the SFO responds to physiological changes, with the hypothesis and aims as outlined below in bold.

In the first series of experiments, we focused on the response of the SFO to a chronic challenge to energy balance. Numerous studies show that early exposure to overfeeding alters the development of the hypothalamic energy balance circuitry (Plagemann et al., 1999a, 1999b; Davidowa and Plagemann, 2007; Glavas et al., 2010; Schipper et al., 2013) and predisposes an individual to obesity and related conditions (Campbell et al., 1996; Siemelink et al., 2002; Habbout et al., 2012; Yim et al., 2013). Because the neurons of the SFO respond to satiety and feeding signals (Pulman et al., 2006; Ono et al., 2008; Alim et al., 2010), and are altered by an

acute challenge to energy balance such as fasting (Hindmarch et al., 2008), they may also respond to a longer-term, less extreme challenge to energy balance. To that end we examined the effect of overnutrition in the postnatal pre-weaning stage (PD0-21) on gene expression in the SFO, with the following hypothesis:

1. **Early postnatal overnutrition alters gene expression in the SFO.**

As changes in gene expression were addressed using RNA sequencing (RNAseq) of both control and treatment groups, these experiments also generated a full transcriptome of the rat SFO in control conditions. Therefore, in the second series of experiments, we combined RNAseq data with previously published microarray data (Hindmarch et al., 2008) with the following aim:

2. **Generate a verified list of GPCRs and ion channels expressed in the SFO.**

The expression of receptors within the SFO represents the signalling molecules which the SFO may respond, and the ion channels shape the electrical activity of these neurons. This list identified potential targets (GPCRs and ligand-gated ion channels) for signalling molecules at the SFO which have not been previously investigated. Examining the expression of GPCRs revealed high expression of receptors for the signalling molecule neurotensin. Given the high expression level of its receptors, and previously established role of neurotensin in modulation of blood pressure (Rioux et al., 1981) and energy balance (Leinninger et al., 2012), the effect of neurotensin on the SFO was of particular interest. Thus the validated list of GPCRs directly led to the hypothesis of the 3rd chapter:

3. Acute exposure to neurotensin modulates the electrical activity (membrane potential and action potential frequency) of SFO neurons via modulation of ion channels.

In the third series of experiments, we found that neurotensin increases the electrical excitability of dissociated SFO neurons by modulation of voltage-gated K+ and nonselective cation currents. Together, these experiments directly address the gaps in our knowledge of the regulation of homeostasis and the mechanisms by which the SFO responds to environmental changes to maintain a stable internal environment.

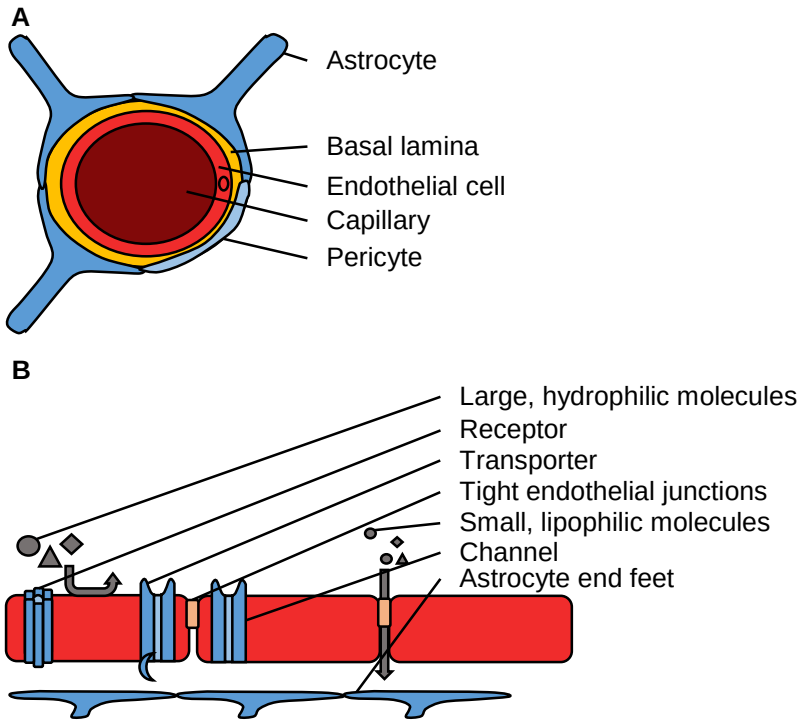

Figure 1.1. The blood-brain barrier is composed of tight endothelial junctions and astrocyte end feet to prevent the passage of large hydrophilic molecules in to the brain (Reese and Karnovsky, 1966). (**A)** Cross-sectional representation of a capillary surrounded by endothelium and astrocyte end feet. (**B)** Diagram representing a longitudinal view of the blood-brain barrier. Small, lipophilic molecules may passively cross the blood-brain barrier while large, hydrophilic molecules cannot. Molecules which can not easily cross the blood-brain barrier may instead cross via transporters or channels, or bind receptors on the endothelium.

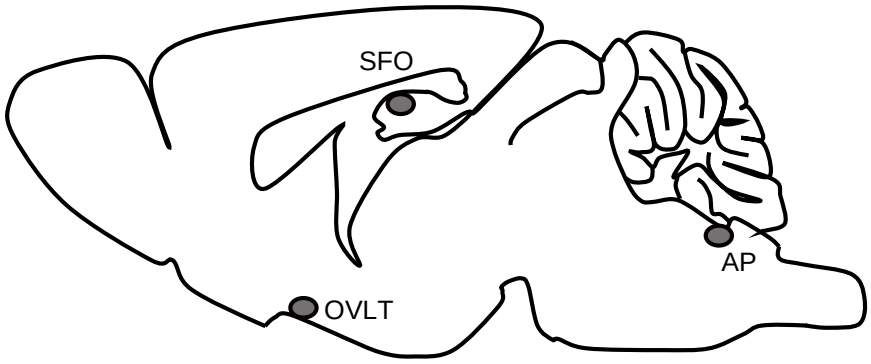

Figure 1.2. Representation of a sagittal section of a rat brain showing the location of the three sensory circumventricular organs: the area postrema (AP) located in the medulla, and vascular organ of the lamina terminalis (OVLT) and subfornical organ (SFO) in the lamina terminalis in the anterior wall of the third ventricle.

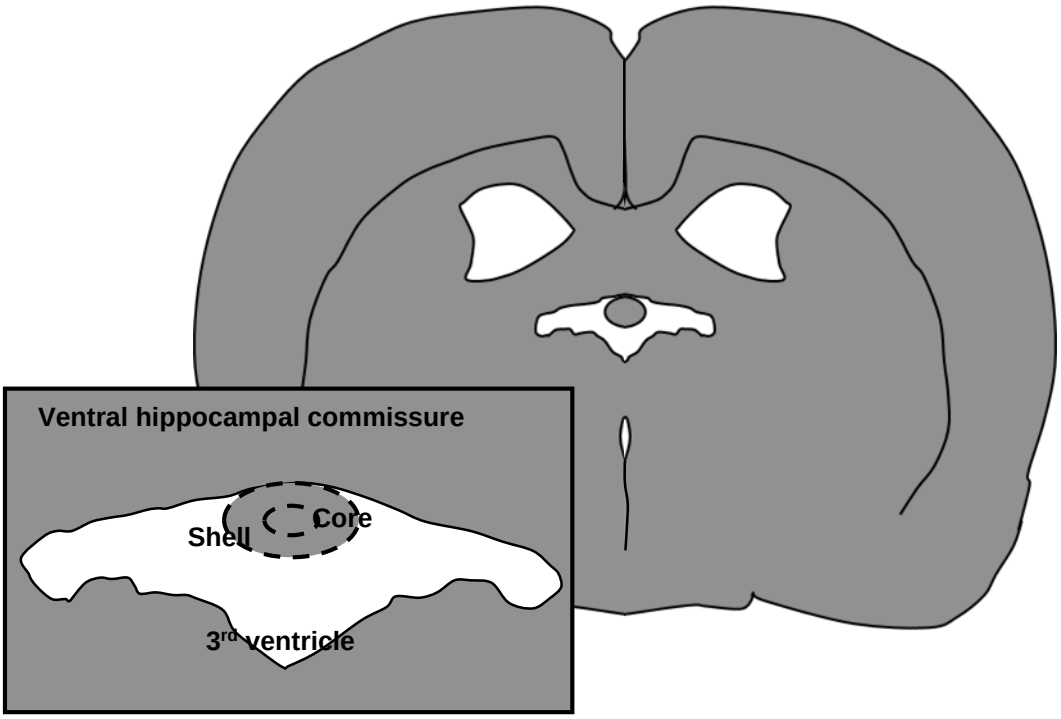

Figure 1.3. Location and subregions (shell and core) of the subfornical organ. Adapted from "Rat brain in stereotaxic coordinates" - Paxinos and Watson, 2005.

1.8. References

Akiyama M et al. (2017) Genome-wide association study identifies 112 new loci for body mass index in the Japanese population. Nat Genet 49:1458–1467 Available at: http://dx.doi.org/10.1038/ng.3951.

Alexander J, Bradley H, Peili C, Richard J Q, Jessy J A (2011) C5a/CD88 signaling alters blood-brain barrier integrity in lupus through nuclear factor-KB. J Neurochem 119:1041–1051.

Alim I, Mark Fry W, Walsh MH, Ferguson A V. (2010) Actions of adiponectin on the excitability of subfornical organ neurons are altered by food deprivation. Brain Res 1330:72–82 Available at: http://dx.doi.org/10.1016/j.brainres.2010.02.076.

Amar S, Mazella J, Checler F, Kitabgi P, Vincent J-P (1985) Regulation of cyclic GMP levels by neurotensin in neuroblastoma clone N1E115. Biochem Biophys Res Commun 129:117–125.

Anand BK, Brobeck JR (1951) Hypothalamic control of food intake in rats and cats. Yale J Biol Med 24:123–140 Available at: http://www.ncbi.nlm.nih.gov/pubmed/14901884%0Ahttp://www.pubmedcentral.nih.gov/articlerender.fcgi?artid=PMC2599116.

Anderson JW, Smith PM, Ferguson A V. (2001) Subfornical organ neurons projecting to paraventricular nucleus: whole-cell properties. Brain Res 921:78–85.

Andersson S, Chang D, Folkers K, Rosell S (1976a) Inhibition of gastric acid secretion in dogs by neurotensin. Life Sci 19:367–370 Available at: http://www.sciencedirect.com/science/article/pii/0024320576900400.

Andersson S, Chang D, Folkers K, Rosell S (1976b) Inhibition of gastric acid secretion in dogs by neurotensin. Life Sci 19:367–370.

Andersson S, Rosell S, Hjelmquist U, Chang D, Folkers K (1977) Inhibition of gastric and intestinal motor activity in dogs by (Gln4) neurotensin. Acta Physiol Scand 100:231–235.

Aponte Y, Atasoy D, Sternson SM (2011) AGRP neurons are sufficient to orchestrate feeding behavior rapidly and without training. Nat Neurosci 14:351.

Atasoy D, Betley JN, Su HH, Sternson SM (2012) Deconstruction of a neural circuit for hunger. Nature 488:172–177.

Bains JS, Ferguson A V (1995) Paraventricular nucleus neurons projecting to the spinal cord receive excitatory input from the subfornical organ. Am J Physiol Integr Comp Physiol 268:R625–R633.

Banks WA, DiPalma CR, Farrell CL (1999) Impaired transport of leptin across the blood-brain barrier in obesity. Peptides 20:1341–1345.

Banks WA, Kastin AJ, Huang W, Jaspan J, Maness LM (1996) Leptin enters the brain by a saturable system independent of insulin. Peptides 17:305–311.

Baver SB, Hope K, Guyot S, Bjørbaek C, Kaczorowski C, O'Connell KMS (2014) Leptin modulates the intrinsic excitability of AgRP/NPY neurons in the arcuate nucleus of the hypothalamus. J Neurosci 34:5486 LP – 5496 Available at: http://www.jneurosci.org/content/34/16/5486.abstract.

Berchtold P, Berger M, Greiser E, Dohse M, Irmscher K, Gries FA, Zimmermann H (1977) Cardiovascular risk factors in gross obesity. Int J Obes 1:219–229.

Biebermann H, Grüters A, Horn R, Luck W, Brabant G, Krude H (1998) Severe early-onset obesity, adrenal insufficiency and red hair pigmentation caused by POMC mutations in humans. Nat Genet 19:155–157.

Black EAE, Smith PM, Mcisaac W, Ferguson A V (2018) Brain-derived neurotrophic factor acts at neurons of the subfornical organ to influence cardiovascular function. Physiol Rep 6:1–10 Available at: https://doi.org/10.14814/phy2.13704.

Blackburn AM, Bloom SR, Long RG, Fletcher DR, Christofides ND, Fitzpatrick ML, Baron JH (1980a) Effect of Neurotensin on Gastric Function in Man. Lancet 315:987–989.

Blackburn AM, Fletcher DR, Adrian TE, Bloom SR (1980b) Neurotensin infusion in man: pharmacokinetics and effect on gastrointestinal and pituitary hormones. J Clin Endocrinol Metab 51:1257–1261.

Bose P, Rompré P-P, Warren RA (2015) Neurotensin enhances glutamatergic EPSCs in VTA neurons by acting on different neurotensin receptors. Peptides 73:43–50.

Boyle PC, Keesey RE (1975) Chonically reduced body weight in rats sustaining lesions of the lateral hypothalamus and maintained on palatable diets and drinking solutions. J Comp Physiol Psychol 88:218–223.

Bozou J-C, de Nadai F, Vincent J-P, Kitabgi P (1989) Neurotensin, bradykinin and somatostatin inhibit cAMP production in neuroblastoma N1E115 cells via both pertussis toxin sensitive and insensitive mechanisms. Biochem Biophys Res Commun 161:1144–1150.

Brief DJ, Davis JD (1984) Reduction of food intake and body weight by chronic intraventricular insulin infusion. Brain Res Bull 12:571–575.

Brimble MJ, Dyball REJ, Forsling ML (1978) Oxytocin release following osmotic activation of oxytocin neurones in the paraventricular and supraoptic nuclei. J Physiol 278:69–78.

Broberger C, Johansen J, Johansson C, Schalling M, Hökfelt T (1998) The neuropeptide Y/agouti gene-related protein (AGRP) brain circuitry in normal, anorectic, and monosodium glutamate-treated mice. Proc Natl Acad Sci 95:15043–15048.

Brown JA, Wright A, Bugescu R, Christensen L, Olson DP, Leinninger GM (2019) Distinct subsets of lateral hypothalamic Neurotensin neurons are activated by leptin or dehydration. Sci Rep 9:1873.

Burton MJ, Rolls ET, Mora F (1976) Effects of hunger on the responses of neurons in the lateral hypothalamus to the sight and taste of food. Exp Neurol 51:668–677.

Cáceda R, Kinkead B, Nemeroff CB (2006) Neurotensin: Role in psychiatric and neurological diseases. Peptides 27:2385–2404 Available at: http://www.sciencedirect.com/science/article/pii/S0196978106002853.

Cador M, Kelley AE, Le Moal M, Stinus L (1986) Ventral tegmental area infusion of substance P, neurotensin and enkephalin: differential effects on feeding behavior. Neuroscience 18:659–669.

Calle EE, Rodriguez C, Walker-Thurmond K, Thun MJ (2003) Overweight, obesity, and mortality from cancer in a prospectively studied cohort of U.S. adults. N Engl J Med 348:1625–1638 Available at: https://doi.org/10.1056/NEJMoa021423.

Campbell DM, Hall MH, Barker DJP, Cross J, Shiell AW, Godfrey KM (1996) Diet in pregnancy and the offspring's blood pressure 40 years later. BJOG An Int J Obstet

Gynaecol 103:273–280.

Carraway R, Leeman SE (1973) The isolation of a new hypotensive peptide, neurotensin, from bovine hypothalami. J Biol Chem 248:6854–6861.

Cerqueira DR, Ferreira HS, Moiteiro ALBB, Fregoneze JB (2016) Effects of interleukin-1 beta injections into the subfornical organ and median preoptic nucleus on sodium appetite, blood pressure and body temperature of sodium-depleted rats. Physiol Behav 163:149–160 Available at: http://dx.doi.org/10.1016/j.physbeh.2016.05.003.

Chalon P, Vita N, Kaghad M, Guillemot M, Bonnin J, Delpech B, Le Fur G, Ferrara P, Caput D (1996) Molecular cloning of a levocabastine-sensitive neurotensin binding site. FEBS Lett 386:91–94.

Ciriello J, Zhang TX (1997) Cardiovascular effects of neurotensin microinjections into the nucleus of the solitary tract. Brain Res 749:35–43.

Clineschmidt B V., McGuffin JC (1977) Neurotensin administered intracisternally inhibits responsiveness of mice to noxious stimuli. Eur J Pharmacol 46:395–396.

Clineschmidt B V., McGuffin JC, Bunting PB (1979) Neurotensin: Antinocisponsive action in rodents. Eur J Pharmacol 54:129–139.

Considine R V, Sinha MK, Heiman ML, Kriauciunas A, Stephens TW, Nyce MR, Ohannesian JP, Marco CC, McKee LJ, Bauer TL, Caro JF (1996) Serum immunoreactive-leptin concentrations in normal-weight and obese humans. Endocrinologist 334:292–295 Available at: https://insights.ovid.com/crossref?an=00019616-199607000-00020.

Contreras RJ, Fox E, Drugovich ML (1982) Area postrema lesions produce feeding deficits in

the rat: Effects of preoperative dieting and 2-deoxy-D-glucose. Physiol Behav 29:875–884 Available at: http://www.sciencedirect.com/science/article/pii/0031938482903389 [Accessed October 9, 2015].

Cottrell GT, Ferguson A V. (2004) Sensory circumventricular organs: Central roles in integrated autonomic regulation. Regul Pept 117:11–23.

Cowley MA et al. (2003) The distribution and mechanism of action of ghrelin in the CNS demonstrates a novel hypothalamic circuit regulating energy homeostasis. Neuron 37:649–661 Available at: https://doi.org/10.1016/S0896-6273(03)00063-1.

Dai L, Smith PM, Kuksis M, Ferguson A V. (2013) Apelin acts in the subfornical organ to influence neuronal excitability and cardiovascular function. J Physiol 591:3421–3432.

Davidowa H, Li Y, Plagemann A (2003) Altered responses to orexigenic (AGRP, MCH) and anorexigenic (α-MSH, CART) neuropeptides of paraventricular hypothalamic neurons in early postnatally overfed rats. Eur J Neurosci 18:613–621.

Davidowa H, Plagemann A (2004) Hypothalamic neurons of postnatally overfed, overweight rats respond differentially to corticotropin-releasing hormones. Neurosci Lett 371:64–68.

Davidowa H, Plagemann A (2007) Insulin resistance of hypothalamic arcuate neurons in neonatally overfed rats. Neuroreport 18:521–524.

Davidowa H, Ziska T, Plagemann A (2004) Arcuate neurons of overweight rats differ in their responses to amylin from controls. Neuroreport 15:2801–2805.

Di Paola ED, Richelson E (1990) Cardiovascular effects of neurotension and some analogues on rats. Eur J Pharmacol 175:279–283.

Donevan SD, Van Vugt DA, Ferguson A V. (1989) Subfornical organ activation stimulates luteinizing hormone secretion in the rat. Brain Res 488:398–402.

Duffy KR, Pardridge WM (1987) Blood-brain barrier transcytosis of insulin in developing rabbits. Brain Res 420:32–38.

Elde R, Schalling M, Ceccatelli S, Nakanishi S, Hökfelt T (1990) Localization of neuropeptide receptor mRNA in rat brain: Initial observations using probes for neurotensin and substance P receptors. Neurosci Lett 120:134–138 Available at: http://www.sciencedirect.com/science/article/pii/030439409090187E.

Epstein LH, Paluch RA, Gordy CC, Dorn J (2000) Decreasing sedentary behaviors in treating pediatric obesity. Arch Pediatr Adolesc Med 154:220–226.

Ert MG, Pinnock RD, Mantyh PW (1984) Neurotensin stimulates inositol phospholipid hydrolysis in rat brain slices. Brain Res 323:193–197.

Ertl G, Bauer B, Becker H-H, Rose G (1993) Effects of neurotensin and neuropeptide Y on coronary circulation and myocardial function in dogs. Am J Physiol Circ Physiol 264:H1062–H1068.

Farkas RH, Chien PY, Nakajima S, Nakajima Y (2017) Properties of a slow nonselective cation conductance modulated by neurotensin and other neurotransmitters in midbrain dopaminergic neurons. J Neurophysiol 76:1968–1981.

Fassio A, Evans G, Grisshammer R, Bolam JP, Mimmack M, Emson PC (2000) Distribution of the neurotensin receptor NTS1 in the rat CNS studied using an amino-terminal directed antibody. Neuropharmacology 39:1430–1442.

Felix D (1976) Peptide and acetylcholine action on neurones of the cat subfornical organ. Naunyn Schmiedebergs Arch Pharmacol 292:15–20.

Ferguson A V. (1988) Systemic angiotensin acts at the subfornical organ to control the activity of paraventricular nucleus neurons with identified projections to the median eminence. Neuroendocrinology 47:489–497.

Ferguson A V., Kasting NW (1986) Electrical stimulation in subfornical organ increases plasma vasopressin concentrations in the conscious rat. Am J Physiol Integr Comp Physiol 251:R425–R428.

Ferguson A V, Day TA, Renaud LP (1984a) Subfornical organ efferents influence the excitability of neurohypophyseal and tuberoinfundibular paraventricular nucleus neurons in the rat. Neuroendocrinology 39:423–428.

Ferguson A V, Day TA, Renaud LP (1984b) Subfornical organ stimulation excites paraventricular neurons projecting to dorsal medulla. Am J Physiol Integr Comp Physiol 247:R1088–R1092.

Fischer H, Gottschlich R, Seelig A (1998) Blood-brain barrier permeation: Molecular parameters governing passive diffusion. J Membr Biol 165:201–211.

Frederich RC, Hamann A, Anderson S, Löllman B, Lowell BB, Flier JS (1995) Leptin levels reflect body lipid content in mice: Evidence for diet-induced resistance to leptin action. Nat Med 1:1311–1314.

Friedman SM, Pauls H (1952) The effect of pitressin infusion on blood pessure of the rabbit, cat, and rat. Am Heart J 44:131–142.

Froguel P, Clement K, Vaisse C, Lahlou N, Cabrol S, Pelloux V, Cassuto D, Gourmelen M, Dina C, Chambaz J, Lacorte J-M, Basdevant A, Bougnères P, Lebouc Y, Guy-Grand B (1998) A mutation in the human leptin receptor gene causes obesity and pituitary dysfunction. Nature 392:398–401 Available at: http://www.nature.com/doifinder/10.1038/32911%5Cnpapers2://publication/doi/10.1038/32911.

Ganote CE, Grantham JJ, Moses HL, Burg MB, Orloff J (1968) Ultrastructural studies of vasopressin effect on isolated perfused renal collecting tubules of the rabbit. J Cell Biol 36:355–367 Available at: http://jcb.rupress.org/content/36/2/355.abstract.

Gevaert B, Wynendaele E, Stalmans S, Bracke N, D'Hondt M, Smolders I, Van Eeckhaut A, De Spiegeleer B (2016) Blood-brain barrier transport kinetics of the neuromedin peptides NMU, NMN, NMB and NT. Neuropharmacology 107:460–470.

Giles ME, Fernley RT, Nakamura Y, Moeller I, Aldred GP, Ferraro T, Penschow JD, McKinley MJ, Oldfield BJ (1999) Characterization of a specific antibody to the rat angiotensin II AT1 receptor. J Histochem Cytochem 47:507–515 Available at: https://doi.org/10.1177/002215549904700409.

Glavas MM, Kirigiti MA, Xiao XQ, Enriori PJ, Fisher SK, Evans AE, Grayson BE, Cowley MA, Smith MS, Grove KL (2010) Early overnutrition results in early-onset arcuate leptin resistance and increased sensitivity to high-fat diet. Endocrinology 151:1598–1610.

Goedert M, Lightman SL, Emson PC (1984) Neurotensin in the rat anterior pituitary gland: effects of endocrinological manipulations. Brain Res 299:160–163.

Gross PM (1991) Morphology and physiology of capillary systems in subregions of the

subfornical organ and area postrema. Can J Physiol Pharmacol 69:1010–1025 Available at: http://www.ncbi.nlm.nih.gov/pubmed/1954559.

Gross PM (1992) Circumventricular organ capillaries. Prog Brain Res 91:219–233.

Grossman SP, Dacey D, Halaris AE, Collier T, Routtenberg A (1978) Aphagia and adipsia after preferential destruction of nerve cell bodies in hypothalamus. Science (80-) 202:537 LP – 539 Available at: http://science.sciencemag.org/content/202/4367/537.abstract.

Gruber K, McRae-Degueurce A, Wilkin LD, Mitchell LD, Johnson AK (1987) Forebrain and brainstem afferents to the arcuate nucleus in the rat : potential pathways for the modulation of hypophyseal secretions. Neurosci Lett 75:1–5 Available at: http://www.ncbi.nlm.nih.gov/pubmed/3574762 [Accessed November 13, 2015].

Habbout A, Delemasure S, Goirand F, Guilland J, Chabod F, Sediki M, Rochette L, Vergely C (2012) Postnatal overfeeding in rats leads to moderate overweight and to cardiometabolic and oxidative alterations in adulthood. Biochimie 94:117–124 Available at: http://dx.doi.org/10.1016/j.biochi.2011.09.023.

Hawkins MF, Baker JD, Baumeister AA (1989) Neurotensin-induced polydipsia: a structure-activity study. Brain Res 487:188–191.

Herriot AM, Thomas DE, Hart KH, Warren J, Truby H (2008) A qualitative investigation of individuals'experiences and expectations before and after completing a trial of commercial weight loss programmes. J Hum Nutr Diet 21:72–80.

Hindmarch C, Fry M, Yao ST, Smith PM, Murphy D, Ferguson A V (2008) Microarray analysis of the transcriptome of the subfornical organ in the rat: regulation by fluid and food

deprivation. Am J Physiol Regul Integr Comp Physiol 295:R1914-20.

Hollis JH, McKinley MJ, D'Souza M, Kampe J, Oldfield BJ (2008) The trajectory of sensory pathways from the lamina terminalis to the insular and cingulate cortex: a neuroanatomical framework for the generation of thirst. Am J Physiol Integr Comp Physiol 294:R1390–R1401.

Huang S, Egan J, Fry WM (2019) Electrophysiological Properties of Rat Subfornical Organ Neurons Expressing Calbindin D28K. Neuroscience 404:459–469 Available at: https://www.sciencedirect.com/science/article/pii/S0306452219301198?dgcid=rss_sd_all.

Jacobsen L, Madsen P, Jacobsen C, Nielsen MS, Gliemann J, Petersen CM (2001) Activation and functional characterization of the mosaic receptor SorLA/LR11 *. J Biol Chem 276:22788–22796.

Kangawa K, Minamino N, Fukuda A, Matsuo H (1983) Neuromedin K: A novel mammalian tachykinin identified in porcine spinal cord. Biochem Biophys Res Commun 114:533–540 Available at: http://www.sciencedirect.com/science/article/pii/0006291X83908136.

Kawano H, Masuko S (2010) Region-specific projections from the subfornical organ to the paraventricular hypothalamic nucleus in the rat. Neuroscience 169:1227–1234 Available at: http://dx.doi.org/10.1016/j.neuroscience.2010.05.065.

Kérouac R, Rioux F, St-Pierre S (1981) Mechanism of neurotensin-induced pressor effect and tachycardia in guinea pigs. Life Sci 28:2477–2487.

Kim E et al. (2016) An obligatory role for neurotensin in high fat diet-induced obesity. Nature 533:411–415.

Kobayashi H, Ogawa Y, Shintani M, Ebihara K, Shimodahira M, Iwakura T, Hino M, Ishihara T, Ikekubo K, Kurahachi H, Nakao K (2002) A novel homozygous missense mutation of melanocortin-4 receptor (MC4R) in a Japanese woman with severe obesity. Diabetes 51:243 LP – 246 Available at: http://diabetes.diabetesjournals.org/content/51/1/243.abstract.

Koistinen, Karonen, Iivanainen, Koivisto (1998) Circulating leptin has saturable transport into intrathecal space in humans. Eur J Clin Invest 28:894–897 Available at: https://doi.org/10.1046/j.1365-2362.1998.00386.x.

Kojima M, Hosoda H, Date Y, Nakazato M, Matsuo H, Kangawa K (1999) Ghrelin is a growth-hormone-releasing acylated peptide from stomach. Nature 402:656–660 Available at: https://doi.org/10.1038/45230.

Kubo T, Kihara M (1990) Modulation of the aortic baroreceptor reflex by neuropeptide Y, neurotensin and vasopressin microinjected into the nucleus tractus solitarii of the rat. Naunyn Schmiedebergs Arch Pharmacol 342:182–188.

Kuksis M, Smith PM, Ferguson A V. (2014) Hydrogen sulfide regulates cardiovascular function by influencing the excitability of subfornical organ neurons. PLoS One 9:1–11.

Kurt G, Woodworth HL, Fowler S, Bugescu R, Leinninger GM (2019) Activation of lateral hypothalamic area neurotensin-expressing neurons promotes drinking. Neuropharmacology 154:13–21.

Lakhi S, Snow W, Fry M (2013) Insulin modulates the electrical activity of subfornical organ neurons. Neuroreport 24:329–334.

Larsen PJ, Møller M, Mikkelsen JD (1991) Efferent projections from the periventricular and

medial parvicellular subnuclei of the hypothalamic paraventricular nucleus to circumventricular organs of the rat: A Phaseolus vulgaris-leucoagglutinin (PHA-L) tracing study. J Comp Neurol 306:462–479.

Leeman SE (1973) The isolation of a new hypotensive from bovine hypothalamus. J Biol Chem 248:6854–6861.

Leinninger GM, Opland DM, Jo Y, Faouzi M, Cappellucci LA, Rhodes CJ, Gnegy ME, Jill B, Pothos EN, Seasholtz AF, Thompson RC (2012) Leptin action via neurotensin neurons controls orexin, the mesolimbic dopamine system and energy balance. Cell Metab 14:313–323.

Lenkei Z, Corvol P, Llorens-Cortes C (1995) The angiotensin receptor subtype AT1A predominates in rat forebrain areas involved in blood pressure, body fluid homeostasis and neuroendocrine control. Mol Brain Res 30:53–60.

Levine AS, Kneip J, Grace M, Morley JE (1983) Effect of centrally administered neurotensin on multiple feeding paradigms. Pharmacol Biochem Behav 18:19–23.

Li AH, Hwang H-M, Tan PP, Wu T, Wang H-L (2017) Neurotensin excites periaqueductal gray neurons projecting to the rostral ventromedial medulla. J Neurophysiol 85:1479–1488.

Limonta P, Maggi R, Giudici D, Martini L, Flavio P (1981) Role of the subfornical organ (SFO) in the control of gonadotropin secretion. Brain Res 229:75–84.

Lind RW, Hoesen GW van, Johnson AK (1982) An HRP study of the connections of the subfornical organ of the rat. J Comp Neurol 210:265–277.

Lind RW, Swanson LW, Ganten D (1984) Angiotensin II immunoreactivity in the neural

afferents and efferents of the subfornical organ of the rat. Brain Res 321:209–215.

Liposits Z, Paull WK, Wu P, Jackson IMD, Lechan RM (1987) Hypophysiotrophic thyrotropin releasing hormone (TRH) synthesizing neurons - Ultrastructure, adrenergic innervation and putative transmitter action. Histochemistry 88:1–10.

Lobo Antunes J, Zimmerman EA (1978) The hypothalamic magnocellular system of the rhesus monkey: An immunocytochemical study. J Comp Neurol 181:539–565.

Locke AE et al. (2015) Genetic studies of body mass index yield new insights for obesity biology. Nature 518:197 Available at: https://doi.org/10.1038/nature14177.

Lundgren H, Bengtsson C, Blohme G, Lapidus L, Sjostrom L (1989) Adiposity and adipose tissue distribution in relation to incidence of diabetes in women: results from a prospective population study in Gothenburg, Sweden. Int J Obes 13:413–423.

Malmersjö S, Liste I, Dyachok O, Tengholm A, Arenas E, Uhlén P (2009) Ca2+ and cAMP signaling in human embryonic stem cell–derived dopamine neurons. Stem Cells Dev 19:1355–1364.

Mangiapane ML, Simpson JB (1979) Pharmacologic independence of subfornical organ receptors mediating drinking. Brain Res 178:507–517 Available at: http://linkinghub.elsevier.com/retrieve/pii/0006899379907108.

Mangiapane ML, Simpson JB (1980) Subfornical organ: forebrain site of pressor and dipsogenic action of angiotensin II. Am J Physiol 239:R382-9 Available at: http://www.ncbi.nlm.nih.gov/pubmed/7435651 [Accessed November 13, 2015].

Mangiapane ML, Simpson JB (1983) Drinking and pressor responses after acetylcholine

injection into subfornical organ. AJP Regul Integr Comp Physiol 244:R508-13.

Martin S, Navarro V, Vincent JP, Mazella J (2002) Neurotensin receptor-1 and -3 complex modulates the cellular signaling of neurotensin in the HT29 cell line. Gastroenterology 123:1135–1143.

Massi M, Caro G De, Mazzarella L, Epstein AN (1986) The role of the subfornical organ in the drinking behavior of the pigeon. Brain Res 381:289–299.

Mazella J, Zsürger N, Navarro V, Chabry J, Kaghad M, Caput D, Ferrara P, Vita N, Gully D, Maffrand J-P (1998) The 100-kDa neurotensin receptor is gp95/sortilin, a non-G-protein-coupled receptor. J Biol Chem 273:26273–26276.

McKinley MJ, McAllen RM, Giles ME, Penschow J, Sunn N, Uschakov A, Oldfield BJ (2003) The sensory circumventricular organs of the mammalian brain. Adv Anat Cell Biol 172:III–XII, 1–122, back cover.

McNay DEG, Briançon N, Kokoeva M V, Maratos-Flier E, Flier JS (2012) Remodeling of the arcuate nucleus energy-balance circuit is inhibited in obese mice. J Clin Invest 122:142–152 Available at: https://doi.org/10.1172/JCI43134.

Merchant RE, McVicar DW, Merchant LH, Young HF (1992) Treatment of recurrent malignant glioma by repeated intracerebral injections of human recombinant interleukin-2 alone or in combination with systemic interferon-α. Results of a phase I clinical trial. J Neurooncol 12:75–83 Available at: https://doi.org/10.1007/BF00172459.

Miller T, Smith R, Pestronk A, David W, Rothstein J, Simpson E, Andres P, Mahoney K, Allred P, Alexander K (2012) Results of a Phase 1, Double-Blind, Placebo-Controlled, Dose-

Escalation Study of the Safety, Tolerability, and Pharmacokinetics of ISIS 333611 Administered Intrathecally to Patients with Familial ALS Due to SOD1 Gene Mutations. Neurology 78:S25.001.

Mimee A, Smith PM, Ferguson A V (2013) Circumventricular organs: targets for integration of circulating fluid and energy balance signals? Physiol Behav 121:96–102.

Minamino N, Kangawa K, Matsuo H (1983) Neuromedin B: A novel bombesin-like peptide identified in porcine spinal cord. Biochem Biophys Res Commun 114:541–548 Available at: http://www.sciencedirect.com/science/article/pii/0006291X83908148.

Minamino N, Kangawa K, Matsuo H (1985) Neuromedin U-8 and U-25: novel uterus stimulating and hypertensive peptides identified in porcine spinal cord. Biochem Biophys Res Commun 130:1078–1085.

Miselis RR (1982) The subfornical organ's neural connections and their role in water balance. Peptides 3:501–502 Available at: http://www.sciencedirect.com.uml.idm.oclc.org/science/article/pii/0196978182901152 [Accessed December 14, 2017].

Mumford AD, Parry LJ, Summerlee AJS (1989) Lesion of the subfornical organ affects the haemotensive response to centrally administered relaxin in anaesthetized rats. J Endocrinol 122:747–755.

Nakazato M, Murakami N, Date Y, Kojima M, Matsuo H, Kangawa K, Matsukura S (2001) A role for ghrelin in the central regulation of feeding. Nature 409:194–198 Available at: https://doi.org/10.1038/35051587.

Nemeroff CB, Bissette G, Prange AJ, Peter T, Barlow TS, Lipton MA (1977) Neurotensin: Central nervous system effects of a hypothalamic peptide. Brain Res 128:485–496.

Nielsen SJ, Popkin BM (2019) Patterns and trends in food portion sizes, 1977-1998. J Am Med Assoc 289:4–7.

O'Connor WT (2001) Functional neuroanatomy of the ventral striopallidal GABA pathway: New sites of intervention in the treatment of schizophrenia. J Neurosci Methods 109:31–39 Available at: http://www.sciencedirect.com/science/article/pii/S0165027001003983.

Obara H, Kusunoki M, Mori M, Mikawa K, Iwai S (1989) The effects of various peptides on the isolated pulmonary artery. Peptides 10:241–243.

Ohlson L-O, Larsson B, Svärdsudd K, Welin L, Eriksson H, Wilhelmsen L, Björntorp P, Tibblin G (1985) The influence of body fat distribution on the incidence of diabetes mellitus: 13.5 years of follow-up of the participants in the study of men born in 1913. Diabetes 34:1055 LP – 1058 Available at: http://diabetes.diabetesjournals.org/content/34/10/1055.abstract.

Oishi M, Inagaki C, Fujiwara M, Takaori S, Yajima H, Akazawa Y (1981) Possible mechanisms of the triphasic effects of neurotensin on the rat blood pressure. Jpn J Pharmacol 31:1043–1049.

Oka Y, Ye M, Zuker CS (2015) Thirst driving and suppressing signals encoded by distinct neural populations in the brain. Nature 520:349–352.

Ono K, Kai A, Honda E, Inenaga K (2008) Hypocretin-1/orexin-A activates subfornical organ neurons of rats. Neuroreport 19:69–73.

Paull WK, Gibbs FP (1983) The corticotropin releasing factor (CRF) neurosecretory system in

intact, adrenalectomized, and adrenalectomized-dexamethasone treated rats. An immunocytochemical analysis. Histochemistry 78:303–316.

Pelleymounter MA, Cullen MJ, Baker MB, Hecht R, Winters D, Boone T, Collins F (1995) Effects of the obese gene product on body weight regulation in ob/ob mice. Science (80-) 269:540 LP – 543 Available at: http://science.sciencemag.org/content/269/5223/540.abstract.

Petersen CM, Nielsen MS, Jacobsen L, Tommerup N, Rasmussen HH, Røigaard H, Madsen P, Søren K, Chem JB, Nykjær A, Gliemann J, Moestrup SK (1997) Molecular identification of a novel candidate sorting receptor purified from human brain by receptor-associated protein affinity chromatography. J Biol Chem 272:3599–3605.

Phillips M, Camacho A (1981) Horseradish peroxidase study in the rat of the neural connections of the organum vasculosum of the lamina terminalis. Neurosci Lett 25:201–204.

Piekut DT, Joseph SA (1986) Co-existence of CRF and vasopressin immunoreactivity in parvocellular paraventricular neurons of rat hypothalamus. Peptides 7:891–898.

Plagemann A, Harder T, Rake A, Melchior K, Rohde W (1999a) Increased number of galanin-neurons in the paraventricular hypothalamic nucleus of neonatally overfed weanling rats. Brain Res 818:160–163.

Plagemann A, Harder T, Rake A, Waas T, Melchior K, Ziska T, Rohde W, Do G (1999b) Observations on the orexigenic hypothalamic neuropeptide Y-system in neonatally overfed weanling rats. J Neuroendocrinol 11:541–546.

Pócsai K, Kálmán M (2015) Glial and perivascular structures in the subfornical organ:

distinguishing the shell and core. J Histochem Cytochem 63:367–383 Available at: https://www.ncbi.nlm.nih.gov/pubmed/25673286.

Polson DA, Thompson MP (2003) Adiponutrin mRNA expression in white adipose tissue is rapidly induced by meal-feeding a high-sucrose diet. Biochem Biophys Res Commun 301:261–266 Available at: http://www.sciencedirect.com/science/article/pii/S0006291X02030279.

Potts PD, Hirooka Y, Dampney RAL (1999) Activation of brain neurons by circulating angiotensin II. Direct effects and baroreceptor-mediated secondary effects. Neuroscience 90:581–594 Available at: http://www.sciencedirect.com/science/article/pii/S0306452298005727.

Public Health Agency of Canada, Canadian Institute for Health (2011) Obesity in Canada.

Pulman KJ, Fry WM, Cottrell GT, Ferguson A V (2006) The subfornical organ: a central target for circulating feeding signals. J Neurosci 26:2022–2030.

Qiu J, Fang Y, Rønnekleiv OK, Kelly MJ (2010) Leptin excites proopiomelanocortin neurons via activation of TRPC channels. J Neurosci 30:1560–1565.

Ratner C, Skov LJ, Raida Z, Bächler T, Bellmann-Sickert K, Foll C Le, Sivertsen B, Dalbøge LS, Hartmann B, Beck-Sickinger AG, Madsen AN, Jelsing J, Holst JJ, Lutz TA, Andrews ZB, Holst B (2016) Effects of peripheral neurotensin on appetite regulation and its role in gastric bypass surgery. Endocrinology 157:3482–3492.

Reese TS, Karnovsky MJ (1966) Fine Structural Localization of a Blood-Brain Barrier To Exogenous Peroxidase. J Cell Biol 34:207–217.

Reijerkerk A, Lopez-ramirez MA, Hof B van het, Drexhage JAR, Kamphuis WW, Kooij G, Vos JB, Kraan TCTM van der P, Zonneveld AJ Van, Horrevoets AJ, Prat A, Romero IA, Vries HE De (2013) MicroRNAs Regulate Human Brain Endothelial Cell-Barrier Function in Inflammation : Implications for Multiple Sclerosis. J Neurosci 33:6857–6863.

Rentsch J, Levens N, Chiesi M (1995) Recombinant OB-Gene Product Reduces Food-Intake in Fasted Mice. Biochem Biophys Res Commun 214:131–136 Available at: http://www.sciencedirect.com/science/article/pii/S0006291X85722668.

Rioux F, Kérouac R, St-Pierre S (1982) Analysis of the biphasic depressor-pressor effect and tachycardia caused by neurotensin in ganglion-blocked rats. Neuropeptides 3:113–127 Available at: http://www.sciencedirect.com/science/article/pii/0143417982900075.

Rioux F, Quirion R, St-Pierre S, Regoli D, Jolicoeur FB, Bélanger F, Barbeau A (1981) The hypotensive effect of centrally administered neurotensin in rats. Eur J Pharmacol 69:241–247 Available at: http://www.ncbi.nlm.nih.gov/pubmed/7215426.

Rogers RC, Hermann GE (1987) Oxytocin, oxytocin antagonist, TRH, and hypothalamic paraventricular nucleus stimulation effects on gastric motility. Peptides 8:505–513.

Rosas-Arellano MP, Solano-Flores LP, Ciriello J (1996) Neurotensin projections to subfornical organ from arcuate nucleus. Brain Res 706:323–327.

Roseberry AG, Liu H, Jackson AC, Cai X, Friedman JM (2004) Neuropeptide Y-mediated inhibition of proopiomelanocortin neurons in the arcuate nucleus shows enhanced desensitization in ob/ob mice. Neuron 41:711–722.

Rosell S, Rökaeus Åk, Chang D, Folkers K (1978) Indirect vascular actions of (Gln4)-

neurotensin in canine adipose tissue. Acta Physiol Scand 102:143–147.

Rosell S, Thor K, Rökaeus Å, Nyquist O, Lewenhaupt A, Kager L, Folkers K (1980) Plasma concentration of neurotensin-like immunoreactivity (NTLI) and lower esophageal sphincter (LES) pressure in man following infusion of (GIn 4)-neurotensin. Acta Physiol Scand 109:369–375.

Roth J, Pehl U, Kueth M, Harre E, Gerstberger RUD, Hu T (2002) Role of IL-6 in LPs-induced nuclear STAT3 translocation in sensory circumventricular organs during fever in rats. J Appl Physiol 92:2657–2666.

Saper CB, Loewy AD, Swanson LW, Cowan WM (1976) Direct hypothalamo-autonomic connections. Brain Res 117:305–312.

Sarret P, Beaudet A, Vincent J-P, Mazella J (1998) Regional and cellular distribution of low affinity neurotensin receptor mRNA in adult and developing mouse brain. J Comp Neurol 394:344–356 Available at: https://doi.org/10.1002/(SICI)1096-9861(19980511)394:3%3C344::AID-CNE6%3E3.0.CO.

Sarret P, Krzywkowski P, Segal L, Nielsen MS, Petersen CM, Mazella J, Stroh T, Beaudet A (2003a) Distribution of NTS3 receptor/sortilin mRNA and protein in the rat central nervous system. J Comp Neurol 461:483–505 Available at: http://doi.wiley.com/10.1002/cne.10708.

Sarret P, Perron A, Stroh T, Beaudet A (2003b) Immunohistochemical distribution of NTS2 neurotensin receptors in the rat central nervous system. J Comp Neurol 461:520–538.

Sato M, Kiyama H, Tohyama M (1992) Different postnatal development of cells expressing mRNA encoding neurotensin receptor. Neuroscience 48:137–149.

Sato M, Shiosaka S, Tohyama M (1991) Neurotensin and neuromedin N elevate the cytosolic calcium concentration via transiently appearing neurotensin binding sites in cultured rat cortex cells. Dev Brain Res 58:97–103.

Sawchenko PE, Swanson LW (1983) The organization of forebrain afferents to the paraventricular and supraoptic nuclei of the rat. J Comp Neurol 218:121–144.

Sayk F, Wobbe I, Twesten C, Meusel M, Wellhöner P, Derad I, Dodt C (2015) Prolonged blood pressure elevation following continuous infusion of angiotensin II—a baroreflex study in healthy humans. Am J Physiol Integr Comp Physiol 309:R1406–R1414.

Schipper L, Bouyer K, Oosting A, Simerly RB, van der Beek EM (2013) Postnatal dietary fatty acid composition permanently affects the structure of hypothalamic pathways controlling energy balance in mice. Am J Clin Nutr 98:1395–1401 Available at: https://doi.org/10.3945/ajcn.113.069229.

Shankar K, Harrell A, Liu X, Gilchrist JM, Ronis MJJ, Badger TM (2008) Maternal obesity at conception programs obesity in the offspring. Am J Physiol Integr Comp Physiol 294:R528–R538 Available at: https://doi.org/10.1152/ajpregu.00316.2007.

Shapiro RE, Miselis RR (1985) The central neural connections of the area postrema of the rat. J Comp Neurol 234:344–364 Available at: http://www.ncbi.nlm.nih.gov/pubmed/3988989 [Accessed November 13, 2015].

Shi W, Bunney B (2018) Roles of intracellular cAMP and protein kinase A in the actions of dopamine and neurotensin on midbrain dopamine neurons. J Neurosci 12:2433–2438.

Siemelink M, Verhoef A, Dormans J, Span P, Piersma A (2002) Dietary fatty acid composition

during pregnancy and lactation in the rat programs growth and glucose metabolism in the offspring. Diabetologia 45:1397–1403.

Simpson JB, Routtenberg A (1972) The subfornical organ and carbachol-induced drinking. Brain Res 45:135–152.

Sims JS, Lorden JF (1986) Effect of paraventricular nucleus lesions on body weight, food intake and insulin levels. Behav Brain Res 22:265–281.

Slusher BS, Zacco AE, Maslanski JA, Norris TE, McLane MW, Moore WC, Rogers NE, Ignarro LJ (1994) The cloned neurotensin receptor mediates cyclic GMP formation when coexpressed with nitric oxide synthase cDNA. Mol Pharmacol 46:115–121.

Smith PM, Chambers AP, Price CJ, Ho W, Hopf C, Sharkey KA, Ferguson A V (2008) The subfornical organ: a central nervous system site for actions of circulating leptin. Am J Physiol Integr Comp Physiol 296:R512–R520 Available at: http://ajpregu.physiology.org/cgi/doi/10.1152/ajpregu.90858.2008.

Smith PM, Ferguson A V. (2012) Cardiovascular Actions of Leptin in the Subfornical Organ are Abolished by Diet-Induced Obesity. J Neuroendocrinol 24:504–510.

Smith PM, Ferguson A V (1997) Vasopressin acts in the subfornical organ to decrease blood pressure. Neuroendocrinology 66:130–135 Available at: https://www.karger.com/DOI/10.1159/000127230.

Smith PM, Rozanski G, Ferguson A V. (2010) Acute electrical stimulation of the subfornical organ induces feeding in satiated rats. Physiol Behav 99:534–537.

Smith PM, Samson WK, Ferguson A V. (2007) Cardiovascular actions of orexin-A in the rat

subfornical organ. J Neuroendocrinol 19:7–13.

Stanley BG, Hoebel BG, Leibowitz SF (1983) Neurotensin: effects of hypothalamic and intravenous injections on eating and drinking in rats. Peptides 4:493–500.

Statistics Canada (2015) Overweight and obese adults (self-reported), 2009.

Statistics Canada (2019) Body mass index, overweight or obese, self-reported, adult, age groups (18 years and older). :Table 13-10-0096-20.

Sun-young K, Hyun Seok H, Minho M, Inhee M (2013) Disruption of blood-brain barrier in Alzheimer disease pathogenesis. Tissue Barriers 1:e23993.

Sundler F, Håkanson R, Hammer RA, Alumets J, Carraway R, Leeman SE, Zimmerman EA (1977) Immunohistochemical localization of neurotensin in endocrine cells of the gut. Cell Tissue Res 178:313–321.

Swanson LW, Kuypers HGJM (1980) The paraventricular nucleus of the hypothalamus: Cytoarchitectonic subdivisions and organization of projections to the pituitary, dorsal vagal complex, and spinal cord as demonstrated by retrograde fluorescence double-labeling methods. J Comp Neurol 194:555–570 Available at: https://doi.org/10.1002/cne.901940306.

Swanson LW, Lind RW (1986) Neural projections subserving the initiation of a specific motivated behavior in the rat: new projections from the subfornical organ. Brain Res 379:399–403.

Szathmari A, Champier J, Ghersi-Egea JF, Jouvet A, Watrin C, Wierinckx A, Fèvre Montange M (2013) Molecular characterization of circumventricular organs and third ventricle ependyma in the rat: Potential markers for periventricular tumors. Neuropathology 33:17–29.

Takahashi Y, Smith P, Ferguson A, Pittman QJ (1997) Circumventricular organs and fever. Am J Physiol 273:R1690-5 Available at: http://www.ncbi.nlm.nih.gov/pubmed/9374811 [Accessed November 13, 2015].

Tanaka J, Saito H, Kaba H, Seto K (1987) Subfornical organ neurons act to enhance the activity of paraventricular vasopressin neurons in response to intravenous angiotensin II. Neurosci Res 4:424–427 Available at: http://www.sciencedirect.com/science/article/pii/0168010287900083.

Tanaka K, Masu M, Nakanishi S (1990) Structure and functional expression of the cloned rat neurotensin receptor. Neuron 4:847–854 Available at: https://doi.org/10.1016/0896-6273(90)90137-5.

Thibault D, Albert PR, Pineyro G, Trudeau LÉ (2011) Neurotensin triggers dopamine D2 receptor desensitization through a protein kinase C and β-arrestin1-dependent mechanism. J Biol Chem 286:9174–9184.

Townend JN, Al-Ani M, West JN, Littler WA, Coote JH (1995) Modulation of cardiac autonomic control in humans by angiotensin II. Hypertension 25:1270–1275.

Tsuda K, Masuyama Y (1993) Effects of neurotensin on norepinephrine release in blood vessels of spontaneously hypertensive rats. Am J Hypertens 6:473–479.

Twells LK, Gregory DM, Reddigan J, Midodzi WK (2014) Current and predicted prevalence of obesity in Canada: a trend analysis. C open 2:E18–E26 Available at: https://www.ncbi.nlm.nih.gov/pubmed/25077121.

Ueno M, Akiguchi I, Hosokawa M, Kotani H, Kanenishi K, Sakamoto H (2000) Blood-brain

barrier permeability in the periventricular areas of the normal mouse brain. Acta Neuropathol 99:385–392.

Valette M, Poitou C, Kesse-Guyot E, Bellisle F, Carette C, Le Beyec J, Hercberg S, Clément K, Czernichow S (2014) Association between melanocortin-4 receptor mutations and eating behaviors in obese patients: A case-control study. Int J Obes 38:883–885.

Van Den Buuse M, Catanzariti R (2000) Stimulation of the ventral tegmental area enhances the effect of vasopressin on blood pressure in conscious rats. Br J Pharmacol 129:29–36.

Walker N, Lepee-Lorgeoux I, Fournier J, Betancur C, Rostene W, Ferrara P, Caput D (1998) Tissue distribution and cellular localization of the levocabastine-sensitive neurotensin receptor mRNA in adult rat brain. Mol Brain Res 57:193–200.

Wall KM, Nasr M, Ferguson A V. (1992) Actions of endothelin at the subfornical organ. Brain Res 570:180–187.

Wang D, He X, Zhao Z, Feng Q, Lin R, Sun Y, Ding T, Xu F, Luo M, Zhan C (2015) Whole-brain mapping of the direct inputs and axonal projections of POMC and AgRP neurons . Front Neuroanat 9:40 Available at: https://www.frontiersin.org/article/10.3389/fnana.2015.00040.

Weiss S, Schmidt BH, Sebben M, Kemp DE, Bockaert J, Sladeczek F (1988) Neurotransmitter-induced inositol phosphate formation in neurons in primary culture. J Neurochem 50:1425–1433 Available at: https://doi.org/10.1111/j.1471-4159.1988.tb03026.x.

Whyment A, Top M Van Den, Lee K, Whyment AD, Blanks AM, Spanswick D (2004) Orexigen-sensitive NPY / AgRP pacemaker neuons in the hypothalamic arcuate nucleus.

Nat Neurosci 7:493–494.

Wilkin LD, Mitchell LD, Ganten D, Johnson AK (1989) The supraoptic nucleus: Afferents from areas involved in control of body fluid homeostasis. Neuroscience 28:573–584 Available at: http://www.sciencedirect.com/science/article/pii/0306452289900067.

Yamada M, Yamada M, Watson MA, Richelson E (1993) Neurotensin stimulates cyclic AMP formation in CHO-rNTR-10 cells expressing the cloned rat neurotensin receptor. Eur J Pharmacol Mol Pharmacol 244:99–101.

Yamashita S, Nakamura T, Shimomura I, Nishida M, Yoshida S, Kotani K, Kameda-Takemuara K, Tokunaga K, Matsuzawa Y (1996) Insulin resistance and body fat distribution. Diabetes Care 19:287–291 Available at: http://europepmc.org/abstract/MED/8742584.

Yaswen L, Diehl N, Brennan MB, Hochgeschwender U (1999) Obesity in the mouse model of pro-opiomelanocortin deficiency responds to peripheral melanocortin. Nat Med 5:1066–1070 Available at: https://doi.org/10.1038/12506.

Yengo L, Sidorenko J, Kemper KE, Zheng Z, Wood AR, Weedon MN, Frayling TM, Hirschhorn J, Yang J, Visscher PM (2018) Meta-analysis of genome-wide association studies for height and body mass index in ~700000 individuals of European ancestry. Hum Mol Genet 27:3641–3649.

Yim HE, Ha KS, Bae IS, Yoo KH, Hong YS, Lee JW (2013) Overweight, hypertension and renal dysfunction in adulthood of neonatally overfed rats. J Nutr Biochem 24:1324–1333 Available at: http://www.sciencedirect.com/science/article/pii/S0955286312002847.

Zhang Y, Proenca R, Maffei M, Barone M, Leopold L, Friedman JM (1994) Positional cloning

of the mouse obese gene and its human homologue. Nature 372:425.

2. The transcriptome of the rat subfornical organ is altered in response to early postnatal overnutrition

2.1. Abstract

Early postnatal overnutrition in humans is associated with long-term negative outcomes including obesity, increased risk of type-II diabetes, and cardiovascular disease. Hypothalamic neurons from rodents exposed to early postnatal overnutrition show altered expression of satiety signals and receptors, and exhibit altered responses to many satiety signals, suggesting a hypothalamic link between early overnutrition and development of these sequelae. Importantly, several hypothalamic nuclei receive information regarding circulating hormones (such as insulin, leptin and ghrelin) from the subfornical organ (SFO), a forebrain sensory circumventricular organ which lacks a blood brain barrier. Previous transcriptomic studies indicate that challenges to energy balance and hydration status stimulate changes in gene expression within the SFO, including genes encoding ion channels and receptors. In order to determine if early postnatal overnutrition also causes changes in SFO gene expression which may be associated with homeostatic dysregulation, we performed whole transcriptome sequencing on SFO tissue from rats raised in small (4 pups), or control (large, 12 pups) litters. Illumina RNA sequencing was performed on SFO tissue from rats raised from small and large litters, and read sequences were aligned to the Rat Rnor_6.0 genome. Control data were further compared to previously published microarray data set for validation. We found statistically significant ($p < 0.05$) changes in expression of 12 transcripts, three of which have likely roles in neuronal excitability, neurite outgrowth and differentiation, and food intake (*Manf, Slc24a4, Cracr2b*). Additionally, gene ontology analysis identified a trend among significantly altered transcripts in roles for oxidative stress response. We conclude that the SFO transcriptome is subtly altered by early postnatal

overnutrition, and recommend further investigation of the effect of early postnatal overnutrition on SFO physiology and morphology.

2.2. Introduction

In humans, early postnatal overnutrition results in accelerated growth and weight gain, is predictive of childhood (Gittner et al., 2013) and adult obesity (Rzehak et al., 2017), and is correlated with increased risk of type II diabetes (Eriksson et al., 2003) and heart disease (Camhi and Katzmarzyk, 2010). Similar effects are seen in rodents raised in small litters as a model of early postnatal overnutrition: rats from small litters gain more weight relative to controls (Wiedmer et al., 2002), a trend which persists into adulthood (Habbout et al., 2013). Moreover, rodents show increased visceral white adipose tissue (Cordeiro et al., 2009), hypertension (Plagemann et al., 1992), hyperinsulinemia (Plagemann et al., 1992), and hyperleptinemia (Plagemann et al., 1999a) following early postnatal overnutrition. When fed a high fat diet, small litter rats display persistent hyperphagia and increased caloric intake (Glavas et al., 2010), suggesting early overnutrition primes rats for later weight gain. Numerous studies indicate that altered neurophysiological development plays a key role (Rodrigues et al., 2009; Glavas et al., 2010; Habbout et al., 2013). Increased densities of galanin and neuropeptide Y (NPY) neurons in the arcuate nucleus of the hypothalamus (ARC) are found in small litter rats compared to control rats, despite lower overall density of neurons (Plagemann et al., 1999b). Galanin neuron density is similarly increased in the paraventricular nucleus of the hypothalamus (PVN; Plagemann et al., 1999a). Neurons may additionally show altered responses to hormones following postnatal overnutrition; for example leptin and insulin resistance is seen in hypothalamic neurons (Glavas et al., 2010) in the face of increased central levels of both peptides (Glavas et al., 2010; Plagemann et al., 1999b). Altered responses to the neuropeptides cocaine and amphetamine

regulated transcript (CART), NPY, and corticotropin-releasing hormones are also observed in the PVN, ARC, and ventromedial nucleus of the hypothalamus (VMN) (Davidowa et al., 2003; Davidowa and Plagemann, 2004)

The subfornical organ (SFO) is a small forebrain sensory circumventricular organ found on the anteroventral aspect of the third ventricle, between the columns of the fornix and attached to the hippocampal commissure. Sensory circumventricular organs are specialised structures uniquely lacking a blood-brain barrier (Gross and Weindl, 1987). They express a wide variety of receptors for circulating hormones and signaling molecules, which when activated modulate electrical activity of SFO neurons to allow transduction of information from the periphery to the brain (Fry and Ferguson, 2007a). The SFO receives synaptic inputs from homeostatic regulatory regions including the nucleus of the solitary tract (NTS) (Tanaka et al., 1997), the lateral hypothalamus (LH) (Lind et al., 1984), and the median preoptic nucleus (MPN) (Lind et al., 1984). The SFO also sends axonal projections to various other centres including the PVN (Miselis, 1982), ARC (Gruber et al., 1987; Whyment et al., 2004), the LH (Burton et al., 1976; Miselis, 1982), the MPN (Lind et al., 1982, 1984), the supraoptic nucleus (SON) (Lind et al., 1982; Sawchenko and Swanson, 1983), and the vascular organ of the lamina terminalis (OVLT) (Lind et al., 1982). Critical roles for the SFO have been established in osmoregulation (Felix, 1976), cardiovascular output (Mangiapane and Simpson, 1983), and energy homeostasis (Smith et al., 2010). Stimulation of the SFO results in feeding in satiated rats (Smith et al., 2010), and microarray data shows strong expression of receptors for hormones involved in energy balance including adiponectin, leptin, amylin, and ghrelin, the activity of which is confirmed in SFO neurons (Hindmarch et al., 2008, and references therein).

That the SFO plays a key role in integration of signals related to energy balance and cardiovascular regulation is highlighted by the observation that acute fasting or water restriction dramatically modulates its transcriptome, causing significant alteration of hundreds of transcripts (Hindmarch et al., 2007). Interestingly, research performed on the impact of postnatal overnutrition on the brain has focused on other nuclei such as the ARC, (Davidowa and Plagemann, 2000; Juan De Solis et al., 2016), VMN (Davidowa et al., 2002), and the PVN (Davidowa and Plagemann, 2004; Plagemann et al., 1999a), but not the SFO which is a key centre communicating information from the periphery to the hypothalamus. In order to evaluate possible roles of SFO in the long term effects of early postnatal overnutrition, we compared the transcriptomes of the SFO of six-week-old male rats raised in small litters (4 pups) to those raised in larger (control) litters (12 pups) using RNA sequencing. Here we report statistically significant (false discovery rate corrected, $p<0.05$) 1.16 – 1.7 fold changes (in either direction) in 12 SFO transcripts involved in neuronal excitability, neuron differentiation and outgrowth, food intake, and/or response to oxidative stress, from rats raised in small litters compared to those raised in large litters.

2.3. Methods

2.3.1. Animals and diets

All procedures were approved by the University of Manitoba Animal Care Committee in accordance with the Canadian Council for Animal Care. Two groups of 8 timed-pregnant dams, all birthing on the same day were used for these studies. For each group of 8 dams on postnatal day one (PD 1), all of the pups were mixed and randomly assigned to a dam: 2 dams received 12 pups to form a large litter, whereas 6 dams received 4 pups to form a small litter. The litters were composed of equal numbers of male and female pups. This procedure was repeated a second

time with a separate set of 8 dams and their pups, for a total of 16 dams; 4 large litters and 12 small litters. Weights between control and small litter rats (n=48, male and female each) on PD 3 were 12.4 ± 0.3 g and 12.9 g ± 0.3 g respectively were not significantly different ($p > 0.05$, t-test).

After weaning, rats were kept in a light-controlled facility (12 hours light: 12 hours dark), and given *ad libitum* access to standard rat chow. Pups were weaned at PD 21 into cages of two males or two females.

Male rats were sacrificed on PD 42-47, between the hours of 9 am and 12 pm (2:45 – 5:45 following lights on). Briefly, rats were decapitated, the brain removed and placed in ice-cold oxygenated artificial cerebrospinal fluid (composition, in mM: 126 NaCl, 2.5 KCl, 1.25 NaH_2PO_4, 2 $MgCl_2$, 10 D-glucose, 26 $NaHCO_3$, 0.5 $CaCl_2$) for 2 minutes. A 3 mm block of tissue was cut at the level of the hypothalamus (approximately 9 to 6 mm interaural in the coordinates of the Paxinos and Watson rat brain atlas (Paxinos and Watson, 2007)), and a vibratome was used to prepare a brain slice containing the SFO, which was dissected out, using caution not to harvest choroid plexus. Brain tissue was stored in RNAlater at -20 °C until time of RNA extraction. Only SFO tissue from male rats was used for RNA sequencing. To reduce biological variability, SFO tissue was pooled (Hindmarch et al., 2006, 2008; Colombari et al., 2011). Briefly, 6 males from each large litter were pooled in to a single RNA sample for sequencing, providing 4 large litter samples of 6 SFO each. For small litters, the 2 males from the 3 litters (for a total of 6 SFO) were pooled, resulting in 4 small litter samples of 6 SFO each.

2.3.2. RNA extraction and sequencing

RNA extraction and sequencing were performed at the ABM laboratory in Vancouver. RNA extraction was performed using the PureLink RNA Mini Kit (Thermo Fisher Scientific),

and analysed using a Bioanalyzer (Agilent). RNA integrity number values (RIN) were assessed using the RNA 6000 pico kit on an Agilent 2100 Bioanalyzer; all RIN values were between 7.7 and 8.6. Two micrograms of sample were prepared for library construction using the TruSeq Standard mRNA Library Prep Kit (Illumina). Briefly, the RNA was subject to polyA enrichment, fragmentation, and cDNA synthesis. Indexed adaptors were ligated to the cDNA library, and then libraries were pooled in equal molar ratio. Quality of library was assessed using an Agilent Bioanalyzer prior to sequencing; library sizes ranged from 401 to 427. Sequencing was performed on the NextSeq 500 platform with 2x 75 bp end sequencing. For each sample, sequencing produced between 42.8 and 54.7 million reads: reads were aligned to Rat Rnor_6.0 reference genome and annotation (GCF_000001895.5) using Hisat2 with the parameters (--rf --mm --dta); mapping rates were between 86.76% and 88.52%. Stringtie was used to estimate FPKM for each sample and differential expression between small and control litter rats was performed using DESeq2. Differentially expressed genes were identified according to $\log_2$(fold change) > 0.5 or < -0.5 with adjusted p-values < 0.05 (Wald test with Benjamini-Hochberg multiple test correction, as previously described (Love et al., 2014)). Functional annotation with gene ontology and pathway annotation was performed using KOBAS (Xie et al., 2011).

2.3.4. Validation of RNA sequencing data

Relative expression of transcripts identified by RNAseq in control rats were compared against those from the control group of an existing microarray dataset (Hindmarch et al., 2008). The rats used in the experiments performed by Hindmarch et al were slightly older (10-12 week) male Sprague Dawley rats from Harlan Sera-lab, Loughborough, UK; litter size is unknown. There were also minor differences in sample collection: dissections occurred at slightly different times in the morning (9 AM – 12 PM in our study vs 11 AM – 1 PM), rat brains used in this

study were cooled in aCSF before SFO dissection whereas those from Hindmarch's study were immediately placed in a cooled brain matrix post-removal. In both cases, choroid plexus was removed and the SFO was carefully dissected out under microscope from a larger slice, however Hindmarch et al used a single 1 mm section, whereas we have used a larger 3 mm section, which was then cut on a vibratome to reveal the SFO. In both studies, samples were stored in RNAlater at -20℃.

Ensembl Gene ID was used as the annotation feature for matching unique genes from each experiment. To allow for fair comparison between microarray and RNAseq data, only those transcripts which could be mapped back to the microarray were included. Of the 31100 probe sets present on the GeneChip Rat Genome 230 2.0 Array, 12779 were not annotated with Ensembl gene IDs and were excluded from analysis, whereas 10910 probes were annotated both with Ensembl gene IDs (of which 8914 were unique Ensembl IDs) and marked as present on the microarray. In the case of RNA-sequencing data, 15628 transcripts with associated Ensembl gene IDs were considered present (FPKM>0.5), and for comparison of the two datasets, only the transcripts with Affy IDs and associated Ensembl IDs which were detected and called as present by both methods were included.

2.4. Results

2.4.1. Effect on body weight of early overnutrition

To confirm that rearing as small litters induced larger body weight, males were weighed at six weeks of age. Consistent with previously published observations (Habbout et al., 2012, 2013), male rats raised in small litters showed significantly increased body weight relative to control rats, with weights of 418.5 ± 4.5 g and 382.9 ± 6.9 g (mean ± SE) for small and control litters respectively ($p = 7.6 \times 10^{-5}$, t-test).

2.4.2. Differential expression analysis

Of the 32884 transcripts identified for the Rat Rnor 6.0 genome assembly, 15630 were identified as present in the SFO. To determine the effect of postnatal overnutrition on the transcriptome of the SFO, differential expression analysis was performed using DESeq2. Statistically significant changes in relative expression were detected for 12 transcripts ($p<0.05$, with multiple test correction). Specifically, 4 transcripts were upregulated and 8 were downregulated in response to postnatal overnutrition. Gene ontology terms were found in oxidative stress response, and regulation of protein folding/activity were detected by KOBAS gene ontology analysis (Table A1).

2.4.3. Comparison to microarray data

In order to validate the present RNAseq experiment, sequencing data from control litters was compared to control data from previously published microarray data from the SFO (Hindmarch et al., 2008). Of the 18321 Affymetrix probe IDs which could be mapped to Ensembl IDs, 10910 were detected by the microarray; these mapped to 9115 unique Ensembl IDs. Of those, only 174 transcripts were detected by the microarray, but were not detected by RNA sequencing. Conversely, 3586 transcripts were detected exclusively by RNA sequencing (Figure 2.2), suggesting higher sensitivity of detection of weakly expressed transcripts. Relative expression (FPKM and relative intensity) of transcripts present in both data sets were compared (Figure 2.3), and were demonstrated to have good concordance (Pearson's $r = 0.65455$; $p<0.001$ Student's two tailed t-test).

2.5. Discussion

The objective of this study was to determine if there are changes in SFO gene expression associated with early overnutrition in rat pups that may be related to the development of sequelae such obesity, type II diabetes (Eriksson et al., 2003) and heart disease (Camhi and Katzmarzyk, 2010) observed in humans and rodents (Plagemann et al., 1992; Habbout et al., 2013). We observed statistically significantly differential expression in 12 transcripts (Figure 2.1); of these one was identified as a pseudogene (*AABR07030823.1*) and one is currently uncharacterised. Of particular interest are three transcripts, mesencephalic astrocyte-derived neurotrophic factor (*Manf*), EF-hand calcium-binding domain-containing protein 4A (*Cracr2b*), and solute carrier family 24 member 4 (*Slc24a4*), as they may alter neuronal excitability or development. Ultimately we found only subtle changes in few transcripts, leading us to conclude that the SFO does not show the dramatic changes following early postnatal overnutrition compared to changes elicited by acute food or water restriction (Hindmarch et al., 2007).

Manf is a neurotrophic factor whose roles in the CNS have yet to be fully elucidated. Increasing evidence suggests Manf participates in neurite outgrowth and neuronal differentiation (Tseng et al., 2017) as well as protection against cell damage in Parkinson's disease (Voutilainen et al., 2009), cerebral ischemia (Airavaara et al., 2009), and endoplasmic reticulum stress (Apostolou et al., 2008; Hellman et al., 2011). Recent data suggests that Manf, acting at the level of the PVN, plays a role in regulation of energy balance. Specifically Manf protein and transcript levels rise in response to fasting and fall following feeding; Manf overexpression or direct injection to the hypothalamus causes hyperphagia and increased body weight, whereas Manf knockdown results in hypophagia and decreased weight gain in 3 month old mice (Yang et al.,

2017). Whether Manf also acts to negatively regulate energy balance via the SFO is unknown. Additionally, given its roles in neurite outgrowth and neuronal differentiation in the cortex (Tseng et al., 2017), there is also potential for altered SFO neuron development resulting from decreased *Manf* expression.

Slc24a4 is a member of a family of potassium-dependent Na^+/Ca^{2+} exchangers, exchanging one Ca^{2+} ion and one K^+ ion for four Na^+ ions (Schnetkamp, 1995). Altered ion transport accomplished by downregulation of *Slc24a4* expression may result in changes to neuronal excitability and calcium-dependent pathways via decreased calcium extrusion. Intriguingly, in rat PVN, this transporter has an established role in energy balance: *Slc24a4* knockout mice show hypophagia and weight loss due to constitutive activation of the melanocortin-4-receptor (Li and Lytton, 2014), a transcript which we also detected in the SFO. Importantly, altered expression of another Slc member (the Slc12a1 ($Na^+/K^+/2Cl^-$) transporter) in hypothalamo-neurohypophyseal neurons causes a mild change in Cl- homeostasis but has dramatic effects on neuronal excitability and ultimately osmoregulation (Konopacka et al., 2015). The effect on calcium levels may additionally be altered by upregulation of *Cracr2b*, a regulator of intracellular CRAC Ca++ channels (Srikanth et al., 2010). Although the changes in expression in these genes are small, they have the potential to alter SFO neuron electrical behaviour: SFO neurons have high input resistance, typically 2 GOhm, so alteration of resting membrane currents of a few pA causes alteration of action potential activity (Fry and Ferguson, 2007b). Further work to determine specific actions and localisation of the Manf, Slc24a4, and Cracr2b proteins in the SFO will improve our knowledge of their electrophysiological and developmental effects, and will inform our understanding of any roles they may play in the development of negative health outcomes secondary to early postnatal overnutrition.

Related functions of differentially expressed transcripts identified using KOBAS show a trend of changes in transcripts for proteins that are involved in oxidative stress response and protein phosphorylation. Expression of heat shock protein 105 kDa (*Hsph1*), heat shock 27kDa protein 1 (*Hspb1*), and oxidative stress regulators including *Manf* (Oh-hashi et al., 2015), cysteine-rich with EGF-like domain protein 2 (*Creld2*) (Oh-hashi et al., 2009), and cysteine and histidine rich domain containing 1 (*Chordc1*) (Gano and Simon, 2010) was significantly altered by postnatal overnutrition. Previous studies have found increased oxidative stress following early postnatal overnutrition in plasma (Habbout et al., 2012) and liver (Conceição et al., 2013). While the small litter rats in this study may not have been obese, evidence suggests they were predisposed to adult obesity (Habbout et al., 2013; Rzehak et al., 2017). While to our knowledge no studies have specifically examined the effect of early postnatal overnutrition on oxidative stress in the brain, recent research indicates a link between adult overnutrition or obesity and neural oxidative stress (Zhang et al., 2005; White et al., 2009; Morrison et al., 2010). Of considerable interest then, is whether or not the observed changes in gene expression are associated with future development of obesity, and whether or not this altered pattern of expression represents pathology or compensatory action. Additionally, it will be important to investigate whether the observed changes are unique to the SFO, unique to areas regulating energy balance and other aspect of homeostasis, or globally observed in the brains of animals subjected to early overnutrition.

Of note, the rats in this study were sacrificed peripubertally at PD 42-47. This raises a question of whether a change in onset of puberty may have played a role in the differential gene expression observed. Smith and Spencer (2018) demonstrated that the age of male puberty onset was not affected in small litters of four pups per litter, compared to litters of 12, despite their

accelerated weight gain. In contrast, the age of puberty onset was significantly delayed in litters of 20 pups. Therefore, we do not believe that different age of puberty was a factor driving the observed changes in gene expression. Whether the onset of male puberty causes changes in transcription in the SFO is unknown, and to our knowledge, such changes in SFO transcription have not been reported.

Through comparing relative expression of SFO transcripts obtained via RNA sequencing in our control group to the data from the control group of a previously published microarray data (Hindmarch et al., 2008), we show correlation between data from the two techniques and validate our present dataset in a manner similar to that by other researchers comparing RNAseq and microarray datasets (Mortazavi et al., 2008; Malone and Oliver, 2011; Guo et al., 2013). We have achieved this level of replication despite that the data were produced by different laboratories, by different personnel, with rats from different suppliers and of different ages (six weeks versus 10-12 weeks). We have presented a correlation of a restricted number of transcripts (10910). The number of transcripts shared between the two datasets was low relative to the total number of present unique transcripts found by each technique (15937 by the microarray and 15630 by RNAseq). This is due to limitations in mapping transcripts between the two datasets. To ensure a fair comparison, only those Affymetrix probes which could be mapped to the ENSEMBL IDs from the Rat Rnor_6.0 genome assembly were used (18321 probes); as such, data from unannotated probes on the Affymetrix microarray could not be included (12778 probes). This mapping issue has been encountered previously by other investigators who demonstrated similar issues with mapping Affymetrix IDs to Ensembl gene IDs (Chen et al., 2011; Black et al., 2014). A more recent microarray analysis of the rat SFO has also been published employing laser microdissection to dissect the SFO without the overlying ependymal

cell layer (Szathmari et al., 2013, 2015). We expect our data to be similar to these except with regard to transcripts overrepresented within the ependymal layer, which was included in both our data and microarray data from Hindmarch et al. (2008).

The microarray study of Hindmarch et al. (2008) examining gene expression changes in rat SFO demonstrated significant changes in expression of 48 transcripts following the extreme conditions of 72 h water restriction, and 687 transcripts following 48 h food restriction. Differentially expressed transcripts included ion channels, neuropeptides and hormone receptors, and signaling molecules including neurotrophins. These results suggest the SFO is a dynamic sensor, changing its properties in response to both severe and mild challenges to homeostasis. Thus, we were intrigued when the present RNA sequencing experiment indicated that early overnutrition altered expression of only 12 transcripts, 9 of which were related to oxidative stress, and 3 transcripts with known roles in neuronal excitability and/or energy homeostasis.

Electrophysiological evidence in small litter rat neurons shows altered response to amylin in ARC and PVN (Davidowa et al., 2004) and CART in VMN (Davidowa et al., 2003; Davidowa and Plagemann, 2004), respectively. Based on this data and the sensory transduction role of SFO for circulating homeostatic signals, we anticipated changes in transcripts associated with receptors and ion channels. It is interesting then that no changes in expression of receptors and ion channels were detected. It is possible that food and water restriction used in Hindmarch et al. (2008) was a powerful and acute stimulus, whereas the early overnutrition investigated here was a mild and prolonged manipulation, not strong enough to evoke a robust changes in gene expression. Furthermore, while the reported changes are statistically significant, they are relatively subtle (<2-fold change). Thus we have come to the conclusion that early postnatal overnutrition does not cause robust changes in gene expression in the SFO such as those seen in

the hypothalamus (Chen et al., 2008; Collden et al., 2015). However, some of the altered transcripts may be suited to modulate electrical excitability or neuronal differentiation. It is unclear whether these changes are reflective of early postnatal overnutrition, or whether they are predictive of changes in physiology which manifest later in life in postnatally overnourished rats, and further research along the developmental timescale will be necessary to determine this. Future research investigating the underpinnings of the effects of early postnatal overnutrition on long-term negative health outcomes should include the role of the SFO, with particular focus on the 12 transcripts we have identified.

We have for the first time examined the effect of postnatal overnutrition on the SFO transcriptome, while also producing the first RNAseq transcriptome of the SFO, building on previous microarray work (Hindmarch et al., 2008). We expect that the sequencing data presented here will provide a valuable resource for other researchers. Our raw data have been deposited in to the Sequence Read Archive (SRA) at NCBI, and we encourage other researchers to examine our data for future research investigating roles of the SFO in homeostasis.

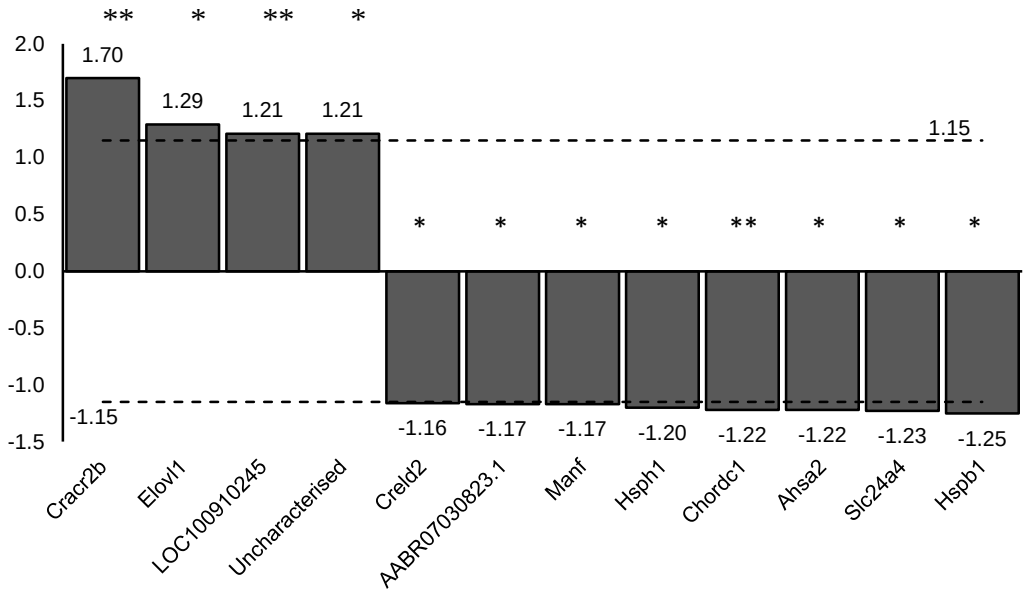

Figure 2.1. Fold regulation of transcripts significantly changed ($p<0.05$; * indicates $p < 0.05$; ** $p <0.01$) by postnatal overnutrition in rat subfornical organ. *Cracr2b* = EF-hand calcium-binding domain-containing protein 4A; *Elovl1* = Elongation of very long chain fatty acids protein 1; *LOC100910245* = Ribose-phosphate pyrophosphokinase 2-like; *Creld2* = Cysteine-rich with EGF-like domain protein 2; *AABR07030823.1* is a pseudogene; *Manf* = Mesencephalic astrocyte-derived neurotrophic factor; *Hsph1* = Heat shock protein 105 kDa; *Chordc1* = Cysteine and histidine-rich domain-containing protein 1; *Ahsa2* = AHA1, activator of heat shock protein ATPase 2 ($p=0.01485$); *Slc24a4* = Solute carrier family 24 member 4; *Hspb1* = Heat shock 27kDa protein 1. Dotted lines indicate fold-change cut-offs, greater than 1.15 fold up- or downregulation.

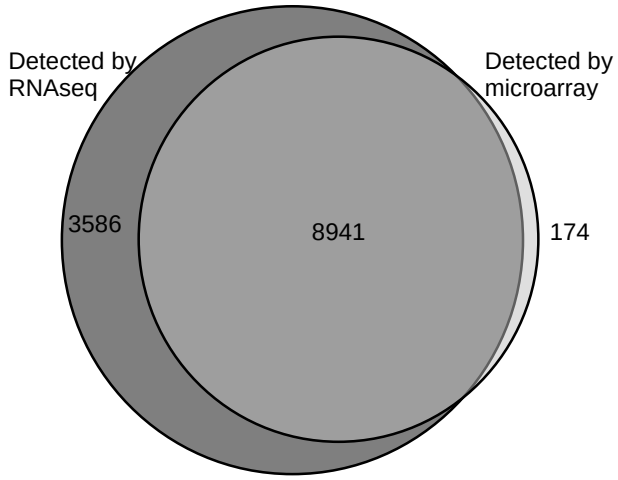

Figure 2.2. Overlap between previously published microarray data and RNA sequencing transcriptomes. Only transcripts which could be mapped between the RNAseq dataset and microarray dataset via Ensembl IDs were included. 8941 unique transcripts (unique Ensembl IDs) were detected by both the microarray and RNAseq. 3586 and 174 transcripts were exclusively detected by RNAseq and microarray respectively.

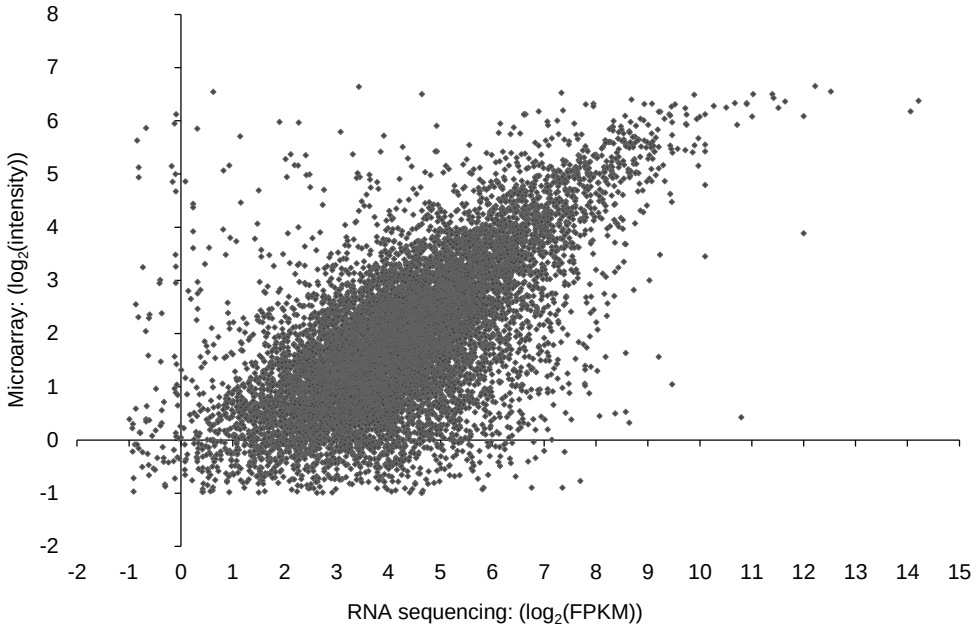

Figure 2.3. Comparison of rat subfornical organ relative expression (FPKM) values to publicly available rat subfornical organ Affymetrix microarray relative expression (intensity) (Hindmarch et al., 2008). Relative expression levels were determined based on log2 transformed average expression values in all control samples in each experiment. 8941 unique Ensembl gene ID annotated transcripts detected by both methods are included; of these 1969 Affy IDs map to the same Ensembl identified as at least one other Affy ID, such that 10910 points are included. Good concordance exists between the two methods despite differing experimental conditions, as demonstrated by the Pearson correlation coefficient (r = 0.65455).

2.6. References

Airavaara M, Shen H, Kuo C-C, Peränen J, Saarma M, Hoffer B, Wang Y (2009) Mesencephalic astrocyte-derived neurotrophic factor reduces ischemic brain injury and promotes behavioral recovery in rats. J Comp Neurol 515:116–124 Available at: http://www.ncbi.nlm.nih.gov/pubmed/19399876 [Accessed December 15, 2017].

Apostolou A, Shen Y, Liang Y, Luo J, Fang S (2008) Armet, a UPR-upregulated protein, inhibits cell proliferation and ER stress-induced cell death. Exp Cell Res 314:2454–2467 Available at: http://www.sciencedirect.com.uml.idm.oclc.org/science/article/pii/S0014482708001870 [Accessed December 15, 2017].

Black MB, Parks BB, Pluta L, Chu TM, Allen BC, Wolfinger RD, Thomas RS (2014) Comparison of microarrays and RNA-Seq for gene expression analyses of dose-response experiments. Toxicol Sci 137:385–403.

Burton MJ, Rolls ET, Mora F (1976) Effects of hunger on the responses of neurons in the lateral hypothalamus to the sight and taste of food. Exp Neurol 51:668–677.

Camhi SM, Katzmarzyk PT (2010) Tracking of cardiometabolic risk factor clustering from childhood to adulthood. Int J Pediatr Obes 5:122–129 Available at: http://informahealthcare.com/doi/abs/10.3109/17477160903111763.

Chen H, Liu Z, Gong S, Wu X, Taylor WL, Williams RW, Matta SG, Sharp BM (2011) Genome-wide gene expression profiling of nucleus accumbens neurons projecting to ventral pallidum using both microarray and transcriptome sequencing. Front Neurosci 5:1–11.

Chen H, Simar D, Lambert K, Mercier J, Morris MJ (2008) Maternal and postnatal overnutrition differentially impact appetite regulators and fuel metabolism. Endocrinology 149:5348–

5356.

Collden G, Balland E, Parkash J, Caron E, Langlet F, Prevot V, Bouret SG (2015) Neonatal overnutrition causes early alterations in the central response to peripheral ghrelin. Mol Metab 4:15–24 Available at: http://dx.doi.org/10.1016/j.molmet.2014.10.003.

Colombari SA, Colombari E, Freiria-oliveira AH, Antunes VR, Song T, Hindmarch C, Ferguson A V, Fry M, Murphy D, Paton JFR (2011) Switching control of sympathetic activity from forebrain to hindbrain in chronic dehydration. J Physiol 589:4457–4471.

Conceição EPS, Franco JG, Oliveira E, Resende AC, Amaral TAS, Peixoto-Silva N, Passos MCF, Moura EG, Lisboa PC (2013) Oxidative stress programming in a rat model of postnatal early overnutrition — role of insulin resistance. J Nutr Biochem 24:81–87 Available at: http://dx.doi.org/10.1016/j.jnutbio.2012.02.010 [Accessed September 24, 2017].

Cordeiro A, Rodrigues DS, Pereira RO, José M, Soares VDM, Martins MR, Teixeira MT, Patrícia É, Souza G, Moura AS (2009) Long-term effects of overfeeding during lactation on insulin secretion — the role of GLUT-2. J Nutr Biochem 20:435–442 Available at: http://dx.doi.org/10.1016/j.jnutbio.2008.05.002.

Davidowa H, Heidel E, Plagemann A (2002) Differential involvement of dopamine D1 and D2 receptors and inhibition by dopamine of hypothalamic VMN neurons in early postnatally overfed juvenile rats. Nutr Neurosci 5:27–36 Available at: http://www.ncbi.nlm.nih.gov/pubmed/11929195.

Davidowa H, Li Y, Plagemann A (2003) Altered responses to orexigenic (AGRP, MCH) and anorexigenic (α-MSH, CART) neuropeptides of paraventricular hypothalamic neurons in

early postnatally overfed rats. Eur J Neurosci 18:613–621.

Davidowa H, Plagemann A (2000) Decreased inhibition by leptin of hypothalamic arcuate neurons in neonatally overfed young rats. Neuroreport 11:2795-8.

Davidowa H, Plagemann A (2004) Hypothalamic neurons of postnatally overfed, overweight rats respond differentially to corticotropin-releasing hormones. Neurosci Lett 371:64–68.

Davidowa H, Ziska T, Plagemann A (2004) Arcuate neurons of overweight rats differ in their responses to amylin from controls. Neuroreport 15:2801–2805.

Eriksson JG, Forsén T, Tuomilehto J, Osmond C, Barker DJP (2003) Early adiposity rebound in childhood and risk of Type 2 diabetes in adult life. Diabetologia 46:190–194 Available at: http://link.springer.com/10.1007/s00125-002-1012-5.

Felix D (1976) Peptide and acetylcholine action on neurones of the cat subfornical organ. Naunyn Schmiedebergs Arch Pharmacol 292:15–20.

Fry M, Ferguson A V. (2007a) The sensory circumventricular organs: Brain targets for circulating signals controlling ingestive behavior. Physiol Behav 91:413–423.

Fry M, Ferguson A V (2007b) Subthreshold oscillations of membrane potential of rat subfornical organ neurons. Neuroreport 18:1389–1393 Available at: https://insights-ovid-com.uml.idm.oclc.org/pubmed?pmid=17762719 [Accessed May 24, 2018].

Gano JJ, Simon JA (2010) A proteomic investigation of ligand-dependent HSP90 complexes reveals CHORDC1 as a novel ADP-dependent HSP90-interacting protein. Mol Cell Proteomics 9:255–270 Available at: http://www.ncbi.nlm.nih.gov/pubmed/19875381 [Accessed December 13, 2017].

Gittner LS, Ludington-Hoe SM, Haller HS (2013) Utilising infant growth to predict obesity status at 5 years. J Paediatr Child Health 49:564–574.

Glavas MM, Kirigiti MA, Xiao XQ, Enriori PJ, Fisher SK, Evans AE, Grayson BE, Cowley MA, Smith MS, Grove KL (2010) Early overnutrition results in early-onset arcuate leptin resistance and increased sensitivity to high-fat diet. Endocrinology 151:1598–1610.

Gross PM, Weindl A (1987) Peering through the windows of the brain. J Cereb Blood Flow Metab 7:663–672.

Gruber K, McRae-Degueurce A, Wilkin LD, Mitchell LD, Johnson AK (1987) Forebrain and brainstem afferents to the arcuate nucleus in the rat : potential pathways for the modulation of hypophyseal secretions. Neurosci Lett 75:1–5 Available at: http://www.ncbi.nlm.nih.gov/pubmed/3574762 [Accessed November 13, 2015].

Guo Y, Sheng Q, Li J, Ye F, Samuels DC, Shyr Y (2013) Large Scale Comparison of Gene Expression Levels by Microarrays and RNAseq Using TCGA Data. PLoS One 8:1–10.

Habbout A, Delemasure S, Goirand F, Guilland J, Chabod F, Sediki M, Rochette L, Vergely C (2012) Postnatal overfeeding in rats leads to moderate overweight and to cardiometabolic and oxidative alterations in adulthood. Biochimie 94:117–124 Available at: http://dx.doi.org/10.1016/j.biochi.2011.09.023.

Habbout A, Li N, Rochette L, Vergely C (2013) Postnatal overfeeding in rodents by litter size reduction induces major short- and long-term pathophysiological consequences. J Nutr 143:553–562 Available at: http://jn.nutrition.org/cgi/doi/10.3945/jn.112.172825.

Hellman M, Arumäe U, Yu L, Lindholm P, Peränen J, Saarma M, Permi P (2011) Mesencephalic

astrocyte-derived neurotrophic factor (MANF) has a unique mechanism to rescue apoptotic neurons. J Biol Chem 286:2675–2680 Available at: http://www.ncbi.nlm.nih.gov/pubmed/21047780 [Accessed December 12, 2017].

Hindmarch C, Fry M, Yao ST, Smith PM, Murphy D, Ferguson A V (2008) Microarray analysis of the transcriptome of the subfornical organ in the rat: regulation by fluid and food deprivation. Am J Physiol Regul Integr Comp Physiol 295:R1914-20.

Hindmarch C, Yao S, Beighton G, Paton J, Murphy D (2006) A comprehensive description of the transcriptome of the hypothalamoneurohypophyseal system in euhydrated and dehydrated rats. Proc Natl Acad Sci U S A 103:1609–1614.

Juan De Solis A, Baquero AF, Bennett CM, Grove KL, Zeltser LM (2016) Postnatal undernutrition delays a key step in the maturation of hypothalamic feeding circuits. Mol Metab 5:198–209 Available at: http://dx.doi.org/10.1016/j.molmet.2016.01.003.

Konopacka A et al. (2015) Osmoregulation requires brain expression of the renal Na-K-2Cl cotransporter NKCC2. J Neurosci 35:5144–5155 Available at: http://www.ncbi.nlm.nih.gov/pubmed/25834041 [Accessed December 15, 2017].

Li X-F, Lytton J (2014) An essential role for the K+-dependent Na+/Ca2+-exchanger, NCKX4, in melanocortin-4-receptor-dependent satiety. J Biol Chem 289:25445–25459 Available at: http://www.ncbi.nlm.nih.gov/pubmed/25096581 [Accessed December 12, 2017].

Lind RW, Hoesen GW van, Johnson AK (1982) An HRP study of the connections of the subfornical organ of the rat. J Comp Neurol 210:265–277.

Lind RW, Swanson LW, Ganten D (1984) Angiotensin II immunoreactivity in the neural

afferents and efferents of the subfornical organ of the rat. Brain Res 321:209–215.

Love MI, Huber W, Anders S (2014) Moderated estimation of fold change and dispersion for RNA-seq data with DESeq2. Genome Biol 15:550 Available at: http://genomebiology.biomedcentral.com/articles/10.1186/s13059-014-0550-8.

Malone JH, Oliver B (2011) Microarrays, deep sequencing and the true measure of the transcriptome. BMC Biol 9:34 Available at: http://www.biomedcentral.com/1741-7007/9/34.

Mangiapane ML, Simpson JB (1983) Drinking and pressor responses after acetylcholine injection into subfornical organ. AJP Regul Integr Comp Physiol 244:R508-13.

Miselis RR (1982) The subfornical organ's neural connections and their role in water balance. Peptides 3:501–502 Available at: http://www.sciencedirect.com.uml.idm.oclc.org/science/article/pii/0196978182901152 [Accessed December 14, 2017].

Morrison CD, Pistell PJ, Ingram DK, Johnson WD, Liu Y, Fernandez-Kim SO, White CL, Purpera MN, Uranga RM, Bruce-Keller AJ, Keller JN (2010) High fat diet increases hippocampal oxidative stress and cognitive impairment in aged mice: implications for decreased Nrf2 signaling. J Neurochem 114:1581–1589.

Mortazavi A, Williams BA, McCue K, Schaeffer L, Wold B (2008) Mapping and quantifying mammalian transcriptomes by RNA-Seq. Nat Methods 5:621–628 Available at: http://www.nature.com/doifinder/10.1038/nmeth.1226.

Oh-hashi K, Koga H, Ikeda S, Shimada K, Hirata Y, Kiuchi K (2009) CRELD2 is a novel

endoplasmic reticulum stress-inducible gene. Biochem Biophys Res Commun 387:504–510 Available at: http://www.sciencedirect.com.uml.idm.oclc.org/science/article/pii/S0006291X09013990 [Accessed December 13, 2017].

Oh-hashi K, Norisada J, Hirata Y, Kiuchi K (2015) Characterization of the Role of MANF in Regulating the Secretion of CRELD2. Biol Pharm Bull 38:722–731 Available at: https://www.jstage.jst.go.jp/article/bpb/38/5/38_b14-00825/_article [Accessed December 13, 2017].

Paxinos G, Watson C (2007) The Rat Brain in Stereotaxic Coordinates, 6th ed. Elsevier Inc.

Plagemann A, Harder T, Rake A, Melchior K, Rohde W (1999a) Increased number of galanin-neurons in the paraventricular hypothalamic nucleus of neonatally overfed weanling rats. Brain Res 818:160–163.

Plagemann A, Harder T, Rake A, Voits M, Fink H, Rohde W, Dörner G (1999b) Perinatal elevation of hypothalamic insulin, acquired malformation of hypothalamic galaninergic neurons, and syndrome X-like alterations in adulthood of neonatally overfed rats. Brain Res 836:146–155.

Plagemann A, Harder T, Rake A, Waas T, Melchior K, Ziska T, Rohde W, Do G (1999c) Observations on the orexigenic hypothalamic neuropeptide Y-system in neonatally overfed weanling rats. J Neuroendocrinol 11:541–546.

Plagemann A, Heidrich I, Gotz F, Rohde W, Dorner G (1992) Obesity and enhanced diabetes and cardiovascular risk in adult rats due to early postnatal overfeeding. Exp Clin Endocrinol 99:154–158 Available at: http://www.ncbi.nlm.nih.gov/pubmed/1526266.

Rodrigues AL, De Moura EG, Fonseca Passos MC, Potente Dutra SC, Lisboa PC (2009) Postnatal early overnutrition changes the leptin signalling pathway in the hypothalamic-pituitary-thyroid axis of young and adult rats. J Physiol 587:2647–2661 Available at: http://doi.wiley.com/10.1113/jphysiol.2009.169045.

Rzehak P, Oddy WH, Mearin ML, Grote V, Mori TA, Szajewska H, Shamir R, Koletzko S, Weber M, Beilin LJ, Huang R-C, Koletzko B (2017) Infant feeding and growth trajectory patterns in childhood and body composition in young adulthood. Am J Clin Nutr 106:568–580 Available at: http://ajcn.nutrition.org/lookup/doi/10.3945/ajcn.116.140962.

Sawchenko PE, Swanson LW (1983) The organization of forebrain afferents to the paraventricular and supraoptic nuclei of the rat. J Comp Neurol 218:121–144.

Schnetkamp PPM (1995) Calcium homeostasis in vertebrate retinal rod outer segments. Cell Calcium 18:322–330 Available at: http://www.sciencedirect.com.uml.idm.oclc.org/science/article/pii/0143416095900284 [Accessed December 14, 2017].

Smith JT, Spencer SJ (2012) Preweaning over- and underfeeding alters onset of puberty in the rat without affecting kisspeptin 1. Biol Reprod 86:1–8.

Smith PM, Rozanski G, Ferguson A V. (2010) Acute electrical stimulation of the subfornical organ induces feeding in satiated rats. Physiol Behav 99:534–537.

Srikanth S, Jung H-J, Kim K-D, Souda P, Whitelegge J, Gwack Y (2010) A novel EF-hand protein, CRACR2A, is a cytosolic Ca2+ sensor that stabilizes CRAC channels in T cells. Nat Cell Biol 12:436–446 Available at: http://www.nature.com/doifinder/10.1038/ncb2045 [Accessed December 12, 2017].

Szathmari A, Champier J, Ghersi-Egea JF, Jouvet A, Watrin C, Wierinckx A, Fèvre Montange M (2013) Molecular characterization of circumventricular organs and third ventricle ependyma in the rat: Potential markers for periventricular tumors. Neuropathology 33:17–29.

Szathmari A, Jouvet A, Mottolese C, Champier J, Fèvre Montange M (2015) Anatomical, molecular and pathological consideration of the circumventricular organs. Neurochirurgie 61:90–100 Available at: http://dx.doi.org/10.1016/j.neuchi.2013.04.006.

Tanaka J, Hayashi Y, Shimamune S, Nomura M (1997) Ascending pathways from the nucleus of the solitary tract to the subfornical organ in the rat. Brain Res 777:237–241.

Tseng K-Y, Danilova T, Domanskyi A, Saarma M, Lindahl M, Airavaara M (2017) MANF is essential for neurite extension and neuronal migration in the developing cortex. eNeuro 4:214–217 Available at: http://eneuro.sfn.org/lookup/doi/10.1523/ENEURO.0214-17.2017 [Accessed December 12, 2017].

Voutilainen MH, Back S, Porsti E, Toppinen L, Lindgren L, Lindholm P, Peranen J, Saarma M, Tuominen RK (2009) Mesencephalic astrocyte-derived neurotrophic factor is neurorestorative in rat model of parkinson's disease. J Neurosci 29:9651–9659 Available at: http://www.ncbi.nlm.nih.gov/pubmed/8929429 [Accessed December 15, 2017].

White CL, Pistell PJ, Purpera MN, Gupta S, Hise TL, Keller JN, Ingram DK, Morrison CD, Bruce-keller AJ (2009) Effects of high fat diet on Morris maze performance, oxidative stress, and inflammation in rats: Contributions of maternal diet. Neurobiol Dis 35:3–13 Available at: http://dx.doi.org/10.1016/j.nbd.2009.04.002.

Whyment A, Top M Van Den, Lee K, Whyment AD, Blanks AM, Spanswick D (2004) Orexigen-sensitive NPY / AgRP pacemaker neuons in the hypothalamic arcuate nucleus.

Nat Neurosci 7:493–494.

Wiedmer P, Ortmann S, Klaus S (2002) Energy metabolism of young rats after early postnatal overnutrition. Br J Nutr 88:301 Available at: http://www.journals.cambridge.org/abstract_S000711450200168X.

Xie C, Mao X, Huang J, Ding Y, Wu J, Dong S, Kong L, Gao G, Li CY, Wei L (2011) KOBAS 2.0: A web server for annotation and identification of enriched pathways and diseases. Nucleic Acids Res 39:316–322.

Yang S, Yang H, Chang R, Yin P, Yang Y, Yang W, Huang S, Gaertig MA, Li S, Li XJ (2017) MANF regulates hypothalamic control of food intake and body weight. Nat Commun 8:579 Available at: http://www.ncbi.nlm.nih.gov/pubmed/28924165 [Accessed December 12, 2017].

Zhang X, Dong F, Ren J, Driscoll MJ, Culver B (2005) High dietary fat induces NADPH oxidase-associated oxidative stress and inflammation in rat cerebral cortex. Exp Neurol 191:318–325.

2.7. Connection between Chapter 2 and 3:

In addition to the first evidence that gene expression in the SFO is altered by early postnatal overnutrition, the data presented in chapter 2 also present a transcriptome of the rat SFO. However, to be certain that a transcript is truly expressed in the area of interest, RNAseq experiments require further validation, preferably with a secondary method. The preliminary comparison of the expression data from RNAseq with that from a previously published microarray as presented in chapter 2 indicate a good concordance between the two datasets. Thus in chapter 3 we combined the RNAseq data from chapter 2 with microarray data and information from the International Union of Pharamcologists database to produce a list of GPCRs and ion channels with validated expression in the SFO. GPCRs and ion channels are of particular interest as they determine the intrinsic electrical properties of neurons and allow binding of ligands to modulate the behaviour of neurons. Thus, the complement of GPCRs and ion channels expressed in the SFO is directly related to the ability of the SFO to sense signals of the physiological state and transduce this information to other homeostatic nuclei.

3. The verified ion channelome of the rat subfornical organ

3.1. Abstract

The subfornical organ (SFO) is a sensory circumventricular organ (CVO) located in the anteroventral third ventricle with critical roles in regulation of energy balance, osmoregulation, and cardiovascular output. Due to the unique absence of a blood-brain barrier in sensory CVOs and their synaptic connections to and from homeostatic control centres, sensory CVOs are critical to homeostasis. The ability of the SFO to detect and transduce circulatory signals is mediated by the population of ion channels and G-protein-coupled receptors (GPCR) expressed. To identify the ion channelome and GPCR transcriptome of the SFO, we mined our previously published RNAseq transcriptome of the rat SFO, compared the relative expression values to the microarray data from Hindmarch et al. for validation, and compared both datasets were compared to the IUPHAR Guide to Pharmacology database. We report the expression of 35 voltage-gated ion channels, 19 ligand-gated ion channels 13 other ion channels, and 75 GPCRs in the SFO. We also present electrophysiological data on voltage-gated K^+, Na^+ and Ca^{2+} currents in conjunction with expression data of α subunits for voltage-gated cation channels, and current clamp recordings indicating the presence of receptors for neurotensin, endothelin, and substance P. Furthermore, we have assembled a full updated list of expression of ion channels and receptors in the SFO. Here we present a dataset which reflect the channelome and GPCR-ome of the SFO which may serve as an important resource for further studies of ion channel and GPCR function in the SFO and regulation of energy balance and cardiovascular output.

3.2. Introduction

Most of the mammalian central nervous system (CNS) is protected from the constituents of the circulation by a blood-brain barrier. In contrast, sensory circumventricular organs (CVOs),

are unique structures in that they contain fenestrated capillaries which allow molecules to move freely from the circulation to the interstitial fluid between neurons. Neurons of sensory CVOs, which include the organum vasculosum of the lamina terminalis (OVLT), area postrema (AP), and the subfornical organ (SFO) express a wide variety of membrane receptors, placing them in a privileged position to detect circulating signals of physiological states. Moreover, neurons from sensory CVOs make synaptic connections with hypothalamic and brainstem homeostatic control centres (Phillips and Camacho, 1981; Lind et al., 1982; Shapiro and Miselis, 1985). The wide variety of receptors expressed by sensory CVO neurons allow them to respond to a numerous signalling molecules, and the complement of ion channels determine the unique electrophysiological properties of sensory CVO neurons (Fry and Ferguson, 2007; Medlock et al., 2018).

The SFO is a forebrain sensory CVO located on the anteroventral aspect of the third ventricle with demonstrated roles in homeostasis including hydromineral balance and osmoregulation (Felix, 1976; Mangiapane and Simpson, 1980a; Oka et al., 2015), cardiovascular output (Mangiapane and Simpson, 1983; Dai et al., 2013; Black et al., 2018), and energy balance (Smith et al., 2008, 2010), as well as immune function (Roth et al., 2002; Cerqueira et al., 2016) and reproduction (Limonta et al., 1981; Donevan et al., 1989). For example, the SFO has long been demonstrated as a sensor for angiotensin II (AngII) to drive thirst and modulate blood pressure (Mangiapane and Simpson, 1980a) via the renin-angiotensin system. The SFO also responds to numerous other signalling molecules to modules blood pressure and heart rate, as indicated by SFO microinjection studies (Smith and Ferguson, 1997, 2012; Smith et al., 2007; Black et al., 2018). The role of the SFO in modulation of cardiovascular output is further supported by lesion (Mangiapane and Simpson, 1980b; Mumford et al., 1989) and electrical

stimulation experiments (Ishibashi and Nicolaidis, 1981; Ferguson and Kasting, 1986). Similarly, animals with SFO lesions show decreased water and salt intake in response to AngII (Thunhorst et al., 1999), and stimulation of SFO neurons using DREADDs (Designer Drugs Exclusively Activated by Designer Drugs) promotes drinking and salt intake (Nation et al., 2016). A recent optogenetics study also shows subpopulations of SFO neurons which trigger or suppress thirst (Oka et al., 2015). Furthermore, SFO neurons show changes in electrical excitability when stimulated with numerous homeostatic hormones and neuropeptides such as angiotensin (Ono et al., 2001), ghrelin (Pulman et al., 2006), vasopressin (Washburn et al., 1999), orexin (Ono et al., 2008), and others. In addition to detecting signals within the circulation, the SFO also receives synaptic input from areas including the lateral hypothalamus (Gruber et al., 1987), the median preoptic nucleus (Gruber et al., 1987), the nucleus of the solitary tract (Miselis, 1982), and the paraventricular and supraoptic nuclei (Larsen et al., 1991; Cottrell and Ferguson, 2004). The SFO also sends axonal projections to various regions including the median preoptic nucleus (Lind et al., 1982, 1984), the paraventricular nucleus (Miselis, 1982) and the supraoptic nucleus (Lind et al., 1982; Sawchenko and Swanson, 1983), the arcuate nucleus of the hypothalamus (Gruber et al., 1987; Whyment et al., 2004), the lateral hypothalamus (Burton et al., 1976; Miselis, 1982), and OVLT (Lind et al., 1982). Therefore, the SFO is in a privileged position to integrate information regarding the homeostatic state of the periphery, transduce this information to homeostatic control centres and receive feedback from these same centres.

In 2008 (Hindmarch et al.) a microarray study demonstrated that the transcriptome of the SFO in rat was dramatically altered by both challenges to water and energy balance strongly suggesting that it is a dynamic integrator of homeostatic information; in contrast, very few changes in gene expression were observed in response to similar stimuli in the AP (Hindmarch et

al., 2011). These data also revealed the first list of G-protein-coupled receptors (GPCR) and ion channels expressed in the SFO under normal (control) conditions. Expression of selected individual transcripts, including a number of receptors with intriguing therapeutic potential have since been investigated (Smith et al., 2008; Alim et al., 2010; Smith and Ferguson, 2012; Hindmarch and Ferguson, 2015), however full-scale validation of the earlier transcriptomic data using similar conditions has not been undertaken. Recently, we published a study that utilised RNAseq to evaluate changes in SFO gene expression in rat caused by early postnatal overnutrition (Peterson et al., 2018). Preliminary comparison of the datasets generated by Hindmarch et al. (2008) and Peterson et al. (2018) indicated concordance between gene expression levels (R^2= 0.428; Two-way t-test)). In this study, we have mined both published datasets, and cross-referenced against the IUPHAR/BPS Guide to Pharmacology database (Ireland et al., 2017) in order to carry out a detailed analysis of expression of GPCRs and ion channels, thus providing a validated SFO-specific "GPCR-ome" and "ion channel-ome". These data will be of great interest to those investigating SFO physiology and its roles in regulation of homeostasis.

3.3. Methods

3.3.1. Cross-validation of RNAseq vs microarray gene expression data

Relative expression of transcripts identified by RNAseq in control rats (Peterson et al., 2018) were compared against those from control rats from a published Affymetrix 230 2.0 genome chip microarray dataset (Hindmarch et al., 2008) using gene ID as the common identifier. At all steps, alternate gene names were also manually checked to ensure no targets were missed. As the resulting list of genes found to be expressed by both RNAseq and microarray showed a good positive correlation ($R^2 = 0.43$) (Peterson et al., 2018) this list was compared against the IUPHAR/BPS Guide to Pharmacology database to identify the list of ion channels and GPCRs. Ion channels were further separated in to 3 categories based on their IUPHAR classification: ligand-gated ion channels (5-HT3 receptors, acid-sensing ion channels, epithelial sodium channels, $GABA_A$ receptors, glycine receptors, ionotropic glutamate receptors, IP3 receptors, nicotinic acetylcholine receptors, P2X receptors, and ZAC receptors), voltage-gated ion channels (CatSper and two-pore channels, cyclic nucleotide-regulated channels, potassium channels, ryanodine receptors, transient receptor potential channels, voltage-gated calcium channels, voltage-gated proton channels, and voltage-gated sodium channels), or other ion channels (aquaporin, chloride channels, connexins and pannexins, piezo channels, sodium-leak channel, non-selective, store-operated ion channels).

To identify transcripts only detected by one method, the IUPHAR database was also compared against the individual present lists for both RNAseq and microarray. The Rnor_6.0 genome assembly and the Affymetrix 230 2.0 genome chip annotation files were further checked against the database to differentiate between undetected transcripts and undetectable transcripts

(not in Rnor_6.0 annotation or no probe on the microarray); 10 were not present in Rnor_6.0, whereas 121 had no associated probes on the Affymetrix 230 2.0 genome chip.

3.3.2. Electrophysiological validation of selected GPCR and ion channel expression

Animal procedures and primary SFO neuron culture

All procedures were approved by the University of Manitoba Animal Care Committee in accordance with the Canadian Council for Animal Care. Male Sprague Dawley rats (150 ± 10 g) were provided *ad libitum* access to standard rat chow and water and kept in a light-controlled facility. Dissociated SFO cultures were prepared as previously reported (Pulman et al., 2006). Briefly, rats were sacrificed between the hours of 8 am and 12 pm (1:45 – 5:45 following lights on), the brain removed and placed in ice-cold oxygenated artificial cerebrospinal fluid (composition, in mM: 126 NaCl, 2.5 KCl, 1.25 NaH_2PO_4, 2 $MgCl_2$, 10 D-glucose, 26 $NaHCO_3$, 0.5 $CaCl_2$) for 2 minutes. A 3 mm block of tissue at the level of the hypothalamus containing the SFO was cut, placed in Hibernate A media (Gibco), and the SFO was microdissected away from the surrounding tissue. Isolated SFO was incubated in 10 mL Hibernate A media containing 5 mg of papain (Worthington) for 30 minutes at 37 ˚C, then washed three times in Hibernate A supplemented with 1X B-27 (Gibco) and gently triturated. Cells were centrifuged at approximately 3000g for 5 minutes and resuspended in Neurobasal A (Gibco) supplemented with 1X B-27 and 1X Glutamax (Gibco) and finally plated on glass-bottom culture dishes (MatTek). Cells were cultured for up to 5 days.

Electrophysiology and drugs

For all electrophysiology recordings, only cells with a starting access resistance of <30 MΩ and less than a 30% change, membrane seals >1 GΩ, and stable holding current in current

clamp were used. Data were acquired using a HEKA EPC10 patch clamp amplifier and Patchmaster 2x73.5 software (Mahone Bay, Nova Scotia, Canada). Cells were allowed to stabilise for at least 2 minutes after forming whole cell seal before recording.

For current clamp recordings, extracellular recording solution (Table 1, physiological) was perfused through the culture dish via a peristaltic pump at a flow rate of ~2 mL/min. Electrodes pulled from borosilicate glass (Sutter Instruments) had resistance of 2-5 MΩ when filled with intracellular solution (Table 2, physiological). Following 4 minutes of stable baseline recording, 10 nM neurotensin (Tocris; 1909), 100 pM endothelin (Tocris; 1160), or 1 μM substance P (Sigma; S6883) were washed over the cell for 2 minutes. Changes in membrane potential and action potential frequency of neurons during the response period (first 300 s following drug application) was determined in Spike 2 version 6.18 software, compared against a 100 s baseline period. Cells were considered responsive to the drug if either the membrane potential changed 2 or more standard deviations from the mean control membrane potential, or if they showed at least 2-fold change in action potential frequency, based on the greatest change from baseline in a 100 s interval during the response period.

For investigation of voltage-gated K^+ currents in SFO neurons, two voltage clamp protocols were performed to observe two distinct subtypes of K^+ currents observable in SFO neurons: the transient I_A and delayed-rectifier I_K. In order to record the total voltage-gated K+ current (I_{TOT}), neurons were subjected to a series of 500 ms depolarising steps in 10 mV increments from −70 to +30 mV following a 500 ms −80 mV hyperpolarising prepulse to remove inactivation. In order to record I_K, neurons were subjected to a series of 500 ms depolarising steps in 10 mV increments from −70 to +30 mV following a 500 ms −40 mV prepulse to

inactivate transient currents (Anderson et al., 2001; Medlock et al., 2018). To reveal the I_A component, I_K was subtracted from I_{TOT}.

For investigation of voltage-gated Na^+ currents, voltage dependence of inactivation, transient current density, and persistent current density were investigated. To measure transient current density, 15 ms-long 10 mV voltage steps from −90 to +50 mV were applied to neurons following a −100 mV pre-pulse. Persistent currents were elicited using a ramp from −100 mV to 0 mV over 1 s. In order to examine time dependent recovery from inactivation of Na^+ current, neurons were subjected to two 15 ms +20 mV pulses with a 2-910 ms recovery pulse at −80 mV between.

For voltage-gated Ca^{2+} currents, neurons were subjected to500 ms depolarising 10 mV voltage steps from −70 to +40 mV, preceded by a hyperpolarising a 500 ms −100 mV prepulse to remove inactivation. A current-voltage plot was constructed using the earliest time point at each voltage step from when the current activated.

3.4. Results

3.4.1. Development of complete list of GPCR and ion channel expression in the SFO

We have validated the expression of 67 ion channels and 75 GPCRs expressed in the SFO by RNAseq and microarray. Of the unvalidated transcripts identified, RNAseq uniquely detected 120 GPCRs and 103 ion channels, of which 89 and 32 respectively were lacking the associated probe on the microarray. Microarray identified 1 GPCR and 5 ion channels which RNAseq could not, of which 3 ion channels were not found in the Rnor 6 annotation used to identify transcripts. For GPCRs and most ion channel groups there is a correlation between RNAseq FPKM and microarray relative intensity ($R^2 = 0.36 – 0.82$; $p < 0.01$, ANOVA; Figure 3.1). Interestingly, no correlation was found between relative expression levels for both methods

for ligand gated ion channels ($R^2 = 0.086$; $p = 0.22$, ANOVA). A full list of all identified GPCRs and ion channels is available as supplementary data (Appendix Table A3.1).

3.4.2. Validation of selected receptors in SFO neurons

After examining the GPCR expression dataset, our attention was drawn to the expression of receptors for 3 neuropeptides in particular: neurotensin, substance P, and endothelin (Figure 3.2). Specifically, the expression levels of receptors for neurotensin and endothelin were notably higher than that of the type 1 angiotensin II receptor (24.4 FPKM/4.24 intensity). We were also intrigued by the expression of tachykinin receptors given their established role in water balance (Polidori et al., 1998). To investigate whether binding at these receptors can modulate the electrical excitability of SFO neurons, we applied their endogenous ligands to dissociated SFO neurons in current clamp and examined effects on membrane potential and action potential frequency.

Neurotensin

Neurotensin is a tridecapeptide first extracted from bovine hypothalamus and noted for its powerful hypotensive effect in rodents (Leeman, 1973; Rioux et al., 1981; Hawkins et al., 1989). Since its initial discovery, numerous roles have been identified for central neurotensin including energy balance (Levine et al., 1983; Cooke et al., 2009), water homeostasis (Rioux et al., 1981), and stress response (Rowe et al., 1997; Steele et al., 2017), among others (Clineschmidt and McGuffin, 1977; Fuxe et al., 1992). Moreover, though central and peripheral sources of neurotensin were long thought to be entirely separate (Nemeroff et al., 1977), recent *c-fos* evidence indicates that peripheral injections of neurotensin activate hypothalamic centres (Ratner et al., 2016). Whether this occurs via crossing the blood-brain barrier (Gevaert et al., 2016) or transduction from areas without a blood-brain-barrier including the SFO is currently unclear.

RNAseq and microarray data show expression of two receptors for the neuropeptide neurotensin (*Ntsr2* and *Ntsr3*), with particularly high expression levels (*Ntsr2*: 41.2 FKM/13.8 intensity, *Ntsr3*: 45.6 FPKM/0.83605 intensity; Figure 3.2). Given the marked expression of neurotensin receptors *Ntsr2* and *Ntsr3* and neurotensin's well-established roles in the same homeostatic processes as the SFO, including cardiovascular output (Leeman, 1973; Rioux et al., 1981; Mangiapane and Simpson, 1983; Hawkins et al., 1989; Dai et al., 2013; Black et al., 2018), feeding (Levine et al., 1983; Smith et al., 2008, 2010; Cooke et al., 2009), and osmoregulation (Felix, 1976; Mangiapane and Simpson, 1980a; Rioux et al., 1981; Oka et al., 2015), we sought to investigate the electrical effects of neurotensin on SFO neurons.

To validate the existence of neurotensin receptor proteins and to investigate the physiological role of neurotensin receptors in SFO neurons, we applied neurotensin to cultured dissociated SFO neurons (Figure 3.3A). Application of 10 nM neurotensin depolarised and/or increased action potential frequency of 42.9% (9/21) of dissociated SFO neurons. Mean depolarisation among responsive neurons was 5.2 ± 2.3 mV (n=9/21) and mean change in action potential frequency among responsive neurons was 1.9 ± 0.4 Hz (n=9/21).

Substance P

Tachykinins and their receptors are widely expressed in the central and peripheral nervous systems (Mantyh et al., 2018), in addition to the immune (Rameshwar and Gascón, 1996) and digestive systems (Mantyh et al., 2018), among others. Given the established role of central tachykinins in mediating angiotensin-induced water intake (Polidori et al., 1998) and salt intake (Polidori et al., 1994), we sought to investigate whether the *Tacr1* expression in the SFO translated to electrical effects. We validated the expression of *Tacr1* against microarray data, however its physiological relevance or which cells it is expressed in is not yet clear. We did not

see expression of any other tachykinin receptors above the threshold in either method (*Tacr1* = 1.80 FPKM/1.43 intensity; *Tacr2* = 0.03 FPKM/0.03 intensity*; Tacr3* = 0.28 FPKM/0.08 intensity). Although there are numerous mammalian tachykinins, we chose the endogenous ligand substance P an due to its high binding affinity to TACR1 relative to other tachykinins (Hershey and Krause, 1990). Application of 100 μM substance P depolarised and increased action potential frequency of SFO neurons such that length of action potential bursts was increased (Figure 3.3B; n=2/3).

Endothelin

Endothelin receptors ETRA and ETRB are the 45th and 3rd most highly expressed GPCRs in the SFO, respectively (*Etra*:10.4 FPKM./2.41 intensity; *Etrb*: 175.7 FPKM/33.9 intensity). Moreover, direct microinjection experiments show that endothelin at the SFO increase blood pressure (Wall et al., 1992), though due to the nature of *in vivo* experiments, it is not clear which cells are the site of endothelin action at the SFO. Recent evidence suggests that at least some ETRB receptors (ETRA was not investigated) are expressed on glial cells, where they act to promote lactate release from osmosensory Na_x cells, though those results focused on the role of endothelins in sensing of salt balance as opposed to blood pressure (Hiyama et al., 2013). Moreover, neither of these experiments examining endothelins at the SFO investigated the effects of endothelin on SFO neurons specifically, leaving some uncertainty as to whether endothelin receptors are expressed on neurons. The effects of endothelin on the electrical activity of single isolated rat SFO neurons has not been investigated. To further investigate the electrical effects of endothelin on SFO neurons, endothelin β was applied to dissociated neurons. Application of 100 pM endothelin β substantially depolarised SFO neurons (Figure 3.3C; n=3/7), confirming expression of a receptor for endothelin in rat SFO neurons specifically.

3.4.3. Validation of voltage-gated ion currents in SFO neurons.

One goal of the present study is to advance reconciliation of the observed ion currents with ion channel gene expression, in order gain a better understanding of the electrophysiological properties of SFO neurons. To that end, we have provided a validated list of ion channels expressed in the SFO as supplementary data (Supplementary Table 3.1). As numerous studies have investigated the properties of voltage-gated cation currents in SFO neurons (Washburn et al., 2000; Washburn and Ferguson, 2001a; Fry and Ferguson, 2007), we have focused on those channels and provided a list of voltage-gated K^+, Na^+, and Ca^{2+} channels expressed in the SFO alongside representative traces of these currents from SFO neurons.

Voltage-gated K^+ channels.

The validated dataset shows the presence of K^+ channels alpha subunits which encode both inactivating and non-inactivating K^+ currents, as has been previously observed (Washburn et al., 1999; Washburn and Ferguson, 2001a; Medlock et al., 2018). We validated the expression of 4 K_v1 channel subunits (*Kcna2,4-6*), the $K_v2.1$ channel subunit (*Kcnb1*), 4 K_v3 channel subunits (*Kcnc1-4*), the $K_v4.3$ channel subunit (*Kcnd3*), the $K_v6.2$ channel subunit (*Kcng2*), the $K_v7.5$ channel subunit (*Kcnq5*), $K_v10.1$ channel subunit (*Kcnv1*), and 2 K_v11 channels subunits (*Kcnh2,6*). RNAseq uniquely detected 2 K_v1 channel subunits (*Kcna1,3*), the $K_v2.2$ channel subunit (*Kcnb2*), the $K_v4.1$ channel subunit (*Kcnd1*), the Kv5.1 subunit (*Kcnf1*), 2 K_v6 channel subunits (*Kcng1,4*), 3 K_v7 channel subunits (*Kcnq2-4*), the $K_v8.1$ channel subunit (*Kcnv1*), the $K_v9.2$ channel subunit (*Kcns2*), the $K_v11.3$ channel subunit (*Kcnh7*), and the $K_v12.3$ channel subunit (*Kcnh4*). Microarray uniquely identified $K_v4.2$ (*Kcnd2*), as it is not present the most current rat gene annotation (Rnor 6).

In order to evaluate the contribution of I_A and I_K to the total K^+ current in SFO neurons, we subjected dissociated SFO neurons to several voltage protocols in voltage clamp by either removing inactivation with a hyperpolarising prepulse at −80 mV, or isolating I_K from I_A via a depolarising prepulse. We then generated a current-voltage plot from the peak outward current at each voltage step to illustrate the differences between voltage-dependence of activation (Figure 3.4D). We observed transient voltage-gated K^+ currents inactivated by depolarising voltage near −40 mV, the bulk of which are fully activated within a few ms but begin to inactivate within 100 ms, typical of I_A, and non-inactivating currents which display slower activation and inactivation times (Figure 3.4A-C) typical of I_K. Furthermore, I_A activated at a lower voltage than I_K, and had a larger peak current magnitude (Figure 3.4).

Voltage-gated Na^+ channels.

The importance of voltage-gated Na^+ currents in shaping the unique electrical properties of SFO neurons has been shown by previous authors (Washburn et al., 2000; Fry and Ferguson, 2007; Fry et al., 2008; Kuksis and Ferguson, 2015). In addition to the rapid upstroke of the action potential, Na^+ currents are thought to contribute to the subthreshold oscillations and bursting behaviour seen in SFO neurons (Washburn et al., 2000; Fry and Ferguson, 2007), and can be modulated by binding of signalling molecules (Fry et al., 2008; Kuksis and Ferguson, 2015). We have validated the expression of Na^+ channel α subunits $Na_v1.1$ (*Scn1a*: 4.10 FPKM/3.00 intensity), $Na_v1.2$ (*Scn2a*: 10.29 FPKM/4.72 intensity), $Na_v1.3$ (*Scn3a*: 6.43 FPKM/2.98 intensity), and $Na_v1.7$ (*Scn9a*: 8.62 FPKM/6.10 intensity). Furthermore, we have detected expression of $Na_v1.6$ (*Scn8a*: 3.45 FPKM/0.12 intensity) which is not validated by microarray.

In order to evaluate Na^+ current properties in SFO neurons, we separated transient and persistent Na^+ currents and examined their properties separately, in addition to the time-dependent recovery from inactivation of voltage-gated Na^+ currents. We observed large, transient Na^+ currents which fully activated and inactivated within 10 ms (Figure 3.5A-B), from which we generated inactivation and activation conductance curves. The activation curve revealed a voltage of ½ activation of -13.5 mV and a slope factor of -7.0, whereas the inactivation curve revealed a voltage of ½ inactivation of -45.2 mV and a slope factor of -4.1 (Figure 3.5C). We consistently observed persistent Na^+ currents (Figure 3.5D) when neurons were subjected to a 1 s ramp to remove the influence of transient voltage-gated Na^+ currents. Finally, we noted a relatively slow recovery from inactivation with a time constant τ of 120 ms (full recovery in approximately 300 ms) (Figure 3.5E-F); resurgent Na^+ currents are not observed in SFO neurons (data not shown).

Voltage-gated Ca^{2+} channels.

Though commonly studied for their effects on neurotensin release at synapses, voltage-gated Ca^{2+} currents at the soma also contribute to the intrinsic electrical properties of neurons. During the upstroke of an action potential, voltage-gated Ca^{2+} channels also allow for the influx of depolarising current to the neuron, though less than voltage-gated Na^+ channels. However, this influx of Ca^{2+} may also influence Ca^{2+}-dependent signalling pathways. Depending on the kinetics of the Ca^{2+} channel, they may also activate at a more hyperpolarised potential than voltage-gated Na^+ channels, and if this current is significantly large the neuron may reach the threshold for action potential firing. This is evident in some neurons which show a rebound depolarisation following hyperpolarisation, which removes their inactivation. Voltage-gated Ca^{2+} channels can also be modulated by binding of signalling molecules to membrane receptors: in SFO neurons, potentiation of Ca^{2+} channels in addition to other cations contributes to

depolarisation of neurons in response to Ang II (Washburn and Ferguson, 2001b) and hydrogen sulfide (Kuksis and Ferguson, 2015).

Electrophysiological evidence also shows the presence of L (Ca_v1), P/Q, and R-type (Ca_v2) Ca^{2+} currents in SFO neurons (Washburn and Ferguson, 2001b). We have validated the expression of 2 L-type channels (*Cacna1c:* 2.11 FPKM/1.58 intensity; Cacna1d: 2.99 FPKM/0.93 intensity) as well as N-type (*Cacna1b:* 5.85 FPKM/3.68 intensity), and further detected via RNAseq but not validated the expression of P/Q-type (*Cacna1a:* 4.67 FPKM/0.51 intensity), R-type (*Cacna1e*: 0.60 FPKM/ 0.10 intensity), and T-type channels (Ca_v3: *Cacna1g*: 8.68 FPKM/1.05 intensity; *Cacna1h*: 2.89 FPKM/0.43 intensity; *Cacna1i*: 4.15 FPKM/0.59 intensity). In voltage clamp recordings we observed the presence of low-voltage activated Ca^{2+} currents in addition to high-voltage activated Ca^{2+} currents (Figure 3.6). Furthermore, we also occasionally observed after-hyperpolarisation firing characteristic of T-type Ca^{2+} currents in current clamp recordings (Figure 3.6C).

3.5. Discussion

In this study we have provided a validated list of GPCRs and ion channels that are expressed in the rat SFO. Based on transcriptomic data, we have identified three transcripts whose effects on SFO neurons were not recorded previously and have demonstrated the action of ligands for these selected GPCRs (neurotensin, substance P, and endothelin), and provided examples of voltage gated-ion currents together with ion channel expression data. Together, these data will improve our understanding of the interaction with signalling molecules and electrical properties of SFO neurons.

The SFO plays a critical role in regulation of energy balance (Smith et al., 2010), fluid balance (Felix, 1976), and cardiovascular output (Mangiapane and Simpson, 1983). Previously published microarray data (Hindmarch et al., 2008; Szathmari et al., 2013) strengthened the evidence of the role of the SFO in these processes, while providing new research targets. We have validated the expression of transcripts for GPCRs and ion channels from the microarray dataset of Hindmarch et al. (2008). We are confident in these data as we have previously shown a positive correlation between expression levels of all comparable transcripts in the 2 datasets (Peterson et al., 2018), which is reflected in the GPCR, voltage-gated ion channel, and other ion channel data (Figure 3.1). RNAseq has superior dynamic range over microarray (Nagalakshmi et al., 2008), and due its difference in design does not suffer from limitations such as cross-hybridisation and limited probesets as does microarray. Moreover, when compared to protein expression levels, investigators report that RNAseq provides a more accurate measure of expression compared to microarray (Fu et al., 2009).

3.5.1. GPCRs

There is considerable interest in characterising the response of SFO neurons to a wide variety of signalling molecules and physiological stimuli (Lakhi et al., 2013; Oka et al., 2015; Nation et al., 2016; Simpson and Ferguson, 2017; Black et al., 2018). We have begun to investigate the expression and physiological relevance of three GPCRs with established roles in osmoregulation and cardiovascular output: *Ntsr2, Tacr1,* and *Etrb* (Leeman, 1973; Rioux et al., 1981; Massi et al., 1991; Wall et al., 1992). Our data suggest that *Ntsr2* and *Etrb* are among the most highly expressed GPCR transcripts in the SFO.

Neurotensin receptors

The tridecapeptide neurotensin and its receptors are of interest as they play roles in multiple homeostatic processes: neurotensin decreases food intake at the AP and NTS (Ratner et al., 2016), and via interaction with leptin in other nuclei (Hawkins et al., 1989), and ICV injected neurotensin increases drinking (Rioux et al., 1981) and has marked but variable effects on blood pressure (Leeman, 1973; Kérouac et al., 1981; Rioux et al., 1981; Ertl et al., 1993). There are at least two possible sources of NT input to the SFO: from the circulation (Reinecke, 1985), and from neurotensinogenic projections originating in the arcuate nucleus of the hypothalamus (Rosas-Arellano et al., 1996). Previous research provides evidence for binding of neurotensin to the SFO (Quirion et al., 1982) and evidence for protein expression of NTSR2 (Sarret et al., 2003b) and NTSR3 (Sarret et al., 2003a); taken together, these studies suggest a role for neurotensin in the regulation of blood pressure and thirst at the SFO. Current clamp recordings (Figure 3.3A) show that neurotensin depolarises neurons and promotes action potential firing in the SFO; the ionic mechanism is the subject of chapter 4. As both *NTSR2* and *NTSR3* are strongly expressed in the SFO, further research is required to dissect the individual contributions of these receptors to the

depolarising effect of neurotensin. However, NTSR3 has a primarily subcellular membrane localisation (Sarret et al., 2003a) and is thought to be concerned with intracellular trafficking (Evans et al., 2011) and neurotensin turnover (Petersen et al., 1997), suggesting that NTSR2 is likely to play the predominant role in neurotensin-mediated modulation of electrical activity.

Tachykinin receptors

Tachykinins are a large group of peptides first extracted from horse tissue and noted for their contractile effects on rabbit intestine (V Euler and Gaddum, 1931); this first tachykinin was named substance P. It is now evident that numerous other tachykinins exist (Pernow and Silva, 1955; Chapman et al., 1960; Kangawa et al., 1983; Minamino et al., 1983), and these are also implicated in numerous homeostatic processes including though not limited to cardiovascular regulation (Burcher et al., 1977; Loesch and Burnstock, 1988), nausea (Saito et al., 2013), salt appetite (Massi et al., 1991), water intake (Polidori et al., 1998). Specifically, central exposure to tachykinins inhibits salt and water intake (Massi et al., 1991). Notably, tachykinins show an inhibitory effect on angiotensin II-induced drinking (Polidori et al., 1998), one of the earliest and best-described roles of the SFO. In mammals, numerous distinct endogenous tachykinins have been discovered with differing affinities for their receptors. Tachykinins can be separated in to four distinct groups: Tac1, which encodes substance P, neurokinin A, neurokinin B, and neuropeptide γ, Tac2 which encodes neurokinin B, and Tac4, which encodes hemokinins and endokinins. Currently, 3 receptors have been identified: TACR1, TACR2, and TACR3, also known as neurokinin receptors 1-3.

However, not all tachykinin receptors are equally implicated in the homeostatic effects of tachykinins: TACR1 versus TACR3 appear to have different roles, as TACR3 agonists inhibit need-free sodium intake, whereas TACR1 agonists do not (Polidori et al., 1994), and instead

more strongly affect water intake (Polidori et al., 1998). Whereas previous research found evidence of TACR1 and TACR3 receptors at the SFO via radioligand binding (Saffroy et al., 1988; Larsen et al., 1992) and *c-fos* expression (Michl et al., 2001), we found that only mRNA *Tacr1* expression levels were above our threshold. Whether SFO neurons are affected by tachykinins to modulate salt and water intake is currently unclear, though we show that application of the tachykinin substance P to dissociated SFO neurons causes marked depolarisation (Figure 3.3), suggesting a role of tachykinins acting on SFO neurons. Further experiments with selective agonists and antagonists are required to more fully understand the response and distinguish what differing roles, if any, the different tachykinins receptors may play at the SFO.

Endothelin receptors

Our data also indicate the expression of receptors for the peptide hormone endothelin β (Figure 3.2 and Figure 3.3). *Etrb* (175.7 FPKM/33.9 intensity) was the most strongly expressed endothelin receptor, however we also observed expression of *Etra* (10.5 FPKM/2.41 intensity). Endothelins (ET-1 -2, and -3) were first discovered for their action as a potent vasoconstrictors (Hickey et al., 2017). However, receptors have since been discovered in a variety of tissues, including the brain (Motegi, 2016), and direct injection of endothelin to SFO increases blood pressure (Wall et al., 1992), suggesting endothelin modulates blood pressure through multiple systems. Previous research in mice showed the expression of endothelin receptors on Na_x-positive glia, and presented that endothelins can modulate synaptic activity via lactate release from glial cells (Hiyama et al., 2013). Notably, the expression profile of Na_x differs between mice and rats: mice may exclusively express Na_x within the SFO in ependymal cells, whereas evidence exists for Na_x in rat SFO ependymal cells and neurons (Nehmé et al., 2012). A 2009

study showed that ependymal cells may express ETRB, and show changes in intracellular Ca^{2+} concentrations, opening the possibility to ependymal signalling (Genzen et al., 2009). Other glial cells may also participate in or modulate signalling through the release of gliotransmitters (Navarrete and Araque, 2008), or changes in lactate production (Hiyama et al., 2013). Thus, there remains some uncertainty as to the expression profile of endothelin receptors in rats, as both RNAseq and microarray data here include glial cells, neurons, and the overlying ependymal layer. Whether neuronal, glial cells, epithelia cells, or a combination, are implicated in the hypertensive effect of endothelin action at the SFO is unclear (Wall et al., 1992), though the evidence we present here (Figure 3.3) suggests at least some activation of endothelin receptors on SFO neurons.

3.5.2. Voltage-gated cation channels

While receptors recognise and bind signalling molecules to initiate cell signalling cascades, ion channels shape the intrinsic electrical properties of neurons. There is an ongoing effort to characterise the specific ion currents of neurons and their responses to signalling molecules associated with specific channels in numerous cell types. Previous labs have attempted this using single-cell PCR with some success (Eberwine et al., 1992; Ono et al., 2005; Hoyda et al., 2007, 2009); however, this technique is particularly susceptible to contamination due to the difficulty in maintaining a RNase-free environment for patch clamping (Sucher et al., 2000). Furthermore, it can suffer from a high false negative rate due to the small amount of available cytoplasm for the reaction, decreasing the probability of high quality RNA for the reaction. Thus although a positive result is indicative of the presence of a channel transcript, a negative result may not indicate its absence. To aid the effort of reconciling channel expression data with electrophysiological data, we have extracted the population of voltage-gated K^+, Ca^{2+},

and Na^+ channel α subunits expressed in the SFO, with a focus on the K_v, Na_v, and Ca_v families, which share a well-conserved 4x6 transmembrane domain structure (Ertal et al., 2000; Goldin et al., 2000; Gutman et al., 2005).

Voltage-gated K^+ channels

Voltage-gated K^+ channels are a diverse class of protein, having members with different numbers of transmembrane segments (2, 4, 6, or 7) and methods of activation. Among the K_v family of voltage-gated K^+ channels, there are 12 subfamilies (K_v1-12 or KCNA-D, F-H, Q, S and V2). The best studied among these are the Shaker (K_v1/KCNA), Shab (K_v2/KCNB), Shaw (K_v3/KCNC), and Shal (K_v4/KCND) families. The K_v alpha subunit group also includes K_v5/KCNF, K_v6/KCNG, K_v8/KCNV, and K_v9/KCNS, KCNQ channels (K_v7), and the Ether a-go-go family, including EAG (K_v10/KCNH1,5), ERG (K_v11/KCNH2,6,7), and ELK (K_v12/KCNH3,4,8), which are not considered here.

The K_v family of voltage-gated K^+ channels share a conserved general structure of 4 heteromultimeric segments each composed of 6 transmembrane segments, centred around a pore formed from hairpin loops in each segment (Doyle et al., 1998). Voltage-gated K^+ channels exhibit considerable variable within their biophysical properties due to the splice variants of each subunit (Wang et al., 1996; Ohya et al., 1997), modifier subunits (Kramer et al., 1998), multiple potential heterotetrametric combinations of subunits, (Gutman et al., 2005), and post-translational modifications (Henke et al., 2004; Gubitosi-Klug et al., 2005). In this study, as in previous studies (Washburn et al., 1999; Washburn and Ferguson, 2001a; Medlock et al., 2018), we have demonstrated the presence of 2 distinct subclasses of voltage-gated K+ current: the rapidly activating and inactivating I_A current (Figure 3.4C), and the slow-inactivating delayed-rectifier I_K currents (Figure 3.4B).

The transient I_A current activates at hyperpolarised (<-40) potentials opposing depolarising current through other cation channels such as nonspecific cation channels and voltage-gated Na^+ channels, though it is quickly inactivated and thus overcome by voltage-gated Na^+ currents at more depolarised potentials. In SFO neurons, I_A is also thought to contribute to the characteristic membrane potential oscillations which are involved in SFO bursting behaviour (Medlock et al., 2018). Comparatively, I_K facilitates membrane repolarisation (Segal et al., 2018). The currents presented here are due to a combination of voltage-gated K^+ ion channels which were identified via RNAseq and microarray. Without being able to determine the ion channel subunits expressed within a particular neuron, it can be difficult to identify the specific ion channel complement based on current properties alone. Current information suggests that, of those subunits found to be expressed in the SFO, the $K_v1.1$ - $K_v1.6$, $K_v2.1$ and $K_v2.2$, $K_v3.1$ and $K_v3.2$, $K_v7.2$ and $K_v7.3$, as well as the K_v10 family subunits contribute to I_K, whereas the $K_v3.3$ and $K_v3.4$, as well as $K_v4.1$ and $K_v4.3$ contribute to I_A (Ono et al., 2005; Judge et al., 2008), though the currents produced by some subunits and specific combinations continue to be investigated. Other subunits, such as $K_v5.1$, $K_v6.1$, $K_v6.2$, $K_v6.4$, and $K_v9.2$, are non-functional unless associated with a member of the K_v2 family (Kramer et al., 1998; Judge et al., 2008), likely acting to modulate the I_K currents typically produced by those channels.

This SFO channelome provides an updated list of ion channels known to be expressed in the SFO which can be further investigated. We have validated the expression of 20 of 41 known voltage-gated K^+ channels in the K_v family, and present 9 transcripts detected uniquely by RNAseq which require further validation.

Voltage-gated Na^+ channels

Voltage-gated Na^+ channels play critical roles in driving neuronal excitability, where they are classically thought of as driving the rapid depolarisation phase of the action potential through allowing the rapid entry of Na^+ ions. They also to contribute to sub-threshold oscillations of membrane potential which contribute to the characteristic bursting firing patterns seen in some SFO neurons (Fry et al., 2008). In mammals, there are 9 voltage-gated Na^+ channelα subunits. The fully assembled channels are composed of four 6-transmembrane domains each with a filter pore between the 5^{th} and 6^{th} segments, connected by 3 linkers. The $Na_v1.1$-$Na_v1.3$ and $Na_v1.6$ isoforms are of particular interest as they are most heavily expressed in the CNS (Goldin et al., 2000).

The voltage-gated Na^+ current includes both a transient component, which activates and inactivates within 15 ms, and a persistent component. Subthreshold persistent Na^+ (I_{NaP}) current is unique in that, although it rapidly activates, it does not inactivate: unlike the rapidly inactivating components that produce transient currents, I_{NaP} may last several hundred ms. Only a small portion of transient Na^+ current comprises the non-inactivating portion, estimated at <4% of the peak transient current in some neuronal subtypes (Cummins et al., 2017b). In SFO neurons specifically, I_{NaP} is implicated in the subthreshold membrane potential oscillations (Fry and Ferguson, 2007).

Some components of Na^+ currents are notably different in SFO neurons. Intriguingly, SFO neurons display remarkably slow recovery from inactivation time constant (τ) of 120 ms, and fully recovering in ~300 ms (Figure 3.5E-F). Comparatively, hippocampal CA1 neurons fully recover within 20 ms (Cummins et al., 2017a), and fast-firing Purkinje neurons within 10 ms (Aman and Raman, 2007). The slow recovery from inactivation may be related to $Na_v1.7$

expression seen in SFO, which is preferentially expressed in PNS neurons as opposed to CNS neurons , but which was reported in HEK cells to show a considerably slower recovery from inactivation with a τ of 40 ms (Huang et al., 2014), compared to τ values of ~5 ms for $Na_v1.1$ and $Na_v1.6$ (Patel et al., 2015), ~15 ms for $Na_v1.3$ (Cummins et al., 2001). The recovery from inactivation seen in SFO neurons is slower still; the mechanism behind this is unknown.

The SFO is comprised of several subpopulations of neurons, between which the intrinsic electrical properties determined by ion channels subtly differ. Differential distributions of voltage-gated Na^+ channels underlie some of the electrical differences between the neurons in the shell and core SFO: a greater proportion of shell SFO neurons are more depolarised and are more electrically active than core SFO neurons, though core SFO neurons display a bursting firing pattern (Huang et al., 2019). Notably, core and shell SFO neurons also differ in their projections: both the core and shell subregions project to the PVN, though core SFO neurons project to magnocellular cells, whereas shell SFO neurons project to the parvocellular cells (Kawano and Masuko, 2010). This is an important distinction as these PVN cells differ in their pathways, such that magnocellular cells secrete oxytocin and vasopressin via the posterior pituitary, and parvocellular cells secrete corticotropin release hormone, vasopressin, and thyrotropin-releasing hormone on to the anterior pituitary. The core SFO neurons also send more axonal projections to the limbic bed nucleus stria of the terminalis (Swanson and Lind, 1986; McKinley et al., 2003; Hollis et al., 2008). Ultimately, these differences in electrical properties of SFO neurons may be linked to distinct physiological outputs. Further research is necessary to examine the differential distribution of voltage-gated Na^+ channels from the shell and the core regions of the SFO to fully understand how they contribute to differences in electrical behaviour.

Voltage-gated Ca^{2+} channels

Voltage-gated Ca^{2+} channels are composed of a pore-forming and voltage-sensing α_1 subunit, and in most types have 4 auxiliary subunits: the co-transcribed α_2 and δ subunits, the trafficking or membrane-localisation β subunit, and the γ subunit. The pore-forming subunits are sufficient to produce a Ca^{2+} current (Perez–Reyes et al., 1989) and are split in to 3 subgroups based on the current properties they confer and their sensitivity to different Ca^{2+} channel blockers: Ca_v1 (composed of CACNA1C, D, S, and F), which produce a long-lasting L-type current, Ca_v2 which produce P/Q-, N-, and R-type currents (CACNA1A, B, and E, respectively), and Ca_v3, which produce transient T-type currents (CACNAG-I) (Ertal et al., 2000). We have validated the expression of 2 L-type subunits ($Ca_v1.2$ and $Ca_v1.3$), and the N-type subunit ($Ca_v2.2$) as present via both RNAseq and microarray. Comparatively, RNAseq detected all known P/Q-, N-, and R-type subunits, and all known T-type subunits in the SFO. The roles of voltage-gated Ca^{2+} channels are broad and depend on their location, intensity, and the duration of Ca^{2+} influx.

L-type calcium channels are activated at depolarised membrane potentials and produce a long-lasting, slowly deactivating inward current (Helton et al., 2005). We did not observe the expression of $Ca_v1.1$ or $Ca_v1.4$; this is unsurprising as these are not highly expressed in the brain, and are instead primarily localised in skeletal muscle (Bannister and Beam, 2013) and the retina (Morgans, 2001; Berntson et al., 2003), respectively. Presynaptically, L-type channels have been shown to play a role in neurotransmitter release (Mortensen, 2013; Subramanian et al., 2013). However voltage-gated Ca^{2+} channels may also be localised to the cell soma or dendrites, and depending on their cell localisation, L-type channels may play different roles: in hippocampal neurons, the L-type channels we detected are thought to be primarily localised to the soma and

dendrites, where they contribute to excitation-transcription coupling (Biase et al., 2010). Excitation-transcription coupling is a mechanism by which electrical activity alters transcription to cause short or long term changes in cells, and is important for synaptic plasticity.

Both the Ca_v1 and Ca_v2 subfamilies are thought to alter gene expression via excitation-transcription-coupling (Wheeler et al., 2012). Similar to L-type channels, the Ca_{v2} group of P/Q-, N-, and R-type channels are also activated at depolarised voltages, though they are resistant to the L-type blockers and unlike L-type channels all are primarily expressed in neurons. Evidence suggests that all channels in this group can also be localised presynaptically and increase Ca^{2+} levels to promote neurotransmitter release (Wu et al., 1999; Huang et al., 2011). Furthermore, modulation of voltage-gated Ca^{2+} currents influences the electrical excitability of neurons. In SFO neurons, N-type Ca^{2+} currents are potentiated by binding of angiotensin or NaHS to increase electrical excitability in concordance with voltage-gated K^+ or Na^+ channels (Washburn and Ferguson, 2001b; Kuksis and Ferguson, 2015; Simpson and Ferguson, 2018). Furthermore, influx of Ca^{2+} via voltage-gated channels can be secondary to modulation of other voltage-gated channels to increase electrical excitability, and simply reflecting an increasing in action potential firing, as is the case with ghrelin in SFO neurons (Pulman et al., 2006).

T-type channels are unique among voltage-gated Ca^{2+} channels in that they activate at more hyperpolarised potentials (~−60 mV) and are inactivated quickly relative to L-type channels (Carbone and Lux, 1984; Bossu and Feltz, 1986). Structurally, T-type channels share a conserved pore-forming subunit structure with other voltage gated Ca^{2+} channels (Jan and Jan, 1990; Perez-Reyes, 2015), though they appear to lack auxiliary subunits (Leuranguer et al., 1998). Peterson et al. detected by RNAseq all 3 known T-type α subunit transcripts, whereas none were detected via microarray (Hindmarch et al., 2008). T-type channels are involved in

Ca^{2+}-mediated rebound depolarisation (also known as low-threshold spike) which follows hyperpolarisation, and may lead to a burst of firing mediated by Na^{+} channels (Jahnsen and Llinás, 1982; Jahnsen and Llinas, 1984). This is most evident in neurons with high frequency firing: expression of T-type Ca^{2+} channels is required for repetitive firing in the thalamus (Kim et al., 2001). Though the expression of T-type Ca^{2+} were only observed in the RNAseq dataset, the presence of rebound depolarisation action potential firing has been previously reported in SFO neurons (Washburn and Ferguson, 2001a). Furthermore, Washburn et al (Washburn and Ferguson, 2001a) also noted the presence of low-voltage activated Ca^{2+} currents in addition to high-voltage activated Ca^{2+} currents, though these are the first data to connect physiological evidence of low-voltage activated Ca^{2+} currents with expression data for the SFO. The physiological significance of the occasional presence of T-type Ca^{2+} currents is currently unclear. Neither the RNAseq nor the microarray data distinguish between peripheral or core SFO neurons, or neuronal and non-neuronal cells within the SFO; further research in to the specific expression pattern and subcellular localisation of the voltage-gated cation channels discussed here would help to resolve their physiological roles.

3.5.3. Conclusion

We have validated the expression of 75 GPCRs, 35 voltage-gated ion channels, 19 ligand-gated ion channels, and 13 other ion channels, expressed in the SFO via RNAseq and microarrray. We found a correlation between the relative expression levels from RNAseq and microarray data for all groups; intriguingly, the ligand-gated ion channels showed a poor correlation (Pearson's $R^2 = 0.03$) which was not statically significant ($p>0.05$). We have validated the expression of many receptors and ion channels previously known to be expressed in the SFO, including receptors for angiotensin and a subset of Na^{+}, K^{+}, and Ca^{2+} ion channels.

These include intriguing potential targets of future research including GPCRs, and voltage-gated Ca^{2+}, K^{+} and Na^{+} channel subunits.

The list of validated transcripts detected by both methods, as well as those detected by either RNAseq or microarray only, or not detected by either is available as supplementary data (Supplementary Table 1) and will aid in future research on SFO physiology. Given the role of SFO in energy balance, osmoregulation, and cardiovascular output, we expect these data will be useful to researchers interested in these processes and the development of treatments for obesity and hypertension.

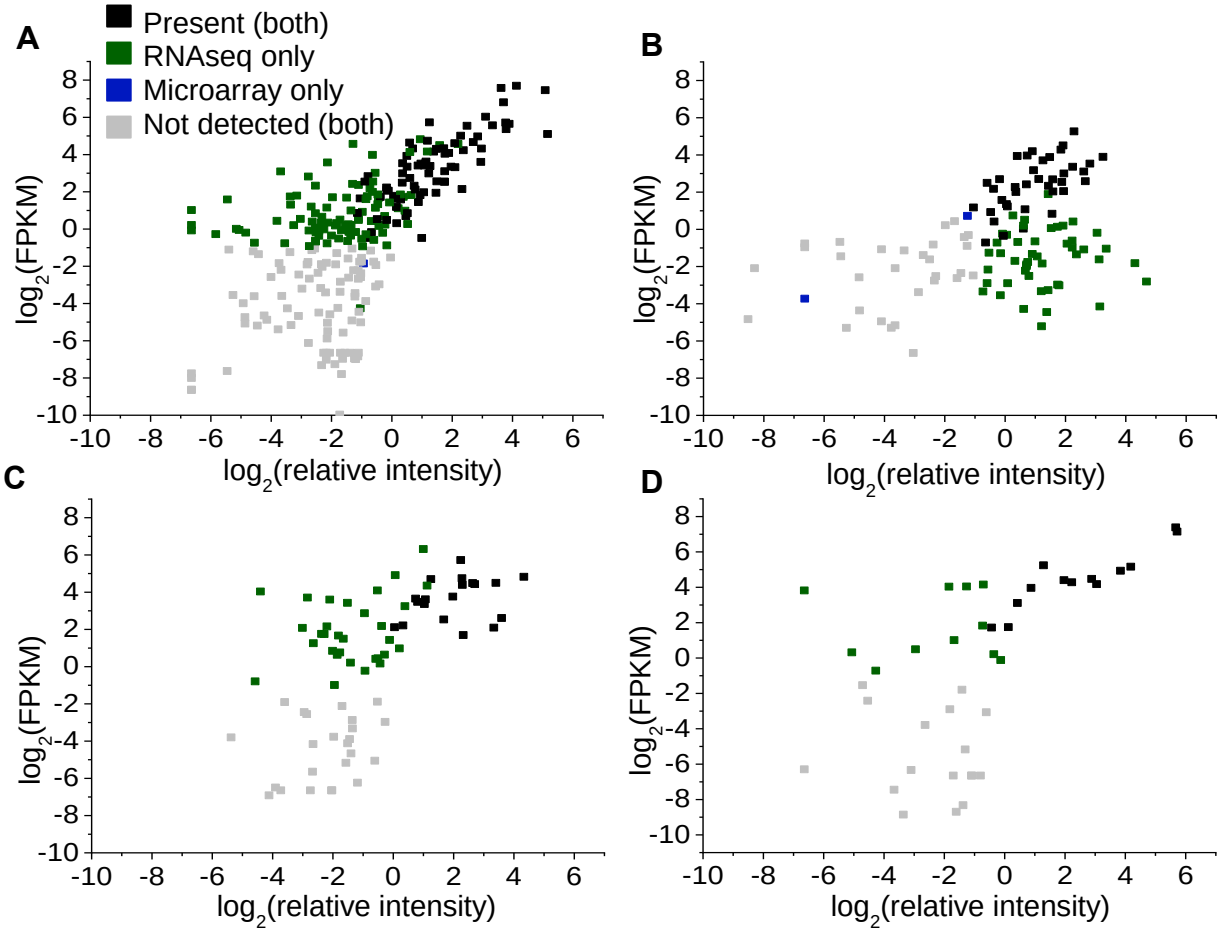
A
Present (both)
RNAseq only
Microarray only
Not detected (both)
log2(FPKM)
log2(relative intensity)
B
log2(FPKM)
log2(relative intensity)
C
log2(FPKM)
log2(relative intensity)
D
log2(FPKM)
log2(relative intensity)

Figure 3.1. Validation of RNAseq transcript relative expression levels using microarray data for **(A)** GPCRs (for 75 validated transcripts: R^2=0.62; p ≈ 0), **(B)** voltage-gated ion channels (for 40 validated transcripts: R^2=0.38; p = 2.17 x 10^{-5}), **(C)** ligand-gated ion channels (for 19 validated transcripts: R^2=0.08; p = 0.22), and **(D)** other ion channels (of 13 validated transcripts: R^2=0.82; p = 2.17 x 10^{-5}). Correlation was assessed only for transcripts detected by both methods. Ligand-gated ion channels include 5-HT3 receptors, acid-sensing ion channels, epithelial sodium channels, $GABA_A$ receptors, glycine receptors, ionotropic glutamate receptors, IP3 receptors, nicotinic acetylcholine receptors, P2X receptors, and ZAC receptors. Voltage-gated ion channels include CatSper and two-pore channels, cyclic nucleotide-regulated channels, potassium channels, ryanodine receptors, transient receptor potential channels, voltage-gated calcium channels, voltage-gated proton channels, and voltage-gated sodium channels. Other ion channels include aquaporin, chloride channels, connexins and pannexins, piezo channels, sodium-leak channel, non-selective, store-operated ion channels.

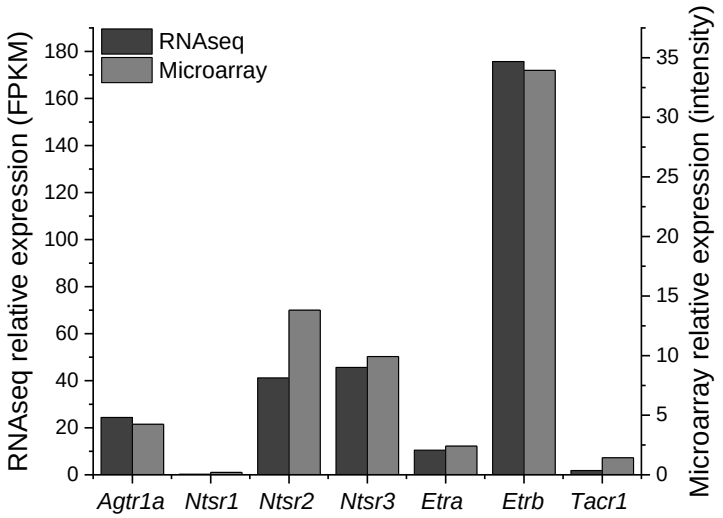

Figure 3.2. Relative expression levels from RNAseq (left axis) and microarray (right axis) of selected transcripts chosen for electrophysiological validation. Relative expression level of the angiotensin receptor is provided for comparison.

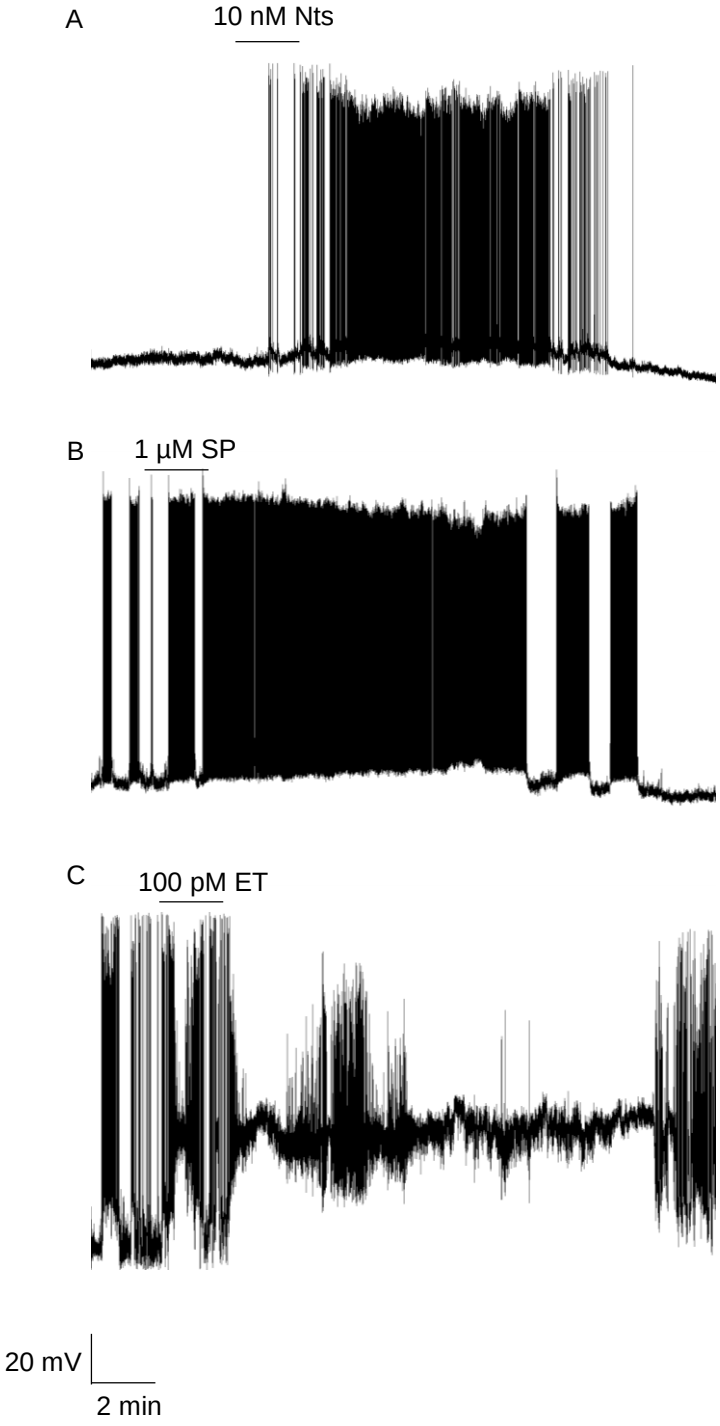
A
10 nM Nts
B
1 µM SP
C
100 pM ET
20 mV
2 min

Figure 3.3. Effects of neuropeptides neurotensin (Nts), Substance P (SP), and endothelin (ET) on dissociated SFO neurons. **(A)** Dissociated SFO neurons depolarise and increase action potential frequency in response to neurotensin. At 10 nM neurotensin (Nts), 42.9% of dissociated SFO neurons depolarise on average by 6.2 ± 2.3 mV (n=8) and increase action potential frequency by on average 1.9 ± 0.4 Hz (n=9). RNAseq data show expression of at least two receptors for neurotensin: *Ntsr2* and *Ntsr3*. **(B)** Dissociated SFO neurons depolarise and increase action potential frequency in response to substance P (SP). RNAseq data show expression of at least one receptor for SP: *Tacr1*. **(C)** Dissociated SFO neurons depolarise considerably in response to endothelin (ET). A receptor for endothelin (*Etrb*) is the 3rd most highly expressed GPCR in the SFO transcriptome.

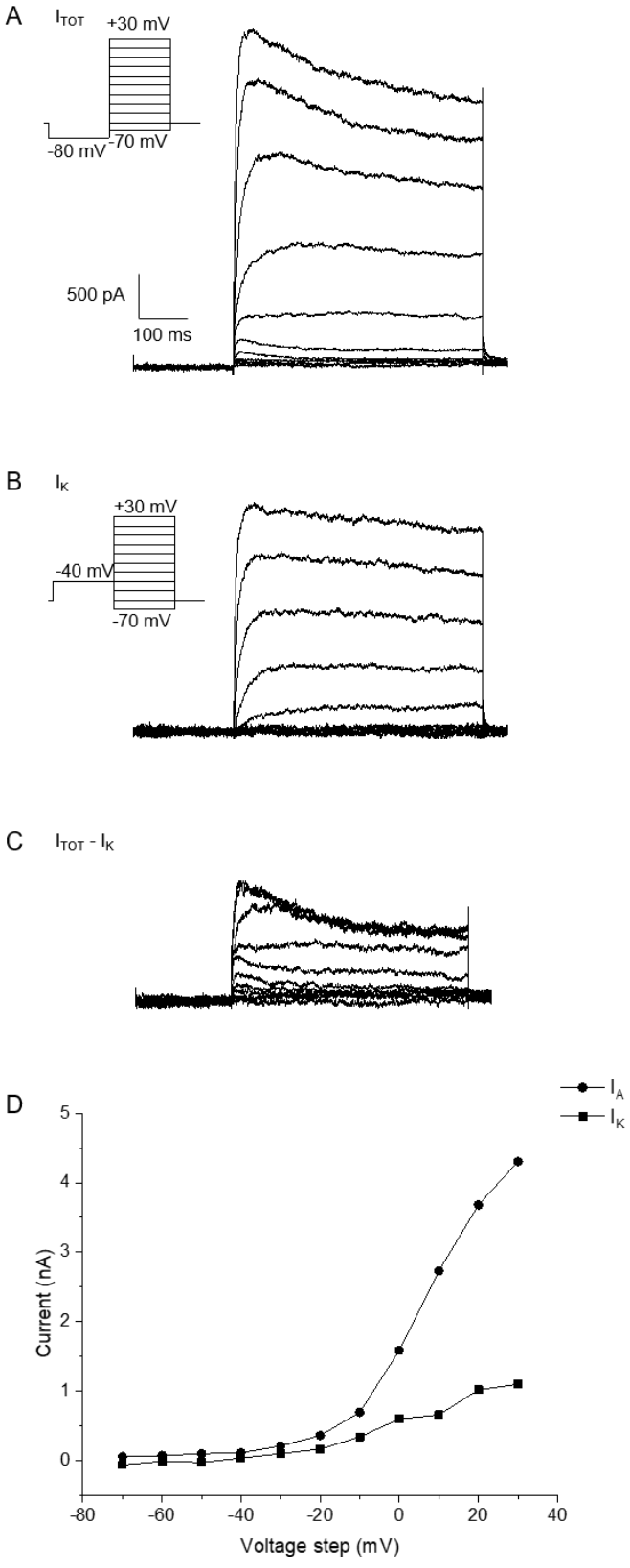
A
I_{TOT}
+30 mV
-80 mV
-70 mV
500 pA
100 ms
B
I_K
+30 mV
-40 mV
-70 mV
C
I_{TOT} - I_K
D
I_A
I_K
Current (nA)
Voltage step (mV)

Figure 3.4. SFO neurons display two distinct subtypes of voltage-gated K^+ current. K^+ currents were elicited using 10 mV current steps from -65 to +35 mV, using either a hyperpolarising (−100 mV) pre-pulse to record total K^+ current (I_{TOT}, **A**), or a depolarising pre-pulse (-30 mV) to examine only delayed-rectifier currents (I_K, **B**). Transient K^+ currents (I_A) are shown as the current remaining after subtracting I_K from total current **(C)**. **(D)** The VI plot generated from the currents in B and C show the differences between the I_A in I_K in terms of peak current and voltage-dependence of activation.

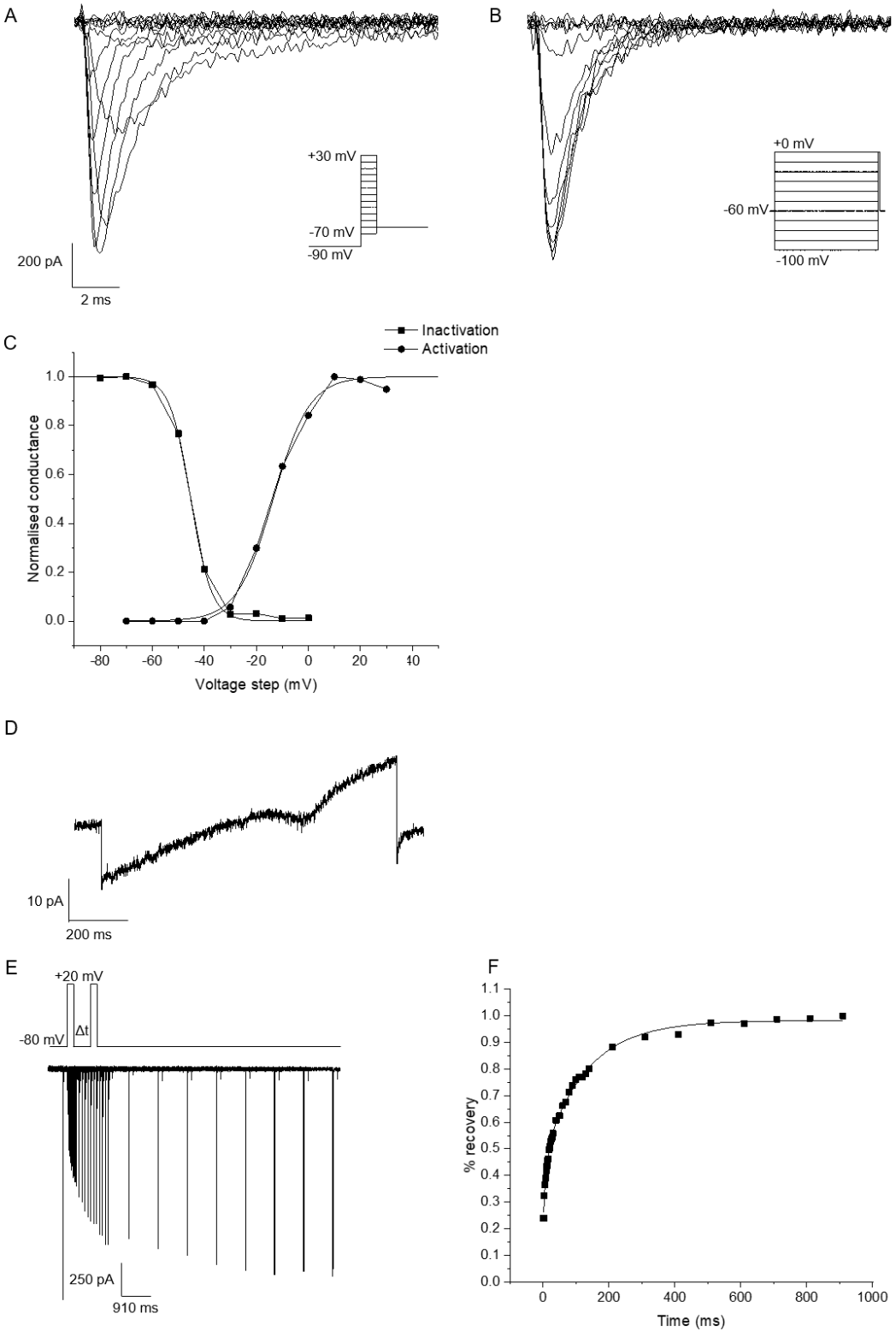
A
+30 mV
-70 mV
-90 mV
200 pA
2 ms
B
+0 mV
-60 mV
-100 mV
C
Inactivation
Activation
Normalised conductance
Voltage step (mV)
D
10 pA
200 ms
E
+20 mV
-80 mV
Δt
250 pA
910 ms
F
% recovery
Time (ms)

Figure 3.5. Properties of voltage-gated Na+ currents in SFO neurons. **(A)** Representative transient Na^+ currents from a SFO elicited using 15 ms 10 mV steps from −70 to +60 mV, following a −90 mV pre-pulse. **(B)** Representative recording from SFO neuron subjected to pre-pulses ranging from −100 mV to 0 mV I 10 mV steps, followed by a 15 ms pulse at 0 mV to investigate inactivation properties of voltage-gated Na^+ current in SFO neurons. **(C)** Results from A and B were used to generate activation and inactivation conductance curves for transient Na+ currents in this neuron. **(D)** Representative voltage trace of SFO neuron subjected to 1 s prolonged ramp from −100 to 0 mV. Persistent Na^+ current does not inactivate as quickly as transient Na^+ currents. **(E)** Representative trace of a SFO neuron subjected to two pulses at +20 mV with varying times between pulses (2-910 ms). **(F)** Results from E are plotted to investigate time-dependent recovery from inactivation, indicating a slow recovery from inactivation with a time constant of 120 ms.

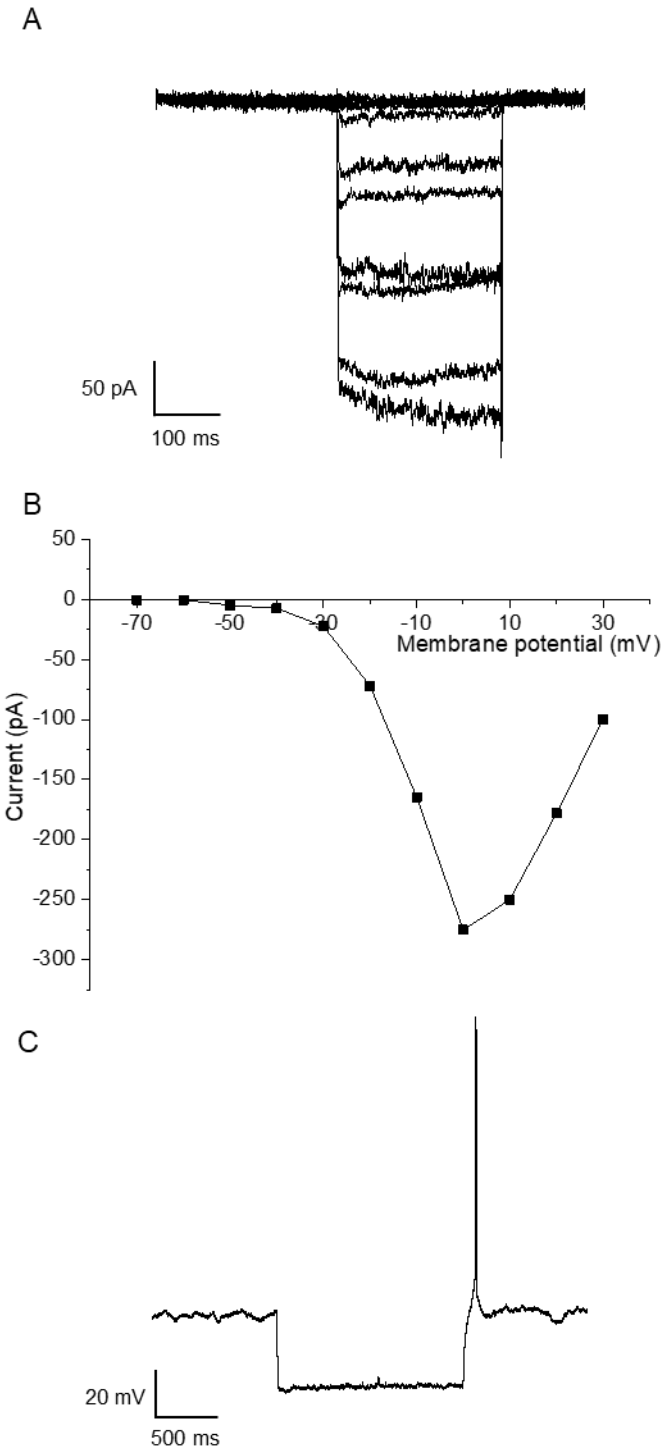
A
50 pA
100 ms
B
50
0
-50
-100
-150
-200
-250
-300
-70
-50
-30
-10
10
30
Membrane potential (mV)
Current (pA)
C
20 mV
500 ms

Figure 3.6. Numerous subtypes of channels make up voltage-gated Ca^{2+} current in SFO neurons. **(A)** Representative traces of voltage-gated Ca^{2+} currents from a dissociated SFO neuron. Ca^{2+} currents were investigated in Na^{+} and K^{+}-free solution and elicited using 10 mV current injections from -60 mV to +30 mV **(B)**. Current-voltage plot generated from Ca^{2+} current recording in A. Note inward current beginning at -50 mV, indicating the activation of low-voltage activated Ca^{2+} channels (T-type). **(C)** Activation of T-type channels causes a short-lived depolarisation, in this case reaching the action potential firing threshold of the neuron.

Table 3.1. Extracellular recording solutions used.

	Concentration (mM)			
Compound	Physiological	K+ Currents	Sodium Currents	Calcium Currents
NaCl	140	140	50	120
KCl	5	4	---	---
$CaCl_2$	2	1	1	---
$MgCl_2$	1	1	1	1
$BaCl_2$	---	---	1	1
$CslCl_2$	---	---	1	
$BaCl_2$	---	---	1	---
$CdCl_2$	---	---	0.3	---
TEA	---	---	100	10
4-AP	---	---	---	1
HEPES	10	10	10	10
Dextrose	`10	10	10	10
TTX	---	0.0005	---	0.0005

Table 3.2. Intracellular recording solutions used.

	Concentration (mM)			
Compound	Physiological	K+ Currents	Sodium Currents	Calcium Currents
K+ gluconate	130	120	---	---
$CsMeSO_4$	---	---	120	---
$CsCl_2$	---	---	---	140
NaCl	---	10	10	---
$CaCl_2$	1	---	---	0.1
KCl	10	---	---	---
$MgCl_2$	---	1	1	1
EGTA	5	10	---	10
HEPES	10	10	10	10
Dextrose	---	---	10	---
NaATP	4	4	2	2
NaGTP	0.1	0.1	0.2	0.2

3.6. References.

Alim I, Mark Fry W, Walsh MH, Ferguson A V. (2010) Actions of adiponectin on the excitability of subfornical organ neurons are altered by food deprivation. Brain Res 1330:72–82 Available at: http://dx.doi.org/10.1016/j.brainres.2010.02.076.

Aman TK, Raman IM (2007) Subunit dependence of Na channel slow inactivation and open channel block in cerebellar neurons. Biophys J 92:1938–1951.

Anderson JW, Smith PM, Ferguson A V. (2001) Subfornical organ neurons projecting to paraventricular nucleus: whole-cell properties. Brain Res 921:78–85.

Bannister RA, Beam KG (2013) CaV1.1: The atypical prototypical voltage-gated Ca2 + channel. Biochim Biophys Acta - Biomembr 1828:1587–1597.

Berntson A, Taylor WR, Morgans CW (2003) Molecular identity, synaptic localization, and physiology of calcium channels in retinal bipolar cells. J Neurosci Res 71:146–151.

Biase V Di, Obermair GJ, Szabo Z, Altier C, Bourinet E, Flucher BE (2010) Expression of postsynaptic CaV 1.2 calcium channel clusters is independent of interactions with AKAP79/150 and PDZ proteins. J Neurosci 28:13845–13855.

Black EAE, Smith PM, Mcisaac W, Ferguson A V (2018) Brain-derived neurotrophic factor acts at neurons of the subfornical organ to influence cardiovascular function. Physiol Rep 6:1–10 Available at: https://doi.org/10.14814/phy2.13704.

Bossu JL, Feltz A (1986) Inactivation of the low-threshold transient calcium current in rat sensory neurones: evidence ofr a dual process. J Physiol 376:341–357.

Burcher E, Atterhog JH, Pernow B, Rosell S (1977) Cardiovascular effects of substance P:

effects on the heart and regional blood flow in the dog. Raven Press New York.

Burton MJ, Rolls ET, Mora F (1976) Effects of hunger on the responses of neurons in the lateral hypothalamus to the sight and taste of food. Exp Neurol 51:668–677.

Carbone E, Lux HD (1984) A low voltage-activated, fully inactating Ca channel in vertebrate sensory neurones. Nature 310:501–502.

Cerqueira DR, Ferreira HS, Moiteiro ALBB, Fregoneze JB (2016) Effects of interleukin-1 beta injections into the subfornical organ and median preoptic nucleus on sodium appetite, blood pressure and body temperature of sodium-depleted rats. Physiol Behav 163:149–160 Available at: http://dx.doi.org/10.1016/j.physbeh.2016.05.003.

Chapman LF, Ramos A, Goodell H, Wolff HG (1960) Neurokinin--a polypeptide formed during neuronal activity in man. Observations on the axon reflex and antidromic dorsal root stimulation. Trans Am Neurol Assoc 85:42–45.

Clineschmidt B V., McGuffin JC (1977) Neurotensin administered intracisternally inhibits responsiveness of mice to noxious stimuli. Eur J Pharmacol 46:395–396.

Cooke JH, Patterson M, Patel SR, Smith KL, Ghatei MA, Bloom SR, Murphy KG (2009) Peripheral and central administration of xenin and neurotensin suppress food intake in rodents. Obesity 17:1135–1143.

Cottrell GT, Ferguson A V. (2004) Sensory circumventricular organs: Central roles in integrated autonomic regulation. Regul Pept 117:11–23.

Cummins TR, Aglieco F, Renganathan M, Herzog RI, Dib-Hajj SD, Waxman SG (2001) Nav1.3 sodium channels: rapid repriming and slow closed-state inactivation display quantitative

differences after expression in a mammalian cell line and in spinal sensory neurons. J Neurosci 21:5952–5961 Available at: http://www.ncbi.nlm.nih.gov/pubmed/11487618.

Cummins TR, Donnelly DF, Haddad GG (2017a) Effect of metabolic inhibition on the excitability of isolated hippocampal CA1 neurons: developmental aspects. J Neurophysiol 66:1471–1482.

Cummins TR, Xia Y, Haddad GG (2017b) Functional properties of rat and human neocortical voltage-sensitive sodium currents. J Neurophysiol 71:1052–1064.

Dai L, Smith PM, Kuksis M, Ferguson A V. (2013) Apelin acts in the subfornical organ to influence neuronal excitability and cardiovascular function. J Physiol 591:3421–3432.

Donevan SD, Van Vugt DA, Ferguson A V. (1989) Subfornical organ activation stimulates luteinizing hormone secretion in the rat. Brain Res 488:398–402.

Doyle DA, Doyle DA, Cabral M, Pfuetzner RA, Kuo A, Gulbis JM, Cohen SL, Chait BT, Mackinnon R (1998) The structure of the potassium channel: molecular basis of K+ conduction and selectivity. Science (80-) 280:69–77.

Eberwine J, Yeh H, Miyashiro K, Cao Y, Nair S, Finnell R, Zettel M, Coleman P (1992) Analysis of gene expression in single live neurons. Proc Natl Acad Sci U S A 89:3010–3014 Available at: http://www.pubmedcentral.nih.gov/articlerender.fcgi?artid=48793&tool=pmcentrez&rendertype=abstract.

Ertal EA, Campbell KP, Harpold MM, Hofman F, Mori Y, Perez-Reyes E, Schwartz A, Snutch TP, Tanabe T, Birnbaumer L, Tsein RW, Catterall WA (2000) Nomenclature of voltage-

gated calcium channels. Neuron 25:533–535.

Ertl G, Bauer B, Becker H-H, Rose G (1993) Effects of neurotensin and neuropeptide Y on coronary circulation and myocardial function in dogs. Am J Physiol Circ Physiol 264:H1062–H1068.

Evans SF, Irmady K, Ostrow K, Kim T, Nykjaer A, Saftig P, Blobel C, Hempstead BL (2011) Neuronal brain-derived neurotrophic factor is synthesized in excess, with levels regulated by sortilin-mediated trafficking and lysosomal degradation. J Biol Chem 286:29556–29567.

Felix D (1976) Peptide and acetylcholine action on neurones of the cat subfornical organ. Naunyn Schmiedebergs Arch Pharmacol 292:15–20.

Ferguson A V., Kasting NW (1986) Electrical stimulation in subfornical organ increases plasma vasopressin concentrations in the conscious rat. Am J Physiol Integr Comp Physiol 251:R425–R428.

Fry M, Cottrell GT, Ferguson A V. (2008) Prokineticin 2 influences subfornical organ neurons through regulation of MAP kinase and the modulation of sodium channels. Am J Physiol Integr Comp Physiol 295:R848–R856.

Fry M, Ferguson A V (2007) Subthreshold oscillations of membrane potential of rat subfornical organ neurons. Neuroreport 18:1389–1393 Available at: https://insights-ovid-com.uml.idm.oclc.org/pubmed?pmid=17762719 [Accessed May 24, 2018].

Fu X, Fu N, Guo S, Yan Z, Xu Y, Hu H, Menzel C, Chen W, Li Y, Zeng R, Khaitovich P (2009) Estimating accuracy of RNA-Seq and microarrays with proteomics. BMC Genomics 10:1–9.

Fuxe K, Von Euler G, Agnati LF, Pich EM, O'Connor WT, TanganelliI S, Li XM, Tinner B, Cintra A, Carani C, Benfenati F (1992) Intramembrane interactions between neurotensin receptors and dopamine D 2 receptors as a major mechanism for the neuroleptic-like action of neurotensin. Ann N Y Acad Sci 668:186–204.

Genzen JR, Platel JC, Rubio ME, Bordey A (2009) Ependymal cells along the lateral ventricle express functional P2X7 receptors. Purinergic Signal 5:299–307.

Gevaert B, Wynendaele E, Stalmans S, Bracke N, D'Hondt M, Smolders I, Van Eeckhaut A, De Spiegeleer B (2016) Blood-brain barrier transport kinetics of the neuromedin peptides NMU, NMN, NMB and NT. Neuropharmacology 107:460–470.

Goldin AL, Barchi RL, Caldwell JH, Hofmann F, Howe JR, Hunter JC, Kallen RG, Mandel G, Meisler MH, Netter YB, Noda M, Tamkun MM, Waxman SG, Wood JN, Catterall WA (2000) Nomenclature of voltage-gated sodium channels. Neuron 28:365–368.

Gruber K, McRae-Degueurce A, Wilkin LD, Mitchell LD, Johnson AK (1987) Forebrain and brainstem afferents to the arcuate nucleus in the rat : potential pathways for the modulation of hypophyseal secretions. Neurosci Lett 75:1–5 Available at: http://www.ncbi.nlm.nih.gov/pubmed/3574762 [Accessed November 13, 2015].

Gubitosi-Klug RA, Mancuso DJ, Gross RW (2005) The human Kv1.1 channel is palmitoylated, modulating voltage sensing: Identification of a palmitoylation consensus sequence. Proc Natl Acad Sci 102:5964–5968.

Gutman GA, Chandy KG, Grissmer S, Lazdunski M, Mckinnon D, Pardo LA, Robertson GA, Rudy B, Sanguinetti MC, Stu W, Wang X (2005) Nomenclature and molecular relationships of voltage-gated potassium channels. Pharmacol Rev 57:473–508.

Hawkins MF, Baker JD, Baumeister AA (1989) Neurotensin-induced polydipsia: a structure-activity study. Brain Res 487:188–191.

Helton TD, Xu W, Lipscombe D (2005) Neuronal L-Type calcium channels open quickly and are inhibited slowly. J Neurosci 25:10247–10251.

Henke G, Maier G, Wallisch S, Boehmer C, Lang F (2004) Regulation of the voltage gated K+ channel Kv1.3 by the ubiquitin ligase Nedd4-2 and the serum and glucocorticoid inducible kinase SGK1. J Cell Physiol 199:194–199.

Hershey AD, Krause JE (1990) Molecular characterization of a functional cDNA encoding the rat substance P receptor. Science (80-) 247:958–962.

Hickey KA, Rubanyi G, Paul RJ, Highsmith RF (2017) Characterization of a coronary vasoconstrictor produced by cultured endothelial cells. Am J Physiol Physiol 248:C550–C556.

Hindmarch C, Fry M, Yao ST, Smith PM, Murphy D, Ferguson A V (2008) Microarray analysis of the transcriptome of the subfornical organ in the rat: regulation by fluid and food deprivation. Am J Physiol Regul Integr Comp Physiol 295:R1914-20.

Hindmarch CCT, Ferguson A V (2015) Physiological roles for the subfornical organ: a dynamic transcriptome shaped by autonomic state. J Physiol 6:1581–1589 Available at: http://www.ncbi.nlm.nih.gov/pubmed/26227400 [Accessed November 8, 2015].

Hindmarch CCT, Fry M, Smith PM, Yao ST, Hazell GGJ, Lolait SJ, Paton JFR, Ferguson A V, Murphy D (2011) The transcriptome of the medullary area postrema: the thirsty rat, the hungry rat and the hypertensive rat. Exp Physiol 96:495–504 Available at:

http://www.ncbi.nlm.nih.gov/pubmed/21317217 [Accessed October 8, 2015].

Hiyama TY, Yoshida M, Matsumoto M, Suzuki R, Matsuda T, Watanabe E, Noda M (2013) Endothelin-3 expression in the subfornical organ enhances the sensitivity of Nax, the brain sodium-level sensor, to suppress salt intake. Cell Metab 17:507–519 Available at: http://dx.doi.org/10.1016/j.cmet.2013.02.018.

Hollis JH, McKinley MJ, D'Souza M, Kampe J, Oldfield BJ (2008) The trajectory of sensory pathways from the lamina terminalis to the insular and cingulate cortex: a neuroanatomical framework for the generation of thirst. Am J Physiol Integr Comp Physiol 294:R1390–R1401.

Hoyda TD, Fry M, Ahima RS, Ferguson A V. (2007) Adiponectin selectively inhibits oxytocin neurons of the paraventricular nucleus of the hypothalamus. J Physiol 585:805–816.

Hoyda TD, Smith PM, Ferguson A V. (2009) Adiponectin acts in the nucleus of the solitary tract to decrease blood pressure by modulating the excitability of neuropeptide Y neurons. Brain Res 1256:76–84 Available at: http://dx.doi.org/10.1016/j.brainres.2008.12.012.

Huang J, Yang Y, Dib-Hajj SD, van Es M, Zhao P, Salomon J, Drenth JPH, Waxman SG (2014) Depolarized inactivation overcomes impaired activation to produce DRG neuron hyperexcitability in a Nav1.7 mutation in a patient with distal limb pain. J Neurosci 34:12328–12340 Available at: http://www.jneurosci.org/cgi/doi/10.1523/JNEUROSCI.2773-14.2014.

Huang S, Egan J, Fry WM (2019) Electrophysiological Properties of Rat Subfornical Organ Neurons Expressing Calbindin D28K. Neuroscience 404:459–469 Available at: https://www.sciencedirect.com/science/article/pii/S0306452219301198?dgcid=rss_sd_all.

Huang Z, Lujan R, Kadurin I, Uebele VN, Renger JJ, Annette C, Shah MM (2011) Pre-synaptic HCN1 channels regulate excitatory neurotransmission at select cortical synapses by altering CaV3.2 Ca2+ channel activity. Nat Neurosci 14:478–486.

Ireland S, Bruce L, Southan C, Levi-Schaffer F, Sharman JL, Faccenda E, Davies JA, Fabbro D, Pawson AJ, Alexander SPH, Anderton S, Harding SD, Spedding M, Bryant C, Davenport AP, Gray AJG, Doerig C (2017) The IUPHAR/BPS Guide to PHARMACOLOGY in 2018: updates and expansion to encompass the new guide to IMMUNOPHARMACOLOGY. Nucleic Acids Res 46:D1091–D1106.

Ishibashi S, Nicolaidis S (1981) Hypertension induced by electrical stimulation of the subfornical organ (SFO). Brain Res Bull 6:135–139.

Jahnsen AH, Llinás RR (1982) Electrophysiology of mammalian thalamic neurons in vitro. Nature 279:406–408.

Jahnsen H, Llinas RR (1984) Ionic basis for the electroresponsiveness and oscillatory properties of guinea-pig thalamic neurones in vitro. J Physiol 429:227–247.

Jan L, Jan Y (1990) A superfamily of ion channels. Nature 345:672.

Judge S, Smith P, Stewart P, Bever Jr. C (2008) Potassium Channel Blockers and Openers as CNS Neurologic Therapeutic Agents. Recent Pat CNS Drug Discov 2:200–228.

Kangawa K, Minamino N, Fukuda A, Matsuo H (1983) Neuromedin K: A novel mammalian tachykinin identified in porcine spinal cord. Biochem Biophys Res Commun 114:533–540 Available at: http://www.sciencedirect.com/science/article/pii/0006291X83908136.

Kawano H, Masuko S (2010) Region-specific projections from the subfornical organ to the

paraventricular hypothalamic nucleus in the rat. Neuroscience 169:1227–1234 Available at: http://dx.doi.org/10.1016/j.neuroscience.2010.05.065.

Kérouac R, Rioux F, St-Pierre S (1981) Mechanism of neurotensin-induced pressor effect and tachycardia in guinea pigs. Life Sci 28:2477–2487.

Kim D, Song I, Keum S, Lee T, Jeong M-J, Kim S-S, McEnery MW, Shin H-S (2001) Lack of the Burst Firing of Thalamocortical Relay Neurons and Resistance to Absence Seizures in Mice Lacking α1G T-Type Ca2+ Channels. Neuron 31:35–45 Available at: http://www.sciencedirect.com/science/article/pii/S0896627301003439.

Kramer JW, Post MA, Brown AM, Kirsch GE (1998) Modulation of potassium channel gating by coexpression of Kv2.1 with regulatory Kv5.1 or Kv6.1 alpha-subunits. Am J Physiol 274:C1501-10 Available at: http://www.ncbi.nlm.nih.gov/pubmed/9696692.

Kuksis M, Ferguson A V. (2015) Actions of a hydrogen sulfide donor (NaHS) on transient sodium, persistent sodium, and voltage-gated calcium currents in neurons of the subfornical organ. J Neurophysiol 114:1641–1651.

Lakhi S, Snow W, Fry M (2013) Insulin modulates the electrical activity of subfornical organ neurons. Neuroreport 24:329–334.

Larsen PJ, Jessop DS, Chowdrey HS, Mikkelsen JD, Lightman SL (1992) Osmotic regulation of substance P and neurokinin A peptide content and substance P binding sites in distinct hypothalamic nuclei of the rat. Peptides 13:705–712.

Larsen PJ, Møller M, Mikkelsen JD (1991) Efferent projections from the periventricular and medial parvicellular subnuclei of the hypothalamic paraventricular nucleus to

circumventricular organs of the rat: A Phaseolus vulgaris-leucoagglutinin (PHA-L) tracing study. J Comp Neurol 306:462–479.

Leeman SE (1973) The isolation of a new hypotensive from bovine hypothalamus. J Biol Chem 248:6854–6861.

Leuranguer V, Bourinet E, Lory P, Nargeot J (1998) Antisense depletion of β-subunits fails to affect T-type calcium channels properties in a neuroblastoma cell line. Neuropharmacology 37:701–708.

Levine AS, Kneip J, Grace M, Morley JE (1983) Effect of centrally administered neurotensin on multiple feeding paradigms. Pharmacol Biochem Behav 18:19–23.

Limonta P, Maggi R, Giudici D, Martini L, Flavio P (1981) Role of the subfornical organ (SFO) in the control of gonadotropin secretion. Brain Res 229:75–84.

Lind RW, Hoesen GW van, Johnson AK (1982) An HRP study of the connections of the subfornical organ of the rat. J Comp Neurol 210:265–277.

Lind RW, Swanson LW, Ganten D (1984) Angiotensin II immunoreactivity in the neural afferents and efferents of the subfornical organ of the rat. Brain Res 321:209–215.

Loesch A, Burnstock G (1988) Ultrastructural localisation of serotonin and substance P in vascular endothelial cells of rat femoral and mesenteric arteries. Anat Embryol (Berl) 178:137–142.

Mangiapane ML, Simpson JB (1980a) Subfornical organ: forebrain site of pressor and dipsogenic action of angiotensin II. Am J Physiol 239:R382-9 Available at: http://www.ncbi.nlm.nih.gov/pubmed/7435651 [Accessed November 13, 2015].

Mangiapane ML, Simpson JB (1980b) Subfornical organ lesions reduce the pressor effect of systemic angiotensin II. Neuroendocrinology 31:380–384.

Mangiapane ML, Simpson JB (1983) Drinking and pressor responses after acetylcholine injection into subfornical organ. AJP Regul Integr Comp Physiol 244:R508-13.

Mantyh P, Gates T, Mantyh C, Maggio J (2018) Autoradiographic localization and characterization of tachykinin receptor binding sites in the rat brain and peripheral tissues. J Neurosci 9:258–279.

Massi M, Polidori C, Perfumi M, Gentili L, de Caro G (1991) Tachykinin receptor subtypes involved in the central effects of tachykinins on water and salt intake. Brain Res Bull 26:155–160.

McKinley MJ, McAllen RM, Giles ME, Penschow J, Sunn N, Uschakov A, Oldfield BJ (2003) The sensory circumventricular organs of the mammalian brain. Adv Anat Cell Biol 172:III–XII, 1–122, back cover.

Medlock L, Shute L, Fry M, Standage D, Ferguson A V. (2018) Ionic mechanisms underlying tonic and burst firing behavior in subfornical organ neurons: a combined experimental and modeling study. J Neurophysiol 120:2269–2281.

Michl T, Jocic M, Schuligoi R, Holzer P (2001) Role of tachykinin receptors in the central processing of afferent input from the acid-threatened rat stomach. Regul Pept 102:119–126 Available at: http://www.sciencedirect.com/science/article/pii/S0167011501003093.

Minamino N, Kangawa K, Matsuo H (1983) Neuromedin B: A novel bombesin-like peptide identified in porcine spinal cord. Biochem Biophys Res Commun 114:541–548 Available

at: http://www.sciencedirect.com/science/article/pii/0006291X83908148.

Miselis RR (1982) The subfornical organ's neural connections and their role in water balance. Peptides 3:501–502 Available at: http://www.sciencedirect.com.uml.idm.oclc.org/science/article/pii/0196978182901152 [Accessed December 14, 2017].

Morgans CW (2001) Localization of the alpha1F calcium channel subunit in the rat retina. Investig Ophthalmol Vis Sci 42:2414–2418.

Mortensen O V. (2013) MKP3 eliminates depolarization-dependent neurotransmitter release through downregulation of L-type calcium channel Cav1.2 expression. Cell Calcium 53:224–230 Available at: http://dx.doi.org/10.1016/j.ceca.2012.12.004.

Motegi SI (2016) Endothelin. Syst Scler 68:155–171.

Mumford AD, Parry LJ, Summerlee AJS (1989) Lesion of the subfornical organ affects the haemotensive response to centrally administered relaxin in anaesthetized rats. J Endocrinol 122:747–755.

Nagalakshmi U, Wang Z, Waern K, Shou C, Raha D, Gerstein M, Snyder M (2008) The transcriptional landscape of the yeast genome defined by RNA sequencing. Science (80-) 320:1344–1349.

Nation HL, Nicoleau M, Kinsman BJ, Browning KN, Stocker SD (2016) DREADD-induced activation of subfornical organ neurons stimulates thirst and salt appetite. J Neurophysiol 115:3123–3129.

Navarrete M, Araque A (2008) Endocannabinoids mediate neuron-astrocyte communication.

Neuron 57:883–893 Available at: https://doi.org/10.1016/j.neuron.2008.01.029.

Nehmé B, Henry M, Mouginot D, Drolet G (2012) The expression pattern of the Na+ sensor, NaX in the hydromineral homeostatic network: A comparative study between the rat and mouse. Front Neuroanat 6:26 Available at: https://www.ncbi.nlm.nih.gov/pubmed/22833716.

Nemeroff CB, Bissette G, Prange AJ, Peter T, Barlow TS, Lipton MA (1977) Neurotensin: Central nervous system effects of a hypothalamic peptide. Brain Res 128:485–496.

Ohya S, Tanaka M, Oku T, Asai Y, Watanabe M, Giles WR, Imaizumi Y (1997) Molecular cloning and tissue distribution of an alternatively spliced variant of an A-type K+ channel α-subunit, Kv4.3 in the rat. FEBS Lett 420:47–53.

Oka Y, Ye M, Zuker CS (2015) Thirst driving and suppressing signals encoded by distinct neural populations in the brain. Nature 520:349–352.

Ono K, Honda E, Inenaga K (2001) Angiotensin II induces inward currents in subfornical organ neurones of rats. J Neuroendocrinol 13:517–523.

Ono K, Kai A, Honda E, Inenaga K (2008) Hypocretin-1/orexin-A activates subfornical organ neurons of rats. Neuroreport 19:69–73.

Ono K, Toyono T, Honda E, Inenaga K (2005) Transient outward K^+ currents in rat dissociated subfornical organ neurones and angiotensin II effects. J Physiol 568:979–991 Available at: http://doi.wiley.com/10.1113/jphysiol.2005.089508.

Patel RR, Barbosa C, Xiao Y, Cummins TR (2015) Human Nav1.6 channels generate larger resurgent currents than human Nav1.1 channels, but the Navβ4 peptide does not protect

either isoform from use-dependent reduction. PLoS One 10:1–19.

Perez-Reyes E (2015) Molecular physiology of low-voltage-activated T-type calcium channels. Physiol Rev 83:117–161.

Perez–Reyes E, Kim HS, Lacerda AE, Horne W, Wei X, Rampe D, Campbell KP, Brown AM, Birnbaumer L (1989) Induction of calcium currents by the expression of the α1-subunit of the dihydropyridine receptor from skeletal muscle. Nature 340:233–236 Available at: https://doi.org/10.1038/340233a0.

Pernow B, Silva MRE (1955) A Comparative Study of Bradykinin mid Substance P. Acta Physiol Scand 34:59–66 Available at: https://doi.org/10.1111/j.1748-1716.1955.tb01224.x.

Petersen CM, Nielsen MS, Jacobsen L, Tommerup N, Rasmussen HH, Røigaard H, Madsen P, Søren K, Chem JB, Nykjær A, Gliemann J, Moestrup SK (1997) Molecular identification of a novel candidate sorting receptor purified from human brain by receptor-associated protein affinity chromatography. J Biol Chem 272:3599–3605.

Peterson CS, Huang S, Lee SA, Ferguson AV, Fry WM (2018) The trancriptome of the Rattus norvegicus subfornical organ is altered in response to early postnatal overnutrition induced by small litter size. IBRO Reports 5:17–23.

Phillips M, Camacho A (1981) Horseradish peroxidase study in the rat of the neural connections of the organum vasculosum of the lamina terminalis. Neurosci Lett 25:201–204.

Polidori C, Ciccocioppo R, De Caro G, Massi M (1998) Further evidence that central tachykinin NK-1 receptors mediate the inhibitory effect of tachykinins on angiotensin-induced drinking in rats. Peptides 19:149–155.

Polidori C, Ciccocioppo R, Epstein AN, de Caro G, Massi M (1994) Effect of tachykinins on the need-free sodium intake of female rats: A continuous intracerebroventricular infusion study. Physiol Behav 56:877–882.

Pulman KJ, Fry WM, Cottrell GT, Ferguson A V (2006) The subfornical organ: a central target for circulating feeding signals. J Neurosci 26:2022–2030.

Quirion R, Gaudreau P, St-Pierre S, Rioux F, Pert CB (1982) Autoradiographic distribution of [3H]neurotensin receptors in rat brain: Visualization by tritium-sensitive film. Peptides 3:757–763.

Rameshwar P, Gascón P (1996) Induction of negative hematopoietic regulators by neurokinin-A in bone marrow stroma. Blood 88:98–106 Available at: http://www.ncbi.nlm.nih.gov/entrez/query.fcgi?db=pubmed&cmd=Retrieve&dopt=AbstractPlus&list_uids=8704207.

Ratner C, Skov LJ, Raida Z, Bächler T, Bellmann-Sickert K, Foll C Le, Sivertsen B, Dalbøge LS, Hartmann B, Beck-Sickinger AG, Madsen AN, Jelsing J, Holst JJ, Lutz TA, Andrews ZB, Holst B (2016) Effects of peripheral neurotensin on appetite regulation and its role in gastric bypass surgery. Endocrinology 157:3482–3492.

Reinecke M (1985) Neurotensin: immunohistochemical localization in central and peripheral nervous system and in endocrine cells and its functional role as neurotransmitter and endocrine hormone. Prog hstochemistry Cytochem 16:III–VIII, 1–172.

Rioux F, Quirion R, St-Pierre S, Regoli D, Jolicoeur FB, Bélanger F, Barbeau A (1981) The hypotensive effect of centrally administered neurotensin in rats. Eur J Pharmacol 69:241–247 Available at: http://www.ncbi.nlm.nih.gov/pubmed/7215426.

Rosas-Arellano MP, Solano-Flores LP, Ciriello J (1996) Neurotensin projections to subfornical organ from arcuate nucleus. Brain Res 706:323–327.

Roth J, Pehl U, Kueth M, Harre E, Gerstberger RUD, Hu T (2002) Role of IL-6 in LPs-induced nuclear STAT3 translocation in sensory circumventricular organs during fever in rats. J Appl Physiol 92:2657–2666.

Rowe WB, Nicot A, Sharma S, Gully D, Walker CD, Rostène WH, Meaney MJ, Quirion R (1997) Central administration of the neurotensin receptor antagonist, SR48692, modulates diurnal and stress-related hypothalamic-pituitary-adrenal activity. Neuroendocrinology 66:75–85.

Saffroy M, Beaujouan JC, Torrens Y, Besseyre J, Bergström L, Glowinski J (1988) Localization of tachykinin binding sites (NK1, NK2, NK3ligands) in the rat brain. Peptides 9:227–241.

Saito H, Yoshizawa H, Yoshimori K, Katakami N, Katsumata N, Kawahara M, Eguchi K (2013) Efficacy and safety of single-dose fosaprepitant in the prevention of chemotherapy-induced nausea and vomiting in patients receiving high-dose cisplatin: A multicentre, randomised, double-blind, placebo-controlled phase 3 trial. Ann Oncol 24:1067–1073.

Sarret P, Krzywkowski P, Segal L, Nielsen MS, Petersen CM, Mazella J, Stroh T, Beaudet A (2003a) Distribution of NTS3 receptor/sortilin mRNA and protein in the rat central nervous system. J Comp Neurol 461:483–505 Available at: http://doi.wiley.com/10.1002/cne.10708.

Sarret P, Perron A, Stroh T, Beaudet A (2003b) Immunohistochemical distribution of NTS2 neurotensin receptors in the rat central nervous system. J Comp Neurol 461:520–538.

Sawchenko PE, Swanson LW (1983) The organization of forebrain afferents to the

paraventricular and supraoptic nuclei of the rat. J Comp Neurol 218:121–144.

Segal M, Rogawski M, Barker J (2018) A transient potassium conductance regulates the excitability of cultured hippocampal and spinal neurons. J Neurosci 4:604–609.

Shapiro RE, Miselis RR (1985) The central neural connections of the area postrema of the rat. J Comp Neurol 234:344–364 Available at: http://www.ncbi.nlm.nih.gov/pubmed/3988989 [Accessed November 13, 2015].

Simpson NJ, Ferguson AV (2018) Tumor necrosis factor alpha potentiates the effects of angiotensin II on subfornical organ neurons. Am J Physiol Integr Comp Physiol 315:R425–R433.

Simpson NJ, Ferguson A V (2017) The pro-inflammatory cytokine tumor necrosis factor alpha excites subfornical organ neurons. J Neurophysiol 1:jn.00238.2017 Available at: http://jn.physiology.org/lookup/doi/10.1152/jn.00238.2017%0Ahttp://www.ncbi.nlm.nih.gov/pubmed/28637815.

Smith PM, Chambers AP, Price CJ, Ho W, Hopf C, Sharkey KA, Ferguson A V (2008) The subfornical organ: a central nervous system site for actions of circulating leptin. Am J Physiol Integr Comp Physiol 296:R512–R520 Available at: http://ajpregu.physiology.org/cgi/doi/10.1152/ajpregu.90858.2008.

Smith PM, Ferguson A V. (2012) Cardiovascular Actions of Leptin in the Subfornical Organ are Abolished by Diet-Induced Obesity. J Neuroendocrinol 24:504–510.

Smith PM, Ferguson A V (1997) Vasopressin acts in the subfornical organ to decrease blood pressure. Neuroendocrinology 66:130–135 Available at:

https://www.karger.com/DOI/10.1159/000127230.

Smith PM, Rozanski G, Ferguson A V. (2010) Acute electrical stimulation of the subfornical organ induces feeding in satiated rats. Physiol Behav 99:534–537.

Smith PM, Samson WK, Ferguson A V. (2007) Cardiovascular actions of orexin-A in the rat subfornical organ. J Neuroendocrinol 19:7–13.

Steele FF, Whitehouse SC, Aday JS, Prus AJ (2017) Neurotensin NTS1 and NTS2 receptor agonists produce anxiolytic-like effects in the 22-kHz ultrasonic vocalization model in rats. Brain Res 1658:31–35 Available at: http://dx.doi.org/10.1016/j.brainres.2017.01.012.

Subramanian J, Dye L, Morozov A (2013) Rap1 signaling prevents L-type calcium channel-dependent neurotransmitter release. J Neurosci 33:7245–7252 Available at: http://www.ncbi.nlm.nih.gov/pubmed/23616533%0Ahttp://www.pubmedcentral.nih.gov/articlerender.fcgi?artid=PMC3657727.

Sucher NJ, Deitcher DL, Baro DJ, Harris Warrick RM, Guenther E (2000) Genes and channels: Patch/voltage-clamp analysis and single-cell RT-PCR. Cell Tissue Res 302:295–307.

Swanson LW, Lind RW (1986) Neural projections subserving the initiation of a specific motivated behavior in the rat: new projections from the subfornical organ. Brain Res 379:399–403.

Szathmari A, Champier J, Ghersi-Egea JF, Jouvet A, Watrin C, Wierinckx A, Fèvre Montange M (2013) Molecular characterization of circumventricular organs and third ventricle ependyma in the rat: Potential markers for periventricular tumors. Neuropathology 33:17–29.

Thunhorst RL, Beltz TG, Johnson AK (1999) Effects of subfornical organ lesions on acutely

induced thirst and salt appetite. Am J Physiol Integr Comp Physiol 277:R56–R65.

V Euler US, Gaddum JH (1931) An unidentified depressor substance in certain tissue extracts. J Physiol 72:74–87 Available at: https://www.ncbi.nlm.nih.gov/pubmed/16994201.

Wall KM, Nasr M, Ferguson A V. (1992) Actions of endothelin at the subfornical organ. Brain Res 570:180–187.

Wang Z, Kiehn J, Yang Q, Brown AM, Wible BA (1996) Membranes and bioenergetics: Comparison of binding and block produced by alternatively spliced Kvβ1 subunits. J Biol Chem 271:28311–28317.

Washburn DL, Ferguson A V. (2001a) Membrane properties of subfornical organ neurons. Clin Exp Pharmacol Physiol 28:575–580.

Washburn DLS, Anderson JW, Ferguson A V. (2000) A subthreshold persistent sodium current mediates bursting in rat subfornical organ neurones. J Physiol 529:359–371.

Washburn DLS, Beedle AM, Ferguson A V. (1999) Inhibition of subfornical organ neuronal potassium channels by vasopressin. Neuroscience 93:349–359.

Washburn DLS, Ferguson A V (2001b) Selective potentiation of N-type calcium channels by angiotensin II in rat subfornical organ neurones. J Physiol 536:667–675.

Wheeler DG, Groth RD, Ma H, Barrett CF, Owen SF, Tsien RW (2012) CaV1 and CaV2 channels engage distinct modes of Ca2+ signaling to control CREB-dependent gene expression. Cell 149:1112–1124.

Whyment A, Top M Van Den, Lee K, Whyment AD, Blanks AM, Spanswick D (2004) Orexigen-sensitive NPY / AgRP pacemaker neuons in the hypothalamic arcuate nucleus.

Nat Neurosci 7:493–494.

Wu LG, Westenbroek RE, Borst JG, Catterall WA, Sakmann B (1999) Calcium channel types with distinct presynaptic localization couple differentially to transmitter release in single calyx-type synapses. J Neurosci 19:726–736 Available at: http://eutils.ncbi.nlm.nih.gov/entrez/eutils/elink.fcgi?dbfrom=pubmed&id=9880593&retmode=ref&cmd=prlinks%5Cnpapers3://publication/uuid/A547EF26-C52E-4EFF-94DC-3C74DAE1F46B.

3.7. Connection between chapters 3 and 4

In the second chapter, we presented a list of ion channels and GPCRs with validated and unvalidated expression in the SFO. Of these we further explored the significance of the receptors for endothelin, substance P, and neurotensin via their effects of electrical excitability of dissociated SFO neurons. These results indicated that marked mRNA expression of *Ntsr2* and *Ntsr3* is paired with robust increases in the electrical excitability of SFO neurons. Considering the converging roles of neurotensin and the SFO in regulation of thirst, cardiovascular output, and energy balance, we further explored the effects of neurotensin on SFO neurons and the ionic mechanism by which neurotensin alters the electrical excitability of SFO neurons in chapter 4.

4. Neurotensin modulates the electrical excitability of subfornical organ neurons.

4.1. Abstract

Neurotensin is a pleiotropic signaling molecule with metabolic and cardiovascular activities. The subfornical organ (SFO), which lacks a blood-brain-barrier, has well-recognized roles in energy homeostasis, hydromineral balance, and cardiovascular output, and has at least two neurotensin inputs: circulating neurotensin in the blood, and neurotensinogenic projections from the arcuate nucleus of the hypothalamus. Moreover, SFO transcriptomic data shows high expression of neurotensin receptor transcripts *Ntsr2* and *Ntsr3*, suggesting neurotensin plays a signalling role at the SFO.

We sought to investigate the electrical effects of neurotensin on dissociated SFO neurons via whole cell patch clamp electrophysiology. Whole-cell current clamp recordings show that at a dose of 100 nM, neurotensin depolarises (7.0 ± 1.8 mV) and increases the action potential frequency (3.3 ± 0.81 Hz) of 53% of SFO neurons (n=12/23). Percent responsive neurons decreased in a dose-dependent manner with an apparent EC_{50} of 7.61 nM. Voltage clamp and current clamp protocols to investigate neurotensin's ionic mechanism of action revealed that neurotensin increases the electrical excitability via modulation of two ion channels: attenuation of delayed-rectifier (I_K) K^+ currents (reversal potential of -75.0 ± 3.8 mV, increased input resistance) and modulation of nonselective cation currents (reversal potential of -51.3 ± 6.1 mV, decreased input resistance). These are the first data to show the direct electrical effects of neurotensin on SFO neurons, in support of the potential role of neurotensin's action at the SFO to modulate homeostasis.

4.2. Introduction

Neurotensin is a tridecapeptide first extracted from bovine hypothalamus and noted for its hypotensive action when injected in to the ventricle of a rat (Leeman, 1973; Rioux et al., 1981; Hawkins et al., 1989). However, regulation of blood pressure has proven more complex, as some studies indicate bi- or triphasic effects of neurotensin on mean arterial pressure and heart rate in rats (Oishi et al., 1981; Rioux et al., 1982; Gully et al., 1996). Furthermore, since the initial discovery of neurotensin additional homeostatic roles for neurotensin in the central nervous system have been identified: in addition to modulation of blood pressure in guinea pigs and rats (Leeman, 1973; Rioux et al., 1981), intracerebroventricular injection of neurotensin promotes drinking (Baker et al., 1989) and supresses feeding in rats (Levine et al., 1983; Cooke et al., 2009). Specific nuclei have been implicated in the pressor, dipsogenic, and energy balance effects of neurotensin: 1. Direct neurotensin injection to the rat nucleus of the solitary tract (NTS) decreases mean arterial pressure (Ciriello and Zhang, 1997), whereas injection to the rat rostral ventrolateral medulla increases basal blood pressure (Ishizuka et al., 1993). 2. Neurotensin microinjection studies have primarily ruled out some nuclei as promoting dipsogenesis in rats via neurotensin, including the paraventricular PVN (Stanley et al., 1983), amygdala, and the preoptic area of the hypothalamus (Baker et al., 1989). Evidence from neurotensinogenic neurons provides insight to other nuclei: activation of neurotensinogenic neurons in the mouse lateral hypothalamus (LH) (Kurt et al., 2019) were shown to promote drinking, though the efferent projections and neuronal inputs of these neurons implicated in thirst require further investigation. 3. Direct injections of neurotensin in rats to the paraventricular nucleus of the hypothalamus (PVN) (Stanley et al., 1983), the NTS (de Beaurepaire and Suaudeau, 1988), and the ventral tegmental area (VTA) (Cador et al., 1986) decrease food

intake. However, some homeostatic nuclei remain uninvestigated, and the full pathways for the pressor, drinking, and feeding effects of neurotensin are still unclear. Furthermore, many early studies did not differentiate between different neurotensin receptor subtypes.

The effect of neurotensin is elicited through at least 3 receptors: The G-protein coupled receptors NTSR1 and 2, and the single transmembrane domain type 1 receptor NTSR3 (also called SORT1). The type 1 and 2 receptors are most similar based on sequence homology, but show differences in expression distribution (Nouel et al., 1999; Fassio et al., 2000; Sarret et al., 2003b; Inoshima et al., 2017) and ligand affinity (Tanaka et al., 1990; Chalon et al., 1996). NTSR3 is the most poorly understood of the known neurotensin receptors, though evidence suggests it is predominantly located on membrane-bound organelles (Sarret et al., 2003a) and may play a role in mediating neurotensin turnover (Petersen et al., 1997). Another single transmembrane domain receptor similar to NTSR3, SorLa/LR11, is thought to bind neurotensin in addition to apolipoprotein E and various propeptides (Jacobsen et al., 2001). Similar to NTSR3, SorLa/LR11 shows a primarily subcellular localisation, expressing approximately 10% on the outer membrane, and is proposed to mediate ligand sorting, trafficking, and endocytosis (Jacobsen et al., 2001).

Neurotensin is produced both peripherally (Sundler et al., 1977; Goedert et al., 1984) and centrally (Carraway and Leeman, 1973; Goedert et al., 1984), though given the different effects of peripheral vs central injections (Sumners et al., 1982), the central and peripheral sources are often considered separate (Nemeroff et al., 1977). As a result, until recently neurotensin was not thought to cross the blood-brain-barrier (BBB) (Gevaert et al., 2016), a network of tight endothelial junctions formed by astrocyte end-feet which isolate the brain from the periphery by preventing passive passage of large, hydrophilic molecules (Risau and Wolburg, 1990).

However, peripherally injected neurotensin induces activity of hypothalamic nuclei, including the paraventricular nucleus of the hypothalamus (PVN) and the NTS, and decreases food intake (Ratner et al., 2016). This effect was shown not to result of interaction of neurotensin with the vagus nerve. Moreover, the apparent ability of neurotensin to cross the BBB does not appear to be relevant to this effect, as prevention of BBB crossing via pegylation did not alter the anorectic effect of neurotensin. Thus the effects of neurotensin in this case are likely mediated through an area of the brain lacking a BBB. While the authors did see increase *c-fos* expression in the area postrema, activity in other sensory circumventricular organs (sensory CVOs) was not examined.

The subfornical organ (SFO) is a sensory CVO, which is a unique structure which lacks a BBB, and a recent transcriptomics study shows high expression levels for NTSR2 and NTSR3 in the SFO (Peterson et al., 2018). Furthermore, neurotensinogenic projections originating in the arcuate nucleus of the hypothalamus project to the SFO (Rosas-Arellano et al., 1996). In addition to neurotensin receptors, the SFO expresses a broad variety of other membrane receptors crucial for regulation of homeostasis, placing it to effectively detect circulating signalling molecules from the periphery. Moreover, the SFO sends axonal projections to important homeostatic centres including the median preoptic nucleus (MPN) (Lind et al., 1982, 1984), the PVN (Miselis, 1982), the supraoptic nucleus (SON) (Lind et al., 1982; Sawchenko and Swanson, 1983), the arcuate nucleus of the hypothalamus (ARC) (Gruber et al., 1987; Whyment et al., 2004), the LH (Burton et al., 1976; Miselis, 1982), the bed nucleus of the stria terminalis (BNST) (Swanson and Lind, 1986; McKinley et al., 2003; Hollis et al., 2008) and vascular organ of the lamina terminalis (Lind et al., 1982). The SFO also receives synaptic input from many of these areas including the MPN (Hernesniemi et al., 1972), the NTS (Miselis, 1982; Zardetto-Smith and Gray, 1987), the ARC (Rosas-Arellano et al., 1996), and the PVN (Lind et al., 1982). Thus the

SFO is situated to detect signals of physiological state, integrate this information with signals from other nuclei, and transduce this information to other homeostatic nuclei to play a critical role in regulation of homeostasis.

Though the classical role of the SFO is as a detector of angiotensin II to increase blood pressure and drive thirst (Mangiapane and Simpson, 1980, 1983), continued research has shown the SFO responds to numerous other signalling molecules to modulate cardiovascular output and thirst, to varying effects. Whereas some molecules such as endothelin and hydrogen sulfide act to increase blood pressure and heart rate (Wall et al., 1992; Kuksis et al., 2014), others such as apelin have the opposite effect (Smith and Ferguson, 2012; Dai et al., 2013). In recent years increased research has expanded the known roles of the SFO to include energy balance, (Smith et al., 2008, 2010), salt appetite (Thunhorst et al., 1999; Nation et al., 2016), and to a lesser extent immune function (Takahashi et al., 1997; Cerqueira et al., 2016) and reproduction (Donevan et al., 1989). Numerous energy balance signalling molecules including leptin (Smith et al., 2008; Smith and Ferguson, 2012), adiponectin (Alim et al., 2010), insulin (Lakhi et al., 2013), and others (Hoyda et al., 2009; Ahmed et al., 2014; Riediger et al., 2017) act at the SFO, and more directly, electrical stimulation of the SFO induces feeding (Smith et al., 2010). Given the established and converging roles of neurotensin and the SFO in regulation of blood pressure, thirst, and feeding, the high expression levels of neurotensin receptor transcripts in the SFO (Peterson et al., 2018), and known neurotensinogenic inputs to the SFO, we sought to characterise the effects of neurotensin on the electrical excitability of SFO neurons.

4.3. Methods

4.3.1. Animals and dissection

All procedures were approved by the University of Manitoba Animal Care Committee in accordance with the guideline from the Canadian Council for Animal Care. Male Sprague Dawley rats (150-175g) were given ad libitum access to standard rat chow and kept in a light-controlled facility. Rats were sacrificed by decapitation between the hours of 8 am and 12pm (1:45 – 5:45 following lights on). The brains were removed and placed in ice-cold oxygenated artificial cerebrospinal fluid (composition, in mM: 126 NaCl, 2.5 KCl, 1.25 NaH_2PO_4, 2 $MgCl_2$, 10 D-glucose, 26 $NaHCO_3$, 0.5 $CaCl_2$) for 2 minutes. A 3 mm block of tissue containing the SFO was cut at the level of the hypothalamus (Paxinos and Watson, 2007), and the tissue surrounding the SFO was dissected under a dissecting microscope. Dissociated SFO cultures were prepared as previously described (Ferguson et al., 1997). Briefly, dissected SFO was incubated in 10 mL Hibernate media (Gibco) containing 5 mg of papain (Worthington) for 30 minutes at 37 ˚C, then washed three times in B-27 (Gibco) supplemented Hibernate, and triturated. Dissociated cells were incubated in Neurobasal (Gibco) supplemented with B-27 and Glutamax (Gibco).

4.3.2. Electrophysiology

All electrophysiological recordings were performed within 5 days of culturing as previous evidence suggests that SFO neurons maintain their electrical properties for at least six days in culture (Ferguson et al., 1997). Data were acquired using a HEKA EPC10 patch clamp amplifier and Patchmaster 2.53 software (Mahone Bay, Nova Scotia, Canada). Cells were visualised under phase contrast microscopy at 400x magnification (Axiovert 135, Carl Zeiss Inc.).

Current Clamp.

Electrodes fashioned from borosilicate glass (Sutter Instruments) with a resistance of 2-5 MΩ when filled with intracellular solution were used. Only cells with stable access resistance (<30% change in MΩ), membrane seals >1 GΩ, and stable membrane potential were used. Neurons used for current clamp experiments had a mean access resistance of 13.58 ± 0.50 MΩ (n=101). Extracellular recording solution was constantly flowed through the culture dish via a peristaltic pump at a flow rate of ~2 mL/min.

For current clamp recordings investing changes in membrane potential, action potential firing frequency, and input resistance, physiological extracellular (composition in mM: 140 NaCl, 5 KCl, 2 $CaCl_2$, 1 $MgCl_2$, 10 HEPES, 10 mM dextrose) and intracellular (composition in mM: 5 EGTA, 130 K gluconate, 10 KCl, 10 HEPES, 1 $CaCl_2$, 4 NaATP, 0.1 NaGTP) solutions were used. Neurons were held without enough current to maintain membrane potential near -60 mV during recording. For dose response, following a 4-minute baseline recording period, 2 mLs of either saline (control) or neurotensin (0.1-100 nM; Tocris, 1909) was washed over the cells, and resting membrane potential and action potential frequency recorded. To determine whether the effect seen in SFO neurons is due to interaction with neurotensin receptors, cells were first washed over the 100 nM NTSR1/2 antagonist SR142948 (Tocris; 2309) for 3 minutes to allow antagonist binding, followed by a 2-minute wash with 100 nM neurotensin.

To gain insight in to the ion channels implicated in the electrical effects of neurotensin on SFO neurons, the reversal potential of the effect and changes in input resistance were calculated. To determine the reversal potential a calculate input resistance, 1-5 pA current steps were applied once baseline had stabilised and at the onset of neurotensin effect or, where no effect was seen, 3 minutes following neurotensin application. The relationship between voltage and current

was plotted (VI plot), the input resistance calculated from the slope, and the reversal potential of the effect from the intersection of the VI plots before and after neurotensin. For all current clamp experiments, a cell was considered responsive to neurotensin if the membrane potential changed by 2 standard deviations from the baseline potential and/or at least doubled in action potential frequency within 3 minutes of neurotensin application.

Voltage Clamp.

For experiments investigating changes in voltage-gated K^+ and nonselective cation currents (I_{NSC}), physiological extracellular (composition in mM: 140 NaCl, 5 KCl, 2 $CaCl_2$, 1 $MgCl_2$, 10 HEPES, 10 mM dextrose) and intracellular (composition in mM: 5 EGTA, 130 K gluconate, 10 KCl, 10 HEPES, 1 $CaCl_2$, 4 NaATP, 0.1 NaGTP) solutions were used. Electrodes fashioned from borosilicate glass (Sutter Instruments) with a resistance of 2-5 MΩ when filled with intracellular solution were used. Only cells with stable access resistance (<30% change in MΩ), membrane seals >1 GΩ, and stable baseline current used. Neurons used for voltage clamp experiments had a mean access resistance of 11.28 ± 0.74 MΩ (n=71). Extracellular recording solution was constantly flowed through the culture dish via a peristaltic pump at a flow rate of ~2 mL/min.

Changes in voltage-gated K^+ currents were investigated by subjecting neurons to 500 ms 10 mV steps from −60 mV to +30 mV, following either a hyperpolarising (−100 mV, to remove inactivation) or depolarising (−30 mV, to inactivate transient currents) pre-pulse. Transient K^+ current (I_A) was measured from the peak current of the resulting difference current of the depolarising and hyperpolarising protocols; delayed rectifier K^+ (I_K) current was measured from the early and late currents at each step from the depolarising protocol. Currents were normalised

to peak current in the control condition, and mean normalised current-voltage (IV) plots before and after 100 nM neurotensin application compared.

Changes in I_{NSC} were investigated using a ramp from −100 mV to 0 mV over 6 s. The point at which the elicited currents before and after 100 nM neurotensin crossed or diverged was examined as an indication of the reversal potential, and current at−100 and 0 mV before and after 100 nM neurotensin were compared to investigate changes in the net direction of current. Mean difference current IV plots were generated by subtracting baseline ramp currents from 100 nM neurotensin ramp current, the value at 10 mV intervals between −90 and 0 mV extracted, and the mean and standard errors calculated from the pooled difference data.

Changes in voltage-gated Na+ currents were performed in low-Na^+, K^+-free extracellular recording solution (composition in mM: 50 NaCl, 100 TEA-Cl,1 $MgCl_2$, 1 $CaCl_2$, 1 $CsCl_2$, 1 $BaCl_2$, 0.3 $CdCl_2$, 10 HEPES, 10 glucose) and internal recording solution (composition in mM: 10 NaCl, 120 $CsMeSO_4$, 1 $MgCl_2$, 10 HEPES, 10 glucose, 2 NaATP, 0.2 NaGTP) to minimise amplitude of Na^+ currents and remove the interference of K^+ currents, To record voltage-dependent Na^+ current, neurons were subjected to a 1 s pre-pulse at −100 mV (to enable full Na^+ channel recovery) followed by 15 ms 10 mV steps from −70 mV to +50 mV. Persistent Na^+ was recorded using 1 s ramp from −100 mV to 0 mV. Peak transient and persistent Na^+ currents and Na^+ conductance were compared before and after application of neurotensin.

4.3.3. Statistics

All statistics were performed using OriginLab 2018 software. Changes in membrane potential and action potential frequency before and after application of a specific dose of neurotensin were tested using a pairwise t-test. Differences between effects of neurotensin doses and saline control, 100 nM neurotensin with or without SR142948 antagonist and saline, were compared via one-way ANOVA with a *post-hoc* t-test and Bonferroni correction. Differences in peak current at −100 and 0 mV derived from long ramp experiments were compared to differences to saline controls (to account for the current run-up or run-down) via a two-way t-test. Welch correction was applied where unequal variance was evident between groups as tested by a two=way test for unequal variance. Differences in proportion of responsive neurons were tested using Chi Square test. Voltage-gated K^+ IV plots and Na^+ conductance plots were fitted to a Boltzmann Curve ($y = A2 + (A1-A2)/(1 + \exp((x-x0)/dx))$) and compared using an F-test.

4.4. Results

4.4.1. Neurotensin directly affects SFO neurons via NTSR2 receptors

Sensitivity of SFO neurons to 100 nM neurotensin, a concentration which we expected to elicit a near-maximum response (Seutin et al., 1989; Werkman et al., 1999), was recorded using current clamp electrophysiology (Figure 4.1). At this concentration, 54.2% (13/24) of cells exhibited a significant response of a depolarisation (n= 10/24; paired t-test, p=0.0054) and/or an increase in action potential frequency (n= 8/24; paired t-test, p=0.0085).

Having determined that the electrical activity of SFO neurons is modulated by neurotensin, to ascertain whether the effects of neurotensin were concentration-dependent, 0.1 – 100 nM neurotensin was applied to cultured SFO neurons, and the percentage of responsive neurons (Figure 4.2A), change in membrane potential (Figure 4.2B), and change in action

potential frequency (Figure 4.2C) were recorded. Between 1-100 nM, proportion of responsive neurons, membrane potential changes, and changes in action potential frequency decreased in a dose-dependent manner; no effect was seen at 100 pM.

Previous studies show the expression of 2 receptors for neurotensin in the SFO: NTSR2 and 3 (Fassio et al., 2000; Sarret et al., 2003b, 2003a; Peterson et al., 2018). To determine which receptors are implicated, we examined whether the high-affinity NTSR1/2 antagonist SR142948 (Werkman et al., 1999; Heine et al., 2019) could block the response to 100 nM neurotensin. Of the 10 neurons treated with 100 nM SR142498, none showed a significant depolarisation or change in action potential frequency when exposed to 100 nM neurotensin (Figure 4.3). The proportion of responsive neurons was significantly different from 100 nM neurotensin without SR14928 pre-treatment (Chi square text, p=0.042) but not saline control (Chi square test, p=1.00). Changes in membrane potential and action potential frequency in the 100 nM SR142928+100 nM neurotensin group did not differ from changes seen in saline control (One-way ANOVA with post-hoc Bonferroni correction, membrane potential p=1.00; action potential p=1.00).

4.4.2. Ionic mechanism of neurotensin-induced changes in membrane potential

Neurotensin attenuates I_K in SFO neuron

Voltage-current plots constructed before and after 100 nM neurotensin application revealed 2 groups of responsive neurons: those which showed a decrease in input resistance and a reversal potential of effect of −51.2 ± 6.19 mV (n=5), and those which showed an increase in input resistance and a reversal potential of effect of −75.0 ±3.92 mV (n=3) (Figure 4.4). This lead us to investigate to possibility of two distinct types of current modulated by neurotensin.

The combination of increased input resistance and a reversal potential of -75 mV suggests the closing of K^+ channels in response to neurotensin. Previous studies demonstrate the presence of two subtypes of voltage-gated K+ current which may be modulated by binding of circulating signalling molecules (Ono et al., 2005; Lakhi et al., 2013). To confirm the effect of neurotensin on voltage-gated K^+ currents, and to investigate which sub-types of K^+ channels are implicated, both the transient I_A and delayed-rectifier I_K K^+ currents were recorded in voltage-clamp before and after neurotensin application (Figure 4.5). A significant decrease in I_K amplitude was seen at both early and late time points (F-test; early $p=1.5 \times 10^{-4}$; late $p=7.3 \times 10^{-12}$). While some current run-down was observed in I_K in saline control conditions, this was not significant (F-test; early p=0.53; late p=0.62). No significant change was detected in I_A currents by neurotensin (F-test; p=0.20).

Neurotensin increases conductance through nonselective cation channels

The reversal potential of those neurons which showed a decrease in input resistance did not match that of the equilibrium potential of any single permeant ion typically implicated in setting neuronal membrane potential (K^+: −80 mV; Na^+: +55 mV; Ca^{2+}: +110 mV, Cl^-: −61 mV). This indicates that a nonselective ion channel is likely modulated. To investigate whether nonselective cation channels are affected by neurotensin, currents were elicited from SFO neurons via a long 6 s ramp from −100 to 0 mV.

One set of neurons (n=4/22 treated with neurotensin) displayed increased inward current below and outward current above approximately -60 mV; these currents were linear in the range of −90 to −20 mV (Figure 4.6). Current-voltage properties combined combined with the reversal potential of −55.9 ± 3.5 mV indicates the modulation of a nonselective cation channel (Pulman et al., 2006). Another set of neurons (n=6/22 treated with neurotensin) showed increased inward

current activated at −30.1 ± 4.8 mV; this suggests the activation of a voltage-gated current, likely a decrease in K^+ currents given the observed decrease in I_K neurotensin. At 0 mV, both the voltage-gated channel (two-way t-test with Welch correction, p=0.0018) and nonselective cation channel (two-way t-test with Welch correction, p=0.039) groups were significantly different than changes in current at 0 mV in saline controls. The remaining neurons (n=12/22 treated with neurotensin) showed no significant response to neurotensin (two-way t-test with Welch correction, p=0.37).

Neurotensin does not alter voltage-gated Na+ channel currents

Neither peak transient Na^+ current, maximum persistent current, nor Na+ conductance were significantly different between baseline and during neurotensin application (Pairwise t-tests: transient p=0.54 and persistent p= 0.54; F-test: conductance p= 0.074; Figure 4.7).

4.5. Discussion

These data are the first to demonstrate that SFO neurons sense neurotensin and respond by increasing electrical activity as measured by changes in membrane potential and action potential frequency. Using whole cell patch clamp electrophysiology, we observed that at 100 nM, 54% of SFO neurons depolarised and/or increased action potential frequency in response to neurotensin, whereas the remaining 46% of neurons showed no response. Neurotensin's effects on membrane potential, action potential frequency, and proportion of responsive cells decreased in a dose-dependent manner, and are absent at 100 pM.

Application of the NTSR1/2-specific antagonist SR142948 completely eliminated the observed depolarisation and increase in action potential frequency. Given that previous immunohistochemistry evidence suggests that NTSR1 is not present in the SFO (Fassio et al., 2000), these data suggest that this response is mediated by NTSR2 only. Though NTSR3 is also

notably strongly expressed in the SFO, its role at the SFO is currently unclear. The intracellular localisation of NTSR3 (Sarret et al., 2003a) and protein affinity chromatography (Petersen et al., 1997) suggest that NTSR3 is likely involved in ligand trafficking and sorting, and is unlikely to play a principal role in signalling. However, heterodimerisation between NTSR3/SORT and NTSR1 was previously reported in the HT29 cell line which altered the affinity of NTSR1 for neurotensin, and properties of the NTSR1 downstream signalling pathway including MAPK phosphorylation and phosphoinositide turnover (Martin et al., 2002). Notably, a similar relationship has not been reported in neurons, nor between NTSR2 and NTSR3.

Using input resistance experiments and voltage-clamp experiments we sought to investigate the ionic mechanisms underlying the excitatory response of SFO neurons to neurotensin. These data show the modulation of two different populations of ion channels in response to neurotensin resulting in depolarisation: attenuation of delayed-rectifier K+ currents and enhancement of nonselective cation current (I_{NSC}). The reversal potentials obtained from long ramp (−55.9 ± 3.5 mV) and input resistance data (−51.2 ± 6.19 mV) indicating modulation of a nonselective cation channel are most similar to that previously reported in SFO neurons by Washburn et al of −48 ± 4 mV (Washburn et al., 1999). Furthermore, insulin (Lakhi et al., 2013) and nesfatin-1 (Kuksis and Ferguson, 2014) have been shown to modulate both exclusively I_K without I_A, and glucose modulates I_{NSC} alone (Medeiros et al., 2012) to alter electrical excitability of SFO neurons. Moreover, Il-1β both decreases outward I_K and increases I_{NSC} resulting in a similar depolarisation and increased action potential frequency in dissociated SFO neurons (Desson and Ferguson, 2003). Whereas in response to Il-1β, depolarisation resulted primarily from nonselective cation channels, in our case, it is not clear whether modulation of these currents occur in the same or different cells.

Some neurons indicated exclusively decreased outward K^+ current: input resistance data from 3 neurons showed a reversal potential very close to the equilibrium potential of K^+ (−75.0 ± 3.8 mV; n=3/8 neurons which responded to neurotensin, of 16 total neurons tested), and long ramps from 6 neurons (of 10 neurons which responded to neurotensin, of 22 neurons total) indicated a decrease in outward current at 0 mV with no change in inward current below −20 mV, suggesting the modulation of a voltage-gated ion channel without changes in nonselective cation channels. However, one neuron displayed increased inward current below −60 mV in addition to decreased K^+ current beginning near −20 mV during the long ramp protocol, suggesting the involvement of both I_{NSC} and I_K (Figure 8). This indicates that in at least some cases both currents can be modulated by neurotensin in the same neuron. Whether I_K is also modulated to a smaller degree in the remaining neurons displaying increased nonselective cation current is not evident from the data.

Central neurotensin is implicated in mediation of numerous homeostatic mechanisms (Leeman, 1973; Rioux et al., 1981; Levine et al., 1983; Cooke et al., 2009). Of these, its effects on blood pressure, water balance, and feeding are most relevant to its expression in the SFO. Numerous intracerebroventricular injection experiments (Quirion et al., 1981; Rioux et al., 1981; Sumners et al., 1982) indicate that neurotensin in the brain modulates blood pressure, though some studies indicate a decrease in blood pressure (Quirion et al., 1981; Rioux et al., 1981) whereas one study found intracerebroventricular injections of neurotensin increased blood pressure (Sumners et al., 1982). Furthermore, some studies indicate bi- or triphasic changes in blood pressure in response to neurotensin (Oishi et al., 1981; Rioux et al., 1982; Gully et al., 1996), and differing pressor effects elicited from intravenous and intracerebroventricular injections (Sumners et al., 1982). The variable effects of neurotensin may be partially explained

by the involvement of peripheral sites in addition to central sites: in the guinea pig, neurotensinogenic fibres lead to the heart as indicated by immunohistochemistry, radioassay, and chromatography (Reinecke et al., 1982), and neurotensin infused in to guinea pig hearts acts as a vasodilator (Bachelard et al., 1986). Conversely, infusion of neurotensin to a rat heart increases mean coronary perfusion pressure (Quirion et al., 1980). Moreover, application of the ganglionic blocker hexamethonium inhibits the effect of intravenous neurotensin, suggesting the involvement of mast cells (Kérouac et al., 1982). Within the central nervous system, different nuclei may be involved in different phases of the triphasic effects of neurotensin: while microinjection to the NTS decrease blood pressure (Ciriello and Zhang, 1997), specific injection to the VTA strengthens increases in blood pressure due to vasopressin (Van Den Buuse and Catanzariti, 2000). If neurotensin at the SFO is implicated in regulation of blood pressure, it is not clear whether it may cause an increase or decrease. Previous direct microinjection experiments indicate that signalling molecules at the SFO may act to either increase (Smith et al., 2007; Kuksis et al., 2014) or decrease (Dai et al., 2013; Black et al., 2018) blood pressure, for example orexin and hydrogen sulfide increase blood pressure (Smith et al., 2007; Kuksis et al., 2014), whereas apelin and brain-derived neurotrophic factor decrease blood pressure (Dai et al., 2013; Black et al., 2018). Furthermore, that these signalling molecules may result in either depolarisation or hyperpolarisation of dissociated SFO neurons, irrespective of their effects on blood pressure. Direct microinjection of neurotensin to the SFO would be needed to clarify the role of neurotensin at the SFO on blood pressure, if any.

Another converging role of the SFO (Mangiapane and Simpson, 1980, 1983) and neurotensin (Rioux et al., 1981; Stanley et al., 1983) is in water homeostasis. Some of the earliest research on SFO physiology show that either electrical stimulation (Robertson et al., 1983) or

injection of angiotensin or acetylcholine (Mangiapane and Simpson, 1980, 1983) to the SFO induce polydipsia. Conversely, lesioning of the SFO disrupts normal thirst and water drinking when dehydrated. Moreover, SFO projects to many centres regulating thirst, including the SON (Lind et al., 1982; Sawchenko and Swanson, 1983), the MPN (Lind et al., 1982, 1984), the OVLT (Lind et al., 1982), the LH (Burton et al., 1976; Miselis, 1982), and the PVN (Miselis, 1982; Oka et al., 2015). Whether the SFO promotes thirst via its projections to the LH is un unclear: evidence suggests that the SFO does not modulate thirst through the LH as the dipsogenic effect of angiotensin microinjection to the SFO is not abolished by LH lesions (Kucharczyk et al., 1976), though these results may also be indicative of redundant pathways, or non-angiotensin-mediated drinking via the SFO to the LH. Evidence for the involvement of SFO projections to the PVN, SON, and MPN suggest the involvement of at least some of these structures: when SFO neurons were specifically stimulated using DREADD-based approach, increased *c-fos* activity was observed in the PVN, SON, and MPN only in mice with an intact SFO, and that this activation increases water and salt appetite (Nation et al., 2016), suggesting that these structures are implicated in SFO-mediated thirst. The best evidence exists for SFO-MPN connections in regulating thirst, as destruction of SFO-MPN projections greatly reduces angiotensin-mediated water drinking (Lind and Johnson, 1982), and activation of glutamatergic SFO neurons projecting to the MPN (but not to the PVN) promotes water drinking (Zimmerman et al., 2016). Notably the MPN also sends axonal projections to the PVN and SON, thus activation of the PVN and SON and SFO by DREADDs may be directly or indirectly due to the activation of SFO neurons.

That both intravenous (Stanley et al., 1983) and intracerebroventricular (Rioux et al., 1981) injections of neurotensin affect water intake has been noted for decades, though the nuclei

on which neurotensin acts to promote drinking remains unclear. Numerous neurotensin direct microinjection studies examining thirst have provided negative results, showing that neurotensin does not act directly on the PVN (Stanley et al., 1983), VTA, LH, amygdala, or the preoptic area of the hypothalamus (Baker et al., 1989) to promote dipsogenesis. Current evidence suggests that neurotensin cells in the LH release neurotensin to cause dipsogenesis (Kurt et al., 2019), though the endpoint of the LH neurotensin projections is unknown. Because LH is protected by the BBB, it cannot directly interact with signalling molecules unless they are specifically transported across the BBB; both the signalling molecule or the inputs to LH neurotensin neurons responsible for the neuron's effects on water homeostasis are also unknown. Projections from the OVLT are one possible source of synaptic input to the LH to modulate thirst (Hübschle et al., 1998), though the SFO also send axonal projections to the LH (Burton et al., 1976; Miselis, 1982).

Neurotensin (Stanley et al., 1983) and the SFO (Smith et al., 2010) also both have established roles in regulation of energy balance. The best understood aspect of the effect of neurotensin on appetite and feeding behaviour has been in the mesolimbic dopamine system nucleus the VTA, where neurotensin is involved in hedonic aspects of feeding (Cador et al., 1986). This appears to be mediated through NTSR1 (Seutin et al., 1989; Woodworth et al., 2017), which is not expressed in the SFO. Knockout studies suggest a clear role for NTSR1 in hedonic food intake, as these mice show increased intake of palatable foods specifically (Remaury et al., 2002; Opland et al., 2013). However, the relative importance of NTSR1 to homeostatic feeding varies depending on the mouse strain, as some NTSR1 knockout mice show hyperphagia and increased body weight (Remaury et al., 2002), others show hypophagia and weight loss (Opland et al., 2013). The homeostatic aspect of neurotensin's effect on feeding is

less well understood, though several nuclei appear to be implicated. Direct injection of neurotensin to the PVN (Stanley et al., 1982) and the NTS (de Beaurepaire and Suaudeau, 1988) suppresses feeding, though the circuits mediating these effects are not fully clear. Neurotensin may act both as a neurotransmitter or a peptide hormone, and the action of neurotensin as a neurotransmitter does not necessarily reflect its action as a peptide hormone. However, in addition to the nuclei noted above at least sensory CVO may respond to plasma neurotensin: circulating neurotensin activates hypothalamic nuclei and causes anorexia in vagotomised rats, but is not removed when neurotensin is prevented from crossing the BBB. The authors suggest this effect is due to homeostatic energy balance nuclei, as they saw no activation of reward regions in the nucleus accumbens or the BNST (Ratner et al., 2016). While activity of another sensory CVO, the area postrema, was increased as indicated by *c-fos* expression, the activity of the SFO was not investigated. Notably, the putative effects of neurotensin on cardiovascular output, fluid intake, and energy balance, are not mutually exclusive: other signalling molecules such as angiotensin II act the SFO to modulate multiple homeostatic properties.

The SFO also has a well-established role in regulation of energy balance. Specific electrical stimulation of the SFO induces feeding even in satiated rats (Smith et al., 2010). Furthermore, mounting evidence shows that the SFO is responsive to multiple energy balance signalling molecules including leptin (Smith et al., 2008; Smith and Ferguson, 2012), adiponectin (Alim et al., 2010), insulin (Lakhi et al., 2013), cholecystokinin (Ahmed et al., 2014), and amylin (Riediger et al., 2017). The only known neurotensinogenic projection to the SFO is from the ARC, which plays a major role in regulation of energy balance (Cowley et al., 2001; van den Top et al., 2004), and is also implicated in regulation of blood pressure (Brody et al., 1986). Given the converging roles of the SFO (Smith et al., 2010) and neurotensin (Levine et

al., 1983) in regulation of feeding, neurotensin may also act at the SFO to affect energy balance, via synaptic neurotensin from the ARC or plasma neurotensin.

In this study, we demonstrated that neurotensin modulates the electrical properties of dissociated SFO neurons, increasing their excitability via changes in I_K and I_{NSC}. The SFO is a potential site where neurotensin can act to affect blood pressure, drinking, and/or feeding, though to clarify the physiological role of the SFO, further research characterising the physiological effects of direct microinjection of neurotensin to the SFO on blood pressure and feeding behaviour is necessary.

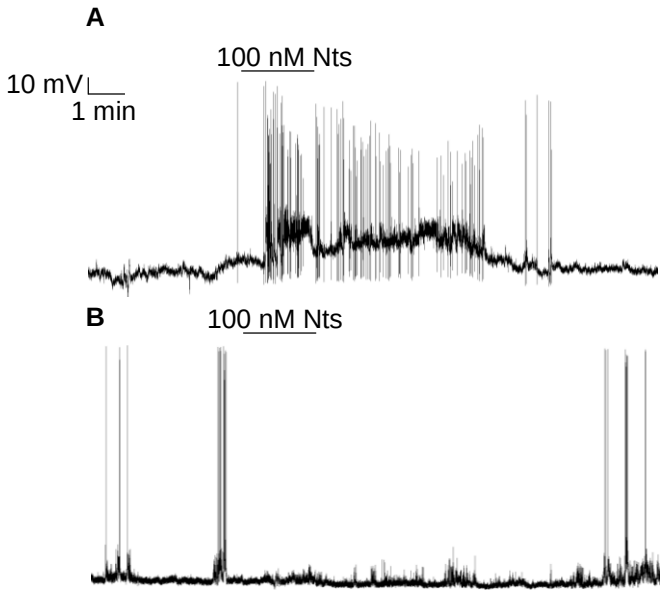

Figure 4.1. Representative current clamp traces showing dissociated SFO neurons which **(A)** depolarised and increased action potential frequency in response to 100 nM neurotensin (Nts) or **(B)** were insensitive to Nts.

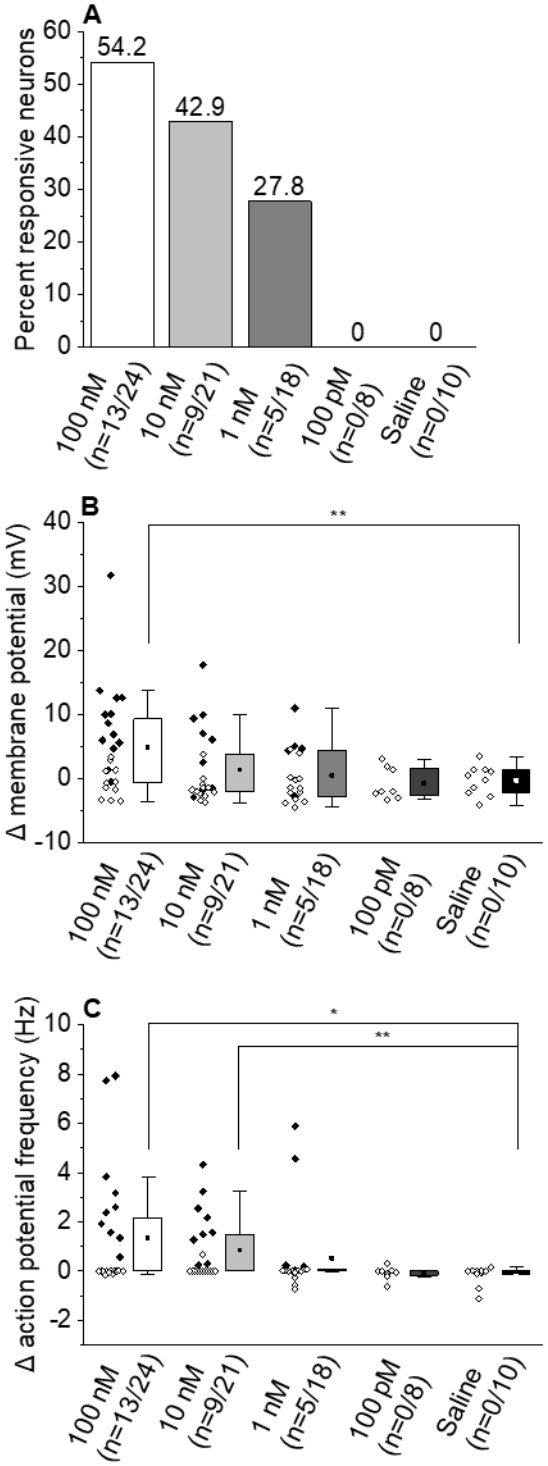
A
Percent responsive neurons
54.2
42.9
27.8
0
0
100 nM (n=13/24)
10 nM (n=9/21)
1 nM (n=5/18)
100 pM (n=0/8)
Saline (n=0/10)
B
Δ membrane potential (mV)
**
C
Δ action potential frequency (Hz)
*
**

Figure 4.2. Neurotensin dose-dependently modulates electrical properties of SFO neurons. **(A)** Percentage of SFO neurons responsive to neurotensin is dependent on dose at concentrations of 0.1 – 100 nM. **(B)** Effect of neurotensin on membrane potential 0.1 – 100 nM. **(C)** Effect of neurotensin on action potential frequency 0.1 – 100 nM. Open points are non-responders whereas filled points indicate responders. Whiskers indicate 1.5 interquartile range, square in box indicates mean. Asterisk indicates statistically significance of responsive neurons vs saline controls * $p < 0.05$; ** $p < 0.01$ (one-way ANOVA with *post hoc* t-test and Bonferroni correction.)

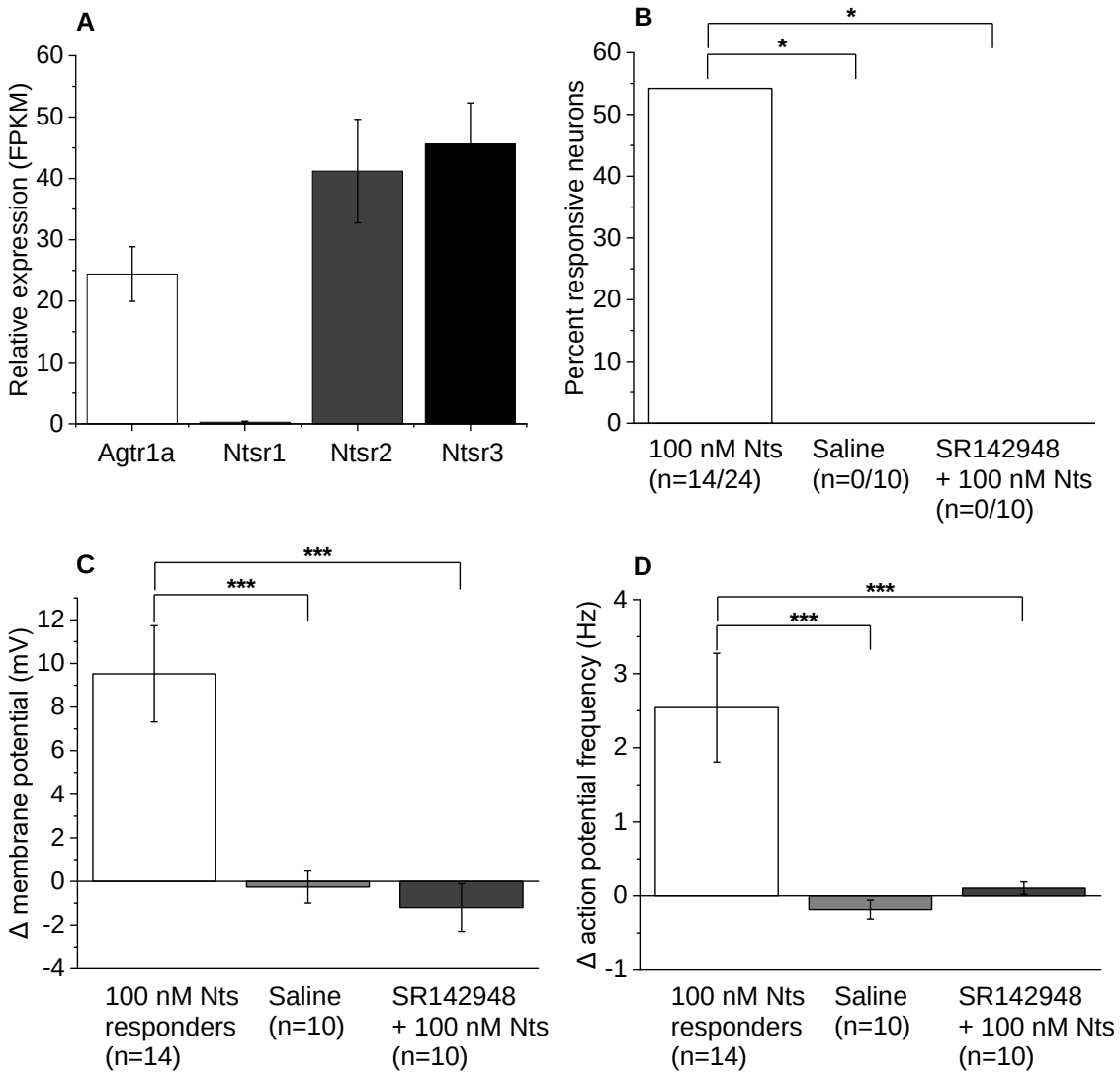
A
Relative expression (FPKM)
60
50
40
30
20
10
0
Agtr1a
Ntsr1
Ntsr2
Ntsr3
B
Percent responsive neurons
*
*
60
50
40
30
20
10
0
100 nM Nts
(n=14/24)
Saline
(n=0/10)
SR142948
+ 100 nM Nts
(n=0/10)
C
Δ membrane potential (mV)
***
***
12
10
8
6
4
2
0
-2
-4
100 nM Nts
responders
(n=14)
Saline
(n=10)
SR142948
+ 100 nM Nts
(n=10)
D
Δ action potential frequency (Hz)
***
***
4
3
2
1
0
-1
100 nM Nts
responders
(n=14)
Saline
(n=10)
SR142948
+ 100 nM Nts
(n=10)

Figure 4.3. Effect of neurotensin on SFO neurons is specific to NTSR2. **(A)** RNAseq expression data shows that *Ntsr2* and *3* are highly expressed in the SFO (mean ± 95% confidence interval), whereas *Ntsr1* expression does not meet the detection cut-off (FPKM<0.5) (Peterson et al., 2018). Angiotensin 2 receptor *Agtr1a* expression is provided for comparison. **(B)** Of 10 neurons pre-treated with the NTSR1/2 specific antagonist SR142948, none showed a significant response to 100 nM neurotensin; this distribution was significantly different from 100 nM neurotensin without antagonist (Chi Square test, p =0.0423). **(C)** Changes in membrane potential and **(D)** action potential frequency were not significantly different from saline controls.

* indicates p< 0.05; ** p<0.01; *** p< 0.001 (Proportion responsive neurons: Chi-square test; Membrane potential and action potential frequency: one-way ANOVA with post-hoc Bonferroni correction).

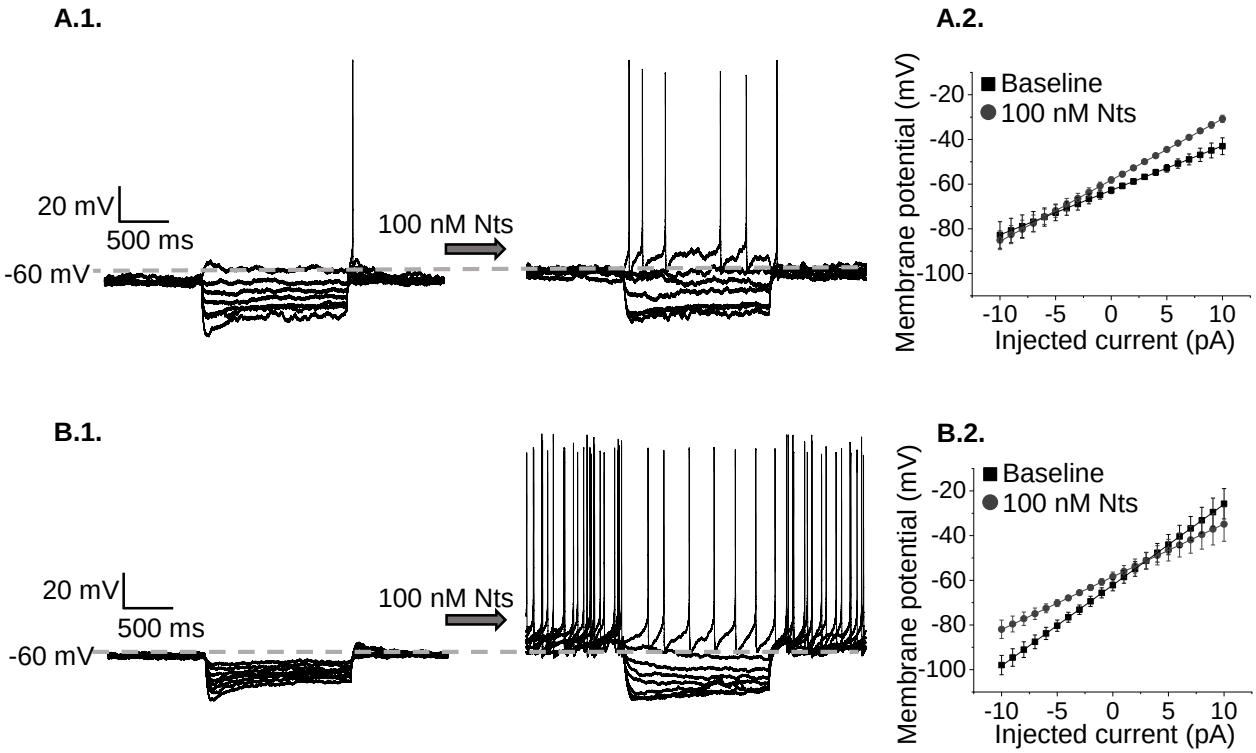

Figure 4.4. Voltage-current (VI) plots were constructed before and after 100 nM neurotensin application. SFO neurons which **(A)** responded and show increased input resistance, or **(B)** responded and decreased increased input resistance. A.1. and B.1. are representative traces of SFO neurons showing changes in membrane potential elicited by current injections before and after 100 nM neurotensin. A.2. and B.2. are VI plots constructed from mean of neurons which (A.2.) responded with increased input resistance (n=3) or (B.2.) responded with decreased input resistance (n=5). Values are reported as mean ± SEM. The combination of increased input resistance and a reversal potential of -75.0 ± 3.8 mV implies the modulation of K^+ channels in one set of neurons. Decreased input resistance and a reversal potential of -51.3 ± 6.1 mV implies the modulation nonselective cation channels.

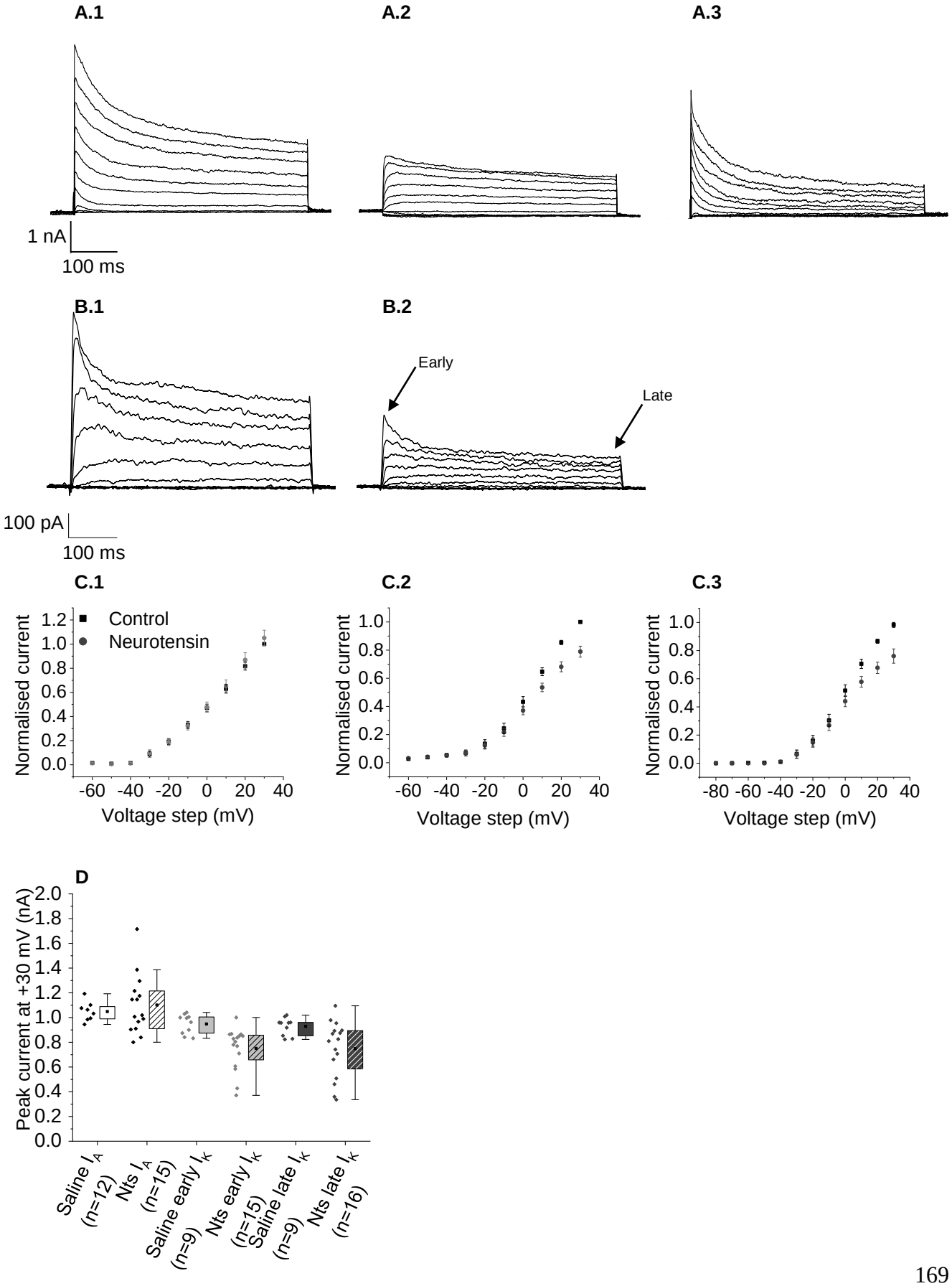
A.1
A.2
A.3
1 nA
100 ms
B.1
B.2
Early
Late
100 pA
100 ms
C.1
C.2
C.3
Control
Neurotensin
Normalised current
Voltage step (mV)
D
Peak current at +30 mV (nA)
Saline I_A (n=12)
Nts I_A (n=15)
Saline early I_K (n=9)
Nts early I_K (n=15)
Saline late I_K (n=9)
Nts late I_K (n=16)

Figure 4.5. Neurotensin attenuates delayed-rectifier K^+ current (I_K), but not transient K^+ (I_A). **(A)** Representative traces showing examples of voltage-gated K+ current. Voltage-gated Na^+ currents are truncated. To investigate voltage-gated K^+ currents, SFO neurons were subjected to 500 ms 10 mV voltage steps from -60 to +30 mV. A.1. Total K^+ current (I_{TOT}) elicited by hold at -100 mV pre-pulse to remove inactivation. A.2. I_K of an SFO neuron. I_A was on inactivated by a -30 mV pre-pulse, revealing only the I_K component. A.3. I_A of an SFO neuron, revealed by subtracting I_K from I_{TOT}. **(B)** I_K of a SFO neuron before (B.1) and after (B.2) 100 nM neurotensin application. Current at both early and late time points is reduced. **(C)** Normalised IV plots showing changes in I_A (C.1) and both early and late I_K (C.2, C.3), expressed as mean ± SEM. Differences between mean IV plots before and after 100 nM neurotensin were significant for early (F-test, $p=1.5x10^{-4}$) and late (F-test, $p=7.3x10^{-12}$) I_K, but not peak I_A (F-test, p=0.20). **(D)** Fold change in peak K^+ current at +30 mV.

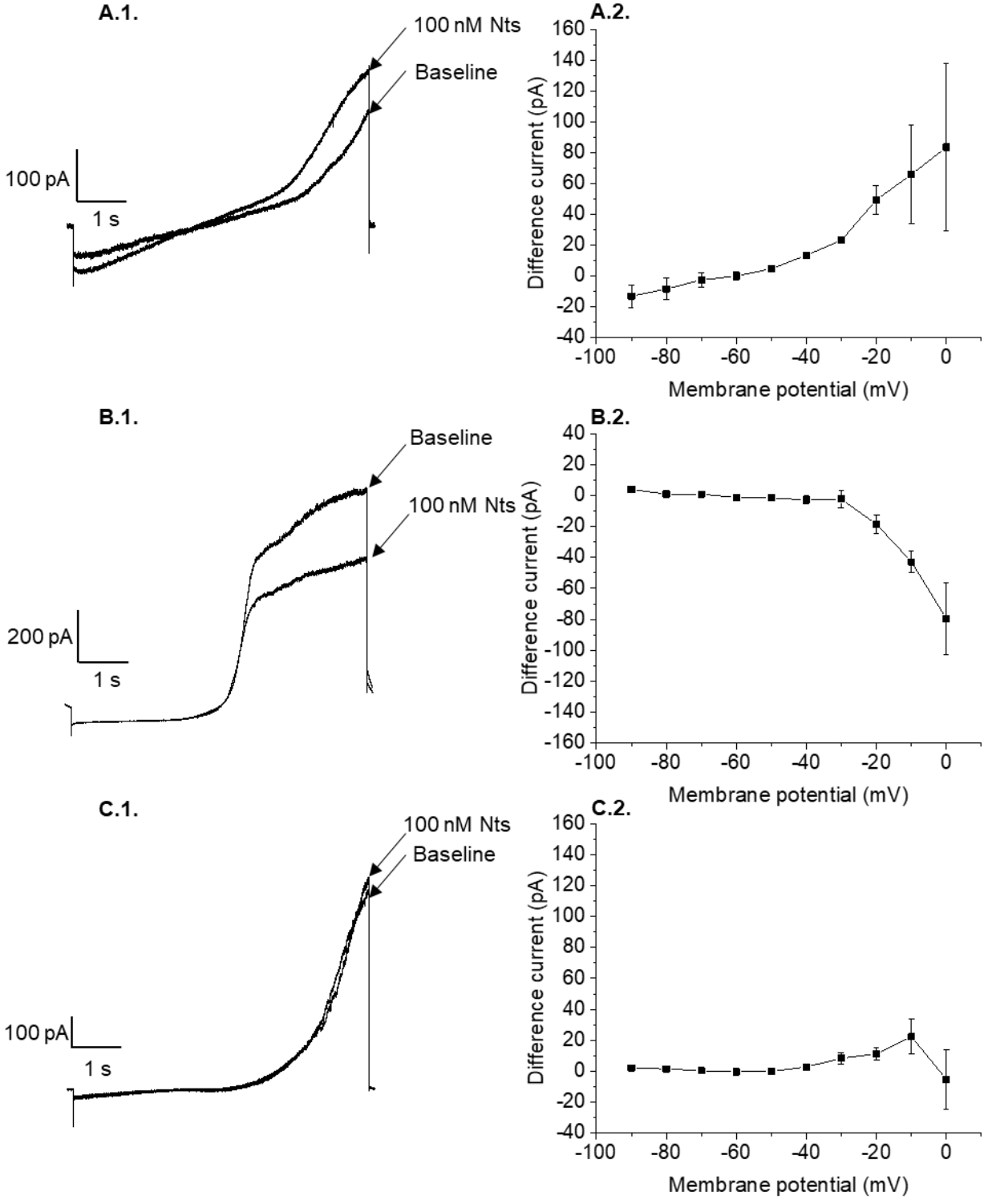
A.1.
100 nM Nts
Baseline
100 pA
1 s
A.2.
Difference current (pA)
Membrane potential (mV)
B.1.
Baseline
100 nM Nts
200 pA
1 s
B.2.
Difference current (pA)
Membrane potential (mV)
C.1.
100 nM Nts
Baseline
100 pA
1 s
C.2.
Difference current (pA)
Membrane potential (mV)

Figure 4.6. Current though nonselective cation channels (I_{NSC}) and voltage-gated K^+ current (I_K) is decreased by neurotensin in SFO neurons. **(A)** A subset of SFO neurons respond to neurotensin through increased I_{NSC}. A.1. Representative trace of a SFO neuron displaying increased current through a nonselective cation channel after application of 100 nM neurotensin (Nts). A.2. Mean (± SEM) difference current of neurons displaying increased I_{NSC} after 100 nM neurotensin application (n=4/22 treated with neurotensin). **(B)** A subset of SFO neurons respond to neurotensin through decreased voltage-gated K^+ conductance. B.1. Representative trace of a SFO neuron displaying decreased delayed-rectified K^+ conductance (I_K) after application of 100 nM neurotensin. B.2. Mean (± SEM) difference current of neurons displaying decreased I_K after 100 nM neurotensin application (n=6/22 treated with neurotensin). **(C)** A subset of SFO neurons do not respond to neurotensin. C.1. Representative trace of a SFO neuron no response to 100 nM neurotensin. C.2. Mean (± SEM) difference current of neurons which did not respond to 100 nM neurotensin (n=12/22 treated with neurotensin).

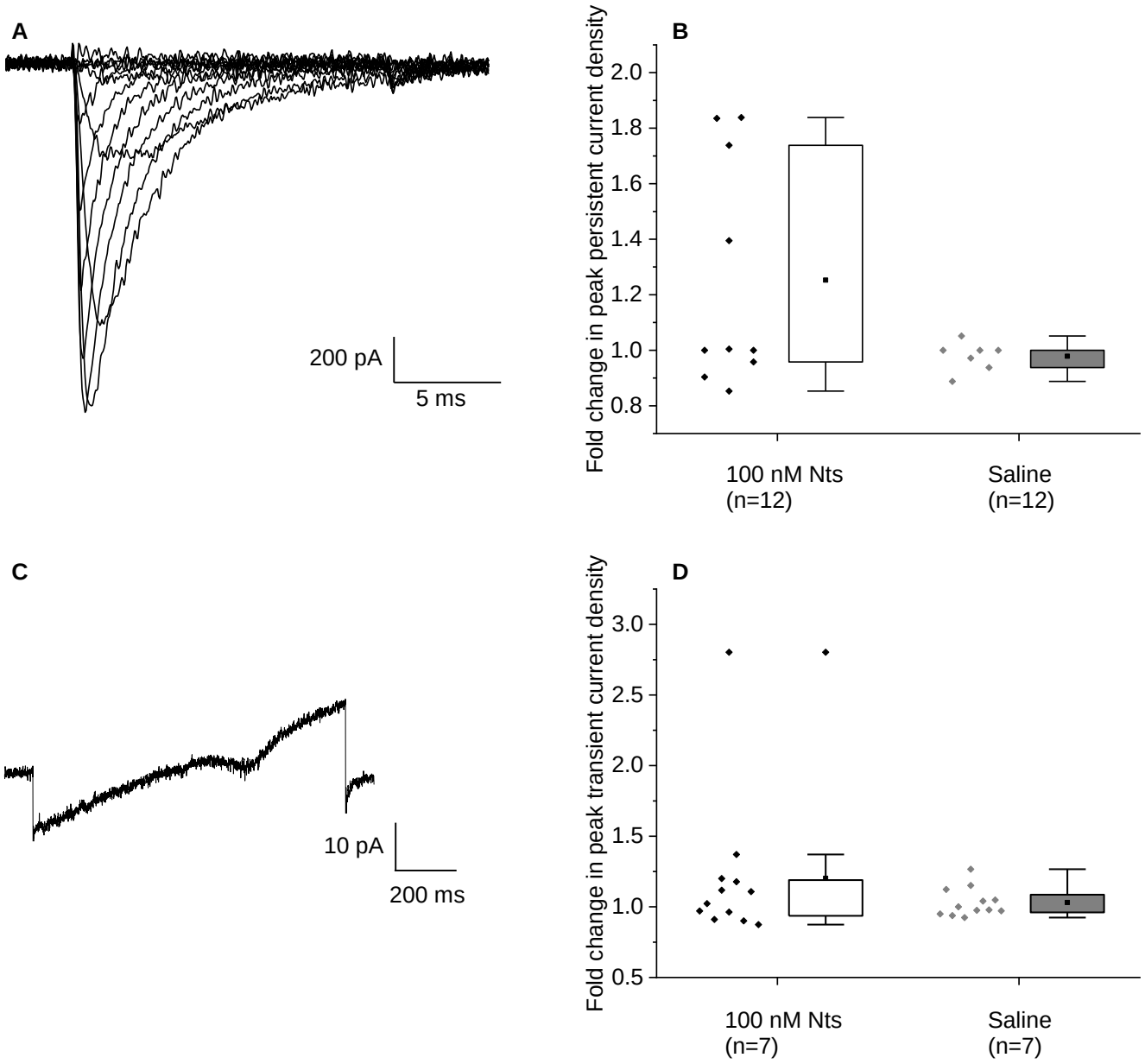

Figure 4.7. Voltage-gated Na^+ currents are not significantly modulated by neurotensin in SFO neurons. **(A)** A representative trace of the transient component of Na^+ current in a SFO neuron, elicited from a prepulse at -90 mV followed by 15 ms voltage steps from -70 to +50 mV. **(B)** Peak density of transient Na+ current in neurotensin-exposed neurons vs saline controls. **(C)** A representative trace of the persistent component of Na^+ current in a SFO neuron, elicited from a 1s ramp from -100 to 0 mV. **(D)** Peak density of persistent Na^+ current in neurotensin-exposed neurons vs saline controls.

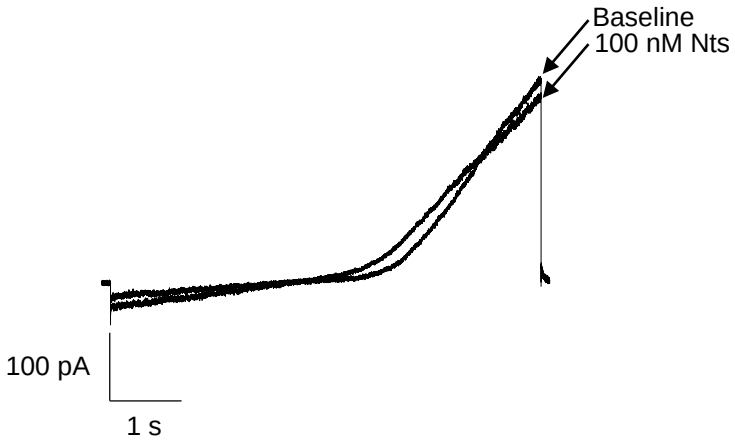

Figure 4.8. I_{NSC} and I_K may be modulated in the same neuron. The long ramp data from 1 SFO neuron indicates an increase in I_{NSCC} and a decrease in I_K to increase the neuron's electrical excitability. Note the increase in inward current at -100 mV, and the linear trend in the neurotensin-exposed neuron which is indicative of an increase in I_{NSC}. The change in the linear trend at approximately -30 mV indicates a decrease in outward K^+ current.

4.6. References

Ahmed A-SF, Dai L, Ho W, Ferguson A V., Sharkey KA (2014) The subfornical organ: a novel site of action of cholecystokinin. Am J Physiol Integr Comp Physiol 306:R363–R373.

Alim I, Mark Fry W, Walsh MH, Ferguson A V. (2010) Actions of adiponectin on the excitability of subfornical organ neurons are altered by food deprivation. Brain Res 1330:72–82 Available at: http://dx.doi.org/10.1016/j.brainres.2010.02.076.

Bachelard H, St-Pierre S, Rioux F (1986) The coronary vasodilator effect of neurotensin in the guinea pig isolated heart. Peptides 7:431–435 Available at: http://www.sciencedirect.com/science/article/pii/0196978186900100.

Baker JD, Hawkins MF, Baumeister AA, Nagy M (1989) Microinjection of neurotensin into the CNS induces hyperdipsia in the rat. Pharmacol Biochem Behav 33:7–10 Available at: http://www.sciencedirect.com/science/article/pii/0091305789904206.

Black EAE, Smith PM, Mcisaac W, Ferguson A V (2018) Brain-derived neurotrophic factor acts at neurons of the subfornical organ to influence cardiovascular function. Physiol Rep 6:1–10 Available at: https://doi.org/10.14814/phy2.13704.

Brody MJ, O'Neill TP, Porter JP (1986) Role of paraventricular and arcuate nuclei in cardiovascular regulation. In: Central and peripheral mechanisms of cardiovascular regulation, pp 443–464. Springer.

Burton MJ, Rolls ET, Mora F (1976) Effects of hunger on the responses of neurons in the lateral hypothalamus to the sight and taste of food. Exp Neurol 51:668–677.

Cador M, Kelley AE, Le Moal M, Stinus L (1986) Ventral tegmental area infusion of substance

P, neurotensin and enkephalin: differential effects on feeding behavior. Neuroscience 18:659–669.

Carraway R, Leeman SE (1973) The isolation of a new hypotensive peptide, neurotensin, from bovine hypothalami. J Biol Chem 248:6854–6861.

Cerqueira DR, Ferreira HS, Moiteiro ALBB, Fregoneze JB (2016) Effects of interleukin-1 beta injections into the subfornical organ and median preoptic nucleus on sodium appetite, blood pressure and body temperature of sodium-depleted rats. Physiol Behav 163:149–160 Available at: http://dx.doi.org/10.1016/j.physbeh.2016.05.003.

Chalon P, Vita N, Kaghad M, Guillemot M, Bonnin J, Delpech B, Le Fur G, Ferrara P, Caput D (1996) Molecular cloning of a levocabastine-sensitive neurotensin binding site. FEBS Lett 386:91–94.

Ciriello J, Zhang TX (1997) Cardiovascular effects of neurotensin microinjections into the nucleus of the solitary tract. Brain Res 749:35–43.

Cooke JH, Patterson M, Patel SR, Smith KL, Ghatei MA, Bloom SR, Murphy KG (2009) Peripheral and central administration of xenin and neurotensin suppress food intake in rodents. Obesity 17:1135–1143.

Cowley MA, Smart JL, Rubinstein M, Cerdán MG, Diano S, Horvath TL, Cone RD, Low MJ (2001) Leptin activates anorexigenic POMC neurons through a neural network in the arcuate nucleus. Nature 411:480.

Dai L, Smith PM, Kuksis M, Ferguson A V. (2013) Apelin acts in the subfornical organ to influence neuronal excitability and cardiovascular function. J Physiol 591:3421–3432.

de Beaurepaire R, Suaudeau C (1988) Anorectic effect of calcitonin, neurotensin and bombesin infused in the area of the rostral part of the nucleus of the tractus solitarius in the rat. Peptides 9:729–733.

Desson SE, Ferguson AV (2003) Interleukin 1β modulates rat subfornical organ neurons as a result of activation of a non-selective cationic conductance. J Physiol 550:113–122.

Donevan SD, Van Vugt DA, Ferguson A V. (1989) Subfornical organ activation stimulates luteinizing hormone secretion in the rat. Brain Res 488:398–402.

Fassio A, Evans G, Grisshammer R, Bolam JP, Mimmack M, Emson PC (2000) Distribution of the neurotensin receptor NTS1 in the rat CNS studied using an amino-terminal directed antibody. Neuropharmacology 39:1430–1442.

Ferguson A V., Bicknell JR, Carew MA, Mason WT (1997) Dissociated adult rat subfornical organ neurons maintain membrane properties and angiotensin responsiveness for up to 6 days. Neuroendocrinology 66:409–415.

Gevaert B, Wynendaele E, Stalmans S, Bracke N, D'Hondt M, Smolders I, Van Eeckhaut A, De Spiegeleer B (2016) Blood-brain barrier transport kinetics of the neuromedin peptides NMU, NMN, NMB and NT. Neuropharmacology 107:460–470.

Goedert M, Lightman SL, Emson PC (1984) Neurotensin in the rat anterior pituitary gland: effects of endocrinological manipulations. Brain Res 299:160–163.

Gruber K, McRae-Degueurce A, Wilkin LD, Mitchell LD, Johnson AK (1987) Forebrain and brainstem afferents to the arcuate nucleus in the rat : potential pathways for the modulation of hypophyseal secretions. Neurosci Lett 75:1–5 Available at:

http://www.ncbi.nlm.nih.gov/pubmed/3574762 [Accessed November 13, 2015].

Gully D, Lespy L, Canton M, Rostene W, Kitabgi P, Le Fur G, Maffrand JP (1996) Effect of the neurotensin receptor antagonist SR48692 on rat blood pressure modulation by neurotensin. Life Sci 58:665–674.

Hawkins MF, Baker JD, Baumeister AA (1989) Neurotensin-induced polydipsia: a structure-activity study. Brain Res 487:188–191.

Heine P, Witt G, Gilardi A, Gribbon P, Kummer L, Plückthun A (2019) High-throughput fluorescence polarization assay to identify ligands using purified G protein-coupled receptor. SLAS Discov Adv Life Sci R&D 0:1–13 Available at: http://journals.sagepub.com/doi/10.1177/2472555219837344.

Hernesniemi J, Kawana E, Bruppacher H, Sandri C (1972) Afferent connections of the subfornical organ and of the supraoptic crest. Cells Tissues Organs 81:321–336.

Hollis JH, McKinley MJ, D'Souza M, Kampe J, Oldfield BJ (2008) The trajectory of sensory pathways from the lamina terminalis to the insular and cingulate cortex: a neuroanatomical framework for the generation of thirst. Am J Physiol Integr Comp Physiol 294:R1390–R1401.

Hoyda TD, Smith PM, Ferguson A V (2009) Gastrointestinal hormone actions in the central regulation of energy metabolism: potential sensory roles for the circumventricular organs. Int J Obes (Lond) 33 Suppl 1:S16-21 Available at: http://www.ncbi.nlm.nih.gov/pubmed/19363501 [Accessed November 13, 2015].

Hübschle T, McKinley MJ, Oldfield BJ (1998) Efferent connections of the lamina terminalis, the

preoptic area and the insular cortex to submandibular and sublingual gland of the rat traced with pseudorabies virus. Brain Res 806:219–231 Available at: http://www.sciencedirect.com/science/article/pii/S0006899398007653.

Inoshima I, Inoshima N, Wilke G, Powers M, Frank K, Wang Y, Wardenburg JB (2017) Neurotensin receptor-1 identifies a subset of ventral tegmental dopamine neurons that coordinate energy balance. Cell Rep 20:1881–1892.

Ishizuka T, Wei X, Kubo T (1993) Cardiovascular effects of microinjections of thyrotropin-releasing hormone, oxytocin and other neuropeptides into the rostral ventrolateral medulla of the rat. Arch Int Pharmacodyn Ther 322:35–44 Available at: http://europepmc.org/abstract/MED/8215715.

Jacobsen L, Madsen P, Jacobsen C, Nielsen MS, Gliemann J, Petersen CM (2001) Activation and functional characterization of the mosaic receptor SorLA/LR11 *. J Biol Chem 276:22788–22796.

Kérouac R, St-Pierre S, Rioux F (1982) Influence of various drugs on the variations of blood pressure, hematocrit and plasma histamine caused by neurotensin and compound 4880 in rats. Neuropeptides 3:145–157 Available at: http://www.sciencedirect.com/science/article/pii/0143417982900105.

Kucharczyk J, Assaf SY, Mogenson GJ (1976) Differential effects of brain lesions on thirst induced by the administration of angiotensin-II to the preoptic region, subfornical organ and anterior third ventricle. Brain Res 108:327–337 Available at: http://www.sciencedirect.com/science/article/pii/000689937690189X.

Kuksis M, Ferguson A V (2014) Cellular Actions of Nesfatin-1 in the Subfornical Organ. J

Neuroendocrinol 26:237–246 Available at: https://doi.org/10.1111/jne.12143.

Kuksis M, Smith PM, Ferguson A V. (2014) Hydrogen sulfide regulates cardiovascular function by influencing the excitability of subfornical organ neurons. PLoS One 9:1–11.

Kurt G, Woodworth HL, Fowler S, Bugescu R, Leinninger GM (2019) Activation of lateral hypothalamic area neurotensin-expressing neurons promotes drinking. Neuropharmacology 154:13–21.

Lakhi S, Snow W, Fry M (2013) Insulin modulates the electrical activity of subfornical organ neurons. Neuroreport 24:329–334.

Leeman SE (1973) The isolation of a new hypotensive from bovine hypothalamus. J Biol Chem 248:6854–6861.

Levine AS, Kneip J, Grace M, Morley JE (1983) Effect of centrally administered neurotensin on multiple feeding paradigms. Pharmacol Biochem Behav 18:19–23.

Lind RW, Hoesen GW van, Johnson AK (1982) An HRP study of the connections of the subfornical organ of the rat. J Comp Neurol 210:265–277.

Lind RW, Johnson AK (1982) Subfornical organ-median preoptic connections and drinking and pressor responses to angiotensin II. J Neurosci 2:1043 LP – 1051 Available at: http://www.jneurosci.org/content/2/8/1043.abstract.

Lind RW, Swanson LW, Ganten D (1984) Angiotensin II immunoreactivity in the neural afferents and efferents of the subfornical organ of the rat. Brain Res 321:209–215.

Mangiapane ML, Simpson JB (1980) Subfornical organ: forebrain site of pressor and dipsogenic action of angiotensin II. Am J Physiol 239:R382-9 Available at:

http://www.ncbi.nlm.nih.gov/pubmed/7435651 [Accessed November 13, 2015].

Mangiapane ML, Simpson JB (1983) Drinking and pressor responses after acetylcholine injection into subfornical organ. AJP Regul Integr Comp Physiol 244:R508-13.

Martin S, Navarro V, Vincent JP, Mazella J (2002) Neurotensin receptor-1 and -3 complex modulates the cellular signaling of neurotensin in the HT29 cell line. Gastroenterology 123:1135–1143.

McKinley MJ, McAllen RM, Giles ME, Penschow J, Sunn N, Uschakov A, Oldfield BJ (2003) The sensory circumventricular organs of the mammalian brain. Adv Anat Cell Biol 172:III–XII, 1–122, back cover.

Medeiros N, Dai L, Ferguson A V (2012) Glucose-responsive neurons in the subfornical organ of the rat—a novel site for direct CNS monitoring of circulating glucose. Neuroscience 201:157–165 Available at: http://www.sciencedirect.com/science/article/pii/S0306452211012954.

Miselis RR (1982) The subfornical organ's neural connections and their role in water balance. Peptides 3:501–502 Available at: http://www.sciencedirect.com.uml.idm.oclc.org/science/article/pii/0196978182901152 [Accessed December 14, 2017].

Nation HL, Nicoleau M, Kinsman BJ, Browning KN, Stocker SD (2016) DREADD-induced activation of subfornical organ neurons stimulates thirst and salt appetite. J Neurophysiol 115:3123–3129.

Nemeroff CB, Bissette G, Prange AJ, Peter T, Barlow TS, Lipton MA (1977) Neurotensin:

Central nervous system effects of a hypothalamic peptide. Brain Res 128:485–496.

Nouel D, Sarret P, Vincent JP, Mazella J, Beaudet A (1999) Pharmacological, molecular and functional characterization of glial neurotensin receptors. Neuroscience 94:1189–1197.

Oishi M, Inagaki C, Fujiwara M, Takaori S, Yajima H, Akazawa Y (1981) Possible mechanisms of the triphasic effects of neurotensin on the rat blood pressure. Jpn J Pharmacol 31:1043–1049.

Oka Y, Ye M, Zuker CS (2015) Thirst driving and suppressing signals encoded by distinct neural populations in the brain. Nature 520:349–352.

Ono K, Toyono T, Honda E, Inenaga K (2005) Transient outward K^+ currents in rat dissociated subfornical organ neurones and angiotensin II effects. J Physiol 568:979–991 Available at: http://doi.wiley.com/10.1113/jphysiol.2005.089508.

Opland D, Sutton A, Woodworth H, Brown J, Bugescu R, Garcia A, Christensen L, Rhodes C, Myers Jr M, Leinninger G (2013) Loss of neurotensin receptor-1 disrupts the control of the mesolimbic dopamine system by leptin and promotes hedonic feeding and obesity. Mol Metab 2:423–434 Available at: https://www.ncbi.nlm.nih.gov/pubmed/24327958.

Paxinos G, Watson C (2007) The Rat Brain in Stereotaxic Coordinates, 6th ed. Elsevier Inc.

Petersen CM, Nielsen MS, Jacobsen L, Tommerup N, Rasmussen HH, Røigaard H, Madsen P, Søren K, Chem JB, Nykjær A, Gliemann J, Moestrup SK (1997) Molecular identification of a novel candidate sorting receptor purified from human brain by receptor-associated protein affinity chromatography. J Biol Chem 272:3599–3605.

Peterson CS, Huang S, Lee SA, Ferguson AV, Fry WM (2018) The trancriptome of the Rattus

norvegicus subfornical organ is altered in response to early postnatal overnutrition induced by small litter size. IBRO Reports 5:17–23.

Pulman KJ, Fry WM, Cottrell GT, Ferguson A V (2006) The subfornical organ: a central target for circulating feeding signals. J Neurosci 26:2022–2030.

Quirion R, Rioux F, Regoli D, St-Pierre S (1980) Pharmacological studies of neurotensin, several fragments and analogues in the isolated perfused rat heart. Eur J Pharmacol 66:257–266 Available at: http://www.sciencedirect.com/science/article/pii/0014299980904574.

Quirion R, Rioux F, St-Pierre S, Bélanger F, Jolicoeur FB, Barbeau A (1981) Hypotensive effects of centrally and peripherally administered neurotensin and neurotensin derivatives in rats. Neuropeptides 1:253–259.

Ratner C, Skov LJ, Raida Z, Bächler T, Bellmann-Sickert K, Foll C Le, Sivertsen B, Dalbøge LS, Hartmann B, Beck-Sickinger AG, Madsen AN, Jelsing J, Holst JJ, Lutz TA, Andrews ZB, Holst B (2016) Effects of peripheral neurotensin on appetite regulation and its role in gastric bypass surgery. Endocrinology 157:3482–3492.

Reinecke M, Weihe E, Carraway RE, Leeman SE, Forssmann WG (1982) Localization of neurotensin immunoreactive nerve fibers in the guinea-pig heart: Evidence derived by immunohistochemistry, radioimmunoassay and chromatography. Neuroscience 7:1785–1795 Available at: http://www.sciencedirect.com/science/article/pii/0306452282900367.

Remaury A, Vita N, Gendreau S, Jung M, Arnone M, Poncelet M, Culouscou J-M, Le Fur G, Soubrié P, Caput D, Shire D, Kopf M, Ferrara P (2002) Targeted inactivation of the neurotensin type 1 receptor reveals its role in body temperature control and feeding behavior but not in analgesia. Brain Res 953:63–72 Available at:

http://www.sciencedirect.com/science/article/pii/S0006899302032717.

Riediger T, Rauch M, Schmid HA (2017) Actions of amylin on subfornical organ neurons and on drinking behavior in rats. Am J Physiol Integr Comp Physiol 276:R514–R521.

Rioux F, Kérouac R, St-Pierre S (1982) Analysis of the biphasic depressor-pressor effect and tachycardia caused by neurotensin in ganglion-blocked rats. Neuropeptides 3:113–127 Available at: http://www.sciencedirect.com/science/article/pii/0143417982900075.

Rioux F, Quirion R, St-Pierre S, Regoli D, Jolicoeur FB, Bélanger F, Barbeau A (1981) The hypotensive effect of centrally administered neurotensin in rats. Eur J Pharmacol 69:241–247 Available at: http://www.ncbi.nlm.nih.gov/pubmed/7215426.

Risau W, Wolburg H (1990) Development of the blood-brain barrier. Trends Neurosci 13:174–178 Available at: http://www.sciencedirect.com/science/article/pii/016622369090043A [Accessed November 13, 2015].

Robertson A, Kucharczyk J, Mogenson GJ (1983) Drinking behavior following electrical stimulation of the subfornical organ in the rat. Brain Res 274:197–200 Available at: http://www.sciencedirect.com/science/article/pii/0006899383905413.

Rosas-Arellano MP, Solano-Flores LP, Ciriello J (1996) Neurotensin projections to subfornical organ from arcuate nucleus. Brain Res 706:323–327.

Sarret P, Krzywkowski P, Segal L, Nielsen MS, Petersen CM, Mazella J, Stroh T, Beaudet A (2003a) Distribution of NTS3 receptor/sortilin mRNA and protein in the rat central nervous system. J Comp Neurol 461:483–505 Available at: http://doi.wiley.com/10.1002/cne.10708.

Sarret P, Perron A, Stroh T, Beaudet A (2003b) Immunohistochemical distribution of NTS2

neurotensin receptors in the rat central nervous system. J Comp Neurol 461:520–538.

Sawchenko PE, Swanson LW (1983) The organization of forebrain afferents to the paraventricular and supraoptic nuclei of the rat. J Comp Neurol 218:121–144.

Seutin V, Massotte L, Dresse A (1989) Electrophysiological effects of neurotensin on dopaminergic neurones of the ventral tegmental area of the rat in vitro. Neuropharmacology 28:949–954.

Smith PM, Chambers AP, Price CJ, Ho W, Hopf C, Sharkey KA, Ferguson A V (2008) The subfornical organ: a central nervous system site for actions of circulating leptin. Am J Physiol Integr Comp Physiol 296:R512–R520 Available at: http://ajpregu.physiology.org/cgi/doi/10.1152/ajpregu.90858.2008.

Smith PM, Ferguson A V. (2012) Cardiovascular Actions of Leptin in the Subfornical Organ are Abolished by Diet-Induced Obesity. J Neuroendocrinol 24:504–510.

Smith PM, Rozanski G, Ferguson A V. (2010) Acute electrical stimulation of the subfornical organ induces feeding in satiated rats. Physiol Behav 99:534–537.

Smith PM, Samson WK, Ferguson A V. (2007) Cardiovascular actions of orexin-A in the rat subfornical organ. J Neuroendocrinol 19:7–13.

Stanley BG, Eppel N, Hoebel BG (1982) Neurotensin injected into the paraventricular hypothalamus suppresses feeding in rats. Ann N Y Acad Sci 400:425–427.

Stanley BG, Hoebel BG, Leibowitz SF (1983) Neurotensin: effects of hypothalamic and intravenous injections on eating and drinking in rats. Peptides 4:493–500.

Sumners C, Phillips MI, Richards EM (1982) Central pressor action of neurotensin in conscious

rats. Hypertension 4:888–893.

Sundler F, Håkanson R, Hammer RA, Alumets J, Carraway R, Leeman SE, Zimmerman EA (1977) Immunohistochemical localization of neurotensin in endocrine cells of the gut. Cell Tissue Res 178:313–321.

Swanson LW, Lind RW (1986) Neural projections subserving the initiation of a specific motivated behavior in the rat: new projections from the subfornical organ. Brain Res 379:399–403.

Takahashi Y, Smith P, Ferguson A, Pittman QJ (1997) Circumventricular organs and fever. Am J Physiol 273:R1690-5 Available at: http://www.ncbi.nlm.nih.gov/pubmed/9374811 [Accessed November 13, 2015].

Tanaka K, Masu M, Nakanishi S (1990) Structure and functional expression of the cloned rat neurotensin receptor. Neuron 4:847–854 Available at: https://doi.org/10.1016/0896-6273(90)90137-5.

Thunhorst RL, Beltz TG, Johnson AK (1999) Effects of subfornical organ lesions on acutely induced thirst and salt appetite. Am J Physiol Integr Comp Physiol 277:R56–R65.

Van Den Buuse M, Catanzariti R (2000) Stimulation of the ventral tegmental area enhances the effect of vasopressin on blood pressure in conscious rats. Br J Pharmacol 129:29–36.

van den Top M, Lee K, Whyment AD, Blanks AM, Spanswick D (2004) Orexigen-sensitive NPY/AgRP pacemaker neurons in the hypothalamic arcuate nucleus. Nat Neurosci 7:493.

Wall KM, Nasr M, Ferguson A V. (1992) Actions of endothelin at the subfornical organ. Brain Res 570:180–187.

Washburn DLS, Smith PM, Ferguson A V (1999) Control of neuronal excitability by an ion-sensing receptor. Eur J Neurosci 11:1947–1954 Available at: https://doi.org/10.1046/j.1460-9568.1999.00619.x.

Werkman TR, Kruse CG, Nievelstein H, Long SK, Wadman WJ (1999) Neurotensin attenuates the quinpirole-induced inhibition of the firing rate of dopamine neurons in the rat substantia nigra pars compacta and the ventral tegmental area. Neuroscience 95:417–423.

Whyment A, Top M Van Den, Lee K, Whyment AD, Blanks AM, Spanswick D (2004) Orexigen-sensitive NPY / AgRP pacemaker neuons in the hypothalamic arcuate nucleus. Nat Neurosci 7:493–494.

Woodworth HL, Batchelor HM, Beekly BG, Bugescu R, Brown JA, Kurt G, Fuller PM, Leinninger GM (2017) Neurotensin receptor-1 identifies a subset of ventral tegmental dopamine neurons that coordinates energy balance. Cell Rep 20:1881–1892.

Zardetto-Smith AM, Gray TS (1987) A direct neural projection from the nucleus of the solitary tract to the subfornical organ in the rat. Neurosci Lett 80:163–166 Available at: http://www.sciencedirect.com/science/article/pii/0304394087906471.

Zimmerman CA, Lin Y-C, Leib DE, Guo L, Huey EL, Daly GE, Chen Y, Knight ZA (2016) Thirst neurons anticipate the homeostatic consequences of eating and drinking. Nature 537:680.

5. Discussion

This thesis describes three sets of experiments which add to the scientific knowledge of the SFO. In the first set of experiments (Chapter 2), we investigated the effects of early postnatal (between PD0-21) overnutrition via a small litter model on gene expression in the rat SFO. We found that early postnatal overnutrition significantly altered the expression of 12 transcripts with shared roles in oxidative stress response and protein folding and activity. Of greatest interest were the changes in the neurotrophic factor *Manf*, the Ca^{2+}-binding protein *Cracr2b*, and the $Na^{+}/K^{+}/Ca^{2+}$ exchanger *Slc24a4*, as their encoded proteins are likely to influence neuronal development and electrical excitability of neurons: *Manf* is a regulator of neurite outgrowth and migration (Tseng et al., 2017), and even small changes in ion concentrations across the plasma membrane such as that caused by changes in expression of a transporter can influence the excitability of neurons (Konopacka et al., 2015). We further performed a preliminary comparison of the RNAseq dataset against previously published microarray data (Hindmarch et al., 2008) to demonstrate concordance between the expression levels.

In the second set of experiments (Chapter 3), we continued our validation of the transcripts in the SFO using the RNAseq data with the microarray data. Given the importance of receptors and ion channels in shaping the behaviour of neurons, we extracted the expression levels of GPCRs and ion channels as outlined in the IUPHAR database from both datasets, to produce a validated set of GPCRs and ion channels expressed in the SFO. We focused on the voltage-gated cation channel transcripts by attempting to correlate our validated expression of voltage-gated K^{+}, Na^{+}, and Ca^{2+} channels with SFO current traces of each. This validated list also includes many receptors whose activity at the SFO have not yet been investigated. We further examined the specific effects of the endogenous ligands for ETRA and ETRB, NTSR2

and NTSR3, and TACR1 on SFO neurons, showing that endothelin, neurotensin, and substance P bind to receptors on SFO neurons to influence the electrical excitability of neurons.

The high expression of neurotensin receptors revealed by the transcriptomic data directly led to the third set of experiments (Chapter 4), where we examined the effects of neurotensin on the electrical activity of SFO neurons. In these experiments, the dose-dependent effect of neurotensin on proportion of responsive neurons, membrane potential, and action potential frequency was investigated using whole cell patch clamp electrophysiology in current clamp configuration. Using a combination of current clamp techniques to investigate changes in input resistance and voltage clamp experiments to examine changes in specific currents in response to neurotensin, we found that attenuation of I_K and an increase in I_{NSC} were responsible for the depolarisation and increase in action potential frequency observed in SFO neurons in response to neurotensin. Moreover, we found that these effects were mediated exclusively by NTSR2.

5.1. Relevance

Together these manuscripts represent a significant contribution to the broader knowledge of the regulation of homeostasis by the SFO. On one level, they address the mechanisms by which the SFO responds to physiological changes. One mechanism by which the SFO addresses changes is through altering gene expression, which may affect the sensitivity of the SFO to detect particular signals or alter its output properties. A SFO microarray study from Hindmarch et al. (2008) showed robust changes in gene expression following short-term challenges to homeostasis by 48-hour fasting or 72-hour water restriction. In chapter 2, we showed that a long-term subtle manipulation of energy balance by early postnatal overnutrition also caused subtle changes in expression of a limited number of transcripts, showing that the SFO is responsive to both acute and chronic physiological challenges. Even subtle disruptions to normal gene

expression levels can have dramatic consequences in early development when the brain is still developing: for example, other researchers have shown that early postnatal overfeeding alters the onset of leptin expression during development of the mouse, which ultimately leads to differences in behaviour of the feeding circuitry and feeding behaviour (Davidowa and Plagemann, 2000; Juan De Solis et al., 2016). Numerous studies show that exposure to early overnutrition is correlated with increased risk of obesity in child- and adulthood (Gittner et al., 2013; Rzehak et al., 2017), cardiovascular disease (Camhi and Katzmarzyk, 2010), and type II diabetes (Eriksson et al., 2003) in humans; thus the consequences of early overnutrition may last in to adulthood.

The electrical response of SFO neurons to circulating signals of physiological state are also critical to understanding how the SFO detects and responds to environmental changes. Gene expression data also contributes to this effort, as understanding the population of ion channels and receptors expressed in the SFO can give us insight in to the electrical properties of its neurons. In chapter 3, we attempted to address the gap in our understanding of the electrical properties of SFO neurons through compiling a list of validated ion channels and GPCRs expressed in the SFO. We further provided examples of voltage-gated cation channel currents from SFO neurons to correlate the expression of voltage-gated K^+, Na^+, and Ca^{2+} channels to the current properties of SFO neurons. We singled out specific K_v family voltage-gated K^+ channels which likely contribute to either the transient I_A or delayed-rectifier I_K portion of SFO voltage-gated K^+ currents. We also found physiological evidence of a subtype of voltage-gated Ca^{2+} channel, the expression of which was not validated by microarray: the low-voltage activated T-type channels. These channels are unique among the Ca_v family of ion channels in that they activate at lower membrane potentials (~−60 mV); we presented an IV plot from a neuron in

non-physiological solutions used to isolate Ca^{2+} current which indicated the opening of low voltage activated voltage-gated Ca^{2+} channels. The specific role and distribution of low voltage gated Ca^{2+} channels in the SFO requires further investigation.

One technique to study individual ion channels is the use of heterologous expression systems to study current properties of specific ion channels in relative isolation (Faivre et al., 1999). While these studies are useful for identifying properties of a current generated by an ion channel, they may not give us full insight in to the properties of the current generated by a channel within a neuron. For example, among voltage-gated cation channels with a 4x6 transmembrane domain configuration, the presence of auxiliary β, γ, and δ subunits can modulate ion channel properties including inactivation and activation kinetics (Auld et al., 1988; Namkung et al., 1998), current amplitude (Gurnett et al., 1996), and membrane trafficking (Isom et al., 1994; Brice and Dolphin, 1999). Furthermore, among K_v-family voltage-gated K^+ channels, some α subunits act as modulators of other α subunits. The effect of an interaction between specific proteins or subunits the current properties of an ion channel can be investigated using heterologous systems by co-expressing the proteins or subunits and comparing the resultant currents with and without the subunit of interest (Körner et al., 2018), though this becomes exponentially more complicated when considering multiple interactions. Ultimately, to fully understand the behaviour of a channel in a specific neuron we must study it in that neuron. To that end, a body of ongoing work is focused on correlating the expression of specific ion channels with current properties in SFO neurons (Washburn and Ferguson, 2001; McKinley et al., 2003; Ono et al., 2005; Fry and Ferguson, 2007; Hindmarch et al., 2008; Medlock et al., 2018). Our ion channelome dataset is a part of this effort and will aid future researchers interested in the SFO and homeostatic regulation.

One benefit of a validated list of GPCRs and ion channels expressed in the SFO is that it provides a list of putative targets with roles in homeostatic regulation. A growing body of work dating back to the 1980s has investigated the electrical and physiological effects of numerous signalling molecules at the SFO including angiotensin II (Mangiapane and Simpson, 1980; Mangiapane et al., 1984; Massi et al., 1986; Ono et al., 2001), leptin (Smith et al., 2008; Smith and Ferguson, 2012), apelin (Dai et al., 2013), and vasopressin (Smith and Ferguson, 1997; Washburn et al., 1999), among many others (McKinley et al., 2003; Alim et al., 2010; Hindmarch and Ferguson, 2015; Black et al., 2018). Our research on the electrical effects of neurotensin adds to this effort.

Now that tools are in place to do so, one benefit to improving our understanding of the intrinsic electrical properties of SFO neurons is to use this information to predict the outputs of SFO neurons. Recently, Medlock et al. (2018) used available information on biophysical properties of current subtypes in the SFO to model SFO neurons using the Hodgkin-Huxley-type model, to model two different electrophysiological phenotypes of SFO neurons (tonic and burst firing neurons) and predict their response to stimuli such as a change in a specific type of current modulated by binding of a signalling molecule to a receptor. The better we understand the intrinsic electrical properties of SFO neurons and how they are modulated by signalling molecules such as neurotensin the more accurate a model of a SFO neuron can become. This model could be improved by increased understanding of the current carried by the ion channels which we have validated the expression of and by examining in detail and spatial distribution of co-occurrence of these ion channels. A predictive model of the SFO can work to further our understanding of the specific electrical mechanisms by which SFO neurons respond to hormones

representing changes in physiological state, thereby improving our understanding of the broader regulation of thirst, cardiovascular output, and energy balance.

One factor to consider when predicting the response of the SFO to physiological changes is that the different homeostatic roles of the SFO are interrelated: Hindmarch et al.'s SFO microarray data (2008) indicates that some transcripts are altered by both thirst and fasting, reflecting that the homeostatic outputs regulated by the SFO are not independent. The interconnectivity of ingestive behaviours has been known for multiple decades: drinking water quenches thirst but also decreases blood osmolarity (Baldes and Smirk, 1934). Conversely, eating can increase the concentrations of glucose, salts, and other solutes in the plasma, thereby increasing osmolarity and driving thirst, which ultimately increases blood pressure (Høst et al., 1996). Thus, a perturbation of one system will affect others as well. For example, a common symptom of type II diabetes is excessive thirst resulting from increased plasma glucose concentrations (Reinehr, 2005). Given the interconnectedness of basic needs, they are also regulated together to ensure survival. One example is the case of dehydration anorexia, which is the body's response to dehydration in which thirst needs override hunger acting to decrease meal size to prevent further increases in plasma osmolarity (Boyle et al., 2012). Though dehydrated hungry rats show many expected responses to negative energy balance, including decreases plasma concentrations of satiety hormones leptin and insulin (Watts et al., 1999), hypothalamic regulation overrides these signals to decrease feeding. The alterations to hunger to preferentially promote drinking over feeding involves activation of the network which inhibits feeding after it has already begun (Salter-Venzon and Watts, 2009). Specifically, PVN and LH neurons show reduced sensitivity to their afferent homeostatic feeding inputs (Salter-Venzon and Watts, 2009). Once thirst is quenched, the inhibitory portion of the feeding network is suppressed and feeding

can continue as usual. Whether the SFO is also implicated in the network of changes induces by dehydration-anorexia aside from its typical role in promoting dipsogenesis is unknown.

Given the position of the SFO to respond to signalling molecules in the circulation and electrical inputs from other homeostatic nuclei, the SFO is well-situated to integrate the impacts of different homeostatic needs, outputs, and behaviours. Indeed, a recent study showed that thirst-promoting *nitric oxide synthase 1* SFO neurons respond to liquid or cold metal at the oral cavity to anticipate the osmotic impacts of eating and drinking behaviours (Zimmerman et al., 2016). The inhibitory effects are anticipatory because the changes in activity of on thirst-promoting neurons occurs before effects on plasma osmolarity takes effect. These data suggest that the SFO anticipates the interactions between fluid homeostasis and cardiovascular output.

5.2. Unanswered questions

The data in the three manuscripts presented in this thesis generated new questions. In chapter 2 (second manuscript) we examined the effect of early postnatal overnutrition on gene expression in the SFO via RNAseq. We noted subtle changes in expression of 12 transcripts at the peripubertal stage (6 weeks) which were significant. Because early postnatal overnutrition is associated with increased risk of obesity (Gittner et al., 2013; Rzehak et al., 2017) and related conditions (Eriksson et al., 2003; Camhi and Katzmarzyk, 2010) in to adulthood, this raises the question as to the changes in SFO gene expression in rats subjected to early postnatal overnutrition throughout later life stages. There are several possibilities, including that these expression changes may resolve, persist in to later life stages, or changes in expression of different genes may be evident in later life stages as a result of early postnatal overnutrition. To address this question, changes in gene expression between control and early postnatal overfed rats who have reached full adulthood (~21 weeks) or in later life (~104 weeks) (Yu et al., 2014)

could be examined using qPCR (to examine specifically the 12 transcripts of interest) or a transcriptomics technique such as RNAseq, microarray, or qPCR array (for a smaller number of genes) to investigate a broader range of potential changes in gene expression.

Further questions were generated as a result of the neurotensin research. Chapter 4 indicated modulation of 2 distinct types of currents, I_{NSC} and I_K to drive the increase in electrical excitability of SFO neurons. Some evidence indicates that this occurs in separate populations of neurons whereas other evidence suggests that in some cases both currents are modulated in a single neuron. Given that the experiments to examine changes in I_{NSC}, I_K, and reversal potential in current clamp were performed in separate cells, we cannot say for certain whether these populations overlap and with what frequency.

Moreover, because the shell and core SFO neurons cannot readily be electrophysiologically distinguished, and dissociation removes anatomical cues as to the identity of SFO neurons, we cannot say whether primarily shell or core neurons respond to neurotensin, or if the differences in electrical response to neurotensin (modulation of I_{NSC} vs I_K) are divided along anatomical lines. There are several possible solutions to this problem, including single cell RT-PCR and single cell transcriptomics, viral transfection, and molecular beacon probes. Electrophysiology and RT-PCR can be performed on the same cell to connect electrophysiological properties of neurons to gene expression and to identify neuronal subtypes for example calbindin vs calretinin-positive (core and shell) or GABA/glutamatergic neurons, and has been previously used with SFO neurons to correlate voltage-gated K^+ current properties to ion channel expression (Ono et al., 2005). Single-cell PCR following electrophysiology to correlate electrical properties of neurons with gene expression has also been successfully

performed in other types of neurons including rat pituitary (Hodne et al., 2010), mouse midbrain neurons (Dey et al., 2017), and in both rat pups and adult rats (Ritter et al., 2015).

RNAseq can similarly be combined with electrophysiology, and while patch clamp and single cell RNAseq have not been combined in the study of SFO neurons, these techniques have been successfully combined to differentiate between neuronal subtypes in pyramidal and interneurons from the mouse cortex (Cadwell et al., 2016; Fuzik et al., 2016) and mouse hippocampal neurons (Zeisel et al., 2015). While these techniques offer the benefit of readily examining multiple genes in the same neuron, it is also a *post-hoc* test which does not allow one to select for a specific phenotype before recording from a neuron. Moreover, while a positive result is likely indicative of true expression of the gene of interest, a negative result does not necessarily indicate lack of expression.

Conversely viral vectors and molecule beacon probes allow for *apriori* detection of neurons with the transcripts of interest, and do not suffer from the same technical challenges as single cell RT-PCR. Both lentivirus (Matsuda et al., 2016) and adenovirus (Vasquez et al., 1998) vectors have been successfully used with SFO cells. Huang et al. (2019) used gold nanoparticle-conjugated molecular beacon probes (SmartFlare) to cause calbindin-expressing SFO neurons to fluoresce allowing for visual identification of potential shell SFO neurons without altering their electrical properties. Both viral transfection and molecular beacon probes could serve as an appropriate solution for identification of SFO neuron subpopulations to determine whether neurotensin-responsive neurons are differentially distributed among the core and peripheral SFO neuron populations. Furthermore, as with single cell RT-PCR, multiple genes can be examined, though this becomes more complicated as each gene needs to be expressed with a different fluorescent probe colour and potentially viewed using a different filter. Future experiments could

include examining differences in response to neurotensin between shell and core SFO neurons, or to connect differences in electrical properties of neurons in as recorded in voltage and current clamp to changes in I_K or I_{NSC} in response to neurotensin.

5.3. Future directions extending this work

The ability of dissociated SFO neurons to respond to neurotensin is one step in understanding the full role of neurotensin signalling at the SFO. To more fully understand the significance of neurotensin signalling at the SFO, we need to examine neurotensin's effects in the fuller physiological context in which this signalling occurs naturally. One route would be to examine the synaptic effects of neurotensin on SFO neurons. Numerous studies indicate that neurotensin modulates synaptic transmission. The specific effect of neurotensin, however, can be varied: for example, in the VTA neurotensin has been shown to either enhance (Bose et al., 2015) or inhibit (Kortleven et al., 2012)) glutamatergic excitatory post-synaptic potentials (EPSPs) and inhibit inhibitory post-synaptic potentials (IPSPs) (Stuhrman and Roseberry, 2015). Moreover, enhancement of glutamatergic transmission may occur through either NTSR1 or NTSR2 depending on the neuronal subtype (Bose et al., 2015). Some research has also proposed a role for NTSR3 or SorLa/LR11 in synaptic transmission, as evidenced by experiments in which NTSR1/NTSR2-specific blockers did not alter the effect of neurotensin (Bose et al., 2015), though due to a lack of widespread pharmacological blockers for NTSR3 and SorLa/LR11 the involvement of eithers of these receptors could not be confirmed. Brain slices containing SFO can be prepared and the SFO visually identified, allowing for recording from SFO neurons with some of their projections and inputs intact, and with the ability to visually identify shell vs core neurons with a fair degree of confidence. Moreover, if the blood vessels are left intact, the effect of neurotensin on SFO vessels can be visually examined at the same time as electrophysiological

experiments. Because ARC stimulation enhances the effect of angiotensin II on SFO neurons, and the ARC sends neurotensinogenic projections to the SFO which terminate near blood vessels, Rosas-Arellano et al. suggested that neurotrensin released from ARC projections could directly dilate SFO blood vessels to improve solute permeability (Rosas-Arellano et al., 1996). Thus the hypothesis on the synaptic and local blood vessel effects of neurotensin at the SFO could be tested concurrently.

Another set of future experiments which would improve our understanding of neurotensin's role in the SFO would be to examine the distribution of neurotensinogenic inputs and neurotensin receptors relative to SFO anatomy. The two major subdivisions of the SFO, its shell and core, can be separated by their expression of calretinin or calbindin, respectively (McKinley et al., 2003; Huang et al., 2019). Using triple immunohistochemistry, we can examine the distribution of neurotensin-producing axonal inputs to the SFO relative to shell and core SFO neurons, and the distribution of neurotensin receptors in shell and core neurons. As shell and core SFO neurons project to different regions of the brain (Swanson and Lind, 1986; McKinley et al., 2003; Hollis et al., 2008; Kawano and Masuko, 2010) and have subtle differences in intrinsic electrical properties (Huang et al., 2019), knowing which neurons or vessels receive neurotensin input and which are competent to respond to neurotensin will give us insight in to the potential roles of neurotensin at the SFO. Similarly, we could triple immunohistochemistry to investigate the distribution of Manf, Cracr2b, and Slc42a4 relative to calbindin (core) and calretinin (shell) SFO neurons.

Numerous experiments involving microinjection to the SFO and monitoring changes in blood pressure and heart rate have been previously performed (Smith et al., 2007; Smith and Ferguson, 2012; Cerqueira et al., 2016). In some cases, these results are the same as an

intracerebroventricular injection as is seen with endothelin injections (Ouchi et al., 1989; Wall et al., 1992), though in many cases the opposite effect is seen such as with leptin (Dunbar et al., 1997; Smith and Ferguson, 2012) and orexin (Lin et al., 2002; Smith et al., 2007). Given this and the bi- or triphasic effects of neurotensin on blood pressure (Oishi et al., 1981; Rioux et al., 1982), we cannot predict what the effect of a direct neurotensin injection the SFO on heart rate and blood pressure would be. A series of direct microinjection experiments would expand our understanding of the physiological consequences of neurotensin at the SFO. While intracerebroventricular injections allow drugs to pass the BBB via injection in to a ventricle, they are not specific to the site of action. Microinjections allow for administration of a drug of interest to a specific site by guiding a cannula to the coordinates of the nucleus of interest. The injection site can be examined after the experiment to confirm the drug was administered to the correct site. By microinjection angiotensin to the SFO as a positive control, which has a well-established effect on blood pressure via the SFO, or the drug vehicle (saline) as a negative control, we can further confirm that the blood pressure and heart rate responses of neurotensin or lack thereof are due to injection of neurotensin as opposed to the cannulation setup.

Combining direct microinjection techniques with the Cre/lox recombination system allows for the study of knockdown or knock-in of genes at a specific nucleus in the brain. In this case, we can microinject a viral vector to generate Cre recombinase enzyme expression directly to the SFO in genetically modified rats with lox sequences flanking a shRNA inserted (Hitz et al., 2007), ensuring knockdown of the target gene to exclusively in the SFO. For example, targeting *Ntsr2* expression allows us to investigate the role of neurotensin action at the SFO specifically, whereas knockdown of *Manf, Cracr2b,* or *Slc24a4* at the SFO allows us to investigate the role of these transcripts in the SFO. As the lox sequences are not activated except

in the presence of the Cre recombinase enzyme, injection controls for this technique include injection of the microinjection vehicle alone to rats expressing the lox sequence (to control for the effects of the injection itself) and injection of the viral vector for Cre recombinase to rats without the lox sequence (to control for the effects of the expression of Cre recombinase enzyme alone). The production of rats with SFO-specific knockdowns allows us to perform a variety of *in vivo* and *in vitro* experiments. For example, to investigate whether binding of neurotensin to NTSR2 specifically is responsible for the effects of neurotensin at the SFO on cardiovascular output as noted in the above paragraph, these *in vivo* microinjection experiments with the same controls can be repeated in NTSR2 knockdown animals. Furthermore, the SFO from Cre/lox-mediated knockdown animals may be used for further electrophysiological studies. For electrophysiological experiments, the Cre/lox system can be used in conjunction with a reporter sequence so that SFO neurons which have successfully knocked down expression of the gene of interest fluoresce (Weber et al., 2011). Using current and voltage clamp electrophysiology, we can compare the intrinsic electrical properties of Cracr2b, or Slc24a4 knockdown SFO neurons to normal SFO neurons, examining electrical properties of neurons including resting membrane potential, action potential frequency and length of action potential bursting behaviour, and properties of Ca^{2+}, Na^{+}, and K^{+} currents (Huang et al., 2019). The four series of experiments proposed above would be a direct continuation of the research outlined in this thesis and will improve our understanding of the regulation of SFO neurons by the signalling molecule neurotensin, and the roles of Manf, Cracr2b, and Slc24a4 in the SFO.

5.4. Conclusion

Taken together, the three manuscripts presented in this thesis add to our knowledge of the SFO, its regulation of homeostasis, challenges to homeostasis, and the electrical properties of its neurons. Specifically, these manuscripts address the response of the SFO to prolonged challenges to energy balance, and the intrinsic electrical properties of the neurons and their ability to detect and respond to signals of physiological state. We expect these data will be of particular interest to researchers interested in the SFO and its role in homeostatic regulation and the treatment of obesity, hypertension, and related conditions.

Alim I, Mark Fry W, Walsh MH, Ferguson A V. (2010) Actions of adiponectin on the excitability of subfornical organ neurons are altered by food deprivation. Brain Res 1330:72–82 Available at: http://dx.doi.org/10.1016/j.brainres.2010.02.076.

Auld VJ, Goldin AL, Krafte DS, Marshall J, Dunn JM, Catterall WA, Lester HA, Davidson N, Dunn RJ (1988) A rat brain Na+ channel α subunit with novel gating properties. Neuron 1:449–461.

Baldes EJ, Smirk FH (1934) The effect of water drinking, mineral starvation and salt administration on the total osmotic pressure of the blood in man, chiefly in relation to the problems of water absorption and water diuresis. J Physiol 82:62.

Black EAE, Smith PM, Mcisaac W, Ferguson A V (2018) Brain-derived neurotrophic factor acts at neurons of the subfornical organ to influence cardiovascular function. Physiol Rep 6:1–10 Available at: https://doi.org/10.14814/phy2.13704.

Bose P, Rompré P-P, Warren RA (2015) Neurotensin enhances glutamatergic EPSCs in VTA neurons by acting on different neurotensin receptors. Peptides 73:43–50.

Boyle CN, Lorenzen SM, Compton D, Watts AG (2012) Dehydration-anorexia derives from a reduction in meal size, but not meal number. Physiol Behav 105:305–314.

Brice NL, Dolphin AC (1999) Differential plasma membrane targeting of voltage-dependent calcium channel subunits expressed in a polarized epithelial cell line. J Physiol 515:685.

Cadwell CR, Palasantza A, Jiang X, Berens P, Deng Q, Yilmaz M, Reimer J, Shen S, Bethge M, Tolias KF, Sandberg R, Tolias AS (2016) Electrophysiological, transcriptomic and morphologic profiling of single neurons using Patch-seq. Nat Biotechnol 34:199–203

Available at: https://www.ncbi.nlm.nih.gov/pubmed/26689543.

Camhi SM, Katzmarzyk PT (2010) Tracking of cardiometabolic risk factor clustering from childhood to adulthood. Int J Pediatr Obes 5:122–129 Available at: http://informahealthcare.com/doi/abs/10.3109/17477160903111763.

Cerqueira DR, Ferreira HS, Moiteiro ALBB, Fregoneze JB (2016) Effects of interleukin-1 beta injections into the subfornical organ and median preoptic nucleus on sodium appetite, blood pressure and body temperature of sodium-depleted rats. Physiol Behav 163:149–160 Available at: http://dx.doi.org/10.1016/j.physbeh.2016.05.003.

Dai L, Smith PM, Kuksis M, Ferguson A V. (2013) Apelin acts in the subfornical organ to influence neuronal excitability and cardiovascular function. J Physiol 591:3421–3432.

Davidowa H, Plagemann A (2000) Decreased inhibition by leptin of hypothalamic arcuate neurons in neonatally overfed young rats. Neuroreport 11:2795-8.

Dey A, Farzanehfar P, Gazina E V, Aumann TD (2017) Electrophysiological and gene expression characterization of the ontogeny of nestin-expressing cells in the adult mouse midbrain. Stem Cell Res 23:143–153 Available at: http://www.sciencedirect.com/science/article/pii/S1873506117301253.

Dunbar JC, Hu Y, Lu H (1997) Intracerebroventricular Leptin Increases Lumbar and Renal Sympathetic Nerve Activity and Blood Pressure in Normal Rats. Diabetes 46:2040 LP – 2043.

Eriksson JG, Forsén T, Tuomilehto J, Osmond C, Barker DJP (2003) Early adiposity rebound in childhood and risk of Type 2 diabetes in adult life. Diabetologia 46:190–194 Available at:

http://link.springer.com/10.1007/s00125-002-1012-5.

Faivre J-F, PG Calmels T, Rouanet S, Javré J-L, Cheval B, Bril A (1999) Characterisation of Kv4. 3 in HEK293 cells: comparison with the rat ventricular transient outward potassium current. Cardiovasc Res 41:188–199.

Fry M, Ferguson A V (2007) Subthreshold oscillations of membrane potential of rat subfornical organ neurons. Neuroreport 18:1389–1393 Available at: https://insights-ovid-com.uml.idm.oclc.org/pubmed?pmid=17762719 [Accessed May 24, 2018].

Fuzik J, Zeisel A, Máté Z, Calvigioni D, Yanagawa Y, Szabó G, Linnarsson S, Harkany T (2016) Integration of electrophysiological recordings with single-cell RNA-seq data identifies neuronal subtypes. Nat Biotechnol 34:175–183 Available at: https://www.ncbi.nlm.nih.gov/pubmed/26689544.

Gittner LS, Ludington-Hoe SM, Haller HS (2013) Utilising infant growth to predict obesity status at 5 years. J Paediatr Child Health 49:564–574.

Gurnett CA, De Waard M, Campbell KP (1996) Dual function of the voltage-dependent Ca2+ channel α2δ subunit in current stimulation and subunit interaction. Neuron 16:431–440.

Hindmarch C, Fry M, Yao ST, Smith PM, Murphy D, Ferguson A V (2008) Microarray analysis of the transcriptome of the subfornical organ in the rat: regulation by fluid and food deprivation. Am J Physiol Regul Integr Comp Physiol 295:R1914-20.

Hindmarch CCT, Ferguson A V (2015) Physiological roles for the subfornical organ: a dynamic transcriptome shaped by autonomic state. J Physiol 6:1581–1589 Available at: http://www.ncbi.nlm.nih.gov/pubmed/26227400 [Accessed November 8, 2015].

Hitz C, Wurst W, Kühn R (2007) Conditional brain-specific knockdown of MAPK using Cre/loxP regulated RNA interference. Nucleic Acids Res 35:e90–e90 Available at: https://doi.org/10.1093/nar/gkm475.

Hodne K, Haug TM, Weltzien F-A (2010) Single-cell qPCR on dispersed primary pituitary cells -an optimized protocol. BMC Mol Biol 11:82 Available at: https://doi.org/10.1186/1471-2199-11-82.

Hollis JH, McKinley MJ, D'Souza M, Kampe J, Oldfield BJ (2008) The trajectory of sensory pathways from the lamina terminalis to the insular and cingulate cortex: a neuroanatomical framework for the generation of thirst. Am J Physiol Integr Comp Physiol 294:R1390–R1401.

Høst U, Kelbaek H, Rasmusen H, Court-Payen M, Christensen NJ, Pedersen-Bjergaard U, Lorenzen T (1996) Haemodynamic Effects of Eating: The Role of Meal Composition. Clin Sci 90:269 LP – 276.

Huang S, Egan J, Fry WM (2019) Electrophysiological Properties of Rat Subfornical Organ Neurons Expressing Calbindin D28K. Neuroscience 404:459–469 Available at: https://www.sciencedirect.com/science/article/pii/S0306452219301198?dgcid=rss_sd_all.

Isom LL, De Jongh KS, Catterall WA (1994) Auxiliary subunits of voltage-gated ion channels. Neuron 12:1183–1194.

Juan De Solis A, Baquero AF, Bennett CM, Grove KL, Zeltser LM (2016) Postnatal undernutrition delays a key step in the maturation of hypothalamic feeding circuits. Mol Metab 5:198–209 Available at: http://dx.doi.org/10.1016/j.molmet.2016.01.003.

Kawano H, Masuko S (2010) Region-specific projections from the subfornical organ to the paraventricular hypothalamic nucleus in the rat. Neuroscience 169:1227–1234 Available at: http://dx.doi.org/10.1016/j.neuroscience.2010.05.065.

Konopacka A et al. (2015) Osmoregulation requires brain expression of the renal Na-K-2Cl cotransporter NKCC2. J Neurosci 35:5144–5155 Available at: http://www.ncbi.nlm.nih.gov/pubmed/25834041 [Accessed December 15, 2017].

Körner J, Meents J, Machtens J-P, Lampert A (2018) β1 subunit stabilises sodium channel Nav1.7 against mechanical stress. J Physiol 596:2433–2445.

Kortleven C, Bruneau LC, Trudeau L-E (2012) Neurotensin inhibits glutamate-mediated synaptic inputs onto ventral tegmental area dopamine neurons through the release of the endocannabinoid 2-AG. Neuropharmacology 63:983–991.

Lin Y, Matsumura K, Tsuchihashi T, Abe I, Iida M (2002) Chronic central infusion of orexin-A increases arterial pressure in rats. Brain Res Bull 57:619–622.

Mangiapane ML, Simpson JB (1980) Subfornical organ: forebrain site of pressor and dipsogenic action of angiotensin II. Am J Physiol 239:R382-9 Available at: http://www.ncbi.nlm.nih.gov/pubmed/7435651 [Accessed November 13, 2015].

Mangiapane ML, Thrasher TN, Keil LC, Simpson JB, Ganong WF (1984) Role for the subfornical organ in vasopressin release. Brain Res Bull 13:43–47.

Massi M, Caro G De, Mazzarella L, Epstein AN (1986) The role of the subfornical organ in the drinking behavior of the pigeon. Brain Res 381:289–299.

Matsuda T, Hiyama TY, Niimura F, Matsusaka T, Fukamizu A, Kobayashi K, Kobayashi K,

Noda M (2016) Distinct neural mechanisms for the control of thirst and salt appetite in the subfornical organ. Nat Neurosci 20:230.

McKinley MJ, McAllen RM, Giles ME, Penschow J, Sunn N, Uschakov A, Oldfield BJ (2003) The sensory circumventricular organs of the mammalian brain. Adv Anat Cell Biol 172:III–XII, 1–122, back cover.

Medlock L, Shute L, Fry M, Standage D, Ferguson A V. (2018) Ionic mechanisms underlying tonic and burst firing behavior in subfornical organ neurons: a combined experimental and modeling study. J Neurophysiol 120:2269–2281.

Namkung Y, Smith SM, Lee SB, Skrypnyk NV, Kim HL, Chin H, Scheller RH, Tsien RW, Shin HS (1998) Targeted disruption of the Ca2+ channel beta3 subunit reduces N- and L-type Ca2+channel activity and alters the voltage-dependent activation of P/Q-type Ca2+ channels in neurons. Proc Natl Acad Sci 95:12010–12015.

Oishi M, Inagaki C, Fujiwara M, Takaori S, Yajima H, Akazawa Y (1981) Possible mechanisms of the triphasic effects of neurotensin on the rat blood pressure. Jpn J Pharmacol 31:1043–1049.

Ono K, Honda E, Inenaga K (2001) Angiotensin II induces inward currents in subfornical organ neurones of rats. J Neuroendocrinol 13:517–523.

Ono K, Toyono T, Honda E, Inenaga K (2005) Transient outward K^+ currents in rat dissociated subfornical organ neurones and angiotensin II effects. J Physiol 568:979–991 Available at: http://doi.wiley.com/10.1113/jphysiol.2005.089508.

Ouchi Y, Kim S, Souza AC, Iijima S, Hattori A, Orimo H, Yoshizumi M, Kurihara H, Yazaki Y

(1989) Central effect of endothelin on blood pressure in conscious rats. Am J Physiol Circ Physiol 256:H1747–H1751.

Reinehr T (2005) Clinical presentation of type 2 diabetes mellitus in children and adolescents. Int J Obes 29:S105–S110.

Rioux F, Kérouac R, St-Pierre S (1982) Analysis of the biphasic depressor-pressor effect and tachycardia caused by neurotensin in ganglion-blocked rats. Neuropeptides 3:113–127 Available at: http://www.sciencedirect.com/science/article/pii/0143417982900075.

Ritter DM, Zemel BM, Lepore AC, Covarrubias M (2015) Kv3.4 channel function and dysfunction in nociceptors. Channels 9:209–217 Available at: https://doi.org/10.1080/19336950.2015.1056949.

Rosas-Arellano MP, Solano-Flores LP, Ciriello J (1996) Neurotensin projections to subfornical organ from arcuate nucleus. Brain Res 706:323–327.

Rzehak P, Oddy WH, Mearin ML, Grote V, Mori TA, Szajewska H, Shamir R, Koletzko S, Weber M, Beilin LJ, Huang R-C, Koletzko B (2017) Infant feeding and growth trajectory patterns in childhood and body composition in young adulthood. Am J Clin Nutr 106:568–580 Available at: http://ajcn.nutrition.org/lookup/doi/10.3945/ajcn.116.140962.

Salter-Venzon D, Watts AG (2009) Site-specific attenuation of food intake but not the latency to eat after hypothalamic injections of neuropeptide Y in dehydrated-anorexic rats. Am J Physiol Regul Integr Comp Physiol 297:R1813–R1821.

Smith PM, Chambers AP, Price CJ, Ho W, Hopf C, Sharkey KA, Ferguson A V (2008) The subfornical organ: a central nervous system site for actions of circulating leptin. Am J

Physiol Integr Comp Physiol 296:R512–R520 Available at: http://ajpregu.physiology.org/cgi/doi/10.1152/ajpregu.90858.2008.

Smith PM, Ferguson A V. (2012) Cardiovascular Actions of Leptin in the Subfornical Organ are Abolished by Diet-Induced Obesity. J Neuroendocrinol 24:504–510.

Smith PM, Ferguson A V (1997) Vasopressin acts in the subfornical organ to decrease blood pressure. Neuroendocrinology 66:130–135 Available at: https://www.karger.com/DOI/10.1159/000127230.

Smith PM, Samson WK, Ferguson A V. (2007) Cardiovascular actions of orexin-A in the rat subfornical organ. J Neuroendocrinol 19:7–13.

Stuhrman K, Roseberry AG (2015) Neurotensin inhibits both dopamine- and GABA-mediated inhibition of ventral tegmental area dopamine neurons. J Neurophysiol 114:1734–1745.

Swanson LW, Lind RW (1986) Neural projections subserving the initiation of a specific motivated behavior in the rat: new projections from the subfornical organ. Brain Res 379:399–403.

Tseng K-Y, Danilova T, Domanskyi A, Saarma M, Lindahl M, Airavaara M (2017) MANF is essential for neurite extension and neuronal migration in the developing cortex. eNeuro 4:214–217 Available at: http://eneuro.sfn.org/lookup/doi/10.1523/ENEURO.0214-17.2017 [Accessed December 12, 2017].

Vasquez EC, Johnson RF, Beltz TG, Haskell RE, Davidson BL, Johnson AK (1998) Replication-Deficient Adenovirus Vector Transfer ofgfpReporter Gene into Supraoptic Nucleus and Subfornical Organ Neurons. Exp Neurol 154:353–365.

Wall KM, Nasr M, Ferguson A V. (1992) Actions of endothelin at the subfornical organ. Brain Res 570:180–187.

Washburn DL, Ferguson A V. (2001) Membrane properties of subfornical organ neurons. Clin Exp Pharmacol Physiol 28:575–580.

Washburn DLS, Beedle AM, Ferguson A V. (1999) Inhibition of subfornical organ neuronal potassium channels by vasopressin. Neuroscience 93:349–359.

Watts AG, Sanchez-Watts G, Kelly AB (1999) Distinct Patterns of Neuropeptide Gene Expression in the Lateral Hypothalamic Area and Arcuate Nucleus Are Associated with Dehydration-Induced Anorexia. J Neurosci 19:6111 LP – 6121.

Weber T, Schönig K, Tews B, Bartsch D (2011) Inducible gene manipulations in brain serotonergic neurons of transgenic rats. PLoS One 6:e28283 Available at: https://doi.org/10.1371/journal.pone.0028283.

Yu Y et al. (2014) A rat RNA-Seq transcriptomic BodyMap across 11 organs and 4 developmental stages. Nat Commun 5:1–11 Available at: http://www.nature.com/doifinder/10.1038/ncomms4230.

Zeisel A, Muñoz-Manchado AB, Codeluppi S, Lönnerberg P, La Manno G, Juréus A, Marques S, Munguba H, He L, Betsholtz C, Rolny C, Castelo-Branco G, Hjerling-Leffler J, Linnarsson S (2015) Cell types in the mouse cortex and hippocampus revealed by single-cell RNA-seq. Science (80-) 347:1138 LP – 1142 Available at: http://science.sciencemag.org/content/347/6226/1138.abstract.

Zimmerman CA, Lin Y-C, Leib DE, Guo L, Huey EL, Daly GE, Chen Y, Knight ZA (2016)

Thirst neurons anticipate the homeostatic consequences of eating and drinking. Nature 537:680.

Appendix

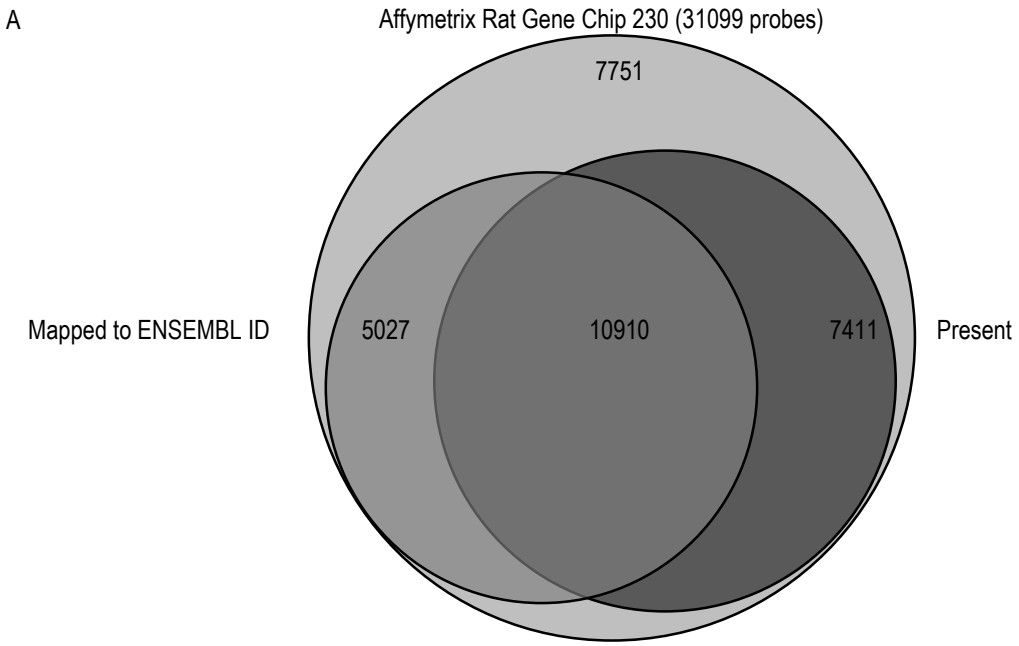
A
Affymetrix Rat Gene Chip 230 (31099 probes)
7751
Mapped to ENSEMBL ID
5027
10910
7411
Present

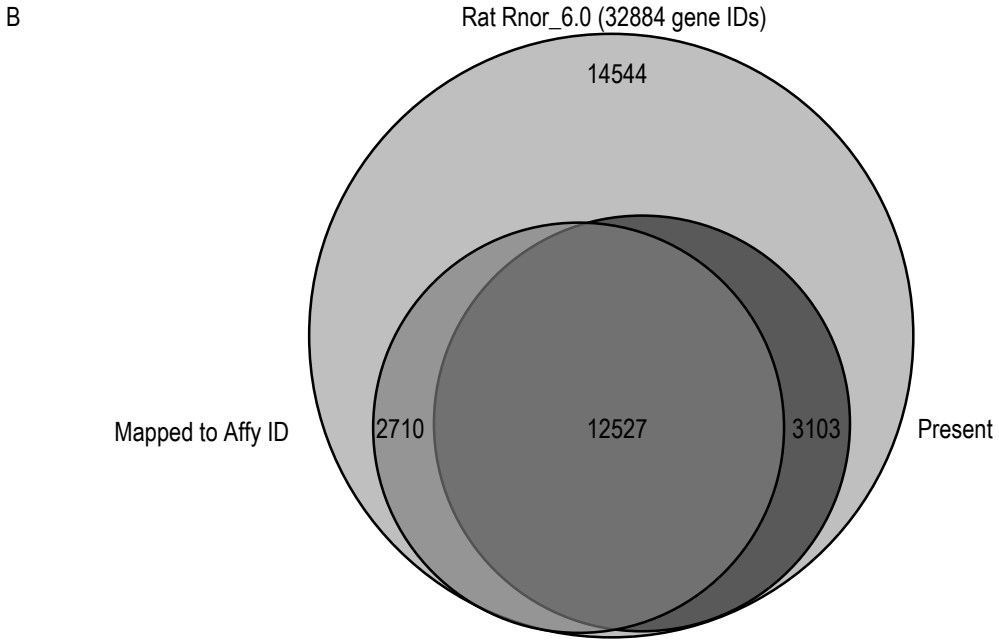
B
Rat Rnor_6.0 (32884 gene IDs)
14544
Mapped to Affy ID
2710
12527
3103
Present

Figure A2.1. Overlap between previously published microarray data and RNA sequencing transcriptomes. (**A)** Of 15630 transcripts detected by RNAseq (compared to Rnor_6.0 rat genome assembly), 12527 transcripts could be mapped to Affymetrix IDs. 2710 transcripts could be mapped but were not expressed within the SFO according to RNAseq. **(B)** Of the 15937 probes called as present on the microarray, 10910 could be mapped to 9115 unique Ensembl IDs.

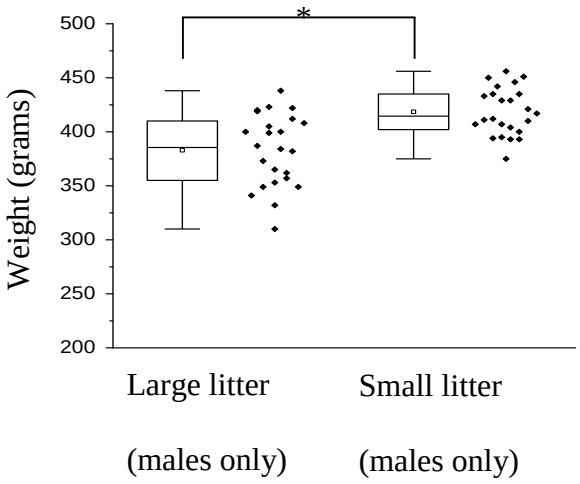

Figure A2.2. Weights of male rats from small and large (control) litters at age 6 weeks. Small litter rats were significantly heavier than controls ($p < 0.05$, t-test).

Table A2.1. Gene ontology analysis (generated by KOBAS) of significantly changed genes.

Gene Ontology Term	ID	Input Number	Background Number	FDR Adjusted p-value
negative regulation of oxidative stress-induced intrinsic apoptotic signaling pathway	GO:1902176	2	15	0.021297
regulation of oxidative stress-induced intrinsic apoptotic signaling pathway	GO:1902175	2	20	0.021297
negative regulation of oxidative stress-induced cell death	GO:1903202	2	31	0.021297
negative regulation of response to oxidative stress	GO:1902883	2	32	0.021297
negative regulation of cellular response to oxidative stress	GO:1900408	2	32	0.021297
intrinsic apoptotic signaling pathway in response to oxidative stress	GO:0008631	2	33	0.021297
chaperone-mediated protein folding	GO:0061077	2	41	0.024176
regulation of oxidative stress-induced cell death	GO:1903201	2	41	0.024176
regulation of cellular response to oxidative stress	GO:1900407	2	48	0.029084
regulation of response to oxidative stress	GO:1902882	2	51	0.029415
cell death in response to oxidative stress	GO:0036473	2	54	0.029854
negative regulation of protein phosphorylation	GO:0001933	3	308	0.041021
negative regulation of intrinsic apoptotic signaling pathway	GO:2001243	2	73	0.041997
cellular response to hydrogen peroxide	GO:0070301	2	73	0.041997
negative regulation of phosphorylation	GO:0042326	3	340	0.043582

Table A3.1: List of GPCRs and ion channels expressed (or not) in the SFO (validated and unvalidated)

Legend:

Validated expression in SFO: present in RNAseq and microarray
RNAseq present, microarray absent
RNAseq absent, microarray present
Absent via RNAseq and microarray
$ indicates not in Rnor 6.0 genome assembly
* indicates no probe on microarray

G-protein coupled receptors:

Gene name	Full gene name	RNAseq FPKM	Microarray intensity	
Ackr1	atypical chemokine receptor 1 (Duffy blood group)	0	0	$
Ackr2	atypical chemokine receptor 2	0.29693	0.66014	
Ackr3	atypical chemokine receptor 3	18.77618	5.16816	
Ackr4	atypical chemokine receptor 4	3.12748	0.48184	
Adcyap1r1	ADCYAP receptor type I	23.8251	0.40937	
Adgra1	adhesion G protein-coupled receptor A1	10.656	2.11026	
Adgra2	adhesion G protein-coupled receptor A2	12.33302	2.19174	
Adgra3	adhesion G protein-coupled receptor A3	20.06078	1.61407	
Adgrb1	adhesion G protein-coupled receptor B1	0	4.69477	$
Adgrb2	adhesion G protein-coupled receptor B2	16.51651	3.38494	
Adgrb3	adhesion G protein-coupled receptor B3	8.60045	3.36904	
Adgrd1	adhesion G protein-coupled receptor D1	0.45511	0.15891	
Adgre1	adhesion G protein-coupled receptor E1	4.16669	0.92202	

Adgre4	adhesion G protein-coupled receptor E4, pseudogene	0.07678	0	*
Adgre5	adhesion G protein-coupled receptor E5	4.29274	0.89141	
Adgrf1	adhesion G protein-coupled receptor F1	0	0.30709	$
Adgrf2	adhesion G protein-coupled receptor F2	0.00772	0.22161	
Adgrf3	adhesion G protein-coupled receptor F3	604	0	*
Adgrf4	adhesion G protein-coupled receptor F4	0	0.22161	
Adgrf5	adhesion G protein-coupled receptor F5	3.04547	0.55072	
Adgrg1	adhesion G protein-coupled receptor G1	65.61031	8.62456	
Adgrg2	adhesion G protein-coupled receptor G2	3.31704	1.30148	
Adgrg3	adhesion G protein-coupled receptor G3	0.21917	0.07846	
Adgrg5	adhesion G protein-coupled receptor G5	0.15741	0.46273	
Adgrg6	adhesion G protein-coupled receptor G6	3.19833	0.73441	
Adgrg7	adhesion G protein-coupled receptor G7	0	0	*
Adgrl1	adhesion G protein-coupled receptor L1	22.75052	2.99926	
Adgrl2	adhesion G protein-coupled receptor L2	5.36998	0.40569	
Adgrl3	adhesion G protein-coupled receptor L3	7.56742	1.02679	
Adgrl4	adhesion G protein-coupled receptor L4	2.33879	0	*
Adgrv1	adhesion G protein-coupled receptor V1	23.73019	4.57428	
Adora1	adenosine A1 receptor	24.99361	1.50477	
Adora2a	adenosine A2a receptor	1.47618	0.46337	
Adora2b	adenosine A2b receptor	3.00796	1.22374	
Adora3	adenosine A3 receptor	0.90222	0.37252	
Adra1a	adrenoceptor alpha 1A	0.4842	0.17	
Adra1b	adrenoceptor alpha 1B	0.54344	0.89038	
Adra1d	adrenoceptor alpha 1D	0.02389	0.07323	
Adra2a	adrenoceptor alpha 2A	3.43953	1.04112	
Adra2b	adrenoceptor alpha 2B	0.03928	0.11701	

Adra2c	adrenoceptor alpha 2C	3.99223	0.64059	
Adrb1	adrenoceptor beta 1	0.58735	0.22594	
Adrb2	adrenoceptor beta 2	1.42202	0.30367	
Adrb3	adrenoceptor beta 3	0.34203	0.49868	
Agtr1a	angiotensin I receptor type a	24.40621	4.23995	
Agtr1b	angiotensin I receptor type b	0	0.30186	
Agtr2	angiotensin II receptor type 2	0.0524	0.48377	
Aplnr	apelin receptor	7.96127	1.27948	
Avpr1a	arginine vasopressin receptor 1A	1.15645	0.10489	
Avpr1b	arginine vasopressin receptor 1B	0	0.46378	
Avpr2	arginine vasopressin receptor 2	0	0.30719	
Bdkrb1	bradykinin receptor B1	0.0531	0.28937	
Bdkrb2	bradykinin receptor B2	0.26839	0.27539	
Brs3	bombesin receptor subtype 3	0.09343	0	*
C3ar1	complement C3a receptor 1	1.16687	0.39242	
C5ar1	complement C5a receptor 1	1.34773	0.6242	
C5ar2	complement component 5a receptor 2	1.20438	0	*
Calcr	calcitonin receptor	32.33745	4.86407	
Calcrl	calcitonin receptor like receptor	5.81745	3.3688	
Casr	calcium sensing receptor	3.26219	1.21124	
Cckar	cholecystokinin A receptor	0.00807	0.42368	
Cckbr	cholecystokinin B receptor	0.19617	0.18343	
Ccr1	C-C motif chemokine receptor 1	1.00766	0.02806	
Ccr10	C-C motif chemokine receptor 10	0.26722	0.14257	
Ccr2	C-C motif chemokine receptor 2	0.11101	0.19493	
Ccr3	C-C motif chemokine receptor 3	0.0811	0.4278	
Ccr4	C-C motif chemokine receptor 4	7	0.226	

Ccr5	C-C motif chemokine receptor 5 (gene/pseudogene)	10.21364	1.41868	
Ccr6	C-C motif chemokine receptor 6	0.06311	0.03285	
Ccr7	C-C motif chemokine receptor 7	0.16422	0	*
Ccr8	C-C motif chemokine receptor 8	0.0079	0	*
Ccr9	C-C motif chemokine receptor 9	366	0	*
Ccrl2	C-C motif chemokine receptor like 2	1.19507	0.36802	
Celsr1	cadherin EGF LAG seven-pass G-type receptor 1	7.92936	0	*
Celsr2	cadherin EGF LAG seven-pass G-type receptor 2	6.69445	1.51356	
Celsr3	cadherin EGF LAG seven-pass G-type receptor 3	3.86056	2.75926	
Chrm1	cholinergic receptor muscarinic 1	0.08574	0.02599	
Chrm2	cholinergic receptor muscarinic 2	1.40418	0.46417	
Chrm3	cholinergic receptor muscarinic 3	1.1405	0.27358	
Chrm4	cholinergic receptor muscarinic 4	1.27274	0.2299	
Chrm5	cholinergic receptor muscarinic 5	0.70391	0.29485	
Cmklr1	chemerin chemokine-like receptor 1	1.57917	0.20017	
Cnr1	cannabinoid receptor 1	20.02889	7.83229	
Cnr2	cannabinoid receptor 2	0.39146	0.04664	
Crhr1	corticotropin releasing hormone receptor 1	0.651	0.17306	
Crhr2	corticotropin releasing hormone receptor 2	0.71781	0.58285	
Cx3cr1	C-X3-C motif chemokine receptor 1	15.85633	0.64111	
Cxcr1	C-X-C motif chemokine receptor 1	0	0.33861	
Cxcr2	C-X-C motif chemokine receptor 2	0.09434	0.21821	
Cxcr3	C-X-C motif chemokine receptor 3	0.27746	0.52108	
Cxcr4	C-X-C motif chemokine receptor 4	16.98855	3.6953	
Cxcr5	C-X-C motif chemokine receptor 5	0.42206	0.09627	

Cxcr6	C-X-C motif chemokine receptor 6	0.26415	0	*
Cysltr1	cysteinyl leukotriene receptor 1	0.33377	0.36547	
Cysltr2	cysteinyl leukotriene receptor 2	0.04466	0.18682	
Drd1	dopamine receptor D1	0.29312	0.14566	
Drd2	dopamine receptor D2	0.44887	0.61526	
Drd3	dopamine receptor D3	0.21568	0.41543	
Drd4	dopamine receptor D4	0	0.23911	
Drd5	dopamine receptor D5	0.10866	0.12669	
Ednra	endothelin receptor type A	10.45032	2.40702	
Ednrb	endothelin receptor type B	175.73241	33.9357	
F2r	coagulation factor II thrombin receptor	12.1799	7.72788	
F2rl1	F2R like trypsin receptor 1	0.12777	0.74662	
F2rl2	coagulation factor II thrombin receptor like 2	0.16403	0.37064	
F2rl3	F2R like thrombin or trypsin receptor 3	0.09665	0.30447	
Ffar1	free fatty acid receptor 1	0	0	*
Ffar2	free fatty acid receptor 2	0.03415	0.05658	
Ffar3	free fatty acid receptor 3	0.00446	0	*
Ffar4	free fatty acid receptor 4	0.18805	0	*
Fpr1	formyl peptide receptor 1	0.00347	0	*
Fpr2	formyl peptide receptor 2	0.00814	0	*
Fpr2	formyl peptide receptor 2	0.00814	0	*
Fpr3	formyl peptide receptor 3	0.03784	0	*
Fshr	follicle stimulating hormone receptor	0	0	*
Fzd1	frizzled class receptor 1	10.63276	1.82697	
Fzd2	frizzled class receptor 2	7.93329	2.33763	
Fzd3	frizzled class receptor 3	8.11519	0.68142	
Fzd4	frizzled class receptor 4	1.23995	1.1179	
Fzd5	frizzled class receptor 5	8.53842	0.07761	

Fzd6	frizzled class receptor 6	3.62239	1.21921	
Fzd7	frizzled class receptor 7	4.50452	0	*
Fzd8	frizzled class receptor 8	2.16433	1.15766	
Fzd9	frizzled class receptor 9	3.81997	0	*
Gabbr1	gamma-aminobutyric acid type B receptor subunit 1	207.41576	17.5055	
Gabbr2	gamma-aminobutyric acid type B receptor subunit 2	9.9972	4.26628	
Galr1	galanin receptor 1	0.43504	0.04129	
Galr2	galanin receptor 2	4.82825	0	*
Galr3	galanin receptor 3	1.26458	0.196	
Gcgr	glucagon receptor	0.02967	0.03426	
Ghrhr	growth hormone releasing hormone receptor	0.00452	0.31465	
Ghsr	growth hormone secretagogue receptor	0.0684	0.54898	
Gipr	gastric inhibitory polypeptide receptor	0.29599	0.47705	
Glp1r	glucagon like peptide 1 receptor	1.89684	0.50796	
Glp2r	glucagon like peptide 2 receptor	0.03326	0.39967	
Gnrhr	gonadotropin releasing hormone receptor	0.00873	0.45799	
Gpbar1	G protein-coupled bile acid receptor 1	0.03991	0	*
Gper1	G protein-coupled estrogen receptor 1	1.14087	0.34469	
Gpr1	G protein-coupled receptor 1	0.58802	0.08544	
Gpr101	G protein-coupled receptor 101	5.32934	0	
Gpr107	G protein-coupled receptor 107	20.19762	3.29636	
Gpr112l	adhesion G protein-coupled receptor G4	0	0	$ *
Gpr119	G protein-coupled receptor 119	0	0	
Gpr119	G protein-coupled receptor 119	0	0	
Gpr12	G protein-coupled receptor 12	0.78289	0.38839	
Gpr132	G protein-coupled receptor 132	0.14795	0	*

Gpr135	G protein-coupled receptor 135	1.95202	0	*
Gpr137	G protein-coupled receptor 137	53.04756	2.37091	
Gpr139	G protein-coupled receptor 139	0.10061	0	*
Gpr141	G protein-coupled receptor 141	0.02844	0	*
Gpr142	G protein-coupled receptor 142	0	0	*
Gpr143	G protein-coupled receptor 143	0.8955	0.43474	
Gpr146	G protein-coupled receptor 146	5.84671	3.33984	
Gpr149	G protein-coupled receptor 149	5.89955	2.81065	
Gpr15	G protein-coupled receptor 15	48	0	*
Gpr150	G protein-coupled receptor 150	1.18012	0.85492	
Gpr151	G protein-coupled receptor 151	0.03179	0	*
Gpr152	G protein-coupled receptor 152	616	0	*
Gpr153	G protein-coupled receptor 153	7.16311	0.57748	
Gpr156	G protein-coupled receptor 156	0.94569	0	*
Gpr157	G protein-coupled receptor 157	1.16238	0	*
Gpr158	G protein-coupled receptor 158	4.42888	5.01543	
Gpr160	G protein-coupled receptor 160	1.13775	0	*
Gpr161	G protein-coupled receptor 161	3.31195	0.76742	
Gpr162	G protein-coupled receptor 162	46.84618	5.62079	
Gpr17	G protein-coupled receptor 17	16.03428	0	*
Gpr171	G protein-coupled receptor 171	0.40328	0	*
Gpr173	G protein-coupled receptor 173	11.95022	0.2277	
Gpr174	G protein-coupled receptor 174	0.03181	0	*
Gpr176	G protein-coupled receptor 176	31.41416	7.19634	
Gpr179	G protein-coupled receptor 179	0.15909	0	*
Gpr18	G protein-coupled receptor 18	0.25467	0	*
Gpr18	G protein-coupled receptor 18	0.25467	0	*
Gpr182	G protein-coupled receptor 182	0.93495	0.18724	

Gpr183	G protein-coupled receptor 183	1.90566	0	*
Gpr19	G protein-coupled receptor 19	11.45561	1.95017	
Gpr20	G protein-coupled receptor 20	0	0.12269	$
Gpr21	G protein-coupled receptor 21	0.05146	0	*
Gpr22	G protein-coupled receptor 22	2.16256	0	*
Gpr25	G protein-coupled receptor 25	0.15954	0	*
Gpr26	G protein-coupled receptor 26	0.29883	0.49801	
Gpr27	G protein-coupled receptor 27	1.79968	0.17276	
Gpr3	G protein-coupled receptor 3	0.81779	0	*
Gpr31	G protein-coupled receptor 31	0.95195	0	*
Gpr33	G protein-coupled receptor 33 (gene/pseudogene)	0	0	*
Gpr34	G protein-coupled receptor 34	15.2159	1.41199	
Gpr35	G protein-coupled receptor 35	0.06189	0	*
Gpr37	G protein-coupled receptor 37	47.44945	10.1082	
Gpr37l1	G protein-coupled receptor 37 like 1	112.07879	13.02	
Gpr39	G protein-coupled receptor 39	527	0	*
Gpr4	G protein-coupled receptor 4	2.48128	0.09761	
Gpr45	G protein-coupled receptor 45	3.25957	0.25544	
Gpr50	G protein-coupled receptor 50	0.02797	0.09863	
Gpr52	G protein-coupled receptor 52	0.88914	0	*
Gpr55	G protein-coupled receptor 55	198	0	*
Gpr55	G protein-coupled receptor 55	198	0	*
Gpr6	G protein-coupled receptor 6	5.86817	0.64627	
Gpr61	G protein-coupled receptor 61	4.58676	0.60478	
Gpr62	G protein-coupled receptor 62	3.47303	0.11255	
Gpr63	G protein-coupled receptor 63	0.71928	0	*
Gpr65	G protein-coupled receptor 65	0.56795	0	*

Gpr68	G protein-coupled receptor 68	2.28106	1.11134	
Gpr75	G protein-coupled receptor 75	5.16736	0.46502	
Gpr83	G protein-coupled receptor 83	2.73483	1.84265	
Gpr84	G protein-coupled receptor 84	2.52822	0.7235	
Gpr85	G protein-coupled receptor 85	11.54069	2.16851	
Gpr87	G protein-coupled receptor 87	0.02452	0	*
Gpr88	G protein-coupled receptor 88	1.20431	1.43845	
Gprc5a	G protein-coupled receptor class C group 5 member A	0.6685	0.66103	
Gprc5b	G protein-coupled receptor class C group 5 member B	191.25851	12.3232	
Gprc5c	G protein-coupled receptor class C group 5 member C	3.39134	0.56878	
Gprc5d	G protein-coupled receptor class C group 5 member D	178	0	*
Gprc6a	G protein-coupled receptor class C group 6 member A	0	0	*
Grm1	glutamate metabotropic receptor 1	0.71739	1.98508	
Grm2	glutamate metabotropic receptor 2	3.53916	1.55891	
Grm3	glutamate metabotropic receptor 3	10.19022	3.89833	
Grm4	glutamate metabotropic receptor 4	0.89122	0.62636	
Grm5	glutamate metabotropic receptor 5	0.87468	0.03479	
Grm6	glutamate metabotropic receptor 6	439	0.14707	
Grm7	glutamate metabotropic receptor 7	5.84938	0.53761	
Grm8	glutamate metabotropic receptor 8	3.08472	1.09351	
Grpr	gastrin releasing peptide receptor	0.04601	0.46934	
Hcar1	hydroxycarboxylic acid receptor 1	2.986	0	*
Hcar2	hydroxycarboxylic acid receptor 2	2.02547	0	
Hcrtr1	hypocretin receptor 1	0.21443	0.46206	
Hcrtr2	hypocretin receptor 2	0.09187	0.42954	

Hrh1	histamine receptor H1	5.0156	1.67177
Hrh2	histamine receptor H2	0.96758	0.02988
Hrh3	histamine receptor H3	2.68744	0.94722
Hrh4	histamine receptor H4	0.00507	0.02272
Htr1a	5-hydroxytryptamine receptor 1A	0.46528	0.02362
Htr1b	5-hydroxytryptamine receptor 1B	1.24547	0.28121
Htr1d	5-hydroxytryptamine receptor 1D	0.16789	0.06222
Htr1f	5-hydroxytryptamine receptor 1F	0.48396	0.40041
Htr2a	5-hydroxytryptamine receptor 2A	0.69648	0.50043
Htr2b	5-hydroxytryptamine receptor 2B	0.02228	0.22903
Htr2c	5-hydroxytryptamine receptor 2C	34.39964	35.835
Htr4	5-hydroxytryptamine receptor 4	0.00653	0.27001
Htr5a	5-hydroxytryptamine receptor 5A	0.8692	0.81053
Htr5b	5-hydroxytryptamine receptor 5B, pseudogene	0.40705	0.28196
Htr6	5-hydroxytryptamine receptor 6	1.05322	0.17264
Htr7	5-hydroxytryptamine receptor 7	0.52494	0.51103
Kiss1r	KISS1 receptor	3.35692	0.09679
Lgr4	leucine rich repeat containing G protein-coupled receptor 4	28.31896	1.92236
Lgr5	leucine rich repeat containing G protein-coupled receptor 5	1.12403	0.74224
Lgr6	leucine rich repeat containing G protein-coupled receptor 6	1.61731	1.38004
Lhcgr	luteinizing hormone/choriogonadotropin receptor	0.04172	0.24058
Lpar1	lysophosphatidic acid receptor 1	52.83691	13.6638
Lpar2	lysophosphatidic acid receptor 2	0.2456	0.20164
Lpar3	lysophosphatidic acid receptor 3	0.77833	0.18664
Lpar4	lysophosphatidic acid receptor 4	1.81721	0.45334

Lpar5	lysophosphatidic acid receptor 5	0.62355	0	*
Lpar6	lysophosphatidic acid receptor 6	3.54239	1.91307	
Ltb4r	leukotriene B4 receptor	0.05224	0.09056	
Ltb4r2	leukotriene B4 receptor 2	0.00253	0	
Mas1	MAS1 proto-oncogene, G protein-coupled receptor	0.02116	0.32631	
Mc1r	melanocortin 1 receptor	0	0	$ *
Mc2r	melanocortin 2 receptor	0.0304	0	*
Mc3r	melanocortin 3 receptor	1.1005	0	*
Mc4r	melanocortin 4 receptor	0.98791	0.21012	
Mc5r	melanocortin 5 receptor	0.00629	0.1991	
Mchr1	melanin concentrating hormone receptor 1	0.64114	0.36188	
Mlnr	motilin receptor	0.00249	0	
Mrgprd	MAS related GPR family member D	0.00391	0	
Mrgpre	MAS related GPR family member E	6.8271	0	*
Mrgprf	MAS related GPR family member F	1.3575	0.07128	
Mrgprg	MAS related GPR family member G	0.00464	0	*
Mtnr1a	melatonin receptor 1A	0.02393	0	*
Mtnr1b	melatonin receptor 1B	0	0	*
Nmbr	neuromedin B receptor	0.16716	0.4886	
Nmur1	neuromedin U receptor 1	0.03102	0.48961	
Nmur2	neuromedin U receptor 2	0.94768	0.14901	
Npbwr1	neuropeptides B and W receptor 1	0.95019	0	*
Npffr1	neuropeptide FF receptor 1	0.95878	0.31395	
Npffr2	neuropeptide FF receptor 2	0.11779	0.68891	
Npsr1	neuropeptide S receptor 1	0.16009	0	*
Npy1r	neuropeptide Y receptor Y1	2.21268	0.68533	
Npy2r	neuropeptide Y receptor Y2	3.00448	0.02283	

Npy4r	neuropeptide Y receptor Y4	0.19228	0.4903	
Npy5r	neuropeptide Y receptor Y5	0.52936	0.15025	
Ntsr1	neurotensin receptor 1	0.2703	0.19789	
Ntsr2	neurotensin receptor 2	41.1987	13.8148	
Olr63	olfactory receptor family 51 subfamily E member 1	0.02672	0	*
Opn3	opsin 3	4.35554	1.70782	
Opn4	opsin 4	0.15798	0.15004	
Opn5	opsin 5	0	0	*
Oprd1	opioid receptor delta 1	0.04002	0.05319	
Oprk1	opioid receptor kappa 1	5.61786	1.27044	
Oprl1	opioid related nociceptin receptor 1	11.57353	1.28169	
Oprm1	opioid receptor mu 1	0.89071	0.17475	
Oxgr1	oxoglutarate receptor 1	0	0	*
Oxtr	oxytocin receptor	0.02752	0.04542	
P2ry1	purinergic receptor P2Y1	17.57994	1.51476	
P2ry10	purinergic receptor P2Y10	0.08298	0.07978	
P2ry12	purinergic receptor P2Y12	17.84347	2.61078	
P2ry13	purinergic receptor P2Y13	3.16884	0	*
P2ry14	purinergic receptor P2Y14	1.62497	0.84874	
P2ry2	purinergic receptor P2Y2	1.02023	0.181	
P2ry4	pyrimidinergic receptor P2Y4	1.31973	0.16055	
P2ry6	pyrimidinergic receptor P2Y6	1.98	1.35207	
Prlhr	prolactin releasing hormone receptor	7.07741	0.14669	
Prokr1	prokineticin receptor 1	0	0.20886	
Prokr2	prokineticin receptor 2	2.30818	0.15666	
Ptafr	platelet activating factor receptor	3.93252	2.07696	
Ptgdr	prostaglandin D2 receptor	1.45959	0.12209	

Ptgdr2	prostaglandin D2 receptor 2	0.08185	0.0423	
Ptger1	prostaglandin E receptor 1	0.18374	0.11792	
Ptger2	prostaglandin E receptor 2	1.40365	0.88667	
Ptger3	prostaglandin E receptor 3	3.22516	0.35377	
Ptger4	prostaglandin E receptor 4	0.28454	0.22226	
Ptgfr	prostaglandin F receptor	0.82609	748	
Ptgir	prostaglandin I2 receptor	0.13499	0	*
Pth1r	parathyroid hormone 1 receptor	4.6881	0.8853	
Pth2r	parathyroid hormone 2 receptor	0.03058	0.22751	
Qrfpr	pyroglutamylated RFamide peptide receptor	0.03008	0	*
Rxfp1	relaxin/insulin like family peptide receptor 1	17.60129	0	*
Rxfp2	relaxin/insulin like family peptide receptor 2	0.54036	0	*
Rxfp3	relaxin/insulin like family peptide receptor 3	4.81719	0	*
S1pr1	sphingosine-1-phosphate receptor 1	50.33706	14.8313	
S1pr2	sphingosine-1-phosphate receptor 2	5.02572	0.17277	
S1pr3	sphingosine-1-phosphate receptor 3	25.44074	6.50061	
S1pr4	sphingosine-1-phosphate receptor 4	0.08228	0	*
S1pr5	sphingosine-1-phosphate receptor 5	17.89621	2.25646	
Sctr	secretin receptor	3.62767	0.72574	
Smo	smoothened, frizzled class receptor	26.81248	2.26709	
Sstr1	somatostatin receptor 1	1.44576	0.71449	
Sstr2	somatostatin receptor 2	1.99533	0.39094	
Sstr3	somatostatin receptor 3	0.34612	0.97125	
Sstr4	somatostatin receptor 4	0.14091	0.30621	
Sstr5	somatostatin receptor 5	0.78612	0.24967	
Sucnr1	succinate receptor 1	403	0	*
Taar1	trace amine associated receptor 1	0	0.38411	

Taar2	trace amine associated receptor 2 (gene/pseudogene)	0.00735	0	*
Taar3	trace amine associated receptor 3, pseudogene	0.00738	0	*
Taar4	trace amine associated receptor 4, pseudogene	0.00541	0	*
Taar5	trace amine associated receptor 5	0	0	*
Taar6	trace amine associated receptor 6	0	0	*
Taar8a	trace amine associated receptor 8	0	0	*
Taar9	trace amine associated receptor 9 (gene/pseudogene)	0	0	*
Tacr1	tachykinin receptor 1	1.80144	1.42783	
Tacr2	tachykinin receptor 2	0.03762	0.03421	
Tacr3	tachykinin receptor 3	0.28038	0.07494	
Tas1r1	taste 1 receptor member 1	0.32517	0	*
Tas1r3	taste 1 receptor member 3	0.00788	0.43487	
Tbxa2r	thromboxane A2 receptor	0.82145	0.55117	
Tpra1	transmembrane protein adipocyte associated 1	19.7842	2.78698	
Trhr	thyrotropin releasing hormone receptor	0.26078	0.69369	
Tshr	thyroid stimulating hormone receptor	2.22802	0.22447	
Uts2r	urotensin 2 receptor	0.60172	0.04256	
Vipr1	vasoactive intestinal peptide receptor 1	0.00799	0.32281	
Vipr2	vasoactive intestinal peptide receptor 2	0.62867	0.1738	
Xcr1	X-C motif chemokine receptor 1	0.20775	0	*

Voltage-gated ion channels:

Gene name	Full gene name	RNAseq FPKM	Microarray intensity	
Cacna 1h	calcium voltage-gated channel subunit alpha1 H	2.88623	1.04682	
Cacna 1i	calcium voltage-gated channel subunit alpha1 I	4.14717	0.58692	
Cacna 1s	calcium voltage-gated channel subunit alpha1 S	0.00272	0.03518	
Catsper1	cation channel sperm associated 1	0	0	*
Catsper2	cation channel sperm associated 2	2.0908	0.36493	
Catsper3	cation channel sperm associated 3	0.01294	0	*
Catsper4	cation channel sperm associated 4	0.01519	0	*
Cnga1	cyclic nucleotide gated channel alpha 1	0.67418	0.22318	
Cnga2	cyclic nucleotide gated channel alpha 2	0	0.59017	
Cnga3	cyclic nucleotide gated channel alpha 3	2.29406	0.09954	
Cnga4	cyclic nucleotide gated channel alpha 4	0.03486	0.16741	
Cngb1	cyclic nucleotide gated channel beta 1	2.34471	0.27996	
Cngb3	cyclic nucleotide gated channel beta 3	0.00475	0	*
Hcn1	hyperpolarization activated cyclic nucleotide gated potassium channel 1	2.55793	1.03223	
Hcn2	hyperpolarization activated cyclic nucleotide gated potassium and sodium channel 2	18.32771	1.86672	
Hcn3	hyperpolarization activated cyclic nucleotide gated potassium channel 3	6.47722	0.88082	
Hcn4	hyperpolarization activated cyclic nucleotide gated potassium channel 4	2.31037	0.02703	
Hvcn1	hydrogen voltage gated channel 1	1.37526	0	*

Kcna1	potassium voltage-gated channel subfamily A member 1	2.6877	3.70805	
Kcna10	potassium voltage-gated channel subfamily A member 10	0.00413	0	*
Kcna2	potassium voltage-gated channel subfamily A member 2	6.01674	6.31347	
Kcna3	potassium voltage-gated channel subfamily A member 3	1.63413	0.25572	
Kcna4	potassium voltage-gated channel subfamily A member 4	2.34605	1.05203	
Kcna5	potassium voltage-gated channel subfamily A member 5	4.53163	0.76695	
Kcna6	potassium voltage-gated channel subfamily A member 6	22.82651	3.78666	
Kcna7	potassium voltage-gated channel subfamily A member 7	0.04535	0	*
Kcnb1	potassium voltage-gated channel subfamily B member 1	4.03142	1.27953	
Kcnb2	potassium voltage-gated channel subfamily B member 2	1.53107	0.05149	
Kcnc1	potassium voltage-gated channel subfamily C member 1	4.15517	3.83402	
Kcnc2	potassium voltage-gated channel subfamily C member 2	5.06581	2.70796	
Kcnc3	potassium voltage-gated channel subfamily C member 3	5.66321	0.66046	
Kcnc4	potassium voltage-gated channel subfamily C member 4	13.06868	2.38833	
Kcnd1	potassium voltage-gated channel subfamily D member 1	1.56502	1.42971	
Kcnd2	potassium voltage-gated channel subfamily D member 2	0	5.14506	$
Kcnd3	potassium voltage-gated channel subfamily D member 3	8.00956	3.85618	

Kcnf1	potassium voltage-gated channel modifier subfamily F member 1	1.76685	0	*
Kcng1	potassium voltage-gated channel modifier subfamily G member 1	5.56212	0	*
Kcng2	potassium voltage-gated channel modifier subfamily G member 2	6.51779	2.16789	
Kcng3	potassium voltage-gated channel modifier subfamily G member 3	0.02246	0.62778	
Kcng4	potassium voltage-gated channel modifier subfamily G member 4	3.81197	0	*
Kcnh1	potassium voltage-gated channel subfamily H member 1	5.3395	1.63155	
Kcnh2	potassium voltage-gated channel subfamily H member 2	15.36578	1.32214	
Kcnh3	potassium voltage-gated channel subfamily H member 3	0.25288	1.1669	
Kcnh4	potassium voltage-gated channel subfamily H member 4	0.89753	0.08577	
Kcnh5	potassium voltage-gated channel subfamily H member 5	0.48013	0.17901	
Kcnh6	potassium voltage-gated channel subfamily H member 6	4.84301	1.2605	
Kcnh7	potassium voltage-gated channel subfamily H member 7	1.06026	0.13415	
Kcnh8	potassium voltage-gated channel subfamily H member 8	0.07979	0.02798	
Kcnj1	potassium voltage-gated channel subfamily J member 1	0.07311	0.0256	
Kcnj10	potassium voltage-gated channel subfamily J member 10	25.75609	0.14313	
Kcnj11	potassium voltage-gated channel subfamily J member 11	2.25877	0.48313	
Kcnj12	potassium voltage-gated channel subfamily J member 12	1.72569	0.17625	

Kcnj13	potassium voltage-gated channel subfamily J member 13	19.73969	0.28315	
Kcnj14	potassium voltage-gated channel subfamily J member 14	4.7599	1.33932	
Kcnj15	potassium voltage-gated channel subfamily J member 15	0.09821	0.455	
Kcnj16	potassium voltage-gated channel subfamily J member 16	15.65715	1.66001	
Kcnj2	potassium voltage-gated channel subfamily J member 2	3.33881	0.12769	
Kcnj3	potassium voltage-gated channel subfamily J member 3	1.59416	0.21389	
Kcnj4	potassium voltage-gated channel subfamily J member 4	0.19662	0.14845	
Kcnj5	potassium voltage-gated channel subfamily J member 5	1.90383	0.71823	
Kcnj6	potassium voltage-gated channel subfamily J member 6	1.02588	1.52052	
Kcnj8	potassium voltage-gated channel subfamily J member 8	0.9019	0.40962	
Kcnj9	potassium voltage-gated channel subfamily J member 9	8.80888	0.05645	
Kcnk1	potassium two pore domain channel subfamily K member 1	9.05503	1.92298	
Kcnk10	potassium two pore domain channel subfamily K member 10	1.64138	0.27097	
Kcnk12	potassium two pore domain channel subfamily K member 12	0.20314	0.17508	
Kcnk13	potassium two pore domain channel subfamily K member 13	0.94288	0.85028	
Kcnk15	potassium two pore domain channel subfamily K member 15	0.02294	0.36587	
Kcnk16	potassium two pore domain channel subfamily K member 16	4.2301	0	*

Kcnk18	potassium two pore domain channel subfamily K member 18	0	0	*
Kcnk2	potassium two pore domain channel subfamily K member 2	14.76248	2.78658	
Kcnk3	potassium two pore domain channel subfamily K member 3	1.33985	0.77552	
Kcnk4	potassium two pore domain channel subfamily K member 4	0.41763	0.54016	
Kcnk5	potassium two pore domain channel subfamily K member 5	1.25308	0.3091	
Kcnk6	potassium two pore domain channel subfamily K member 6	0.39068	0.7491	
Kcnk7	potassium two pore domain channel subfamily K member 7	0.14737	0	*
Kcnk9	potassium two pore domain channel subfamily K member 9	5.1482	0.39337	
Kcnma1	potassium calcium-activated channel subfamily M alpha 1	1.86821	0.39943	
Kcnn1	potassium calcium-activated channel subfamily N member 1	2.16711	0	*
Kcnn2	potassium calcium-activated channel subfamily N member 2	1.52509	1.14841	
Kcnn2	potassium calcium-activated channel subfamily N member 2	3.78492	1.14841	
Kcnn3	potassium calcium-activated channel subfamily N member 3	6.0961	0.47289	
Kcnn4	potassium calcium-activated channel subfamily N member 4	0.36203	0.19609	
Kcnq1	potassium voltage-gated channel subfamily Q member 1	0.31264	1.35497	
Kcnq2	potassium voltage-gated channel subfamily Q member 2	10.21197	0.48689	
Kcnq3	potassium voltage-gated channel subfamily Q member 3	1.03644	0.81711	

Kcnq4	potassium voltage-gated channel subfamily Q member 4	0.83115	0.60978	
Kcnq5	potassium voltage-gated channel subfamily Q member 5	0.78514	0.9625	
Kcns1	potassium voltage-gated channel modifier subfamily S member 1	0.17624	0.32588	
Kcns2	potassium voltage-gated channel modifier subfamily S member 2	2.68343	0.10365	
Kcns3	potassium voltage-gated channel modifier subfamily S member 3	0.42998	0.80784	
Kcnt1	potassium sodium-activated channel subfamily T member 1	4.65921	0.65723	
Kcnt2	potassium sodium-activated channel subfamily T member 2	2.20484	0	*
Kcnu1	potassium calcium-activated channel subfamily U member 1	0.00378	0	*
Kcnv1	potassium voltage-gated channel modifier subfamily V member 1	1.33768	0.62511	
Kcnv2	potassium voltage-gated channel modifier subfamily V member 2	0.05846	0.47579	
Mcoln 1	mucolipin 1	19.47008	3.60541	
Mcoln 2	mucolipin 2	0.00316	0.23505	
Mcoln 3	mucolipin 3	0.59793	0	*
Pkd2	polycystin 2, transient receptor potential cation channel	14.90464	9.48042	
Pkd2l1	polycystin 2 like 1, transient receptor potential cation channel	0.00539	0	*
Pkd2l2	polycystin 2 like 2, transient receptor potential cation channel	0.07989	0.23497	
Ryr1	ryanodine receptor 1	0.06332	0	*

Ryr2	ryanodine receptor 2	0.42116	1.65031	
Ryr3	ryanodine receptor 3	1.78863	2.94162	
Scn10a	sodium voltage-gated channel alpha subunit 10	0.15241	0.38315	
Scn11a	sodium voltage-gated channel alpha subunit 11	0.13666	0.09619	
Scn1a	sodium voltage-gated channel alpha subunit 1	4.10373	3.00307	
Scn2a	sodium voltage-gated channel alpha subunit 2	10.28531	4.72349	
Scn3a	sodium voltage-gated channel alpha subunit 3	6.43042	2.9835	
Scn4a	sodium voltage-gated channel alpha subunit 4	0.05824	0.03241	
Scn5a	sodium voltage-gated channel alpha subunit 5	0.33157	0.16251	
Scn8a	sodium voltage-gated channel alpha subunit 8	3.45493	0.12433	
Scn9a	sodium voltage-gated channel alpha subunit 9	8.62151	6.09753	
Tpcn1	two pore segment channel 1	38.45973	4.87123	
Tpcn2	two pore segment channel 2	3.32282	1.10096	
Trpa1	transient receptor potential cation channel subfamily A member 1	0.04608	0	*
Trpc1	transient receptor potential cation channel subfamily C member 1	0	2.8719	$
Trpc2	transient receptor potential cation channel subfamily C member 2, pseudogene	0	0.54593	$
Trpc3	transient receptor potential cation channel subfamily C member 3	0.61129	0.63875	
Trpc4	transient receptor potential cation channel subfamily C member 4	1.98793	0.63776	
Trpc5	transient receptor potential cation channel subfamily C member 5	2.60359	0.04585	
Trpc6	transient receptor potential cation channel subfamily C member 6	1.68274	0.29628	
Trpc7	transient receptor potential cation channel subfamily C member 7	1.29291	0	*

Trpm1	transient receptor potential cation channel subfamily M member 1	0.19166	0.56845	
Trpm2	transient receptor potential cation channel subfamily M member 2	2.99785	0	*
Trpm3	transient receptor potential cation channel subfamily M member 3	17.00175	0	*
Trpm4	transient receptor potential cation channel subfamily M member 4	0.69027	0.41919	
Trpm5	transient receptor potential cation channel subfamily M member 5	0.12118	0	*
Trpm6	transient receptor potential cation channel subfamily M member 6	0.09396	0	*
Trpm7	transient receptor potential cation channel subfamily M member 7	11.57418	7.014	
Trpm8	transient receptor potential cation channel subfamily M member 8	0.03529	0.04871	
Trpv1	transient receptor potential cation channel subfamily V member 1	0.66109	0.13478	
Trpv2	transient receptor potential cation channel subfamily V member 2	8.26521	0.88011	
Trpv3	transient receptor potential cation channel subfamily V member 3	0.36223	0	*
Trpv4	transient receptor potential cation channel subfamily V member 4	1.19596	1.67714	
Trpv5	transient receptor potential cation channel subfamily V member 5	0	0.07552	
Trpv6	transient receptor potential cation channel subfamily V member 6	0	0.51283	

Ligand-gated ion channels:

Gene name	Full gene name	RNAseq FPKM	Microarray intensity	
Asic1	acid sensing ion channel subunit 1	12.59786	1.67222	
Asic2	acid sensing ion channel subunit 2	13.58714	3.92846	
Asic3	acid sensing ion channel subunit 3	0.18443	0.12909	
Chrna1	cholinergic receptor nicotinic alpha 1 subunit	0.05761	0.3501	
Chrna10	cholinergic receptor nicotinic alpha 10 subunit	112	0.06682	
Chrna2	cholinergic receptor nicotinic alpha 2 subunit	0.03022	0.65417	
Chrna3	cholinergic receptor nicotinic alpha 3 subunit	3.38858	0.19232	
Chrna4	cholinergic receptor nicotinic alpha 4 subunit	4.34396	1.02911	
Chrna5	cholinergic receptor nicotinic alpha 5 subunit	0.02002	0.15652	
Chrna6	cholinergic receptor nicotinic alpha 6 subunit	0	0.07543	
Chrna7	cholinergic receptor nicotinic alpha 7 subunit	9.50312	1.3082	
Chrna9	cholinergic receptor nicotinic alpha 9 subunit	0.03955	0.37896	
Chrnb1	cholinergic receptor nicotinic beta 1 subunit	1.97324	1.15119	
Chrnb2	cholinergic receptor nicotinic beta 2 subunit	12.15794	0.23236	
Chrnb3	cholinergic receptor nicotinic beta 3 subunit	0.07179	0.02408	
Chrnb4	cholinergic receptor nicotinic beta 4 subunit	4.54691	0.76521	
Chrnd	cholinergic receptor nicotinic delta subunit	0	0.14878	
Chrne	cholinergic receptor nicotinic epsilon subunit	0.50452	0.25884	
Chrng	cholinergic receptor nicotinic gamma subunit	0	0.0873	$
Gabra1	gamma-aminobutyric acid type A receptor alpha1 subunit	22.64117	10.5765	
Gabra2	gamma-aminobutyric acid type A receptor alpha2 subunit	12.25983	2.09369	
Gabra3	gamma-aminobutyric acid type A receptor alpha3 subunit	16.40755	0.0472	

Gabra4	gamma-aminobutyric acid type A receptor alpha4 subunit	13.10074	0.13925
Gabra5	gamma-aminobutyric acid type A receptor alpha5 subunit	10.30772	2.04332
Gabra6	gamma-aminobutyric acid type A receptor alpha6 subunit	332	0.43974
Gabrb1	gamma-aminobutyric acid type A receptor beta1 subunit	4.2744	10.09
Gabrb2	gamma-aminobutyric acid type A receptor beta2 subunit	4.23783	0.1239
Gabrb3	gamma-aminobutyric acid type A receptor beta3 subunit	17.06353	0.69508
Gabrd	gamma-aminobutyric acid type A receptor delta subunit	0.13721	0.39011
Gabre	gamma-aminobutyric acid type A receptor epsilon subunit	21.00746	4.89065
Gabrg1	gamma-aminobutyric acid type A receptor gamma1 subunit	30.11948	1.0475
Gabrg2	gamma-aminobutyric acid type A receptor gamma2 subunit	22.45081	6.20191
Gabrg3	gamma-aminobutyric acid type A receptor gamma3 subunit	1.5668	0.8177
Gabrp	gamma-aminobutyric acid type A receptor pi subunit	0.00829	0.05759
Gabrq	gamma-aminobutyric acid type A receptor theta subunit	2.70718	0.91926
Gabrr1	gamma-aminobutyric acid type A receptor rho1 subunit	0.17102	0.13692
Gabrr2	gamma-aminobutyric acid type A receptor rho2 subunit	1.16061	0.37388
Gabrr3	gamma-aminobutyric acid type A receptor rho3 subunit (gene/pseudogene)	0	0.24222
Glra1	glycine receptor alpha 1	0.06746	0.36634

Glra2	glycine receptor alpha 2	2.83469	0.3172	
Glra3	glycine receptor alpha 3	0.10043	0.39159	
Glra4	glycine receptor alpha 4	0.4566	0	*
Glrb	glycine receptor beta	21.58509	6.49287	
Gria1	glutamate ionotropic receptor AMPA type subunit 1	79.77848	1.99502	
Gria2	glutamate ionotropic receptor AMPA type subunit 2	28.35372	20.1097	
Gria3	glutamate ionotropic receptor AMPA type subunit 3	3.24668	4.98878	
Gria4	glutamate ionotropic receptor AMPA type subunit 4	10.76736	0.34915	
Grid1	glutamate ionotropic receptor delta type subunit 1	3.37534	0.20466	
Grid2	glutamate ionotropic receptor delta type subunit 2	2.389	0.15946	
Grik1	glutamate ionotropic receptor kainate type subunit 1	20.46693	2.17376	
Grik2	glutamate ionotropic receptor kainate type subunit 2	4.64253	1.25044	
Grik3	glutamate ionotropic receptor kainate type subunit 3	1.69949	0.29278	
Grik4	glutamate ionotropic receptor kainate type subunit 4	7.30837	0.51606	
Grik5	glutamate ionotropic receptor kainate type subunit 5	26.03991	2.36961	
Grin1	glutamate ionotropic receptor NMDA type subunit 1	26.91762	4.84796	
Grin2a	glutamate ionotropic receptor NMDA type subunit 2A	0.07362	0.25449	
Grin2b	glutamate ionotropic receptor NMDA type subunit 2B	0.27166	0.69505	
Grin2c	glutamate ionotropic receptor NMDA type subunit 2C	5.80179	3.1889	

Grin2d	glutamate ionotropic receptor NMDA type subunit 2D	1.55483	0.2759
Grin3a	glutamate ionotropic receptor NMDA type subunit 3A	1.80165	0.24778
Grin3b	glutamate ionotropic receptor NMDA type subunit 3B	0.0279	0.33715
Htr3a	5-hydroxytryptamine receptor 3A	0.85947	0.52209
Htr3b	5-hydroxytryptamine receptor 3B	0	0.24447
Itpr1	inositol 1,4,5-trisphosphate receptor type 1	6.11613	12.0711
Itpr2	inositol 1,4,5-trisphosphate receptor type 2	1.33751	0.66946
Itpr3	inositol 1,4,5-trisphosphate receptor type 3	1.12491	0.73877
P2rx1	purinergic receptor P2X 1	0.26735	0.08245
P2rx2	purinergic receptor P2X 2	4.4765	0.21751
P2rx3	purinergic receptor P2X 3	1.36384	0.70281
P2rx4	purinergic receptor P2X 4	11.17898	1.74883
P2rx5	purinergic receptor P2X 5	0.05593	0.15855
P2rx6	purinergic receptor P2X 6	52.96405	4.70851
P2rx7	purinergic receptor P2X 7	3.18344	0.28413
Scnn1a	sodium channel epithelial 1 alpha subunit	0.57733	0.04188
Scnn1b	sodium channel epithelial 1 beta subunit	0.12783	0.82864
Scnn1g	sodium channel epithelial 1 gamma subunit	0.23084	0.30849

Other ion channels:

Gene name	Full gene name	RNAseq FPKM	Microarray intensity	
Ano1	anoctamin 1	18.07925	8.27877	
Aqp1	aquaporin 1 (Colton blood group)	15.63078	1.83298	
Aqp2	aquaporin 2	0.00216	0.09731	
Aqp3	aquaporin 3 (Gill blood group)	245	0.11658	
Aqp4	aquaporin 4	142.07014	52.5917	
Aqp5	aquaporin 5	0.00575	0.07878	
Aqp6	aquaporin 6	0	0.46685	
Aqp7	aquaporin 7	0	0.57341	
Aqp8	aquaporin 8	0	0.46919	
Aqp9	aquaporin 9	3.55981	0.60185	
Cftr	cystic fibrosis transmembrane conductance regulator	0.00242	0.32833	
Clcn1	chloride voltage-gated channel 1	0.13418	0.28394	
Clcn2	chloride voltage-gated channel 2	8.64905	1.34019	
Clcn3	chloride voltage-gated channel 3	35.89265	18.1412	
Clcn4	chloride voltage-gated channel 4	19.47461	4.67295	
Clcn5	chloride voltage-gated channel 5	2.01434	0.31307	
Clcn6	chloride voltage-gated channel 6	22.21917	7.38807	
Clcn7	chloride voltage-gated channel 7	16.50765	0.41648	
Clcnka	chloride voltage-gated channel Ka	0	0.30687	
Clcnkb	chloride voltage-gated channel Kb	0.28879	0.37488	
Gja1	gap junction protein alpha 1	167.27918	50.9026	
Gja10	gap junction protein alpha 10	275	0	*
Gja3	gap junction protein alpha 3	0.07257	0.16072	
Gja4	gap junction protein alpha 4	0.92502	0.91373	
Gja5	gap junction protein alpha 5	0.11945	0.65515	

Gja8	gap junction protein alpha 8	0	0	
Gjb1	gap junction protein beta 1	17.83156	0.61288	
Gjb2	gap junction protein beta 2	21.16591	3.90916	
Gjb3	gap junction protein beta 3	0.02782	0.40358	
Gjb4	gap junction protein beta 4	0.00313	0.38416	
Gjb5	gap junction protein beta 5	0.60982	0.05171	
Gjb6	gap junction protein beta 6	37.81746	2.43995	
Gjc1	gap junction protein gamma 1	3.30129	0.73984	
Gjc2	gap junction protein gamma 2	16.40784	0.27802	
Gjc3	gap junction protein gamma 3	14.13007	0	
Gjd2	gap junction protein delta 2	1.40732	0.12901	
Gjd3	gap junction protein delta 3	0.04572	0	*
Gjd4	gap junction protein delta 4	0	0	*
Gje1	gap junction protein epsilon 1	0	0	*
Mip	major intrinsic protein of lens fiber	1.25083	0.02981	
Nalcn	sodium leak channel, non-selective	30.64044	14.3179	
Panx1	pannexin 1	3.35556	1.08723	
Panx2	pannexin 2	13.56859	0	*
Panx3	pannexin 3	0.34563	0.03824	
Piezo1	piezo type mechanosensitive ion channel component 1	1.16172	0.7799	
Piezo2	piezo type mechanosensitive ion channel component 2	0.18806	0.04296	